

# **Formulation and evaluation of self-nanoemulsifying tablets for the delivery of poorly water-soluble drugs**

## **Dissertation**

Zur Erlangung des akademischen Grades

Doctor rerum naturalium (Dr. rer. nat.)

Vorgelegt der  
Naturwissenschaftlichen Fakultät I - Biowissenschaften  
der Martin-Luther-Universität  
Halle-Wittenberg

von Herrn MSc.

**Tamer Hassenen Hamed Ahmed Hassan**

geb. am 02. September 1982 in Port Said, Ägypten

Gutachter:

1. Prof. Dr. Karsten Mäder

2. PD Dr. Annette Meister

3. Prof. Dr. Rolf Schubert

Halle (Saale), den 20.01.2015

Verteidigt am 24.09.2015



*TO THE MEMORY OF  
MY FATHER  
AND  
TO MY FAMILY*



---

**Table of contents**

<b>Table of contents</b>	<b>A</b>
<b>List of abbreviations</b>	<b>E</b>
<b>1. Introduction</b>	<b>1</b>
<b>2. Research objectives</b>	<b>20</b>
<b>3. Materials and methods</b>	<b>21</b>
<b>3.1. Materials</b>	<b>21</b>
<b>3.2. Preliminary experiments</b>	<b>21</b>
3.2.1. Formulations preparation	21
3.2.2. Dispersion test	21
<b>3.3. Formulation and characterization of the semisolid SNEDDS</b>	<b>22</b>
3.3.1. Pseudo-ternary phase diagrams	22
3.3.2. Effect of dilution	22
3.3.3. Selection of formulations for further investigations	22
3.3.4. Characterization of the selected semisolid SNEDDS	24
3.3.4.1. Droplet size distribution	24
3.3.4.2. Percentage transmittance	25
3.3.4.3. Differential scanning calorimetry (DSC)	25
3.3.4.4. Benchtop nuclear magnetic resonance (BT-NMR)	25
3.3.4.5. Proton nuclear magnetic resonance ( <sup>1</sup> H-NMR)	26
3.3.4.6. Electron spin resonance (ESR)	26
<b>3.4. Preparation and characterization of self-nanoemulsifying tablets</b>	<b>26</b>
3.4.1. Preliminary screening of the possible adsorbates	26
3.4.2. Preparation of the Neusilin <sup>®</sup> US2/SNEDDS adsorbates	27
3.4.2.1. Method A	27
3.4.2.2. Method B	27
3.4.3. Effect of SNEDDS content on the adsorbates properties	28
3.4.4. Preparation of tablets for the preliminary studies	28
3.4.4.1. Dispersibility	28
3.4.4.2. Effect of the disintegrant level on the fineness of the dispersion	28
3.4.4.3. Effect of the compression force and tablets shape on the tablets properties	29
3.4.4.4. Lumogen <sup>®</sup> F305 release	29
3.4.5. Incorporation of Progesterone	29

## Table of contents

---

3.4.5.1. Progesterone loading	29
3.4.5.2. Progesterone equilibrium solubility	29
3.4.5.3. Preparation of the Progesterone-loaded adsorbates	30
3.4.5.4. Differential scanning calorimetry (DSC)	30
3.4.5.5. Powder X-ray diffraction (PXRD)	30
3.4.5.6. Fourier transform infrared spectroscopy (FTIR)	30
3.4.6. Powder properties	30
3.4.6.1. Angle of repose	30
3.4.6.2. Bulk and tapped density	31
3.4.6.3. Compressibility	31
3.4.7. Preparation of the self-nanoemulsifying tablets	31
3.4.8. Characterization of the self-nanoemulsifying tablets	32
3.4.8.1. Optical microscopy	32
3.4.8.2. Hardness	32
3.4.8.3. Thickness	32
3.4.8.4. Tensile strength	32
3.4.8.5. Friability	32
3.4.8.6. Disintegration time	32
3.4.9. Droplet size distribution	32
3.4.10. Benchtop nuclear magnetic resonance (BT-NMR)	33
3.4.11. <i>In vitro</i> Progesterone release	33
<b>3.5. <i>In vitro</i> lipid digestion</b>	<b>33</b>
3.5.1. Used media	33
3.5.2. Preparation of the Cithrol® DPHS dispersions	34
3.5.2.1. Ultra-Turrax® method (UTM)	34
3.5.2.2. Solvent evaporation method (SDM)	34
3.5.3. Particle size measurement	34
3.5.4. pH-stat method	35
3.5.5. Back titration method	35
3.5.6. Lipid analysis by high-performance thin layer chromatography (HPTLC) combined with spectrodensitometry	36
3.5.7. Possible drug precipitation during digestion	37
3.5.8. Effect of digestion on the drug release from adsorbates and tablets	37
3.5.9. HPLC method	37
3.5.10. Statistical analysis	37
<b>4. Results and discussion</b>	<b>38</b>

<b>4.1. Preliminary experiments</b>	<b>38</b>
4.1.1. Inclusion of 10 % m/m of polymeric excipients	38
4.1.2. Screening of selected solid and semisolid lipid excipients	40
4.1.2.1. Formulations containing Soluplus®	40
4.1.2.2. Formulations containing Arlacel® LC	42
4.1.2.3. Formulations containing Cithrol® DPHS	43
<b>4.2. Formulation and characterization of the semisolid SNEDDS</b>	<b>44</b>
4.2.1. Selection of an excipient combination	44
4.2.2. Pseudo-ternary phase diagrams	45
4.2.3. Effect of dilution	47
4.2.4. Selection of formulations for further investigations	48
4.2.5. Characterization of the selected semisolid SNEDDS	49
4.2.5.1. Droplet size distribution	49
4.2.5.2. Percentage transmittance	50
4.2.5.3. Differential scanning calorimetry (DSC)	51
4.2.5.4. Benchtop nuclear magnetic resonance (BT-NMR)	52
4.2.5.5. Proton nuclear magnetic resonance ( <sup>1</sup> H-NMR)	55
4.2.5.6. Electron spin resonance (ESR)	59
<b>4.3. Preparation of the self-nanoemulsifying adsorbates</b>	<b>64</b>
4.3.1. Preliminary screening of the possible adsorbates	65
4.3.2. Preparation of the Neusilin® US2/SNEDDS adsorbates	65
4.3.3. Characterization of the Neusilin® US2/SNEDDS adsorbates	66
4.3.3.1. Differential scanning calorimetry (DSC)	66
4.3.3.2. Benchtop nuclear magnetic resonance (BT-NMR)	67
4.3.4. Preparation of tablets for the preliminary studies	71
4.3.4.1. Dispersibility	71
4.3.4.2. Effect of the disintegrant level on the fineness of the dispersion	72
4.3.4.3. Effect of the compression force and tablets shape on the tablets properties	72
4.3.4.4. Lumogen® F305 release	75
<b>4.4. Incorporation of Progesterone</b>	<b>76</b>
4.4.1. Progesterone loading	77
4.4.2. Progesterone equilibrium solubility	77
4.4.3. Differential scanning calorimetry (DSC)	78
4.4.4. Powder X-ray diffraction (PXRD)	79
4.4.5. Fourier transform infrared spectroscopy (FTIR)	80
<b>4.5. Powder properties</b>	<b>81</b>

<b>4.6. Preparation and characterization of the self-nanoemulsifying tablets</b>	<b>82</b>
4.6.1. Powder properties	82
4.6.2. Physical properties and optical microscopy	83
4.6.3. Droplet size distribution	84
4.6.4. Benchtop nuclear magnetic resonance (BT-NMR)	85
4.6.5. <i>In vitro</i> drug release	88
<b>4.7. <i>In vitro</i> lipid digestion</b>	<b>89</b>
4.7.1. Digestibility of the excipients	90
4.7.1.1. Preparation and particle size of the excipient dispersions	90
4.7.1.2. pH-stat method	91
4.7.1.3. Back titration method	92
4.7.1.4. Lipid analysis by high-performance thin layer chromatography (HPTLC) combined with spectrodensitometry	93
4.7.2. Digestibility of the semisolid SNEDDS	95
4.7.3. Possible drug precipitation during digestion	97
4.7.4. Effect of digestion on the drug release from adsorbates and tablets	98
<b>5. Conclusion</b>	<b>99</b>
<b>6. Summary and outlook</b>	<b>100</b>
6.1. English version	100
6.2. German version	103
<b>7. References</b>	<b>107</b>
<b>8. Appendices</b>	<b>I</b>
8.1. Supplementary data	I
8.1.1. Supplementary tables	I
8.1.2. Supplementary figures	X
8.2. Acknowledgement	XV
8.3. Curriculum vitae	XVI
8.4. List of publications	XVII
8.4.1. Research articles	XVII
8.4.2. Conferences contributions	XVII
8.5. Declaration of the original authorship	XVIII



---

**List of abbreviations**

<b>%T</b>	Percentage transmittance
<b><math>\tau_c</math></b>	Rotational correlation time
<b>12-HSA</b>	12-hydroxystearic acid
<b><math>^1\text{H-NMR}</math></b>	Proton nuclear magnetic resonance
<b>2-MAG</b>	2-monoacylglycerols
<b>A</b>	0.1 N HCl
<b><math>a_N</math></b>	Hyperfine coupling constant
<b>B</b>	Phosphate buffer pH 6.8 USB
<b>BCS</b>	Biopharmaceutics classification system
<b>BHA</b>	Butylated hydroxyanisole
<b>BHT</b>	Butylated hydroxytoluene
<b>BS</b>	Bile salts
<b>C<sub>10</sub></b>	Capric acid
<b>C<sub>12</sub></b>	Lauric acid
<b>C<sub>16</sub></b>	Palmitic acid
<b>C<sub>18</sub></b>	Stearic acid
<b>C<sub>18:1</sub></b>	Oleic acid
<b>C<sub>18:2</sub></b>	Linoleic acid
<b>C<sub>8</sub></b>	Caprylic acid
<b>CEH</b>	Carboxyl ester hydrolase
<b>CMC</b>	Critical micelle concentration
<b>CPMG</b>	Carr-Purcell-Meiboom-Gill
<b>CS</b>	Cholesterols
<b>D</b>	Dalton
<b>D<sub>2</sub>O</b>	Deuterium oxide
<b>dB</b>	Decibel
<b>d-DMSO</b>	Deuterated dimethyl sulfoxide
<b>DE</b>	Diesters
<b>DG</b>	Diglycerides
<b>DGDG</b>	Digalactosyldiglycerides
<b>DGMG</b>	Digalactosylmonoglycerides
<b>DPHS</b>	Cithrol <sup>®</sup> DPHS
<b>DSC</b>	Differential scanning calorimetry
<b>EDTA</b>	Ethylenediaminetetraacetate
<b>EP</b>	European Pharmacopeia
<b>EPR</b>	Electron paramagnetic resonance
<b>ESR</b>	Electron spin resonance
<b>F305</b>	Lumogen <sup>®</sup> F305
<b>FA</b>	Fatty acids
<b>FaSSIF</b>	Fasted state simulated intestinal fluid
<b>FeSSIF</b>	Fed state simulated intestinal fluid

<b>FTIR</b>	Fourier transform infrared spectroscopy
<b>GI</b>	Gastrointestinal
<b>HGL</b>	Human gastric lipases
<b>HLB</b>	Hydrophilic-lipophilic balance
<b>HPL</b>	Human pancreatic lipases
<b>HPLC</b>	High-performance liquid chromatography
<b>HPMC</b>	Hydroxypropyl methylcellulose
<b>HPMCAS</b>	Hydroxypropyl methylcellulose acetate succinate
<b>HPMCP</b>	Hydroxypropyl methylcellulose phthalate
<b>HPTLC</b>	High-performance thin-layer chromatography
<b>HS15</b>	Kolliphor <sup>®</sup> HS 15
<b>HTS</b>	High-throughput screening
<b><i>I</i></b>	Nuclear spin quantum number
<b>LBDDS</b>	Lipid-based drug delivery systems
<b>LC</b>	Liquid crystals
<b>LCNP</b>	Liquid crystalline nanoparticles
<b>LFCS</b>	Lipid formulation classification system
<b>MC</b>	Methylcellulose
<b>MCC</b>	Microcrystalline cellulose
<b>MCM</b>	Capmul <sup>®</sup> MCM
<b>ME</b>	Monoesters
<b>MG</b>	Monoglycerides
<b>MLogP</b>	Moriguchi Log P
<b>MRI</b>	Magnetic resonance imaging
<b>ms</b>	Millisecond
<b>mT</b>	Millitesla
<b>MW</b>	Microwave
<b>NaCMC</b>	Sodium carboxymethylcellulose
<b>NLC</b>	Nanostructured lipid carriers
<b>N-US2</b>	Neusilin <sup>®</sup> US2
<b>O/W</b>	Oil in water
<b>P</b>	Progesterone
<b>PCS</b>	Photon correlation spectroscopy
<b>PDI</b>	Polydispersity index
<b>PEG</b>	Polyethylene glycol
<b>PG</b>	Propyl gallate
<b>PL</b>	Phospholipids
<b>PLA2</b>	Phospholipase A2
<b>PLRP2</b>	Pancreatic lipase-related protein 2
<b>PVP</b>	Polyvinylpyrrolidone
<b>PWSD</b>	Poorly water-soluble drug
<b>PXRD</b>	Powder X-ray diffraction
<b>rpm</b>	Revolutions per minute

<b>S</b>	Solid adsorbates
<b>SD</b>	Standard derivation
<b>SDEDDS</b>	Self-double emulsifying drug delivery systems
<b>SDM</b>	Solvent displacement method
<b>SEDDS</b>	Self-emulsifying drug delivery systems
<b>SLD</b>	Static laser diffraction
<b>SLN</b>	Solid lipid nanoparticles
<b>SMEDDS</b>	Self-microemulsifying drug delivery systems
<b>SNEDDS</b>	Self-nanoemulsifying drug delivery systems
<b>S-SEDDS</b>	Solid self-emulsifying drug delivery systems
<b>S-SNEDDS</b>	Solid self-nanoemulsifying drug delivery systems
<b>T</b>	Tablets
<b>TB</b>	Tempolbenzoate
<b>TBHQ</b>	<i>tert</i> -Butyhydroquinone
<b>TE</b>	Triesters
<b>TG</b>	Triglycerides
<b>USP</b>	United States Pharmacopeia
<b>UTM</b>	Ultra-Turrax <sup>®</sup> method
<b>UWL</b>	Unstirred water layer
<b>VLDL</b>	Very low-density lipoproteins
<b>W/O</b>	Water in oil
<b>W/O/W</b>	Water in oil in water



## 1. Introduction

In the last 2 decades, many tools in drug discovery and screening were rapidly developed. Examples are automated synthesis, combinatorial chemistry, molecular genetics and high-throughput screening (HTS) methodologies. Accordingly, a large number of compounds has been identified as potential drug candidates [1-4]. Lipinski *et al.* [1, 2] have proposed the “rule of 5” to identify the potential poorly bioavailable drug candidates. Proposed properties of poor bioavailability include: (a) high molecular weight ( $> 500$  D), (b) high lipophilicity ( $\text{Log } P > 5$  or  $\text{MLogP}^1 > 4.15$ ), (c) possession of more than 5 H-bond donors (e.g. NHs and OHs) and (d) possession of more than 10 H-bond acceptors (e.g. Ns and Os). This rule is only valid for drug candidates that are not substrates for active transporters and efflux mechanisms. Poor bioavailability is always originated from poor aqueous solubility (a and b) or poor intestinal permeability (a, c and d) [6].

Amidon *et al.* [7] have introduced the biopharmaceutics classification system (BCS). BCS provides a classification of drugs according to their maximum dose solubility, dissolution and permeability into four classes (**Fig. 1**). High solubility means that the maximum dose is soluble in 250 ml aqueous media in pH range of 1-7.5 at 37 °C. High dissolution means that not less than 85 % of the administered dose is released within 30 min. High permeability means that more than 90 % of the dose is absorbed. This classification provides a guiding tool to replace individual bioequivalence studies by accurate *in vitro* dissolution tests [8, 9].

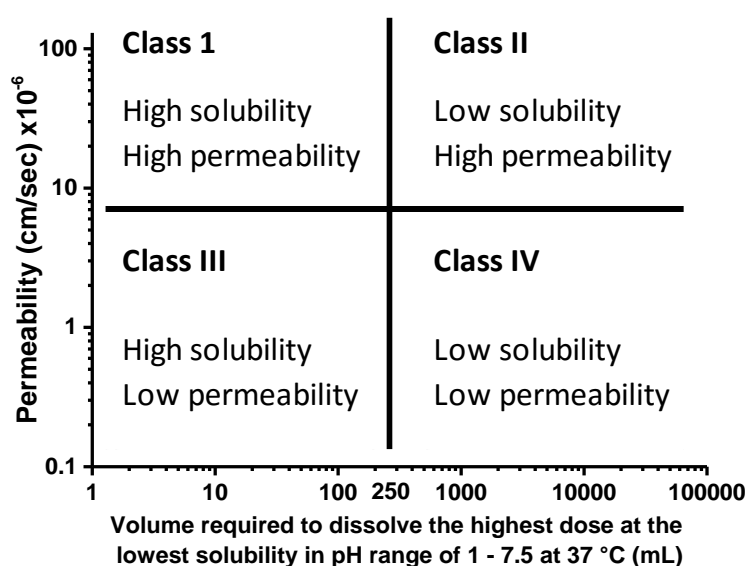


**Fig. 1** Biopharmaceutics classification system of drugs (BCS) adapted from [9, 10].

<sup>1</sup> MLogP is the Moriguchi Log P calculated as described by Moriguchi *et al* [5].

Unfortunately, the number of potential drug candidates, especially those with high molecular weight and high Log P, is progressively increasing. Accordingly, the problem of the poor aqueous solubility ( $< 1 \mu\text{g/ml}$ ) has become dominant in the pharmaceutical industry [1, 2]. Recent studies showed that  $\sim 75\%$  of the drug development candidates are poorly water-soluble. This ratio could be increased to 80-90 % depending on the therapeutic area [11, 12]. As a result, they may fail to reach the market despite their pharmacological activity.

Poorly water-soluble drugs (PWSDs) represent Class II and IV of the BCS [7] and could be classified as grease balls and brick dusts [13]. Brick dusts have a low to moderate lipophilicity and high melting point ( $> 190 \text{ }^\circ\text{C}$ ) because of their strong, stable lattice structure. Their strong intermolecular bonds hinder their solubility in water. On the other hand, grease balls are highly lipophilic compounds ( $\log P > 4$ ) with lower melting point ( $< 190 \text{ }^\circ\text{C}$ ). They are not able to form bonds with the water molecules [14]. Since drugs are absorbed in the dissolved state, several problems are associated with PWSDs such as inter- and intra-patient variability as well as reduced bioavailability. Furthermore, PWSDs dose is always augmented to reach the therapeutic blood level. This leads to local GI tract irritation, toxicity, patient non-compliance, higher costs as well as inefficient treatment [15].

Several strategies have been developed to enhance the water solubility and hereafter the bioavailability of PWSDs. These strategies are described in details in the following reviews: [3, 4, 10, 16-22] and could be briefly summarized into: (a) Physical modifications such as particle size reduction, optimization of crystal habit, cocrystal formation and solid dispersions. (b) Chemical modifications such as the use of buffers, salt formation and complexation (Cyclodextrins). (c) Miscellaneous methods such as the use of surfactants, co-solvents, hydrotrophy, supercritical fluids and lipid-based drug delivery systems (LBDDS).

In this thesis, only the lipid-based approaches, especially the self-nanoemulsifying ones, will be discussed in more details. Lipids represent a large class of compounds that can be classified according to their chemical structures, origin, solubility in organic solvents or biochemical interactions [23-27]. A pioneer in the field of lipid-based systems, Small [28], has introduced a lipid classification system based on lipid/water interactions in bulk water and the behavior of lipids at the air/water interface (**Table 1**).

The use of LBDDS in the oral delivery of PWSDs has generated considerable interest and eventually therapeutical and commercial success [29-31]. LBDDS bioavailability enhancement is ultimately beneficial in the case of grease balls PWSDs, which have adequate solubility in pharmaceutical lipids ( $\log P > 4$ ) [31, 32]. Examples of LBDDS include lipid solutions, lipid

suspensions, liposomes, liquisols, solid lipid nanoparticles (SLN), nanostructured lipid carriers (NLC), mixed micelles, nanocapsules, liquid crystalline nanoparticles (LCNP) (e.g. Cubosomes<sup>®</sup>, Flexisomes<sup>®</sup> and Hexosomes<sup>®</sup>), emulsions, nanoemulsions, microemulsions, and self-emulsifying drug delivery systems [20, 33-45].

**Table 1** Lipid classification system proposed by Small [28].

Class	Bulk interactions with water	Surface interactions with water	Examples
<b>Non-polar</b>	- Insoluble - Crystals or oil	Do not spread to form a monolayer	Cholestanes, benzpyrenes, carotenes, lycopenes and gadusenes
<b>Polar I</b>	- Insoluble, non-swelling - Crystals or oil	Form a stable monolayer	CS, TG, DG, long chain protonated FA, waxes, sterols, oil soluble vitamins and steroidal hormones
<b>Polar II</b>	- Insoluble, swelling - LC	Form a stable monolayer	PL, MG, FA soaps and cerebrosides
<b>Polar IIIA</b>	- Soluble with lyotropic mesomorphism - Crystals or oil → LC → micelles	Form an unstable monolayer	Lysolecithins and surfactants
<b>Polar IIIB</b>	- Soluble without lyotropic mesomorphism - Crystals or oil → micelles	Form an unstable monolayer	BS and saponins

CS: cholesterols; TG: triglycerides; DG: diglycerides; FA: fatty acids; PL: phospholipids; LC: liquid crystals; BS: bile salts.

LBDDS present and maintain the drug in the solubilized form, in which absorption takes place [46, 47]. As a result, the rate-limiting step of drug dissolution is eliminated. Furthermore, they can enhance the bioavailability by different mechanisms depending on their type and amounts such as prolongation of the gastric emptying time; stimulation of bile secretion and interaction with bile salts (BS), phospholipids (PL) and cholesterol (CS) mixed micelles; reduction of the first pass metabolism via stimulation of intestinal lymphatic transport for highly lipophilic drugs ( $\text{Log } P > 5$ ) and reduction of the enterocyte-based metabolism; modulation of intestinal efflux transporters such as P-glycoprotein; permeation enhancement; as well as generation and maintenance of a metastable supersaturable drug state [47-49].

Oral administration of lipids stimulates the secretion of the gastric lipase (HGL) with the consequent secretion of the pancreatic lipase (HPL) and co-lipase from the pancreas along with other esterases such as phospholipase A2 (PLA2), carboxyl ester hydrolase (CEH) and pancreatic lipase related protein 2 (PLRP2) [50-53]. Most of the lipid excipients are esters. Examples are glycerides, PEG esters of fatty acids, polysorbates, PL and CS esters. Ester bonds are generally potential substrates to lipolytic enzymes. Examples of lipid digestion products of different lipid classes are summarized in **Table 2**.

**Table 2** Enzymatic lipolysis of different lipid excipients (adapted from [52]).

Lipid class	Lipolytic enzyme(s)	Digestion products
Glycerides	HPL > HGL	TG → DG + FA → 2-MAG + FA
	CEH, PLRP2, HGL	2-MAG → FA + glycerol
PEG esters	CEH >> PLRP2 > HGL	PEG DE → PEG ME + FA → PEG + FA
Phospholipids	Phospholipase A <sub>2</sub>	Phospholipids → Lyso-1-phospholipids + FA
	PLRP2 > CEH	Phospholipids → Lyso-2-phospholipids + FA
Galactolipids	PLRP2 > CEH	DGDG → DGMG + FA
Cholesterol esters	CEH	Cholesterol ester → cholesterol + FA

HPL: human pancreatic lipases; HGL: human gastric lipases; HTG: triglycerides; DG: diglycerides; FA: fatty acids; 2-MAG: 2-monoacylglycerols; CEH: carboxyl ester hydrolase; PLRP2: pancreatic lipase-related protein 2; DE: diesters; ME: monoesters; DGDG: digalactosyldiglycerides; and DGMG: digalactosylmonoglycerides.

Lipid digestion usually inaugurates in the stomach by the action of HGL [54]. HGL is an acid stable lipase with an optimum activity at pH 3-6 and a maximum activity at pH 5.0-5.4 [43, 52]. HGL is secreted by the chief cells of the gastric fundic glands under the stimulation of meals, stomach motion, gastrin secretion and cholinergic mechanisms [50, 55]. HGL works on the lipid/water interface. Therefore, the ingested lipids need to be emulsified before being digested. The emulsification is usually achieved by the shear action of the stomach along with the surface active actions of the co-administered amphiphiles and digestion products such as monoglycerides (MG) and dietary proteins [52]. Therefore, the contribution of the gastric lipolysis to the whole lipid digestion process is strongly dependent on the gastric residence time, susceptibility of the ingested lipid to digestion and lipid dispersibility pattern in the gastric fluids [47]. In some cases such as incomplete pancreatic function (neonates) or compromised one (cystic fibrosis or chronic alcoholism), gastric lipolysis plays the principal role in the lipid digestion [54, 56]. However, in most cases, gastric lipolysis accounts only for 10-25 % of the total lipid lipolysis [57, 58]. For example, triglycerides (TG) could be partially hydrolyzed in the stomach into diglycerides (DG) and free fatty acids (FA) [54, 57, 59]. FA are protonated under the gastric conditions. In the absence of the bile mixed micelles, protonated FA (especially long chain ones) accumulate on the lipid/water interface with subsequent deactivation of the HGL [52, 55, 56].

HPL is produced in the acinar cells of the pancreas and is secreted along with bile under the stimulation of cholecystokinin and secretin. HPL is active only above pH 5 with a maximum activity at pH 7.0-7.5 [55]. Similar to HGL, HPL works on the lipid/water interface. However, BS always desorb HPL from the interface with the subsequent inhibition of its action [60]. This inhibitory effect is counterbalanced by the formation of HPL/co-lipase equimolar complex, which plays a crucial role in the HPL anchoring to the lipid/water interface. Furthermore, FA



produced during the lipolysis enhance the anchoring of HPL/co-lipase complex on the lipid/water interface with the consequent promotion of further lipid lipolysis [61]. In addition, FA indirectly stimulate the HPL secretion through cholecystokinin release stimulation [62, 63]. Moreover, the presence of the lipid digestion products, especially long chain FA in the small intestine is reported to reduce the gastric motility with the subsequent delay of the gastric emptying rate [64]. This delay may allow more efficient lipid lipolysis and absorption in the upper GI tract as well as higher PWSD dissolution.

Both HGL and HPL have high selectivity toward TG. However, they differ in their specificity. HPL is a regioselective enzyme that hydrolyze only sn-1 or sn-3 positions. On the other hand, HGL can hydrolyze the 3 ester positions [55]. Other lipolytic enzymes such as CEH, PLA2 and PLRP2 do not work on the interface. They hydrolyze the lipid excipients in the dispersed micelles or mixed micelles [52, 53]. Therefore, they are beneficial in the digestion of various lipid excipients [65]. Examples are summarized in **Table 2**.

Bile is composed mainly of digestive enzymes, lipoproteins, CS, BS and PL along with water, bicarbonates, bile pigments and organic wastes [66, 67]. BS, PL and CS are secreted in the form of mixed micelles at a molar ratio BS: PL: CS of 16:4:1 [10, 47]. The interaction of the lipids with the bile mixed micelles plays a crucial role in the lipid lipolysis process as well as the biofate of the accompanied PWSD. Lipid/bile interactions vary from the adsorption of BS on the lipid/water interface of the less polar lipids droplets (TG and DG) to the formation of various colloidal structures such as micelles, mixed micelles and vesicles (**Fig. 2**) with more polar lipids (2-MAG and FA) [68]. Furthermore, BS clean the lipid/water interface by displacing other amphiphiles such as proteins and incorporating of the digestion products, especially long chain 2-MAG and FA, into their mixed micelles. Otherwise, accumulation of the digestion products at the interface would inhibit the action of HPL [52, 69]. On the other hand, the digestion products of medium chain lipids are more polar and do not need the action of BS to be dispersed in the aqueous media.

The biofate of the PWSDs is strongly dependent on the LBDDS dispersion pattern, digestion as well as the interaction of their dispersions and digestion products with the bile mixed micelles rather than the properties of the LBDDS themselves [43, 47]. During lipid dilution and digestion several liquid crystalline (LC) and colloidal phases might occur that have different PWSDs solubilization capacity [68]. The incorporation of the digestion products into the bile mixed micelles strongly increases their PWSDs solubilization capacity. However, this increase is dependent on the FA chain length (long chain > medium chain), the nature of the

colloidal dispersions (vesicles > micelles) and the phase behavior of the digestion products (cubic phases > lamellar phases > colloidal phases) as well as the PWSD lipophilicity [70, 71]. However, some exceptions were also reported [43].

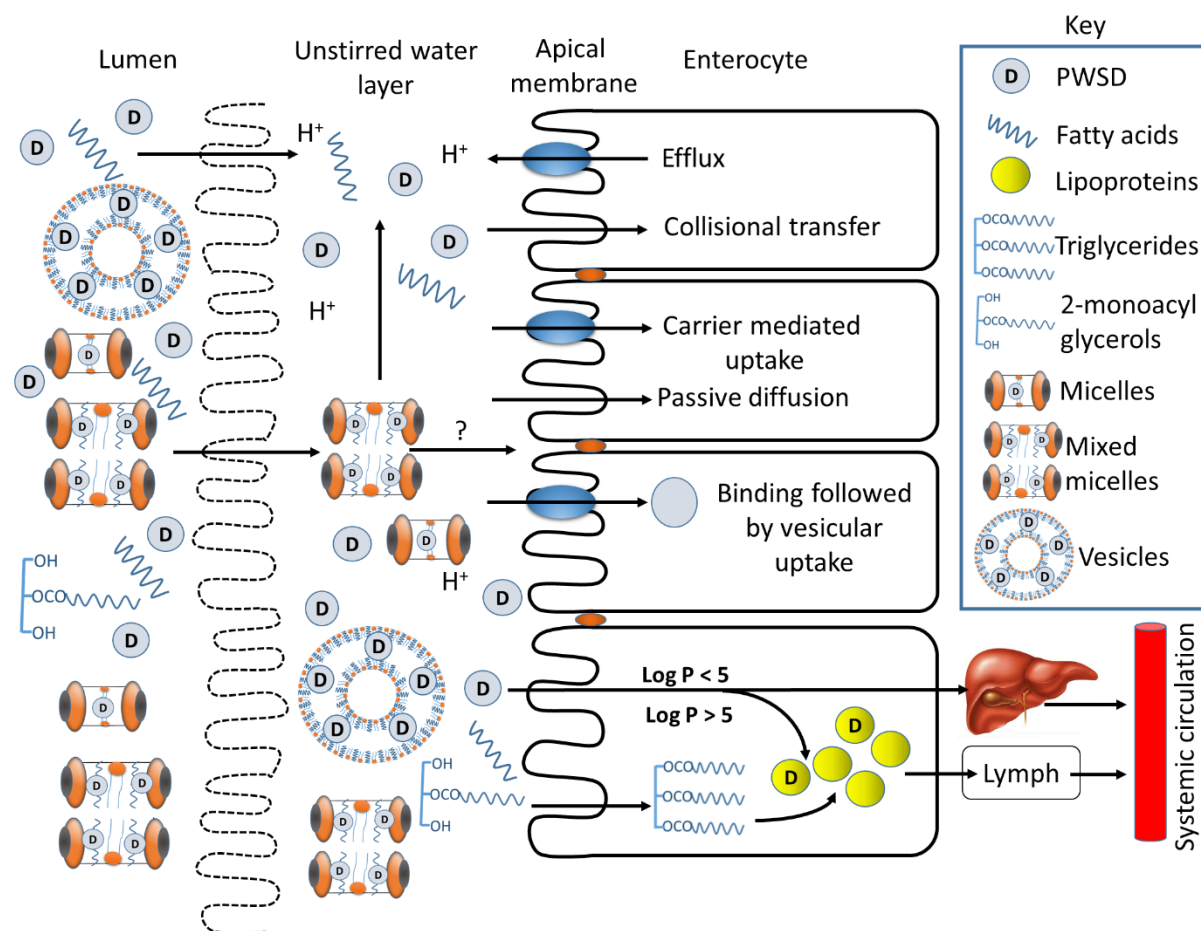


**Fig. 2** Schematic representation of different mechanism of lipids and drugs absorption as well as lipid-mediated bioavailability enhancement (adapted from [47]). For detailed description, please refer to the text.

Furthermore, the incorporation of PWSD, FA and 2-MAG into the bile mixed micelles enhances their mass transfer along the unstirred water layer (UWL) [72, 73]. UWL represents the physical barrier between the bulk fluids in the intestinal lumen and the apical membrane of the enterocyte, where the absorption takes place (**Fig. 2**). UWL has an aqueous acidic microenvironment [74]. Therefore, protonated FA and PWSDs are slowly diffused through it. On the other hand, micelles have higher solubility in the UWL. However, it seems that micelles do not be absorbed intact into the enterocyte [75] as the acidic microenvironment within the UWL accelerates its dissociation [76]. The absorption of the PWSDs and lipids (FA and 2-MAG) into the enterocyte could occur by passive diffusion or carrier-mediated uptake. Furthermore, colloidal structures could be also absorbed by collisional transfer as well as





carrier- or vesicular- mediated uptake (**Fig. 2**). However, the absorbed PWSDs and FA could suffer from the action of the efflux transporters that efflux them back into the UWL [47].

The absorbed lipid digestion products could be directly transported into the portal circulation with a subsequent first pass metabolism. Alternatively, FA and 2-MAG are re-esterified in the endothelial reticulum into TG that constitutes along with CS esters the hydrophobic core of lipoproteins such as chylomicrons and very low-density lipoproteins (VLDL) (**Fig. 2** bottom). The hydrophilic surface of lipoprotein colloidal particles is composed mainly of PL, CS and apolipoproteins [77]. After exocytosis into the interstitial spaces, lipoproteins are selectively taken up by the lymphatic system rather than the blood vessels. The transport of FA into the portal circulation or the lymph may depend on its chain length, degree of unsaturation as well as the class of the administered lipids. However, in some cases contradictory data are reported [78]. Based on their number of carbon atoms, FA could be classified as short (4-6), medium (8-12), long (14-18) or very long chain (20-24) [79]. In most cases, short and medium chain FA are directly transported to the portal circulation while long chain FA are usually involved in the lipoproteins synthesis. Furthermore, increasing the degree of FA unsaturation was found to promote their lymphatic uptake [80-82]. Highly lipophilic absorbed PWSDs (Log P > 5 and TG solubility > 50 mg/g) might be incorporated into lipoproteins (**Fig. 2** bottom) [83]. The transportation of PWSDs along the lymphatic system offers some advantages such as the avoidance of the first pass metabolism, reduction of the enterocyte metabolism [84] and the possible drug targeting (in the case of anticancers and immunomodulators) [85]. However, high PWSD concentration in the lymphatic system may cause local toxicity [47].

Vast varieties of possible lipid excipient combinations are available. Therefore, a classification system was developed to stratify lipid-based formulations into those that could display similar *in vivo* performance. Pouton [10, 31] has established the lipid formulation classification system (LFCS). He itemized LBDDS into five categories (**Table 3**) based on their composition and the possible impact of dilution and digestion on the biofate of the lipid carrier and the drug. Class I formulations are the most lipophilic and are generally regarded as safe. They have the disadvantage that digestion is required to facilitate their dispersion. The digestion products might have different drug solubilization capacity and the solubilization is strongly dependent on the gall bladder activity. This might introduce a variability and food dependency. On the other hand, Class IV formulations are oil-free and rather polar systems based on surfactants and co-solvents. In general, they are less sensitive towards digestion but more sensitive towards dilution. In addition, the presence of organic co-solvents has a negative impact

on the capsule shelf-life stability. Furthermore, the high content of surfactants may cause local irritations in the GI tract, especially if the drug has to be administered on a chronic basis [86].

**Table 3** Lipid formulation classification system (LFCS) proposed by Pouton [10] showing the typical compositions and the properties of the LBDDS.

Excipient	Content in the formulation (% m/m)				
	Class I	Class II	Class IIIA	Class IIIB	Class IV
Oils: MG, DG and TG	100	40-80	40-80	> 20	—
Water-insoluble surfactants (HLB < 12)	—	20-60	—	—	0-20
Water-soluble surfactants (HLB > 12)	—	—	20-40	20-50	30-80
Hydrophilic co-solvents	—	—	0-40	20-50	0-50
Lipophilicity					
Dispersibility					
Digestibility					
Effect of dilution					

Self-emulsifying drug delivery systems represent class II and class III of the LFCS. They are composed of two or more ingredients, which provide the self-emulsifying properties: more hydrophilic amphiphiles, more lipophilic amphiphiles and sometimes co-solvents or precipitation inhibitors. Upon mild agitation and dilution in the GI fluids, these systems transform into oil in water (O/W) emulsions (SEDDS), double emulsions (SDEDDS), microemulsions (SMEDDS) or nanoemulsions (SNEDDS) [16, 87-89]. Microemulsions are thermodynamically stable while nanoemulsions are only kinetically stable. However, in most of the literatures, SNEDDS and SMEDDS are usually subjectively assigned to formulations that provide fine colloidal dispersions. The differences between the nano- and microemulsions are critically discussed in [38, 90] and are summarized in **Table 4**.

**Table 4** Key differences between microemulsions and nanoemulsions.

	Microemulsions	Nanoemulsions
Thermodynamic stability	Stable	Non-stable
Dilution sensitivity	Sensitive	Non-sensitive
Temperature sensitivity	Immediate phase change	Accelerated destabilization

Self-emulsification increases the bioavailability by the circumvention of drug crystal dissolution, which is often insufficient and highly variable for the PWSDs [89]. Compared to the conventional emulsions, SNEDDS are water-free systems. Accordingly, they have better physical and chemical stability. SNEDDS have high patient compliance and palatability as they are always formulated as capsules or tablets. Food has minor effect on drug absorption from SNEDDS compared to other LBDDS. Other advantages include the ease of manufacture and scale-up as well as quick onset of action [31]. In addition, being a mixture of more lipophilic and more hydrophilic amphiphiles, SNEDDS offer high solubilization capacity to a wide spectrum of PWSDs with different degrees of lipophilicity compared to other LBDDS [91].

A good example of a very successful formulation is Neoral<sup>®</sup> / Optoral<sup>®</sup> (Novartis). It is composed of a mixture of MG, DG and TG as lipophilic amphiphiles, Cremophore<sup>®</sup> RH 40 as a hydrophilic amphiphile, propylene glycol and ethanol as co-solvents and tocopherol as an antioxidant [86]. It forms spontaneously transparent dispersions with particle sizes below 100 nm upon dilution with aqueous media [92]. SNEDDS are not only restricted for the oral use [93-97]. Self-emulsifying suppositories [98, 99], intraurethral liquid formulations [100], injections [101-104], implants [105], transdermal [106-111] and ocular systems [112-116] were also reported.

The mechanism of the self-emulsification process is still not clear. However, Reiss [117] have suggested that self-emulsification occurs when the entropy change in the favor of dispersion is higher than the energy required to increase the surface area of the dispersion. The free energy of an emulsion is a function of the energy required to create a new surface between the oil and water phases that could be described by the following equation:

$$\Delta G = \sum_i N_i \pi r_i^2 \sigma$$

Where  $G$  is the free energy associated with the process,  $N$  is the number of droplets,  $r$  is the radius of the droplets and  $\sigma$  is the interfacial energy. The free energy of mixing is ignored.

Crude emulsions are not thermodynamically stable. Therefore, oil and water phases have a high tendency to separate in order to reduce the interfacial energy. The presence of the more hydrophilic amphiphiles stabilizes the interface and reduces the interfacial free energy by formation of a monolayer around the oil droplets. In the case of the SNEDDS, the free energy required to form the emulsion is very small and could be positive or negative. Therefore, the emulsification process takes place spontaneously [95]. The easiness of the emulsification was proposed to be related to the ease of water penetration into the various LC or gel phases formed

on the surface of the droplets [33]. The interface between the oil and the aqueous continuous phase is formed upon addition of the oil/hydrophilic amphiphiles mixture to the water. Water penetrates then into the interface and is solubilized in the oil phase. The extent of water penetration is dependent on its solubilization limit close to the interface [118]. Further aqueous penetration leads to the dispersion of the LC phase. Finally, oil droplets surrounded by LC interface are formed. The extent of the LC interface depends on the hydrophilic amphiphile concentration in the mixture [33, 91, 119, 120].

Several lipid excipients could be formulated as SNEDDS [40, 48, 121]. Based on their polarity, HLB and interaction with the aqueous media, they could be classified as more lipophilic amphiphiles (Polar lipids I and II) and more hydrophilic amphiphiles (Polar lipids IIIa). There are several factors that should be considered in the selection of the lipid excipients. The most important factor is toxicity, especially if the SNEDDS are intended for chronic use. Other factors include the solvent capacity, melting point, digestibility, capsule compatibility, chemical stability, purity, miscibility and their role in promoting the self-dispersibility [32]. More hydrophilic amphiphiles lead to formations, which readily disperse. However, they show in many cases low drug loads and are sensitive to dilution. If the content of the more lipophilic amphiphiles is increased, often higher drug loads can be achieved. However, the self-nanoemulsifying properties are decreased. Therefore, a balanced composition is crucial for the *in vivo* performance.

More lipophilic amphiphiles are mostly referred to as oils or fats depending on their physical states at room temperature. They usually offer high PWSs solubility compared to the more hydrophilic ones. Pharmaceutical lipids could be of natural (**Table 5**), semisynthetic or synthetic origin (**Table 6**). Based on their chain length, medium and long chain lipids are the commonly used oil part of the SNEDDS. Short chain lipids are commonly used as co-surfactants to enhance the film flexibility at the interface and to promote nanoemulsions formation. Very long chain lipids are scarcely used in the SNEDDS formulations [16, 48, 91].

**Table 5** Examples of the commonly used natural lipids in the formulation of SNEDDS. The exact fatty acids composition is tabulated in [48, 122].

	Examples
<b>Long chain lipids</b>	Apricot kernel, Canola, Castor, Corn, Olive, Palm, Peanut, Safflower, Sesame, Soybean and Sunflower oils
<b>Medium chain lipids</b>	Coconut and Palm kernel oils

More lipophilic amphiphiles are generally regarded as safe. They are mostly composed of a mixture of TG and partial glycerides of FA. Furthermore, propylene glycols, PEG and sorbitan

esters of FA as well as free FA (e.g. oleic acid) are commonly used as lipophilic amphiphiles. The solubility of PWSDs in a particular lipid is dependent on the effective ester molar concentration of the lipids [123]. Therefore, the same mass of the medium chain lipids usually afford higher PWSDs solubilization power than long chain ones [32]. Furthermore, depending on their chain length, lipids may have different biofate. The transport through lymphatic circulation, in the most reported cases, is dependent on the lipid chain length (long > medium > short) and the degree of unsaturation [124]. Therefore, the accompanied PWSDs transport through lymphatic system might be enhanced and the first pass metabolism could be reduced when they are incorporated in long chain glycerides. However, the lymphatic transport is also dependent on PWSDs lipid solubility (> 50 mg/g) and lipophilicity ( $\log P > 5$ ). On the other hand, medium chain lipids are usually transported through portal veins to the systematic circulation. Therefore, the accompanied PWSDs could extensively suffer from the first pass metabolism [125, 126].

More hydrophilic amphiphiles are incorporated to promote the dispersibility of the accompanied more lipophilic ones through the reduction of the interfacial tension. They are usually referred to as surfactants. As surfactants can fluidize or solubilize biological membranes, their toxicity must be greatly considered. The toxicity of surfactants is in this order: cationic > anionic > non-ionic. Esters are considered less toxic than ethers. Furthermore, bulky surfactants are deemed to be less toxic than those with single chain [32]. Therefore, non-ionic, bulk, FA ester polymers are the most commonly used hydrophilic amphiphiles in the formulation of SNEDDS (**Table 7**). Furthermore, the HLB value of the surfactant is very important for the self-nanoemulsifying process. To ensure adequate fast dispersibility, surfactants with higher HLB values (> 12) are normally used [91].

Miscellaneous excipients such as co-solvents, precipitation inhibitors and antioxidant might be used to improve the SNEDDS performance, PWSD load and the shelf-life stability. Examples are summarized in **Table 8**. Co-solvents can increase the SNEDDS drug solubilization power. However, the relation between the drug solubility and the co-solvents concentration is nearly logarithmic. Therefore, the use of co-solvents carries a high risk of PWSD precipitation upon dilution in the GI fluids [10, 31]. Furthermore, co-solvents, especially the volatile ones, have an adverse impact on the capsule shelf-life stability, [4, 32, 127, 128]. SNEDDS should not only be able to solubilize PWSDs, but also to maintain drug solubilization throughout the GI tract [89]. Due to its higher co-solvents content, SNEDDS carry a high risk of drug precipitation upon dilution into the GI fluids [31].

**Table 6** Examples of the commonly used semisynthetic and synthetic more lipophilic amphiphiles in the formulation of SNEDDS (adapted from [40, 48, 121]).

Excipient name	HLB	Description	Supplier
<b>Medium chain glycerides</b>			
Capmul® MCM	5.5	C <sub>8</sub> /C <sub>10</sub> MG [58 % MG, 36 % DG, 5 % TG; 80 % C <sub>8</sub> , 20 % C <sub>10</sub> ]	Abitec
Capmul® MCM C10	5-6	C <sub>8</sub> /C <sub>10</sub> MG [> 45 % MG; > 45 % C <sub>10</sub> ]	Abitec
Capmul® MCM C8	5-6	C <sub>8</sub> /C <sub>10</sub> MG [68 % MG, 27 % DG, 3 % TG; > 95 % C <sub>8</sub> , 3 % C <sub>10</sub> ]	Abitec
Captex® 355	1	C <sub>8</sub> /C <sub>10</sub> TG	Abitec
Imwitor® 742	3-4	C <sub>8</sub> /C <sub>10</sub> MG/DG/TG [45-55 % MG]	Sasol
Imwitor® 928	-	C <sub>12</sub> MG/DG/TG of saturated FA [40% MG]	Sasol
Labrafac® CM 10	10	PEG C <sub>8</sub> /C <sub>10</sub> glycerides [50 % C <sub>8</sub> , 50 % C <sub>10</sub> ]	Gattefossé
Labrafac® Lipophile WL 1349	2	C <sub>8</sub> /C <sub>10</sub> TG [50-80 % C <sub>8</sub> , 20-50 % C <sub>10</sub> ]	Gattefossé
Miglyol® 810	-	C <sub>8</sub> /C <sub>10</sub> TG [65-80 % C <sub>8</sub> , 20-35 % C <sub>10</sub> ]	Sasol
Miglyol® 812	-	C <sub>8</sub> /C <sub>10</sub> TG [50-65 % C <sub>8</sub> , 30-45 % C <sub>10</sub> ]	Sasol
Miglyol® 818	-	C <sub>8</sub> /C <sub>10</sub> /C <sub>18:2</sub> TG [45-65 % C <sub>8</sub> , 30-45 % C <sub>10</sub> , 2-5 % C <sub>18:2</sub> ]	Sasol
<b>Long chain glycerides</b>			
Cithrol® GMS 40	3-5	C <sub>18</sub> MG and DG	Croda
Maisine® 35-1	4	C <sub>18:1</sub> / C <sub>18</sub> / C <sub>16</sub> MG [> 50 % C <sub>18</sub> , 10-35 % C <sub>18:1</sub> , < 6 % C <sub>18</sub> , 4-20 % C <sub>16</sub> ]	Gattefossé
Myverol® 18-92	3.7	Distilled sunflower oil MG [7 % C <sub>16</sub> , 4.5 % C <sub>18</sub> , 18.7 % C <sub>18:1</sub> , 67.5 % C <sub>18:2</sub> ]	Eastman
Peccol®	3.3	C <sub>18:1</sub> / C <sub>18:2</sub> / C <sub>18</sub> / C <sub>16</sub> MG [> 60 % C <sub>18:1</sub> , < 35 % C <sub>18:2</sub> , < 6 % C <sub>18</sub> , < 12 % C <sub>16</sub> ]	Gattefossé
Plurol oleique® CC 497	6	Polyglyceryl-3 dioleate	Gattefossé
Plurol® Diisostearate	4.5	Polyglyceryl-3 diisostearate	Gattefossé
Soybean oil	-	C <sub>18:1</sub> /C <sub>18:2</sub> TG	Central Soya
<b>Propylene glycol esters</b>			
Capmul® PG-12	4-5	C <sub>12</sub> ME of propylene glycol	Abitec
Capmul® PG-8	6-7	C <sub>8</sub> ME of propylene glycol	Abitec
Capryol® 90	6	C <sub>8</sub> ME of propylene glycol [> 90 % ME of C <sub>8</sub> ]	Gattefossé
Capryol® PGMC 90	5	C <sub>8</sub> ME of propylene glycol [> 60 % ME, > 90 % C <sub>8</sub> ]	Gattefossé
Captex® 200	-	C <sub>8</sub> /C <sub>10</sub> DE of propylene glycol	Abitec
Captex® 200 P	2	C <sub>8</sub> /C <sub>10</sub> DE of propylene glycol	Abitec
Labrafac® PG	2	C <sub>8</sub> /C <sub>10</sub> DE of propylene glycol	Gattefossé
Lauroglycol® 90	5	C <sub>12</sub> ME of propylene glycol [> 90 % ME, > 95 % C <sub>12</sub> ]	Gattefossé
Lauroglycol® FCC	4	C <sub>12</sub> ME/DE of propylene glycol [45-70 % ME, 30-55 % DE; > 95 % C <sub>12</sub> ]	Gattefossé
Miglyol® 840	-	C <sub>8</sub> /C <sub>10</sub> DE of propylene glycols	Sasol
<b>PEG glycerides</b>			
Labrafil® M 1944 CS	4	C <sub>18:1</sub> PEG-6 glycerides [58-68 % C <sub>18:1</sub> , 22-32 % C <sub>18:2</sub> ]	Gattefossé
Labrafil® M 2125 CS	4	C <sub>18:2</sub> PEG-6 glycerides [24-34 % C <sub>18:1</sub> , 53-63 % C <sub>18:2</sub> ]	Gattefossé
Labrafil® M 2130 CS	4	C <sub>12</sub> PEG-6 glycerides	Gattefossé
Labrafil® WL 2609 BS	6	C <sub>18:2</sub> PEG glycerides [24-34 % C <sub>18:1</sub> , 53-63 % C <sub>18:2</sub> ]	Gattefossé
Tagat® TO	11.3	C <sub>18:1</sub> PEG-25 TG	Evonik



**Table 6;** continued

Excipient name	HLB	Description	Supplier
<b>Sorbitan esters</b>			
Span <sup>®</sup> 20	9	C <sub>12</sub> sorbitan ME	Croda
Span <sup>®</sup> 60	5	C <sub>18</sub> sorbitan ME	Croda
Span <sup>®</sup> 80	4	C <sub>18:1</sub> sorbitan ME	Croda
Tween <sup>®</sup> 85	11	PEG-20 C <sub>18:1</sub> sorbitan TE	Croda
<b>Miscellaneous</b>			
Centrophase <sup>®</sup> 31	4	60 % liquid lecithin, 40 % soybean oil; molecular weight = 800	Central Soya
Cithrol <sup>®</sup> GMO 50	2.8	Glyceryl oleate: propylene glycol (90:10)	Croda

**Table 7** Examples of the commonly used more hydrophilic amphiphiles in the formulation of SNEDDS (adapted from [40, 48, 121]).

Excipient name (former name)	HLB	Description	Supplier
Acconon <sup>®</sup> C-44	13-14	PEG-32 C <sub>12</sub> glycerides	Abitec
Acconon <sup>®</sup> CC-6	12.5	PEG-6 C <sub>8</sub> /C <sub>10</sub> glycerides	Abitec
Acconon <sup>®</sup> MC8-2	14-15	PEG-6 C <sub>8</sub> /C <sub>10</sub> glycerides	Abitec
Gelucire <sup>®</sup> 44/14	14	PEG-32 C <sub>12</sub> glycerides	Gattefossé
Gelucire <sup>®</sup> 50/13	13	PEG-32 C <sub>18</sub> /C <sub>16</sub> glycerides	Gattefossé
Kolliphor <sup>®</sup> EL (Cremophor <sup>®</sup> EL)	13.5	PEG-35 castor oil	BASF
Kolliphor <sup>®</sup> HS 15 (Solutol <sup>®</sup> HS 15)	14-16	PEG-15 esters of 12-hydroxystearic acid	BASF
Kolliphor <sup>®</sup> P188 (Lutrol <sup>®</sup> F68)	29	Poloxamer 188	BASF
Kolliphor <sup>®</sup> RH 40 (Cremophore <sup>®</sup> RH40)	14-16	PEG-40 hydrogenated castor oil (C <sub>16</sub> /C <sub>18</sub> )	BASF
Kolliphor <sup>®</sup> TPGS	13.2	D- $\alpha$ -tocopheryl PEG-1000 succinate	BASF
Labrasol <sup>®</sup>	14	PEG-8 C <sub>8</sub> /C <sub>10</sub> glycerides	Gattefossé
Tween <sup>®</sup> 20	16	PEG-20 C <sub>12</sub> sorbitan ME	Croda
Tween <sup>®</sup> 60	15	PEG-20 C <sub>18</sub> sorbitan ME	Croda
Tween <sup>®</sup> 80	15	PEG-20 C <sub>18:1</sub> sorbitan ME	Croda

Therefore, supersaturable SNEDDS were developed. They contain precipitation inhibitors in order to generate and maintain a metastable drug supersaturation state. Furthermore, they improve the toxicity/safety profile of the SNEDDS by reducing the amounts of the used surfactants [20, 48, 49, 88, 129, 130]. Antioxidants could be incorporated in the SNEDDS to increase the shelf-life stability by protecting the unsaturated lipids or the PWSDs against oxidations [32].

SNEDDS can be formulated as liquid, semisolid or solid dosage forms [33]. The liquid and semisolid SNEDDS are usually filled in soft or hard gelatin capsules while the solid ones are compressed into tablets or filled as freely flowable powders or pellets into hard gelatin capsules. Recently, several novel approaches and patented techniques have been evaluated for the formulation of the SNEDDS [33, 93]. Examples are: self-emulsifying osmotic pumps [93, 131-133], gastroretentive SNEDDS [134, 135], mucoadhesive SNEDDS [136, 137], eutectic

SNEDDS [138, 139], self-emulsifying phospholipids suspension [140-144], self-emulsifying supersaturable systems [144-158], carbon nanotubes-based SNEDDS [159], cationic SNEDDS [160-163], polymeric SNEDDS [164-166], self-emulsifying glasses [167, 168] and self-double emulsifying drug delivery systems (SDED DS) [87, 169-172].

**Table 8** Examples of the miscellaneous excipients used in the formulation of SNEDDS (adapted from [32, 49, 86, 145, 149, 173, 174]).

Excipients class	Examples
<b>Co-solvents</b>	
Diethylene glycol monoethyl ether	Transcutol <sup>®</sup> HP, Transcutol <sup>®</sup> P
Organic solvents	Ethanol, Glycerin, Polypylene glycol, Polyethylene glycol
<b>Precipitation inhibitors</b>	
Water-soluble cellulosic polymers	Hydroxypropyl Methylcellulose (HPMC), Methylcellulose (MC), Hydroxypropyl Methylcellulose Phthalate (HPMCP), Hydroxypropyl Methylcellulose Acetate Succinate (HPMCAS), Sodium Carboxymethylcellulose (NaCMC)
Water-soluble Polyvinylpyrrolidone	Povidone (PVP)
Block co-polymers	Ploxamers (Pluronic <sup>®</sup> F68, Pluronic <sup>®</sup> F127)
Graft co-polymers	Soluplus <sup>®</sup>
<b>Antioxidants</b>	
Natural	$\alpha$ -Tocopherol, $\beta$ -Carotene
Synthetic	Butylated Hydroxytoluene (BHT), Butylated Hydroxyanisole (BHA), <i>tert</i> -Butylhydroquinone (TBHQ), Propyl Gallate (PG)

SNEDDS are associated with some limitations [89] that need to be considered during the formulation development and manufacture. Examples are: (a) The susceptibility of some lipids to oxidation and polymorphism. Lipid oxidation could be reduced by the use of saturated lipids or the incorporation of antioxidants or metal chelators such as EDTA [175]. Polymorphism is always associated with long chain lipids. The influence of the polymorphism can be avoided by heating the lipids at least 20 °C above their melting point and good homogenization. This approach destroys any preformed crystals and promotes the uniformity of the solidified product [176]. (b) PWSD precipitation upon dilution. SNEDDS, especially those with high co-solvents content, carry high risk of PWSD precipitation upon dilution due to the loss of solubilization capacity [10]. The degree of precipitation depends on the lipophilicity of the PWSD as well as the contribution of the hydrophilic amphiphiles and co-solvents to the PWSD solubilization. However, the precipitation kinetics could be in some cases very slow so that the PWSD remains in the supersaturated state for a considerable time. Accordingly, the *in vivo* absorption of the PWSD is not pronouncedly affected [31]. Furthermore, precipitation could be reduced by incorporation of precipitation inhibitors such as HPMC to provide and maintain metastable

supersaturated drug state [152]. (c) SNEDDS can only accommodate low drug dosage. However, the SNEDDS-mediated PWSD bioavailability enhancement may outweigh the dose reduction [31]. (d) SNEDDS are typically formulated as liquid to be encapsulated in soft gelatin capsules. Several drawbacks are associated with such systems such as the interaction with the capsule shell, capsule leakage, instability, possible drug precipitation upon temperature variation as well as the requirement of specialized manufacturing equipment [177-180]. Therefore, alternative formulation strategies, e.g. the inclusion of the SNEDDS into a solid (S-SNEDDS) or semisolid dosage form, are desirable; nonetheless, very challenging.

S-SNEDDS combines the benefits of liquid SNEDDS with those of solid dosage forms and overcomes its limitations. S-SNEDDS were formulated as pellets [181, 182], conventional tablets [183], bilayer tablets [184], effervescent tablets [185], orodispersible tablets [186], capsules [187], tablet-loaded pulsatile capsules [188], osmotic pumps [93, 131-133], microparticles [189-192], nanoparticles [137, 193, 194], mouth dissolving films [195], beads [196, 197], lipid matrices [198] and self-emulsifying glasses [167, 168]. Several approaches were evaluated for the manufacture of the S-SNEDDS [89, 93, 95, 97, 199, 200]. These approaches could be summarized into:

### **(1) The use of solid or semisolid lipids**

Liquid, semisolid and/or solid lipids could be blended so that the final form would have a semisolid or solid consistency. Examples of the evaluated semisolid/solid lipids are: Acconon<sup>®</sup> C-44 [201], Acconon<sup>®</sup> C-50 [202], Gelucire<sup>®</sup> 50/13 [202, 203] and Gelucire<sup>®</sup> 44/14 [65, 201, 203-205]. Compared to other approaches, higher lipid/drug load and scale up simplicity is afforded. Nevertheless, this approach is very challenging because self-nanoemulsifying properties are harder to be achieved with solid lipids. Furthermore, PWSDs could be crystallized out when the molten solid lipids reach room temperature [44].

### **(2) Incorporation of polymeric excipients/amphiphiles**

The liquid SNEDDS is homogeneously distributed in a hydrophilic polymeric matrix such as PEG [206-208]. Alternatively, solid polymeric amphiphiles such as Poloxamer 188 [206] could be used to prepare S-SNEDDS. Poloxamer 188 plays a dual role, as a solidifying agent and more hydrophilic amphiphiles, in the production of S-SNEDDS. In both approaches (1 and 2), the solidified lipids could be directly filled into capsules in the molten state or transformed into powders using cryogenic grinding [209], melt granulation [210] or spray cooling (congealing) [203, 211]. The produced powders could be filled into hard gelatin capsules or compressed into tablets.

### **(3) Lyophilization**

The aqueous phase is removed from O/W emulsions by freeze drying to produce dry emulsions [212]. Direct lyophilization in a suitable PVC blisters [213, 214] could be used to prepare self-nanoemulsifying tablets.

### **(4) Extrusion/spheronization**

The liquid SNEDDS is mixed with a pelletization aid such as MCC and lactose. The produced mass is extruded and spheronized into freely flowable pellets [134, 181, 215-228].

### **(5) Adsorption onto solid carrier**

Liquid SNEDDS are adsorbed onto porous carriers e.g. silicates to prepare apparently dry freely flowable powders. Ideal adsorbent should not interfere with the self-nanoemulsifying properties, have higher adsorption capacity, have superior flow properties, able to produce tablets with acceptable physical properties and able to release 100 % of the incorporated SNEDDS/PWSD. Several silicates with different physical properties and pore sizes were evaluated. Examples are: Aeroperl<sup>®</sup> 300 [184, 229, 230], Aerosil<sup>®</sup> 200 [230-233], Neosyl<sup>®</sup> [234], Neusilin<sup>®</sup> UFL2 [184, 232, 234, 235], Neusilin<sup>®</sup> US2 [187, 230-232, 235-238], Sipernat<sup>®</sup> [232], Sylysia<sup>®</sup> [231, 232] and Zeopharm<sup>®</sup> [187, 230, 232]. Other evaluated non-silicates adsorbents include Fujicalin<sup>®</sup> [184, 234, 235], Hydroxypropyl- $\beta$ -cyclodextrin [233], Magnesium stearate [233], Mannitol [188, 239], MCC [188, 240-242], Polyvinyl alcohol [233] and Sodium carboxymethyl cellulose [233]. The adsorption process could be performed by: (a) Solvent-free methods. The adsorption process could be done by simple trituration in mortar using a pestle [184, 234] or using a mechanical mixer [237]. Alternatively, the liquid SNEDDS/adsorbent mixture could be wet granulated to produce freely flowable granules [231]. (b) Solvent methods. SNEDDS are dissolved in an organic solvent or emulsified in water. The SNEDDS solutions/emulsions are then mixed with the adsorbent and the aqueous/organic phase is removed by rotary evaporation [168], spray drying [141, 150, 190, 233, 239, 243-257] or freeze drying [248].

### **(6) Liquisolid technique**

The carrier, usually MCC, is saturated with the liquid SNEDDS. Excess surface liquid is coated with silicates to produce apparently dry, freely flowable powders [242, 258-260].

### **(7) Fluid bed coating**

Porous silicates/MCC pellets are prepared by extrusion/spheronization. The liquid SNEDDS is then sprayed onto the surface of the porous pellets in a fluid bed coater [261]. Alternatively, liquid SNEDDS are emulsified in water and mixed with a film former such as

Polyvinylpyrrolidone K30. Non-pareil pellets are then coated with the mixture in a fluid bed coater [182, 262].

In all cases, the prepared S-SNEDDS powder could be filled into capsules [187] or compressed into tablets [231]. Although S-SNEDDS are less reactive with the capsule shell than the liquid ones, shell softening is still observed in some cases upon storage [187]. HPMC capsules are superior upon storage of S-SNEDDS compared to hard gelatin ones [187]. Furthermore, due to the relatively low density of SNEDDS adsorbates, tablets are more favorable than capsules. Tablets can hold 2-3 times more powder compared to capsules [237, 263]. However, compression of SNEDDS-loaded adsorbates is not trivial. The SNEDDS could be squeezed out during the compression. Furthermore, the hydrophobic environment inside the produced tablets hinder their disintegration and can lead to incomplete drug release, especially when gel-mediated SNEDDS dispersion takes place or irreversible interaction between the SNEDDS and adsorbent arises [237, 238].

Several approaches were explored to prepare S-SNEDDS tablets. Examples are lyophilization [213, 214], wet granulation [135, 188, 231, 236, 241], dry granulation [189] and direct compression [230, 234, 237]. Alternative approach is to prepare plain tablets with high porosity. Subsequently, tablets are loaded by soaking into the liquid SNEDDS for a certain time [238, 264, 265]. SNEDDS tablets showed high shelf-life stability [236]. In addition, compressed SNEDDS have shown faster *in vitro* dissolution rate and superior *in vivo* activity compared to conventional tablets [231, 239]. However, in some cases the bioavailability enhancement is lower than capsules [264, 265] and incomplete release from tablets was observed [237]. Therefore, PWS release should be monitored in bio-relevant media and the interactions between the SNEDDS and the adsorbents should be thoroughly evaluated.

The formulation of S-SNEDDS is not trivial. The excipient selection is usually based on their solid properties, melting points, toxicity, drug solubility and HLB values [48]. The solid/semisolid physical properties could be evaluated using differential scanning calorimetry (DSC) as well as powder X-ray diffraction (PXRD). However, the performance and dispersibility of the different combinations are difficult to predict. Therefore, phase diagrams are always made to help understanding the phase behavior of the combinations and to estimate the nanoemulsion regions.

DSC is not only useful for determination the melting behavior of lipids [206], it can be also used to evaluate the excipient interactions, lipid polymorphism, drug solubilization [127], type of the produced emulsions and the different states of water associated with the dispersed system

[266-268]. PXRD could also provide information about the physical state of the PWSD within the S-SNEDDS supposing sufficient sensitivity (drug concentration) is obtained. Furthermore, PWSD/SNEDDS interactions could be evaluated by Fourier transform infrared spectroscopy (FTIR).

After ingestion, the SNEDDS will be subjected to gastric and intestinal fluids with different pH values and ions respectively. Solid/semisolid formulations may suffer from poor *in vivo* performance due to the presence of the high melting point lipids [93]. Furthermore, during the melting and dispersion of the solid/semisolid SNEDDS in physiological conditions, several phases might occur based on the temperature as well as the volume, pH and ionic strength of the dispersion media. These phases (ranging from crystals, gels, and lyotropic LC to colloidal structures such as micelles and vesicles) have different impact on the *in vivo* performance (dispersibility, digestibility, absorption of the lipids/PWSD). For example, it was observed in previous studies that Sucrose ester nanodispersions are pH and ion-sensitive and might precipitate under physiological relevant conditions [269]. Therefore, it is important to ensure sufficient lipid mobility and to avoid lipid crystallization and precipitation. Consequently, it is very important to study the robustness of the solid/semisolid SNEDDS to dilution at different pH values (e.g. 1.2 and 6.8) as well as double distilled water to anticipate the effect of various pH-values and ions on the self-nanoemulsifying properties. The droplet size distribution can serve as a control and could be monitored after dilution by photon correlation spectroscopy (PCS). PCS offers the advantage that droplet size distribution could be monitored at physiological temperature. On the other hand, static laser diffraction (SLD) can be used to monitor the droplet size distributions of highly polydisperse dispersions. Furthermore, the evaluation of the mobility of the lipid formulations after dilution, especially at body temperature, is very essential. The molecular mobility of the dispersed SNEDDS components could be evaluated using benchtop nuclear magnetic resonance (BT-NMR) and proton nuclear magnetic resonance ( $^1\text{H-NMR}$ ). In addition, BT-NMR can provide useful information about lipids/adsorbents interactions as well as lipid/water interactions. Electron spin resonance (ESR) has also shown its usefulness for the characterization of lipid nanodispersions in previous studies. For example, ESR has been used in the area of the SLN, which quite frequently do not crystallize and remain for long periods in the state of supercooled melts. It has been shown by ESR that crystallization dramatically decreases the drug load capacity of the lipid nanodispersions and induces a translocation of incorporated compounds from the desired lipophilic environment into more polar microenvironments of the interface and into the aqueous

phase [270]. It is obvious that the characteristics of the microenvironment affect drug stability and release processes. Using the poorly water-soluble spin probe (Tempolbenzoate, TB) as a PWSD model, ESR can be used to characterize the micropolarity and microviscosity and to quantify the distribution of the probe between different microenvironments.

Oral administration of lipids stimulates the secretion of various lipolytic enzymes that hydrolyze the ester bonds, abundantly present in the lipid excipients. For example, TG are hydrolyzed into two free FA and 2-MAG [52]. The breakdown products are then incorporated in the bile mixed micelles. However, lipid digestion might decrease the solubilization capacity of the carrier, and - as a consequence - drug precipitation might occur. Therefore, *in vitro* lipid digestion studies, using bio-relevant dissolution media containing enzymes and naturally occurring surfactants such as BS and PL, are recommended to predict the *in vivo* performance of the SNEDDS [265, 271-273]. The most important methods that are used to assess the *in vitro* lipid digestibility are related to pH-stat measurements and high-performance thin layer chromatography (HPTLC) combined with spectrodensitometry [271, 274]. The pH-stat method is the simplest and the most widely used method for evaluation of *in vitro* lipid digestion. However, this method relies on the ionization state of the FA. The titration should be carried out at pH values, which are at least 2 units higher than the pKa of the acid. Long chain fatty acids (e.g. C<sub>16</sub> and C<sub>18</sub>) might be underestimated due to their higher apparent pKa values and partial localization in more lipophilic environments, which makes them non-accessible for titration. Therefore, back titration at higher pH values is sometimes used to minimize these problems [274]. HPTLC combined with spectrodensitometry gives a more detailed view not only about the released FA but also about the other digestion products such as DG, 2-MAG, PEG esters, etc. [69, 275]. A direct measurement of lipid digestion by optical methods is difficult due to the complex and turbid nature of pancreatin. However, a continuous monitoring of digestion-induced translocation of model compounds has been described using ESR [276, 277]. The beauty of a direct measurement is counterbalanced by the fact that ESR requires paramagnetic molecules and therefore no real PWSD can be monitored.

## 2. Research objectives

### 2.1. General objective

- The main aim of this project is to develop and optimize novel semisolid/solid SNEDDS for the oral delivery of PWSDs. Tablets were selected as a final dosage form. The prepared SNEDDS should conform to the following criteria: (a) Semisolid or solid consistency at room temperature. (b) pH-independent self-nanoemulsification upon mild agitation at 37 °C. (c) High lipid mobility after dilution at physiological conditions. (d) High shelf-life stability due to the avoidance of unsaturated lipid excipients. (e) Less PWSDs precipitation due to the avoidance of co-solvents as well as high content of long chain lipids.

### 2.2. Specific objectives

- To screen and optimize novel lipid excipient combinations for their fitting into the aforementioned criteria. The selection of the lipid excipients was based on their physical properties, lack of unsaturation, novelty, toxicity profile, miscibility and potential advantages in the SNEDDS development.
- To investigate the physical properties of the optimized formulations as well as the possible excipient/excipient and excipient/drug interactions by PXRD and DSC.
- To study the effect of dilution, pH and ionic strength on the droplet size distribution of the selected excipient combinations by PCS.
- To comprehensively characterize the molecular mobility of the selected optimized formulations and their nanodispersions by BT-NMR, <sup>1</sup>H-NMR and ESR.
- To evaluate the digestibility of the lipid excipients as well as their SNEDDS *in vitro* by a pancreatin digestion assay.
- To investigate the SNEDDS-mediated solubility enhancement of the PWSD (Progesterone) in different media as well as the possible impact of the SNEDDS digestion on the Progesterone biofate.
- To incorporate the optimized SNEDDS into a nanoporous carrier with the subsequent production of freely flowable self-nanoemulsifying adsorbates.
- To study the possible interactions between the SNEDDS and the nanoporous using DSC and BT-NMR.
- To evaluate the effect of the disintegrant level and compression pressure on the physical properties and dispersibility of the compressed adsorbates.
- To prepare and characterize SNEDDS tablets with acceptable mechanical properties, low surface lipids as well as the ability to release 100 % of the PWSD in bio-relevant media.



### 3. Materials and methods

#### 3.1. Materials

All materials were used as received from suppliers. Being a mixture of two or more ingredients, semisolid lipids need to be molten and homogenized before use. Furthermore, to avoid the heat stress during the heating and the cooling cycles, semisolid lipids were divided into small portions once received. Liquid excipients were homogenized before use. The chemical structures and the properties of the used materials are summarized in **Table S1** of the supplementary data.

#### 3.2. Preliminary experiments

##### 3.2.1. Formulations preparation

Several combinations (**Table S2 - Table S5** of the supplementary data) were molten together and mixed. Sudan III was used as a PWSD model at a level of 2 mg/g and was then dissolved in the molten mass. The mixtures were cooled down to room temperature and allowed to equilibrate for 24 h at 23 °C and examined for any possible phase separation. Hundred milligrams of the prepared formulations were molded into a cylinder with 6 mm diameter and 2-3 mm thickness so that finally solid tablet-like shapes were produced (**Fig. 3**). Formulations were heated whenever necessary to facilitate molding.

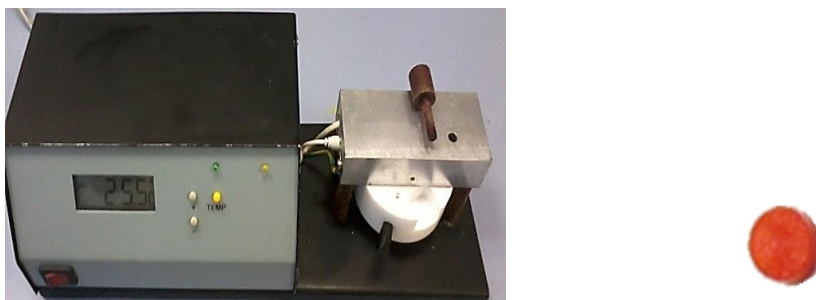


**Fig. 3** Tablets molding machine and an example of the produced tablet-like cylinders (diameter = 6 mm).

##### 3.2.2. Dispersion test

Tablets were dispersed in 10 ml of 0.1 N HCl and phosphate buffer pH 6.8 USP so that the final concentration was 1 % m/V. The dispersions were incubated in a preheated ( $37\pm 1$  °C) end over end mixer (**Fig. 4**) rotating at 10 rpm. The self-emulsification spontaneity and the appearance of the final dispersion were monitored visually at the specified time intervals (10 min, 30 min, 1 h, 2 h, 3 h, 4 h and 24 h).

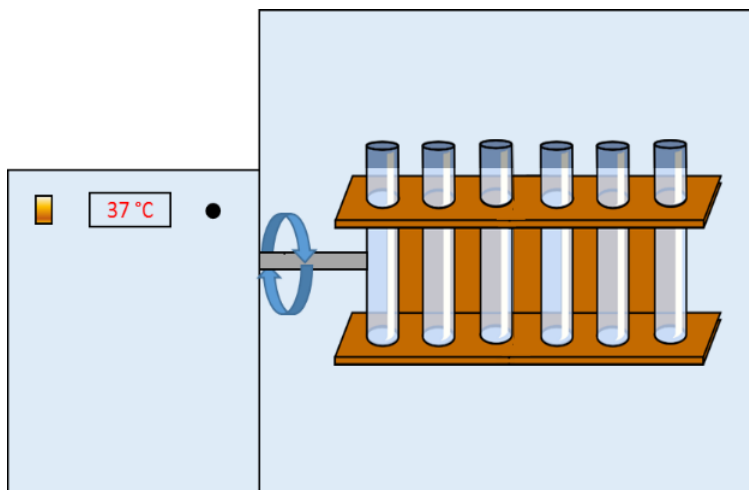


**Fig. 4** Schematic representation of the end over end mixer.

### 3.3. Formulation and characterization of the semisolid SNEDDS

#### 3.3.1. Pseudo-ternary phase diagrams

Cithrol<sup>®</sup> DPHS (DPHS) and Kolliphor<sup>®</sup> HS 15 (HS15) were screened in different ratios (M1 – M4). Capmul<sup>®</sup> MCM (MCM) was tested as a co-emulsifier. Two ratios of DPHS: MCM were extensively tested: 1:1 (M5 – M15) and 2:1 (M16 – M26). Furthermore, different ratios of DPHS: MCM (1:2.5, 1:3 and 1:4) were tested at HS15 content of 40-60 % (M27 – M35). In addition, at constant DPHS content of 20 %, different ratios of MCM: HS15 (M36 – M38) were tested. The exact composition of DPHS, MCM and HS15 combinations is summarized in **Table 9**. The combinations were prepared as described in **Section 3.2.1** and dispersed as described in **Section 3.2.2**. Furthermore, selected dispersions were investigated with a Zeiss Axiolab microscope (Carl Zeiss, Oberkochen, Germany).

#### 3.3.2. Effect of dilution

One gram samples were heated to  $37 \pm 1$  °C in an orbital mixing chilling/heating dry bath (Torrey Pines Scientific Inc., California, USA) operated at 600 rpm. The samples were then diluted with 0.1 N HCl to yield a 90 % m/V lipid dispersion. The diluent was added in 10 % (m/V) incremental steps (**Table 10**) every 15 min. The appearance of the final emulsions was monitored visually.

#### 3.3.3. Selection of formulations for further investigations

Based on the results of the pseudo-ternary phase diagrams and dilution study, three formulations were selected for further characterization (**Table 11**).

**Table 9** Composition of the investigated Cithrol® DPHS, Capmul® MCM and Kolliphor® HS 15 formulations (m %).

Code	Cithrol® DPHS		Kolliphor® HS 15
M1	60		40
M2	40		50
M3	50		60
M4	30		70
	Cithrol® DPHS: Capmul® MCM (1:1)		Kolliphor® HS 15
M5	80		20
M6	75		25
M7	70		30
M8	65		35
M9	60		40
M10	55		45
M11	50		50
M12	40		60
M13	30		70
M14	20		80
M15	10		90
	Cithrol® DPHS: Capmul® MCM (2:1)		Kolliphor® HS 15
M16	80		20
M17	75		25
M18	70		30
M19	65		35
M20	60		40
M21	55		45
M22	50		50
M23	40		60
M24	30		70
M25	20		80
M26	10		90
	Cithrol® DPHS	Capmul® MCM	Kolliphor® HS 15
M27	42.86	17.14	40
M28	45	15	40
M29	48	12	40
M30	35.71	14.29	50
M31	37.50	12.50	50
M32	40	10	50
M33	28.57	11.43	60
M34	30	10	60
M35	32	8	60
M36	20	30	50
M37	20	40	40
M38	20	50	30

**Table 10** Volumes of the added 0.1 N HCl during the dilution study.

Lipid mass (g)	Added 0.1 N HCl volume (ml)	Total 0.1 N HCl volume (ml)	Lipid concentration (% m/V)
1	0.111	0.111	90
1	0.139	0.250	80
1	0.179	0.429	70
1	0.238	0.667	60
1	0.333	1.000	50
1	0.500	1.500	40
1	0.833	2.333	30
1	1.667	4.000	20
1	5.000	9.000	10

**Table 11** Composition of the selected Cithrol<sup>®</sup> DPMS formulations (m %).

Formulation code	Cithrol <sup>®</sup> DPMS	Capmul <sup>®</sup> MCM	Kolliphor <sup>®</sup> HS 15
F1	20	20	60
F2	26.67	13.33	60
F3	30	10	60

### 3.3.4. Characterization of the selected semisolid SNEDDS

#### 3.3.4.1. Droplet size distribution

Formulations were analyzed for droplet size distribution by photon correlation spectroscopy (PCS) using a Zetasizer Nano ZS (Malvern Instruments, Worcestershire, U.K.) with a back scattering angle of 173°. Samples were dispersed as described in **Section 3.2.2** and measured at 37 °C after an equilibration time of 20 min. Each sample was measured 3 times with 12-17 runs over 10 s. The measurement position was fixed in the middle of the cuvette. Z-average diameters and polydispersity indices (PDI) were determined by the cumulant analysis software of the instrument (Zetasizer Software 6.32, Malvern Instruments, Worcestershire, U.K.).

The viscosity of the samples was evaluated at 37 °C using Ubbelohde-viscometer type 1 (Schott Geräte, Hofheim, Germany) using the following equation:

$$\eta = K \cdot (t - F) \cdot \rho$$

Where  $\eta$  is the sample viscosity,  $K$  is a device constant,  $F$  is Hagenbach correction,  $t$  is the time to pass between the two marks (average,  $n=5$ ) and  $\rho$  is the density of the sample. The density of the samples was determined by Mohr-Westphal balance (Wissenschaftlicher Apparatebau Johannes Hammer, Leipzig, Germany). The sample density was found to be constant for all samples (0.997 g/cm<sup>3</sup>). The measured viscosity for F1 was 0.7622 mPa.s, F2 was 0.7722 mPa.s and F3 was 0.7821 mPa.s.

### 3.3.4.2. Percentage transmittance

One percent dispersions (m/V) were prepared as described in **Section 3.2.2**. The optical clarity expressed as percentage transmittance (%T) was measured spectrophotometrically at 650 nm using a Spekol 1200 spectrometer (Analytik Jena GmbH, Jena, Germany). Blank dispersion media were used as references.

### 3.3.4.3. Differential scanning calorimetry (DSC)

DSC investigations were performed using a nitrogen purged Netzsch DSC 200 (Netzsch-Gerätebau GmbH, Selb, Germany). All samples (approx. 15 mg) were accurately weighed in aluminum pans and hermetically sealed to avoid water evaporation. For excipients, formulations and adsorbates, DSC thermograms were generated by cooling the samples to -20 °C. The samples were then equilibrated for 3 min and the heating thermograms at a rate of 5 K/min up to 200 °C were recorded. Furthermore, the second and the third heating and cooling thermograms of F2 was recorded.

### 3.3.4.4. Benchtop nuclear magnetic resonance (BT-NMR)

Samples were filled in test tubes and directly measured with a low-field (20 MHz) benchtop <sup>1</sup>H-NMR-MRI spectrometer (MARAN DRX2, Oxford Instruments Molecular Biotools, Oxford, UK) equipped with an airflow temperature regulation. The transverse magnetization decay was measured by applying the Carr-Purcell-Meiboom-Gill (CPMG) pulse sequence. Data fitting was carried out using the WinDXP analysis software (Oxford Instruments Molecular Biotools, UK) to obtain the resulting T<sub>2</sub>-relaxation time distribution. The used parameters are summarized in **Table 12**. Gauss peak fitting and relative area calculations were performed using OriginPro 2015 (64-bit) b9.2.214 software (Originlab Corporation, Northampton, USA) after taking the log of the X-scale.

**Table 12** The used parameters for the BT-NMR measurements.

Parameter		Excipients and formulations	Adsorbates	Nanoemulsions and SNEDDS release
Number of echoes		3072	2048	4096
Number of scans		64	128	256
Relaxation delay	ms	1000	1000	1200
Receiver gain	%	5	40	40
Pulse sequence		CPMAG (P90 = 3.65 μs)		
Temperature	°C	25 and 37	25	37

### 3.3.4.5. Proton nuclear magnetic resonance ( $^1\text{H-NMR}$ )

Formulations were dispersed in deuterium oxide ( $\text{D}_2\text{O}$ ) (5 % m/V) using an end over end mixer at  $37 \pm 1$  °C. Excipients were dissolved in d-DMSO. HS15 was also dispersed in  $\text{D}_2\text{O}$  (3 % m/V) to investigate the chemical shift corresponding to the micellar form. All  $^1\text{H-NMR}$  spectra were recorded by a Gemini 2000 spectrometer (Varian, Les Ullis, France) operated at 400 MHz at 37 °C. The analysis of the relative signal area and peak width at half amplitude was performed using MestReNova 6.0.2-5475 software (Mestrelabs Research S.L., Santiago de Compostela, Spain). Expected relative signal area calculations were based on the molar fraction of the individual excipient in the dispersion and the relative areas obtained from the dissolved DPHS and MCM in d-DMSO and micellar dispersion HS15 in  $\text{D}_2\text{O}$ .

### 3.3.4.6. Electron spin resonance (ESR)

The nitroxide spin probe Tempolbenzoate (TB) was used as a PWSD model in a concentration of 2 mM/kg. SNEDDS nanodispersions (1, 5, 10 and 20 % (m/V)) in phosphate buffer pH 6.8 USP were prepared. ESR spectra were recorded by means of a 9.3-9.55 GHz X-band spectrometer equipped with a nitrogen gas flow temperature regulation (MiniScope MS200, Magnettech, Berlin, Germany). The used parameters for the ESR measurements are summarized in **Table 13**. The obtained spectra were fitted for either one isotropic rotation state (excipients) or two isotropic rotation states (anhydrous formulations and nanoemulsions). Fitting of the EPR spectra was performed using EPRSIM Nitroxide spectra simulation software V. 4.99 (Biophysical laboratory EPR center, Jožef Stefan Institute, Ljubljana, Slovenia).

**Table 13** The used parameters for the ESR measurements.

Parameter		Excipients and anhydrous formulations	Nanoemulsions
<b>B0-Field</b>	mT	333.97	333.66
<b>Sweep</b>	mT	6.97	4.95
<b>Modulation</b>	mT	0.06	0.1
<b>Sweep time</b>	s	60	1200
<b>MW attenuation</b>	dB	10	10
<b>Spectrometer</b>		X-band	X-band

## 3.4. Preparation and characterization of self-nanoemulsifying tablets

### 3.4.1. Preliminary screening of the possible adsorbates

The SNEDDS were molten at 50 °C and mixed with selected excipients (**Table S6**) in a ratio of 30:70 m/m in a mortar using a pestle for 5 min. The appearance and the flowability of the adsorbates were judged visually.

### 3.4.2. Preparation of the Neusilin<sup>®</sup> US2/SNEDDS adsorbates

Based on the screening results, Neusilin<sup>®</sup> US2 (N-US2) was selected as an adsorbent. Two methods were used in the adsorbates preparation. Method A was used in the preparation of small batches (~10 g) for the preliminary experiments and loading studies. Method B was used for the preparation of relatively large batches (~50 g) for the studying of the powder properties and tablets preparation.

#### 3.4.2.1. Method A

Molten DPHS, MCM and HS15 were mixed together in a small beaker. The molten SNEDDS was mixed with N-US2 in a Fanta dish, which was then heated in an oven at 50 °C for 30 min with occasional mixing. The content was then transferred into a mortar and mixed thoroughly for 5 min (**Fig. 5**).

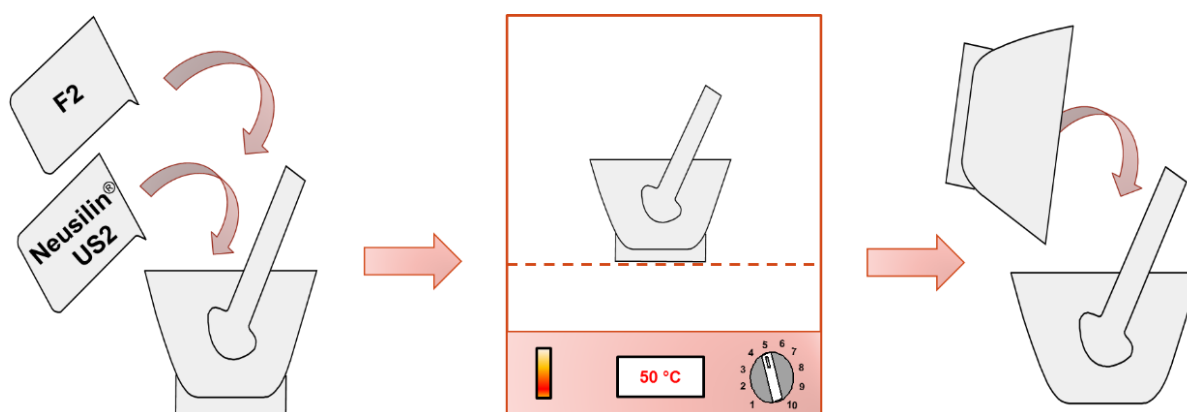


**Fig. 5** Schematic representation of the SNEDDS/Neusilin<sup>®</sup> US2 adsorbates preparation using method A.

#### 3.4.2.2. Method B

Molten DPHS, MCM and HS15 were mixed together at 50 °C in a 500 ml beaker over a heating plate. The mixing process was made by a lab scale mechanical stirrer (RW 20, Janke & Kunkel IKA<sup>®</sup>-Labortechnik, Staufen, Germany) equipped with an 80 mm 3-hole blade stirrer (**Fig. 6**). The beaker diameter was selected so that it allows a very narrow clearance between the blade and the beaker wall to reduce the building up of agglomerates. The beaker was then covered with aluminum foil to avoid dusting and N-US2 was then added gradually through a powder funnel. The stirrer speed was set to 500 rpm. The mixing was stopped after the complete N-US2 addition to free any formed wall or blade stickiness. Subsequently, the mixing was continued for 5 min. At the end of the mixing phase, freely flowable powders were obtained. The powders were allowed to reach the room temperature before any further processing.

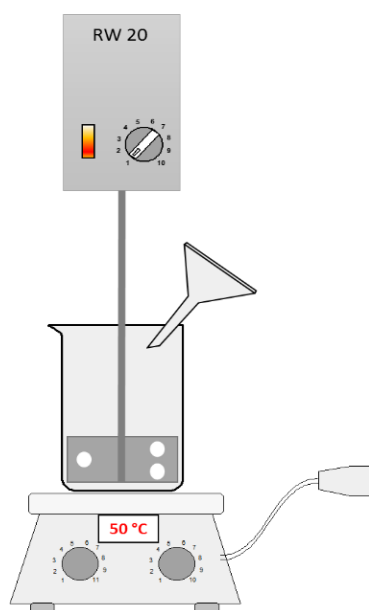


**Fig. 6** Schematic representation of the SNEDDS/Neusilin<sup>®</sup> US2 adsorbates preparation using method B.

### 3.4.3. Effect of SNEDDS content on the adsorbates properties

The semisolid SNEDDS was incorporated (20-90 % m/m) in N-US2 using method A (Section 3.4.2.1). The interactions between the semisolid SNEDDS and the adsorbent were evaluated using both DSC and BT-NMR as described in Section 3.3.4.3 and Section 3.3.4.4 respectively.

### 3.4.4. Preparation of tablets for the preliminary studies

Semisolid and rubbery adsorbates (N1 – N3) were molded into cylinders with a 6 mm diameter and a thickness of 2-3 mm so that finally tablet-like shapes were produced (Section 3.2). The tablets weight was 100 mg. Freely flowable adsorbates (N4 – N8) were compressed on a single punch tableting machine (Korsch AG, Berlin, Germany) using 11 mm flat punch. The tablets weight was 250 mg.

#### 3.4.4.1. Dispersibility

The dispersibility of the prepared tablets was tested in a preheated ( $37 \pm 1$  °C) end over end mixer rotated at 10 rpm. Two dispersion media were used: 0.1 N HCl and phosphate buffer pH 6.8 USP. The volume of the media was selected so that it allows the production of 1 % m/V SNEDDS nanodispersions.

#### 3.4.4.2. Effect of the disintegrant level on the fineness of the dispersion

Kollidon<sup>®</sup> CL-SF (CL-SF) was selected as a disintegrant. Tablets were prepared as described above using three levels of the disintegrant: 5, 7.5 and 10 %. Tablets dispersions were investigated microscopically using a Zeiss Axiolab microscope (Carl Zeiss, Oberkochen, Germany) after 10 min and 60 min.



### **3.4.4.3. Effect of the compression force and tablets shape on the tablets properties**

N7 adsorbates were prepared using method B (Section 3.4.2.2) and mixed with 10 % CL-SF in a mortar using a pestle. The adsorbates were compressed on a single punch tableting machine (Korsch AG, Berlin, Germany) using 11 mm flat or concave punch. The tablets weight was 250 mg. The evaluated compression forces were 2-10 kN, corresponding to compression pressures of 20-105 MPa. Tablets properties were assessed as described in Section 3.4.8.

### **3.4.4.4. Lumogen® F305 release**

In order to visually monitor the SNEDDS release from the produced adsorbates and tablets, Lumogen® F305 (F305) fluorescence dye was used as a PWSD model. F305 was incorporated in the SNEDDS at a concentration of 0.2 % m/m. N7 adsorbates were prepared using method A (Section 3.4.2.1). The adsorbates were mixed with 10 % CL-SF in a mortar using a pestle and the mixture was compressed at 50 MPa as described above. The dispersion study of the SNEDDS, adsorbates and tablets was performed in a preheated ( $37\pm 1$  °C) end over end mixer rotated at 10 rpm. The volume of the dispersion media (0.1 N HCl and phosphate buffer pH 6.8 USP) was selected so that it allows 1 % m/V dispersion of SNEDDS in the chosen medium. The dispersibility was monitored visually. Furthermore, samples were collected after 2 h and centrifuged at 12045 *g* for 5 min in an Eppendorf centrifuge (MiniSpin, Eppendorf AG, Hamburg, Germany) to separate the rest N-US2 powder.

## **3.4.5. Incorporation of Progesterone**

### **3.4.5.1. Progesterone loading**

Progesterone equilibrium solubility was assessed in DPHS, HS15, MCM as well as the SNEDDS at 50 °C. Progesterone was added in excess to 5 g of the corresponding lipid in sealed tubes. Samples were incubated in an end over end mixer at  $50\pm 1$  °C for 24 h. Later, they were centrifuged for 5 min (Avanti J-20XP centrifuged equipped with JLA-16.250 rotor, Beckman Coulter, Miami, USA) at 12045 *g* at 40 °C. The supernatant was diluted with acetonitrile to a suitable concentration range, centrifuged again for 5 min and analyzed by HPLC (Section 3.5.9).

### **3.4.5.2. Progesterone equilibrium solubility**

Progesterone equilibrium solubility measurements were carried out in the following media: double distilled water, 0.1 N HCl, phosphate buffer pH 6.8 USP and simulated intestinal fluids in both fasted (FaSSIF) and fed state (FeSSIF) as well as blank dispersion media containing 1 % m/V of the semisolid SNEDDS. For detailed composition of simulated intestinal fluids, see Section 3.5.1. Progesterone was added in excess to 5 ml of the dispersion media in sealed tubes.

Samples were incubated in an end over end mixer at  $37\pm 1$  °C for 24 h. After that, they were centrifuged for 5 min in an Eppendorf centrifuge (MiniSpin, Eppendorf AG, Hamburg, Germany) at 12045 g. The supernatant was filtered through a 0.2 µm Millipore filter, diluted with acetonitrile to an appropriate concentration range, centrifuged again for 5 min and analyzed by HPLC (Section 3.5.9) [215].

#### **3.4.5.3. Preparation of the Progesterone-loaded adsorbates**

Progesterone was dissolved in the molten SNEDDS. The Progesterone-loaded (15 mg/g) SNEDDS were then adsorbed on N-US2 as described in Section 3.4.2.2.

#### **3.4.5.4. Differential scanning calorimetry (DSC)**

DSC measurements of adsorbates with or without Progesterone as well as pure Progesterone were performed as described in Section 3.3.4.3. For pure Progesterone, small sample weight (approx. 0.3 mg) was used.

#### **3.4.5.5. Powder X-ray diffraction (PXRD)**

Samples were measured using a powder X-ray diffractometer (STADI MP, Stoe, Darmstadt, Germany) equipped with a curved Ge (111) monochromator (CoK $\alpha$  radiation,  $\lambda = 0.178896$  nm) operated at 40 KV and 30 mA and an image plate detector at room temperature. The samples were scanned from 5° ( $2\theta$ ) to 123° ( $2\theta$ ) with a step size of 0.03° ( $2\theta$ ) and a count time of 2000 s per step.

#### **3.4.5.6. Fourier transform infrared spectroscopy (FTIR)**

Solid samples were pressed into potassium bromide tablets and the spectra were recorded using a FTIR spectrometer (IFS 28, Bruker Optik GmbH, Karlsruhe, Germany). Each spectrum (400 to 4000  $\text{cm}^{-1}$ ) was collected with 32 scans and a resolution of 2  $\text{cm}^{-1}$ . Semisolid samples were measured using a FTIR spectrometer (IFS 28, Bruker Optik GmbH, Karlsruhe, Germany) equipped with an ATR attachment (Thermo Spectra Tech, Shelton, USA), a Fresnel ZnSe crystal (angle of incidence 45°, diameter 20 mm) and DTGS detector. Each spectrum (680 to 4000  $\text{cm}^{-1}$ ) was collected with 32 scans and a resolution of 2  $\text{cm}^{-1}$ .

### **3.4.6. Powder properties**

#### **3.4.6.1. Angle of repose**

Angle of repose was determined according to Carr's method [278]. A glass funnel with a pore diameter of 21 mm was used. The funnel was secured with its tip positioned at a fixed height (2 cm, **H**) above a sheet of paper. The powder was slowly poured through the funnel

until the apex of the pile reached the tip of the funnel. The angle of repose was calculated using the formula:

$$\tan \theta = \frac{H}{R}$$

Where  $\theta$  is the angle of repose and  $R$  is the radius of the formed pile. Results are expressed as mean,  $n = 5$ .

### 3.4.6.2. Bulk and tapped density

The bulk and tapped density were calculated according to the European Pharmacopeia method [279]. The bulk volume was assessed by pouring 10 g of the corresponding powder in 100 ml measuring cylinder. The tapped volume was measured using a Stampfvolumeter type STAV 2003 (J. Engelsmann AG, Ludwigshafen, Germany) applying 500 and 1250 taps. If the difference between the 2 obtained tapped volumes was less than 2 %, the volume corresponding to 1250 taps was considered as the tapped volume. Otherwise, the measurements were repeated in 1250 incremental taps steps until the difference between two successive measurements was less than 2 %.

### 3.4.6.3. Compressibility

The compressibility was evaluated according to the United States Pharmacopeia [280] and European Pharmacopeia [281] guidelines, expressed as Carr's compressibility index (CI) and Hausner ratio (HR). The following formulas were used for the calculations:

$$CI = 100 \times \left( \frac{V_{\text{bulk}} - V_{\text{tapped}}}{V_{\text{bulk}}} \right) \quad \& \quad HR = \frac{V_{\text{bulk}}}{V_{\text{tapped}}}$$

### 3.4.7. Preparation of the self-nanoemulsifying tablets

N5, N6 and N7 adsorbates were prepared as described in **Section 3.4.2.2** and mixed with the other excipients (**Table 14**) in a mortar using a pestle. The tablets were compressed on a single punch tableting machine (Korsch AG, Germany) using 11 mm concave punch with a compression pressure corresponding to 50 MPa. The tablets weight was 250 mg.

**Table 14** Composition of the prepared self-nanoemulsifying tablets (m %).

Code	Adsorbates (SNEDDS content)	Kollidon® 90 F	Kollidon® CL-SF	Final SNEDDS load
T1	90 (30)	0	10	27
T2	90 (30)	2.5	7.5	27
T3	90 (40)	0	10	36
T4	90 (40)	2.5	7.5	36
T5	90 (50)	0	10	45
T6	90 (50)	2.5	7.5	45

### **3.4.8. Characterization of the self-nanoemulsifying tablets**

#### **3.4.8.1. Optical microscopy**

The tablets shape and surface were evaluated using a stereomicroscope (SZX9, Olympus, Hamburg, Germany).

#### **3.4.8.2. Hardness**

Six tablets were tested for hardness using TBH-30 hardness tester (Erweka GmbH, Heusenstamm, Germany). Results are expressed as mean  $\pm$  SD.

#### **3.4.8.3. Thickness**

Ten tablets were tested for thickness using a digital micrometer. Results are expressed as mean  $\pm$  SD.

#### **3.4.8.4. Tensile strength**

The tensile strength was calculated according to the United States Pharmacopeia [282]. Results are expressed as mean  $\pm$  SD. For the flat tablets, the following equation was used:

$$\sigma_x = \frac{2F}{\pi DH}$$

For the convex tablets, the following formula was used:

$$\sigma_x = \frac{10F}{\pi D^2} \left[ \frac{2.84 H}{D} - \frac{0.126 H}{W} + \frac{3.15 W}{D} + 0.01 \right]^{-1}$$

Where  $\sigma_x$  is the tensile strength, **F** is the tablets breaking force, **D** is the tablets diameter, **H** is the tablets thickness and **W** is the central cylinder thickness (tablets wall height).

#### **3.4.8.5. Friability**

Ten tablets were dedusted, weighed and placed in the drum of a friability tester (VEB Arzneimittelwerk Dresden, Dresden, Germany). The drum was rotated 100 rotations at 25 rpm. The tablets were then removed and carefully dedusted. The weight loss in % was calculated.

#### **3.4.8.6. Disintegration time**

The disintegration time was determined using a preheated ( $37 \pm 1$  °C) end over end mixer rotated at 10 rpm. Two dispersion media were used: 0.1 N HCl and phosphate buffer pH 6.8 USP. The volume of the disintegration media was selected so that it allows 1 % m/V dispersion of SNEDDS in the chosen medium. The tablets were added to medium and their disintegration was visually checked every 30 s.

### **3.4.9. Droplet size distribution**

Progesterone-loaded and Progesterone-free semisolid SNEDDS, N7 adsorbates and T2 tablets were analyzed for droplet size distributions. One percent dispersions (m/V) of the

SNEDDS, adsorbates and tablets were prepared in 0.1 N HCl and phosphate buffer pH 6.8 USP. The dispersions were incubated in a preheated  $37\pm 1$  °C end over end mixer rotating at 10 rpm. After 2 h, samples were centrifuged at 12045 *g* for 5 min in an Eppendorf centrifuge (MiniSpin, Eppendorf AG, Hamburg, Germany) to separate the rest N-US2. The supernatant was measured at 37 °C as described in **Section 3.3.4.1**.

### **3.4.10. Benchtop nuclear magnetic resonance (BT-NMR)**

Five % m/V dispersions were prepared as described below in deuterated 0.1 N HCl and phosphate buffer pH 6.8 USP (prepared in D<sub>2</sub>O). After 60 min and 120 min, the whole dispersions were analyzed by BT-NMR as described in **Section 3.3.4.4** at 37 °C.

### **3.4.11. *In vitro* Progesterone release**

Progesterone was incorporated in the semisolid SNEDDS at a concentration of 15 mg/g. The *in vitro* release study of the Progesterone-loaded SNEDDS, N7 adsorbates and T2 tablets was performed in a preheated  $37\pm 1$  °C end over end mixer rotated at 10 rpm. The tested media were 0.1 N HCl, phosphate buffer pH 6.8, FaSSIF and FeSSIF. The volume of the dispersion media was selected so that it allows 1 % m/V dispersion of the SNEDDS in the selected medium. 200 µl samples were taken at regular time intervals and centrifuged at 12045 *g* for 5 min in an Eppendorf centrifuge (MiniSpin, Eppendorf AG, Hamburg, Germany). An aliquot of the supernatant was diluted with acetonitrile and centrifuged again for 5 minutes at 12045 *g*. The organic supernatant was filled into a vial for HPLC analysis. The HPLC analysis was performed as described in **Section 3.5.9**.

## **3.5. *In vitro* lipid digestion**

### **3.5.1. Used media**

Simulated intestinal fluids were composed of Sorensen's phosphate buffer pH 6.8 supplemented with sodium chloride, calcium chloride, bile extract and PL (**Table 15**) [215]. Several stock solutions were freshly prepared in distilled water and mixed just before use. The solutions were heated to 37 °C and the pH was adjusted thereafter to 6.8 with 0.1 N sodium hydroxide.

- **Sorensen's phosphate buffer pH 6.8** was composed of 35.6 mM potassium dihydrogen phosphate (4.85 g/L) and 31.1 mM disodium monohydrogen phosphate dihydrate (5.53 g/L).

- **BS-PL preconcentrate** was composed of a mixture of 7.5 mM porcine bile extract (30.43 g/l) and 30 mM Phospholipon<sup>®</sup> 90G (6.04 g/l). Phospholipon<sup>®</sup> 90G was dissolved in distilled water at 50 °C. Simultaneously, the bile extract was added. The mixture was stirred until a clear, brownish solution was obtained.
- **Sodium chloride** stock solution (4.5 M) was prepared by dissolving 26.3 g in 100 ml of distilled water.
- **Calcium chloride** stock solution (0.15 M) was prepared by dissolving 1.66 g of anhydrous calcium chloride in 100 ml of distilled water.
- **Porcine pancreatin** (450 U/ml) was used as an enzyme source.

**Table 15** Composition of the bio-relevant media.

	FaSSIF	FeSSIF
<b>Bile extract (mM)</b>	5	15
<b>Phospholipids (mM)</b>	1.25	3.75
<b>Sodium Chloride (mM)</b>	150	150
<b>Calcium chloride (mM)</b>	5	5
<b>Sorensen's phosphate buffer pH 6.8</b>	q.s.	q.s.
<b>Final pH corrected by 0.1 N NaOH to</b>	6.8	6.8

### 3.5.2. Preparation of the Cithrol<sup>®</sup> DPHS dispersions

Two methods were used to prepare DPHS dispersions: the Ultra-Turrax<sup>®</sup> method (UTM) and the solvent displacement method (SDM).

#### 3.5.2.1. Ultra-Turrax<sup>®</sup> method (UTM)

Molten DPHS was mixed with Sorensen's phosphate buffer pH 6.8 using a rotor-stator mixer (Ultra-Turrax<sup>®</sup> T18 basic, IKA, Staufen, Germany) operated at 24000 rpm for 5 min at room temperature.

#### 3.5.2.2. Solvent evaporation method (SDM)

Molten DPHS was dissolved in acetone to yield 10 % m/m solution. Double distilled water was heated to 50 °C. The organic solution was added dropwise using a syringe to the aqueous phase under agitation (1000 rpm). The produced milky emulsion was then allowed to reach the room temperature under agitation until all acetone was vaporized.

### 3.5.3. Particle size measurement

The droplet size distribution of DPHS dispersions was measured using static laser diffraction (Mastersizer 2000, Malvern Instruments, Worcestershire, U.K.). Samples were added until an

average laser obscuration of about 8 % was obtained. The refractive index was 1.45 and the absorption was 0.001. The stirrer speed was set to 1200 rpm without sonication.

### 3.5.4. pH-stat method

The digestion experiment was carried out under fasted and fed state conditions. One percent m/V dispersions of each excipient or semisolid SNEDDS were prepared in 15 ml FaSSIF or FeSSIF media. In the case of DPHS dispersions, their volumes were deducted from the contribution of buffer volume to the respective media. The respective medium was heated to  $37\pm 1$  °C in a water bath and stirred at 700 rpm. The temperature was maintained constant during the experiment using a thermocouple. For the blank samples, lipids were replaced by a respective volume of Sorensen's phosphate buffer pH 6.8. A pH electrode connected to an autotitrator (DL 21, Mettler Toledo, Giessen, Germany) was placed into the liquid (**Fig. 7**). The start pH was adjusted to 6.8. The digestion was initiated by the addition of pancreatin powder equivalent to 450 U/ml of pancreatic lipase activity. The autotitrator kept the pH constant at 6.8 throughout the experiment by adding 0.1 M sodium hydroxide (Titrisol®). The cumulative consumption of sodium hydroxide was recorded over 120 min [277].

### 3.5.5. Back titration method

The pH-stat titration was performed as described in **Section 3.5.4** for 120 min. At the end of the titration process, the pH was raised from 6.8 to 9 and the required volume of sodium hydroxide was recorded.

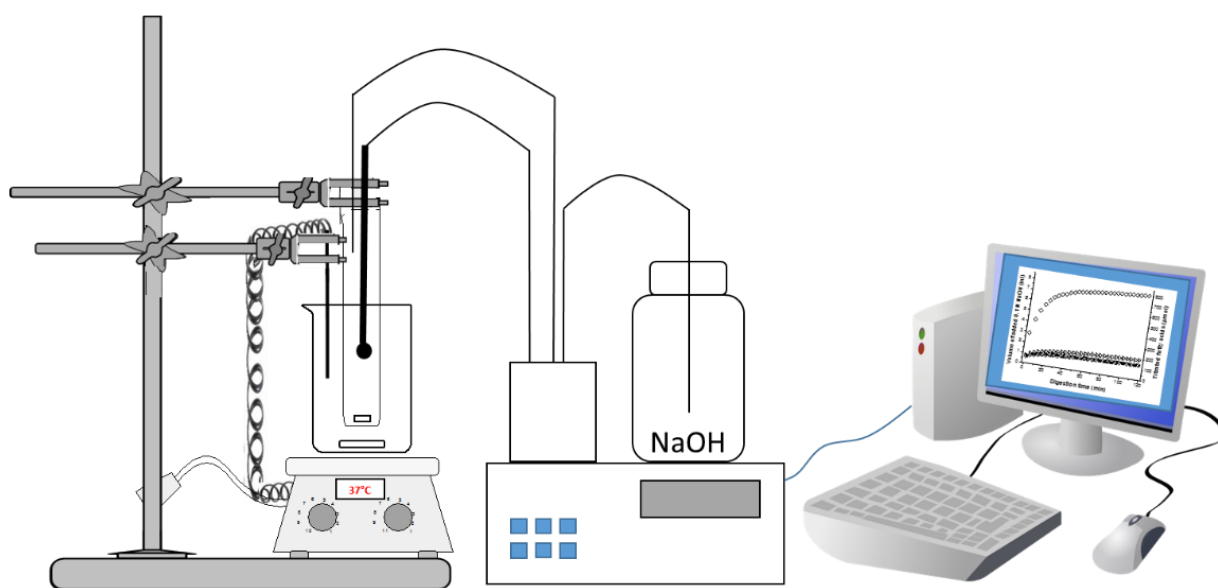


**Fig. 7** Schematic representation of the pH-stat titration method.

### 3.5.6. Lipid analysis by high-performance thin layer chromatography (HPTLC) combined with spectrodensitometry

The pH-stat titration was performed as described in **Section 3.5.4**. At a predetermined time schedule, 100  $\mu\text{l}$  samples were withdrawn and diluted with 900  $\mu\text{l}$  of a chloroform and methanol (1:1 V/V) mixture. The organic mixture stops the enzymatic reaction and causes the precipitation of the enzymes. The mixture was then centrifuged at 12045  $g$  for 10 min in an Eppendorf centrifuge (MiniSpin, Eppendorf AG, Hamburg, Germany) and the supernatant was filled into glass vials and stored in the dark at  $-20\text{ }^{\circ}\text{C}$  for further investigation.

The HPTLC analysis was performed according to [275, 283-285]. 12-hydroxystearic acid (12-HSA) standard solutions were prepared in chloroform and methanol (1:1 V/V) mixture. Samples and standards were separated simultaneously on each plate to avoid inter-assay variations. Standard 12-HSA solutions corresponding to 0.1-2  $\mu\text{g}$  were applied together with 10  $\mu\text{l}$  of samples on silica gel plates (HPTLC Silica gel 60, Merck, Darmstadt, Germany) using an Automatic TLC Sampler 4 (CAMAG, Muttenz, Switzerland). The separation was performed by HPTLC (AMD 2, CAMAG, Muttenz, Switzerland) employing an 11-step gradient based on hexane and ethyl acetate (**Table 16**). Subsequently, the plates were submerged in a copper sulfate solution (15 % copper sulfate pentahydrate, 8 % phosphoric acid (85 % m/V) and 5 % methanol) for 20 s. Residual liquid was removed and the plates were heated in an oven at  $150\text{ }^{\circ}\text{C}$  for 20 min. The stained spots on the plate were quantified by spectrodensitometry at 675 nm (CAMAG TLC Scanner 3, CAMAG, Muttenz, Switzerland). The optical densities were converted into masses using a calibration curve.

**Table 16** The HPTLC gradient that was used for the separation of long chain lipids [285].

Step	Migration distance (mm)	Hexane (% V/V)	Ethyl acetate (% V/V)
1	20.0	70	30
2	25.1	73	27
3	30.2	76	24
4	35.3	79	21
5	40.4	82	18
6	45.5	85	15
7	50.6	88	12
8	55.7	91	9
9	60.8	94	6
10	65.9	97	3
11	71.0	100	0



### **3.5.7. Possible drug precipitation during digestion**

Progesterone was incorporated at 70 % of its saturation solubility in the semisolid SNEDDS (34 mg/g F1; 38.4 mg/g F2; 45.2 mg/g F3) in order to maintain a constant thermodynamic activity across all formulations. Progesterone was dissolved in the molten SNEDDS at 50 °C. Progesterone-loaded SNEDDS were cooled down to room temperature and allowed to equilibrate for 24 h prior to the digestion study. The semisolid SNEDDS were accurately weighed into sealed glass tubes. Then the freshly prepared FaSSIF or FeSSIF was added. One percent m/V was allowed to disperse prior to initiation of digestion in an end over end mixer rotating at a rate of 10 rpm at 37±1 °C. A dispersion volume of 7.5 ml was used in all experiments. The digestion was initiated by the addition of pancreatin powder equivalent to 450 U/ml of pancreatic lipase activity. 200 µl samples were withdrawn at regular time intervals and centrifuged at 12045 *g* for 5 min in an Eppendorf centrifuge (MiniSpin, Eppendorf AG, Hamburg, Germany) in order to separate the micellar phase from, precipitated drug, calcium salts of FA and precipitated parts of pancreatin. An aliquot of the supernatant was diluted with acetonitrile and centrifuged again for 5 min at 12045 *g*. The organic supernatant was filled into a vial for HPLC analysis (**Section 3.5.9**).

### **3.5.8. Effect of digestion on the drug release from adsorbates and tablets**

The release study was performed in both FaSSIF and FeSSIF media as described in **Section 3.4.11**. The digestion was started by the addition of pancreatin powder equivalent to 450 U/ml of pancreatic lipase activity and assessed as described above.

### **3.5.9. HPLC method**

The HPLC system consisted of a Jasco model PU-1580 pump equipped with LG-1580-04 quaternary gradient unit, degasser, AS 1559 intelligent autosampler, UV 1559 intelligent UV/VIS detector. Purospher® Star RP-18 endcapped (5 µm) column (Merck, Darmstadt, Germany) was used as an analytical column. Acetonitrile and double distilled water in a ratio 70:30 V/V were used as the mobile phase at a flow rate of 1 mL/min. The oven temperature was adjusted to 40 °C. Standard Progesterone solutions (5-250 µg/mL) were prepared in acetonitrile. 10 µl were injected and the column effluent was monitored at a wavelength of 240 nm. The retention time for Progesterone was found to be 3.9 min.

### **3.5.10. Statistical analysis**

Unless otherwise stated, results are represented as mean ± SD (n=3). F-test was performed to check if the samples have equal variance. Significance between the mean values was tested using Student's t-test. Probability values  $P < 0.05$  were considered statistically significant.

## 4. Results and discussion

### 4.1. Preliminary experiments

The inclusion of the SNEDDS as a liquid in soft gelatin capsules is associated with several drawbacks such as the interaction with the capsule shell, instability, higher production cost and possible PWSD precipitation [177-180]. Therefore, alternative formulation strategies, e.g. the inclusion of SNEDDS into solid or semisolid dosage forms, are desirable; nevertheless, very challenging because the self-nanoemulsifying properties are difficult to be obtained with solid excipients. Several approaches were developed to produce S-SNEDDS. Among them, the inclusion of polymeric excipients and the use of the solid/semisolid lipids offer higher PWSD load compared to the adsorption onto porous carrier. Ideal SNEDDS should conform to the following criteria: (a) Semisolid or solid consistency at room temperature. (b) pH-independent self-nanoemulsification upon mild agitation at 37 °C. (c) High lipid mobility after dilution at physiological conditions. (d) High shelf-life stability due to the avoidance of the unsaturated lipid excipients. (e) Less PWSDs precipitation due to the avoidance of co-solvents as well as high content of long chain lipids.

#### 4.1.1. Inclusion of 10 % m/m of polymeric excipients

The inclusion of a small amount of polymeric excipients could be useful in the solidification of the liquid/semisolid SNEDDS. Semisolid SNEDDS require less content of the polymeric excipient because they have rather higher solid properties than liquid ones. The solidified formulations could be molded into tablet-like cylinders to be filled into hard gelatin capsule. Alternatively, the solidified lipids could be transformed into powder using cryogenic grinding [209], melt granulation [210] or spray cooling [203, 211]. The produced powder could be filled in the hard gelatin capsules or compressed into tablets. The possible advantages of this approach, compared to the corresponding liquid/semisolid SNEDDS, include the higher stability, less interaction with the capsule shell and less sensitivity to temperature change. This approach is valid for the pharmaceutical industry and has the advantages of the higher SNEDDS/PWSD load compared to other methods that solidify SNEDDS using the adsorption on an inert carrier.

A semisolid SEDDS was selected as reference formulation [181]. The formulation is composed of 50 % m/m Solutol<sup>®</sup> HS 15, the old name of Kolliphor<sup>®</sup> HS 15, as a more hydrophilic amphiphile and 50 % m/m Cithrol<sup>®</sup> GMS 40 as a more lipophilic amphiphile. The formulation was successfully loaded (40 % m/m) on MCC and was formulated as pellets. MCC

is the golden standard of pellets preparation using extrusion/spheronization. However, MCC pellets do not disintegrate and accordingly, the PWSD release occurs by diffusion through inert, insoluble matrix. Therefore, the incomplete release of PWSDs is always associated with MCC pellets. Moreover, drug adsorption to MCC and decomposition of some drugs in the presence of MCC were reported [286-289]. In an attempt to increase the self-emulsifying lipid load up to 90 % and avoid limitations derived by the MCC incorporation, various formulations (P1 – P8) were prepared (**Table S2** of the supplementary data). In all formulations, Sudan III was incorporated as a PWSD model with a Log P of 5.737 [290]. The use of Sudan III as a drug model offers the advantage that drug release and formulation dispersibility can be qualitatively judged visually.

All formulations were solid at room temperature and retained their tablet-like shape after the ejection from the molding machine (**Fig. 3**). P5 – P8 showed a little degree of punch stickiness, which might be avoided by the increase of the relative amount of the polymeric excipients. Low molecular weight PEG is often used as a co-solvent in the SNEDDS preparation. Furthermore, high molecular weight PEG was tested as a solidification aid for liquid SNEDDS at a level of 30-40 % m/m [206-208]. Incorporation of PEG (10 %) with different molecular weights (P1 – P4) in the semisolid formulation resulted in S-SEDDS with proper self-emulsification rate and extent. Drug release was comparable to the parent formulation. However, the release rate was slower. About 50 % of the mass was dispersed within the first 2 h and ~10 % remained undispersed after 24 h. The release did not seem to be pH-dependent and minor difference between formulations in Sudan III release could be observed (**Fig. S1** of the supplementary data).

Cellulose ethers such as Hydroxyethyl Cellulose (HEC) and Hydroxypropyl Methylcellulose (HPMC) are widely used as a gelling and thickening agent. They were reported to increase the release rate of PWSDs from capsule by hydrophilization [291, 292]. Furthermore, they maintain a metastable supersaturation state of the PWSDs. Consequently, they were used in SNEDDS as precipitations inhibitors [293]. Two formulations were prepared with 10 % of low (P5) and high (P6) viscosity grade HEC. The dispersion rate of both formulation was superior to PEG formulations (P1 – P4) with about 50 % of the mass emulsified within the first 0.5 h. The initial dispersion rate of P6 was higher than P5. However, P5 showed less turbid, complete dispersions within the first 3 h. Moreover, P5 showed a higher initial dispersibility in the acidic pH. P5 and P6 dispersions in phosphate buffer were more turbid than in 0.1 N HCl.

Two formulations were prepared with 10 % of low (P7) or high (P8) viscosity grade HPMC. The dispersion rate of both formulations was superior to PEG formulation but slower than HEC ones. About 50 % of the mass was emulsified within the first 1 h. Similar to HEC formulations, the initial dispersion rate was faster in the case of the higher viscosity grade HPMC (P8); nevertheless, in the buffer medium. The dispersions of the lower viscosity grade were less turbid than the higher viscosity ones.

### 4.1.2. Screening of selected solid and semisolid lipid excipients

The use of solid/semisolid excipients to prepare S-SNEDDS is not trivial. The excipient selection is usually based on their solid properties, miscibility, melting points, toxicity, drug solubility and HLB values. However, the performance and dispersibility of the different combinations are difficult to predict, especially for those with high melting point. Combinations of solid, semisolid and liquid amphiphiles were prepared and screened for their dispersibility (**Table S3 - Table S5** of the supplementary data). The solid amphiphiles include Soluplus<sup>®</sup>, Arlacel<sup>®</sup> LC and Cithrol<sup>®</sup> GMS 40 (GMS). The semisolid amphiphiles include Cithrol<sup>®</sup> DPHS (DPHS) and Kolliphor<sup>®</sup> HS 15 (HS15). The liquid amphiphiles include Capmul<sup>®</sup> MCM (MCM) and Captex<sup>®</sup> 355 EP/NF. The selection of these excipients was based on their physical properties, lack of unsaturation, novelty, toxicity profile, miscibility, and potential advantages in the SNEDDS development.

#### 4.1.2.1. Formulations containing Soluplus<sup>®</sup>

Soluplus<sup>®</sup> is a relatively new excipient, which was developed for the melt extrusion [294-298]. It consists of polyvinyl caprolactam-polyvinyl acetate-polyethylene glycol graft copolymer. It has a strong solid character and amphiphilic properties. Soluplus<sup>®</sup> can enhance the solubility of PWSDs by forming solid dispersions as well as by micellar solutions [299-306]. Moreover, Soluplus<sup>®</sup> was investigated as a precipitation inhibitor in supersaturable SNEDDS [49, 307]. However, its potential use as a more hydrophilic amphiphile in SNEDDS formulation was scarcely explored.

Soluplus<sup>®</sup> was screened as a hydrophilic amphiphile in the proposed self-emulsifying formulations (P9 – P25). The composition of the proposed Soluplus<sup>®</sup> formulations and their physical characteristics are summarized in **Table S3** of the supplementary data.

Formulations of Soluplus<sup>®</sup> with GMS (P9 and P10) had a solid consistency and could be molded into a tablet-like dosage form. However, a very slow dispersion rate was observed. The produced mass did not disperse over 24 h, which is too long for a meaningful oral administration (**Fig. S2** of the supplementary data). GMS is a solid long chain MG with low polarity and high

melting temperature (~60 °C). Therefore, its combination with Soluplus<sup>®</sup> has lower polarity and strong solid character. This could be the cause of the very slow dispersibility. Increasing Soluplus<sup>®</sup> content (P2) slightly promoted the 24 h dispersibility. Incorporation of 10 % PEG with different molecular weight in the formulation (P11 – P14) promoted Sudan III release via pore formation in the solid mass. However, the release was medium-dependent and a higher Sudan III release was observed in the acidic medium (**Fig. S3** of the supplementary data). The molecular weight of PEG affected the extent of Sudan III release. Lower molecular weight PEG dissolve faster than higher molecular weight ones. Accordingly, they promoted the initial Sudan III release within the first 3 h. However, the extent of Sudan III release was more or less the same after 24 h because of the fixed amount of PEG in the formulation.

Several approaches were evaluated in order to enhance the dispersibility of Soluplus<sup>®</sup> formulations. The first approach was to substitute GMS with a 1:1 mixture of liquid medium chain lipids (Captex<sup>®</sup> 355 and MCM) (P15 – P17). This approach reduces the melting point and modulates the polarity of the formulation. However, the presence of the liquid lipids adversely affected the solid properties of the formulations. At least 65 % of Soluplus<sup>®</sup> was required to achieve a solid formulation. The formulations did not show any enhancement in Sudan III release within the first 4 h compared to GMS formulations. However, the extent of Sudan III release was significantly higher than that of GMS formulations after 24 h (**Fig. S2** right vs. left of the supplementary data). Variation in the Soluplus<sup>®</sup> content did not pronouncedly enhance the dispersibility.

The second approach to improve the dispersibility of Soluplus<sup>®</sup> formulations was to substitute Soluplus<sup>®</sup> partially with a semisolid hydrophilic amphiphile such as HS15 (P18 – P25). HS15 has a semisolid consistency, lower melting point and nearly the same HLB value of Soluplus<sup>®</sup>. The produced formulation (P18) retained the solid characteristics and showed an enhanced dispersibility (**Fig. S4** of the supplementary data), compared to the parent formulation (P9) (**Fig. S2** of the supplementary data). However, the dispersibility rate was lower than a semisolid formulation [181] consisting of only GMS and HS15.

The third approach was to increase the polarity of the formulation. Accordingly, the content of the hydrophilic excipients was increased on the favor of the lipophilic one (P19 and P20). The formulations kept the solid character to a certain extent. Nevertheless, the dispersibility did not improve (compared to P18 formulation), especially with higher Soluplus<sup>®</sup> content (**Fig. S4** of the supplementary data). Formulations (P21 – P25) represent a combination of the aforementioned approaches. It was found that increasing the Soluplus<sup>®</sup> content in the

formulation contributes to the solid properties of the formulation. Nonetheless, higher Soluplus<sup>®</sup> content is always associated with retarded and incomplete dispersibility.

#### 4.1.2.2. Formulations containing Arlcel<sup>®</sup> LC

Arlcel<sup>®</sup> LC, formerly Arlatone<sup>®</sup> LC, is a 1:1 mixture of sorbitan stearate (HLB 4.7) and sorbityl laurate (HLB 8.6). Arlcel<sup>®</sup> LC is an O/W emulsifier that stabilizes emulsions through the formation of hydrosomes (lamellar LC network) [308]. The composition of the proposed Arlcel<sup>®</sup> LC formulations and their physical characteristics are summarized in **Table S4** of the supplementary data. Although Arlcel<sup>®</sup> LC is composed of a mixture of amphiphiles, Arlcel<sup>®</sup> LC alone (P26) was very slightly dispersible in phosphate buffer pH 6.8 and was non-dispersible in 0.1 N HCl (**Fig. S5** of the supplementary data). Arlcel<sup>®</sup> LC combination with either GMS (P27) or Captex<sup>®</sup> 355/MCM mixture (P28) showed a pH-dependent dispersibility. Both formulations were dispersible only in phosphate buffer pH 6.8 and no dispersibility was observed in 0.1 N HCl medium. P28 formed a stable dispersion in the buffer medium within 10 min while P27 showed slower dispersibility with about 50 % of the mass emulsified within the first 2 h (**Fig. S5** of the supplementary data).

Formulation of Arlcel<sup>®</sup> LC with HS15 (P29) was semisolid. However, it was too soft to retain the tablet-like shape. In contrast to other Arlcel<sup>®</sup> LC formulations, it showed fast, pH-independent dispersibility in both dispersion media due to its relatively higher polarity (**Fig. S5** of the supplementary data). Formulation of Arlcel<sup>®</sup> LC with Soluplus<sup>®</sup> (P30) has showed pH-dependent dispersibility. Complete fine dispersion was observed in 0.1 N HCl medium while coarse incomplete dispersion was obtained in phosphate buffer. About 90 % of the mass remained undispersed after the first 4 h and more than 30 % remained undispersed after 24 h. The incomplete dispersibility of Soluplus<sup>®</sup>/Arlcel<sup>®</sup> LC formulation was improved by incorporation of HS15 in the formulation (P31) with about 50 % of the mass emulsified within the first 3 hr. However, coarse dispersions were still observed in the buffer medium (**Fig. S5** of the supplementary data).

Since the formulation of Arlcel<sup>®</sup> LC and HS15 has showed a pH-independent dispersibility and was too soft to retain the tablet-like shape, GMS was incorporated in the formulation in different concentration (P32 – P36). The purpose of the GMS incorporation was to increase the solid properties of the formulation and to prepare formulations with different polarities. At least 30 % GMS was required to obtain solid formulation (**Table S4** of the supplementary data). However, the semisolid formulation (P32, 20 % GMS) was also able to retain the tablet-like shape. Increasing the GMS content reduced the formulations polarity with a consequent

decrease in their dispersibility. Formulations with lower GMS content (P32 and P33) showed a higher degree of Sudan III release in both media than those of higher GMS content (P34 – P36). However, coarse particles that remained undispersed for 24 h were developed during the dispersion. P34 (50 % GMS) showed lower release in phosphate buffer compared to 0.1 N HCl. Formulations with higher GMS content (P35 and P36) showed incomplete dispersibility in both media with more than 75 % of the tablet-like mass remained non-dispersed for more than 24 h.

### 4.1.2.3. Formulations containing Cithrol<sup>®</sup> DPHS

Cithrol<sup>®</sup> DPHS (DPHS), formerly Arlacel<sup>®</sup> P135, (PEG-30-dipolyhydroxystearate) is a polymeric W/O emulsifier with HLB value of 5.5. DPHS is a polyester-polyether-polyester ABA block copolymer. The middle chain B is poly(ethylene oxide) while the two tails A are poly(12-HSA) [309]. Different combinations of DPHS along with other hydrophilic and lipophilic excipients were prepared (**Table S5** of the supplementary data) and screened for their dispersibility and drug release. Formulations of DPHS (as a lipophilic amphiphile) with Soluplus<sup>®</sup> (P37) or HS15 (P38) (as hydrophilic ones) were non-dispersible over 24 h. Combination between DPHS/GMS as lipophilic amphiphiles and HS15/Soluplus<sup>®</sup> as hydrophilic ones (P39) had a rubbery consistency. Incorporation of GMS successfully promoted the formulation dispersibility. However, incomplete, milky dispersions were produced in both media. Therefore, it was concluded that incorporation of a monoglyceride (MG) in the formulation might be necessary for the self-emulsifying process. The MG may act as a co-surfactant and promote the dispersibility of the formulations. Accordingly, two MG were evaluated: GMS (solid, long chain) and MCM (liquid, middle chain).

DPHS/GMS formulations (P40 – P50) were semisolid. The formulations became softer with the increase of the HS15 content relative to the lipophilic excipients. All formulations provided a turbid, milky and pH-independent dispersions within 1-3 h. The dispersion rate and the turbidity of the produced dispersions were a function of both HS15 content as well as the DPHS/GMS ratio. Faster dispersion rate and lower turbidity were observed with higher content of HS15 and DPHS: GMS ratio close to 1. However, even with a relatively high HS15 content (P50, 80 %), a reasonable amount of the droplets were in the micro-size range. Therefore, the solid MG was substituted with a liquid one.

Compared to the long chain MG, the middle chain ones have a higher flexibility at the interfacial film, which is a crucial requirement for the production of the nanoemulsions [89]. All formulations (P51 – P55) were semisolid at room temperature. The production of nanoemulsions and the pH-independent dispersibility were found to be dependent on the ratio

of DPHS: MCM. Furthermore, formulations containing Soluplus<sup>®</sup> (P39, P54 and P55) have shown pH-dependent dispersibility. Nanoemulsions were produced in double distilled water and 0.1 N HCl whereas coarse dispersions were produced in the buffer media.

## **4.2. Formulation and characterization of the semisolid SNEDDS**

### **4.2.1. Selection of an excipient combination**

Based on the results of the preliminary screening, combinations of DPHS, HS15 and MCM were able to produce SNEDDS. However, the composition should be optimized to ensure fast, pH-independent dispersibility. Other formulations have either produced coarse dispersions or showed pH-dependent dispersibility. DPHS offers some advantages that enable it to be a good candidate for SNEDDS. However, its potential use as a lipophilic excipient in SNEDDS was not yet explored. The proposed advantages include:

- (a) DPHS is semisolid at room temperature. Semisolid formulations have higher viscosity than the liquid ones. Therefore, they usually afford higher drug stability and better handling [93].
- (b) DPHS is a saturated long chain lipid. Saturated lipids are more resistant to oxidation offering longer shelf-life stability than the unsaturated ones while long chain lipids are known to enhance the lymphatic uptake of the accompanied PWSDs. Therefore, the accompanied PWSDs may avoid the first pass metabolism [93]. Furthermore, the digestion products of long chain lipids are able to pronouncedly enhance the solubilization capacity of the bile mixed micelles [47].
- (c) The polymeric nature and the interfacial packing of DPHS enable the manufacture of very stable emulsions at low DPHS content in the presence of additives that are incompatible with traditional W/O emulsifier systems [309]. DPHS has been used to prepare stable semisolid multiple W/O/W emulsions [310-315].
- (d) DPHS is a non-ionic, high molecular weight amphiphile. A published report from the European Food Safety Authority in 2004 [316] demonstrates DPHS safety based on the safety of its starting substances (PEG and 12-HSA) and its average molecular weight (> 5000 D). Furthermore, the Committee for Veterinary Medicinal Products [316] has demonstrated that PEG stearates with 8-40 ethylene oxide units are considered of low oral toxicity. The acute oral median lethal dose (rats) of DPHS is estimated to be more than 2000 mg/kg [317].

HS15, formerly known as Solutol<sup>®</sup> HS 15, is a non-ionic amphiphile that has proved its potential usefulness for drug delivery and possesses a low toxicity [318, 319]. HS15 consists of



a mixture of ~70 % PEG ME and DE of 12-HSA and ~30 % PEG. The HLB is about 15 and the critical micelle concentration is 0.005-0.02 % [86, 320]. MCM is a medium chain MG and DG. It is widely used as a lipophilic excipient in the SNEDDS formulations with HLB value of 4.7.

#### 4.2.2. Pseudo-ternary phase diagrams

Pseudo-ternary phase diagrams are constructed to identify nanoemulsion regions and accordingly the suitable ratios between hydrophobic and hydrophilic amphiphiles. Many studies in the literature describe pseudo-ternary phase diagrams at ambient temperature. However, the mobility and dispersion characteristics of lipid molecules are very sensitive to temperature [321]. The aim of this study is to prepare SNEDDS that are semisolid or solid at room temperature, but have high molecular mobility and kinetic stability at body temperature. Therefore, all experiments were performed at body temperature.

In order to identify and optimize the nanoemulsifying range, different combinations of DPHS, MCM and HS15 (**Table 9**) were prepared. The physical state of these combinations is represented in **Fig. 8**. All DPHS/HS15 combinations (M1 – M4) were semisolid at room temperature. Combinations of HS15 and 1:1 DPHS: MCM (M5 – M15) were liquid at lower HS15 contents. After storage at room temperature for several months, phase separation was observed. At least 40 % m/m of HS15 was required to develop semisolid formulations with 1:1 DPHS: MCM. Increasing DPHS to MCM ratios (M16 – M35) resulted in semisolid formulations, regardless of the HS15 amounts. At 20 % DPHS, the variation of HS15: MCM ratio (M36 – M38) resulted in liquid formulations that did not exhibit phase separation.

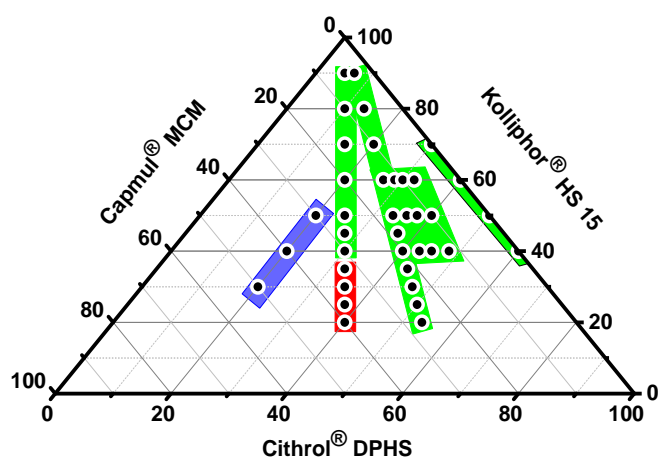


**Fig. 8** Physical state of the different combinations of Kolliphor® HS 15, Cithrol® DPHS and Capmul® MCM after equilibration at 23 °C. The green zone represents semisolid state. The blue zone represents liquid state without any phase separation. The red zone represents liquid state with phase separation.

**Fig. 9** illustrates the pseudo-ternary phase diagrams of 1 % m/V dispersions obtained in different media. The phase diagrams are divided into 3 distinct regions: (a) region, in which

phase separation was observed or dispersions with rather large droplet sizes were obtained, (b) region with a milky dispersions and (c) the isotropic nanoemulsions region. Examples of optical microscopic images of selected dispersions in the three mentioned regions are shown in **Fig. 10**. Although both DPHS and HS15 has an amphiphilic property, their combinations (M1 – M4) were not found to be self-emulsifying over 24 h. The presence of MCM was essential for the self-nanoemulsification, even in a small concentration. At lower HS15 concentration (below 60 %), the process of self-nanoemulsification was sensitive to the ionic strength and pH of the media. The self-nanodispersibility was superior in water and 0.1 N HCl compared to pH 6.8 buffer. However, above 60 % of HS15, this sensitivity was less pronounced. Therefore, at least 60 % of HS15 was found to be required to obtain transparent nanoemulsions in almost all media.

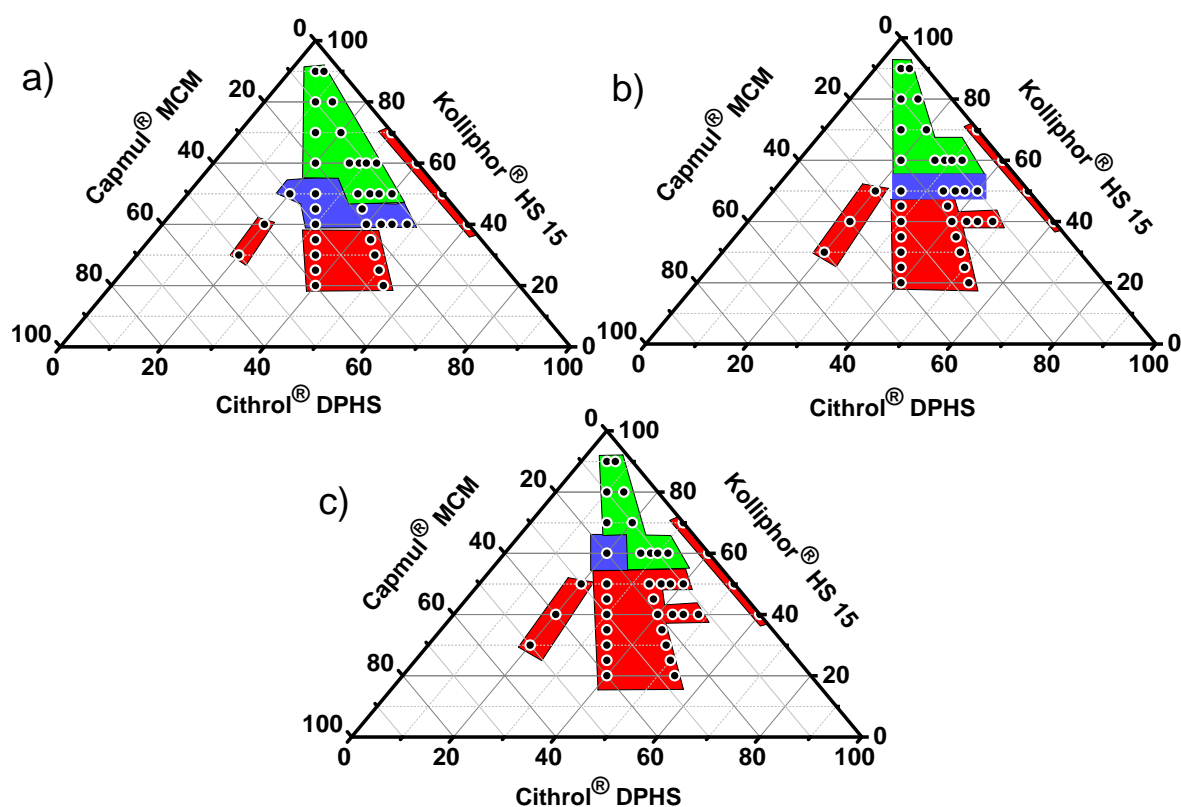


**Fig. 9** Pseudo-ternary phase diagrams of 1 % (m/V) dispersions of different combinations of Kolliphor® HS 15, Cithrol® DPHS and Capmul® MCM in (a) double distilled water, (b) 0.1 N HCl and (c) phosphate buffer pH 6.8 at 37 °C. The green zone represents the nanoemulsions region. The blue zone represents the milky dispersions. The red zone represents no dispersion or dispersions with very large droplet size. The value of 100 in the phase diagrams represents 1 % (m/V) of the dispersion.

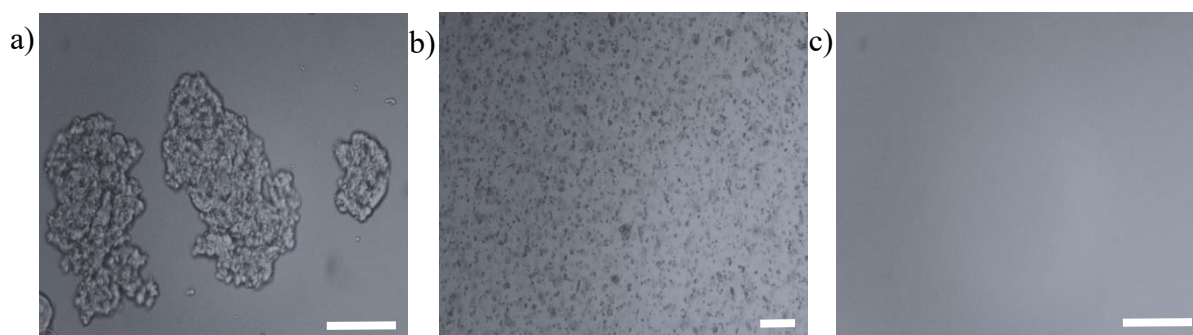


**Fig. 10** Optical microscopic images of selected dispersions in (a) the large droplets size region or no dispersion region, (b) the milky dispersions region and (c) the nanoemulsions region of the pseudo-ternary phase diagrams. The bar represents 100  $\mu\text{m}$ .

Lower amounts of MCM resulted in a slower kinetics of self-nanoemulsification (minutes to hours) while higher amounts resulted in pH- (or ionic strength-) dependent dispersibility as well as the formation of more coarse and unstable dispersions. Substitution of MCM (liquid) with Capmul<sup>®</sup> MCM C10 (solid) did not alter the overall consistency but did result in dispersions with an increased turbidity. Formulations with a DPHS: MCM ratio of 2:1 were optimal in terms of the self-nanoemulsification rate, sensitivity to pH and ionic strength and stability. Increasing the DPHS: MCM ratio to 4:1 or even 5:1 gave SNEDDS with slower self-nanoemulsification rates (in terms of hours). The increase in the viscosity of the more lipophilic part and its semisolid properties accompanied with the increase of DPHS ratio relative to MCM can be attributed to this effect.

#### 4.2.3. Effect of dilution

After oral administration, the GI fluids will dilute the SNEDDS. The degree of dilution and the local pH might be highly variable *in vivo*. Therefore, it is important to mirror the *in vivo* situation by *in vitro* tests. **Fig. 11** demonstrates the effect of dilution on the appearance of the corresponding emulsion. Although the proposed dilution test is not a good simulation to the physiological dilution, it helps us to understand what is happening to the formulation during the dilution and which composition gives stable dispersions upon dilution. Dilution by up to 20 % 0.1 N HCl yields single phase mixtures. The presence of DPHS supports the emulsification of a considerable high amount of water into the oil phase. Upon further dilution, the emulsion was inverted and an O/W emulsion was formed at higher HS15 concentrations. The stability of the formed nanoemulsions was found to be dependent on the HS15 level and DPHS: MCM ratio. At lower HS15 content, the formed emulsions can easily separate into two phases. Higher DPHS: MCM ratio (2:1) are more hydrophobic and were not able to accommodate more water

at lower contents of HS15. Therefore, phase separation was observed. At moderate level of HS15 (40-50 %), stable dispersions with large droplets were formed during dilution.

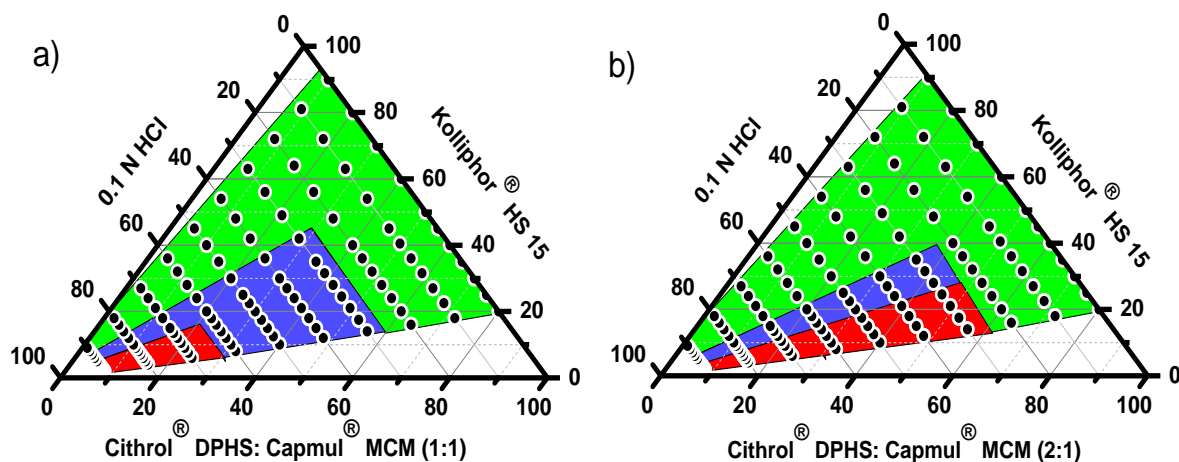


**Fig. 11** Effect of dilution on combinations prepared from Kolliphor® HS 15 and Cithrol® DPHS: Capmul® MCM (a) 1:1 and (b) 2:1 using 0.1 N HCl as a diluent. The green zone represents the one phase or nanoemulsions. The blue zone represents emulsions with large droplets size. The red zone represents 2 phases.

#### 4.2.4. Selection of formulations for further investigations

Based on the aforementioned results, three formulations (**Table 11**) were selected for further investigation. The HS15 content was kept constant at 60 % while the lipophilic part of the formulations was kept at 40 % with different DPHS: MCM ratios. All formulations are semisolid at room temperature (**Fig. 12**) and provided fine dispersions in the three tested media within few minutes (**Fig. 13**). An exception was noticed in the case of the 1 % (m/V) formulation F1 dispersion in phosphate buffer pH 6.8 that was milky at 37 °C (**Fig. 13c left**). A clear dispersion with low turbidity was obtained after this dispersion was cooled to room temperature.

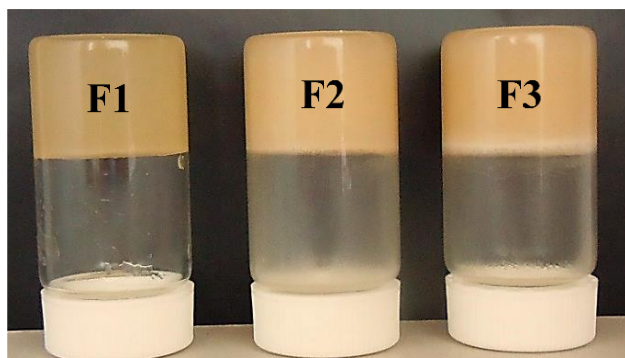


**Fig. 12** Photo of the semisolid SNEDDS after 24 h storage at 23 °C.

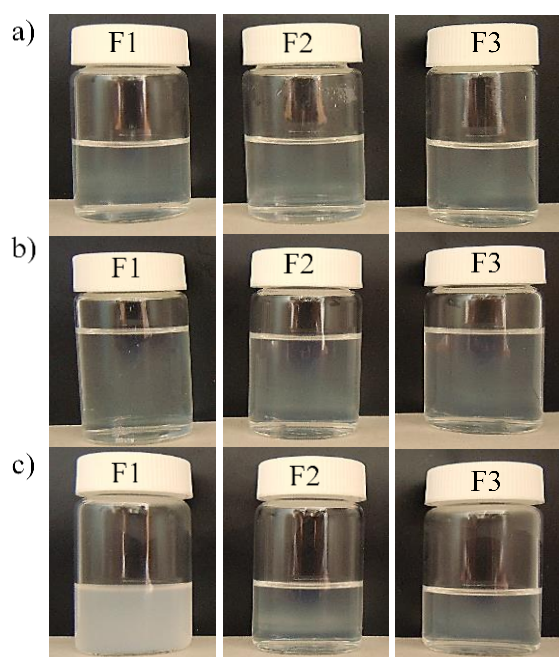


**Fig. 13** Photos of different 1 % (m/V) dispersions of F1, F2 and F3 semisolid SNEDDS in (a) double distilled water, (b) 0.1 N HCl and (c) phosphate buffer pH 6.8 after incubation in an end over end mixer at 37 °C.

#### 4.2.5. Characterization of the selected semisolid SNEDDS

##### 4.2.5.1. Droplet size distribution

One percent dispersions (m/V) of the semisolid SNEDDS and HS15 in different media were incubated in an end over end mixer at  $37 \pm 1$  °C and the formed nanoemulsions were evaluated for the droplet size distribution (Table 17).

**Table 17** Average droplet size diameter of the Kolliphor® HS 15 micelles and the nanoemulsions produced by 1 % (m/V) dispersions of the semisolid SNEDDS in different media measured by dynamic light scattering at 37 °C (mean, n=3).

Formulation / excipient	Double distilled water		0.1 N HCl		Phosphate buffer pH 6.8	
	Z-average (nm)	PDI	Z-average (nm)	PDI	Z-average (nm)	PDI
Kolliphor® HS 15	12.5	0.033	12.7	0.021	11.1	0.022
F1	25.1	0.166	75.3	0.277	NA <sup>a</sup>	NA <sup>a</sup>
F1 (filtered) <sup>b</sup>	27.0	0.145	69.5	0.250	41.3	0.238
F2	18.2	0.245	21.5	0.299	21.7	0.272
F2 (filtered) <sup>b</sup>	16.6	0.091	18.3	0.086	19.3	0.107
F3	19.9	0.334	21.7	0.334	20.5	0.310
F3 (filtered) <sup>b</sup>	17.2	0.179	17.4	0.121	16.9	0.070

<sup>a</sup> NA is not available. Sample was too polydisperse. As a result, data quality was too poor for cumulant analysis.

<sup>b</sup> 0.22 µm filter.

HS15 micelles showed a monomodal distribution with an average hydrodynamic diameter of 11-13 nm. Incorporation of more lipophilic excipients (DPHS and MCM) increased the hydrodynamic diameter. F1 dispersions showed a high degree of sensitivity towards the ionic

strength and pH of the dispersion media. It gave a milky dispersion in the buffer media, which was not suitable for PCS measurements due to the high degree of polydispersity. F2 and F3 formulations showed monomodal volume distributions in all media with an average hydrodynamic diameter of less than 25 nm. The effect of the ionic strength and pH on the particle size distribution of F2 and F3 nanoemulsions was minimal. Moreover, filtered nanoemulsions did not show a prominent change in the droplet size volume distribution (**Fig. 14**).

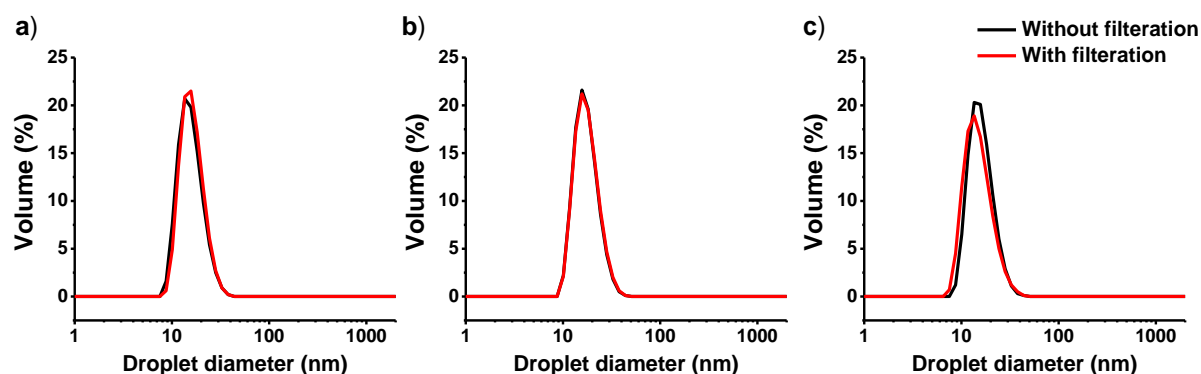


**Fig. 14** Droplet size volume distribution of 1 % (m/V) dispersion of the semisolid self-nanoemulsifying formulation F2 in (a) double distilled water, (b) 0.1 N HCl and (c) phosphate buffer pH 6.8 with or without filtration measured by dynamic light scattering at 37 °C.

#### 4.2.5.2. Percentage transmittance

In order to quantitatively evaluate the optical clarity of the formed nanodispersions, UV-visible spectrophotometer was used to measure the transmitted light at 650 nm. **Fig. 15** demonstrates the values of the percentage transmittance (%T) of 1 % (m/V) dispersions of the semisolid SNEDDS in different media. All dispersions were transparent (%T > 94 %) with the exception of that of F1 dispersions in phosphate buffer pH 6.8.

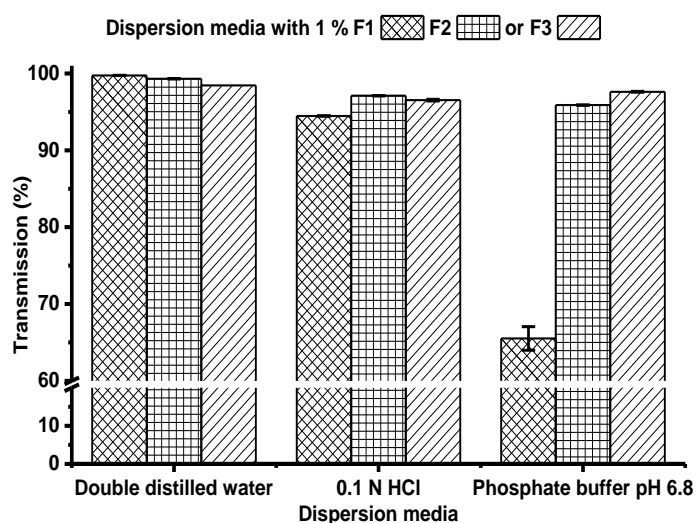


**Fig. 15** Percentage transmittance of 1 % m/V dispersions of the semisolid SNEDDS in different media at 650 nm (mean  $\pm$  SD, n=3).

#### 4.2.5.3. Differential scanning calorimetry (DSC)

To examine the thermal behavior and the possible excipients interactions, DSC measurements were performed on the single excipients, excipient combinations as well as the semisolid SNEDDS (**Fig. 16**). The melting endotherm of DPHS was above the body temperature. HS15, being a mixture of two main components (free PEG and PEG esters), showed two melting endotherms. MCM showed a very broad melting endotherm, which is typical for lipids mixtures. The DSC study indicated an interaction between the the most lipophilic components of the formulations (DPHS and MCM) with a shift of the DPHS melting endotherm towards the MCM melting range. MCM is probably capable of dissolving DPHS in a ratio of 1:1 and 1:2 and to a certain extent in a ratio of 1:3. This points towards the importance of MCM in the formulations and may explain the slower dispersibility observed with decreasing MCM content. Furthermore, the enhancement of the mobility of the mixture compared to DPHS alone at body temperature is expected. A similar pattern was observed between MCM and HS15. On the other hand, the interaction between HS15 and DPHS was not pronounced.

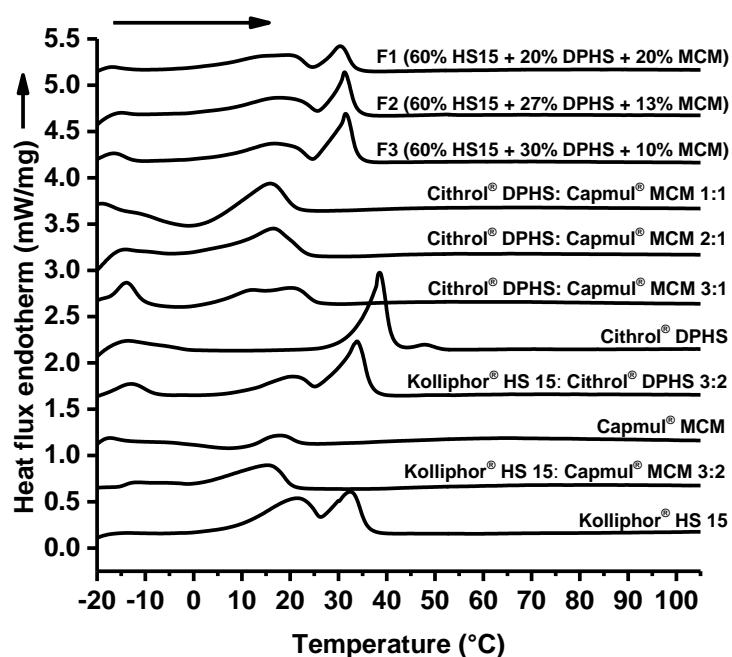


**Fig. 16** Heating DSC thermograms of excipients, excipient combinations and the semisolid SNEDDS.

All semisolid SNEDDS showed a melting endotherm above the room temperature and below 37 °C with a very slight positive shift in the melting endotherm with the increase of the DPHS content in the formulation. Accordingly, all formulations are expected to be highly mobile at body temperature. F2 formulation showed a peak melting endotherm at about 31.5 °C. The second heating cycle showed a very broad melting endotherm and a shifting of the peak melting temperature to about 27.2 °C and crystallization exotherm at about 12.1 °C (**Fig. 17**). The third heating cycle was overlaying the second heating one.

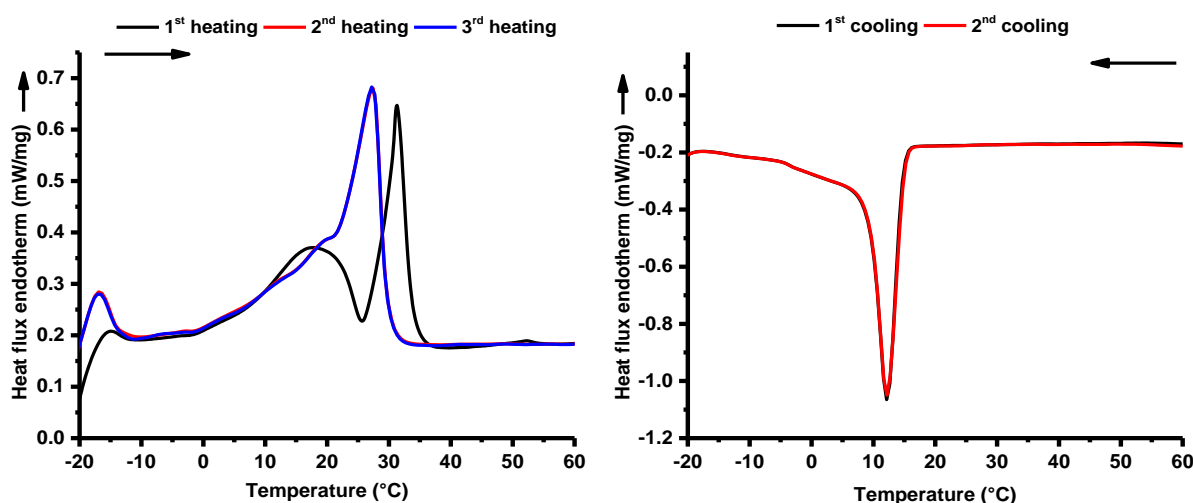


**Fig. 17** Heating (left) and cooling (right) DSC thermograms of the semisolid self-nanoemulsifying formulation F2.

#### 4.2.5.4. Benchtop nuclear magnetic resonance (BT-NMR)

BT-NMR is a non-invasive tool for the analysis of proton possessing compounds such as lipids. Lipid mobility could be assessed as a function of  $T_2$ -relaxation time that is calculated by fitting the NMR exponential decay curves. Additionally, the distribution of  $T_2$ -relaxation times could be calculated from inverse Laplace transformation of the exponential decay data. Mobile lipids have higher  $T_2$ -relaxation time than the mobility-restricted ones [322]. The  $T_2$ -relaxation time distribution of both excipients (**Fig. 18**) and the semisolid SNEDDS (**Fig. 19**) at 25 °C and 37 °C are summarized in **Table 18**.

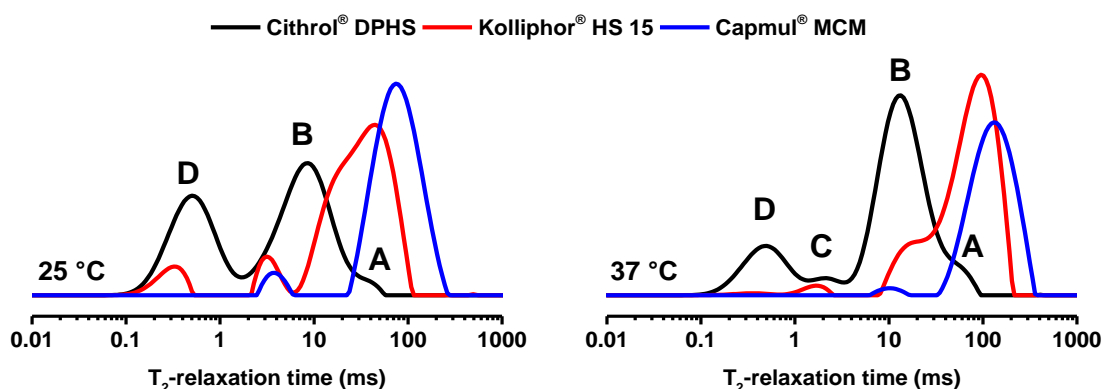


**Fig. 18**  $T_2$ -relaxation time distributions of the excipients at 25 °C and 37 °C.

MCM showed the highest mobility in both temperatures due to its lower viscosity. DPHS showed two main mobility states at 25 °C (State B and D) (**Fig. 18**). This could be attributed to the physical state of DPHS at room temperature. Based on the PXRD study, DPHS occurs in a partial crystalline and partial amorphous system (**Fig. S7** of the supplementary data). The area



under the  $T_2$ -relaxation time distribution indicates that the crystalline part (State D) accounts for ~40 % of the system while the amorphous part (State A and B) accounts for ~60 %. Increasing the temperature to 37 °C resulted in a shift of the  $T_2$ -relaxation time of the amorphous part to a higher mobility with the increase of the State A and B ratio to 78 %. The crystalline state (State D) remained in its position due to the incomplete melting of DPHS chains at 37 °C. Furthermore, a new mobility state (State C) is formed where the lipid chains are partially molten (~5 %).

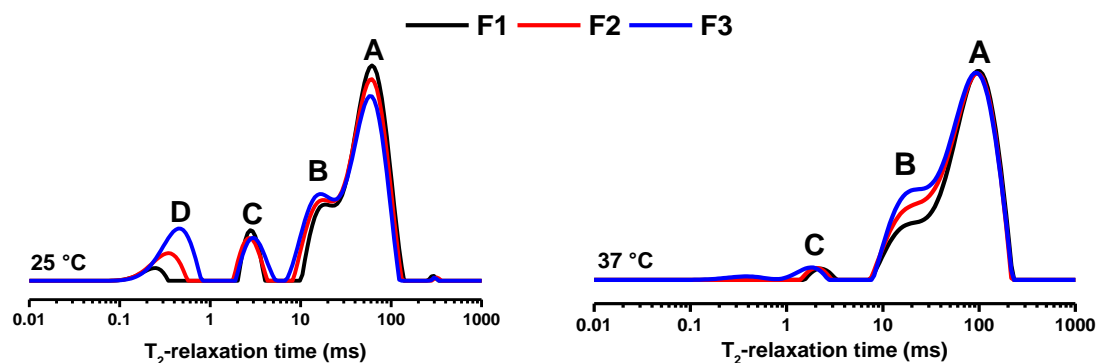


**Fig. 19**  $T_2$ -relaxation time distribution of the semisolid SNEEDS at 25 °C and 37 °C.

**Table 18**  $T_2$ -relaxation times of the excipients and the semisolid SNEEDS at 25 °C and 37 °C.

	State A (ms)		State B (ms)		State C (ms)		State D (ms)		$T_2$ (ms) <sup>a</sup>	
	25 °C	37 °C	25 °C	37 °C	25 °C	37 °C	25 °C	37 °C	25 °C	37 °C
	<b>Cithrol® DPHS</b>	37.0	54.1	8.7	13.5	--	2.2	0.50	0.50	7.8
<b>Kolliphor® HS 15</b>	44.8	95.6	18.5	20.8	3.2	1.7	0.32	--	20.9	74.7
<b>Capmul® MCM</b>	74.2	115.5	3.8	12.7	--	2.3	--	--	81.8	128.8
<b>F1</b>	61.4	95.6	18.5	20.8	2.8	2.3	0.25	--	52.4	80.4
<b>F2</b>	61.4	95.6	17.5	20.8	2.8	2.0	0.34	--	48.8	74.8
<b>F3</b>	61.4	95.6	16.3	20.8	3.0	1.8	0.44	--	44.9	72.5

<sup>a</sup>  $T_2$ -relaxation times were calculated by fitting the exponential decay curves.

HS15 has a more complex structure than DPHS. At least four mobility states could be observed at 25 °C with a superposition of the two highly mobile states (**Fig. 18** left). Increasing the temperature to 37 °C resulted in a shift to higher relaxation times with a reduction in the number of the lower mobility states.

Compared to a weighted average estimate of the excipients mobility, the measured  $T_2$ -relaxation time distribution of the semisolid SNEEDS was shifted toward higher mobility (**Fig. 20**). Furthermore, the measured peaks were narrower than the calculated estimate reflecting mobility enhancement. The improvement in the formulation mobility could be due to the interaction between lipid excipients observed during the DSC study (**Fig. 16**).

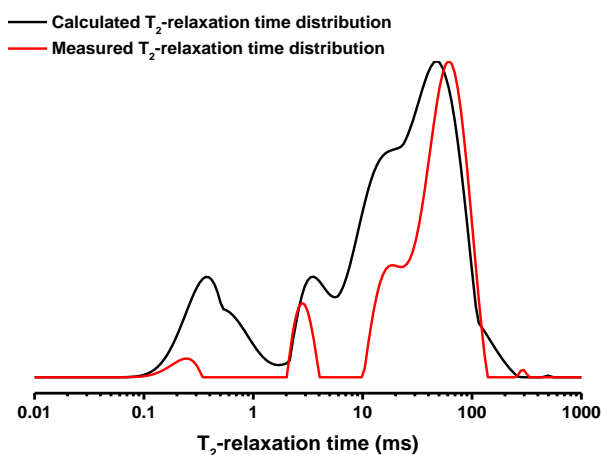


**Fig. 20** Comparison between the calculated and measured  $T_2$ -relaxation time distribution of the semisolid self-nanoemulsifying formulation F2 at 25 °C. The 2 curves are normalized to the same amplitude of the highest peak. The calculated F2 distribution is a weighted average of the measured excipients  $T_2$ -relaxation time distribution (**Fig. 18** left).

$T_2$ -relaxation time distribution of the semisolid SNEDDS showed at least 4 mobility states at 25 °C. The change in the formulation composition did not pronouncedly affect the  $T_2$ -relaxation time distribution (**Table 18**). However, the area under the different mobility states is apparently affected (**Fig. 19**). Therefore, the fitted  $T_2$ -relaxation time decreased with the increase of DPHS content. The increase in the DPHS content in the formulation resulted in an increase of the relatively mobility-restricted states (State B and D) areas and a decrease in the relatively high mobility state (State A) area. The area under the mobility state (State C) remained almost unchanged. State D reflects the crystalline part of the formulation while State B and C probably reflect the amorphous part. Increasing the temperature to 37 °C shifted the  $T_2$ -relaxation time distribution to higher values due to the enhancement of the lipid mobility (**Fig. 19**). Two main mobility states could be observed (State A and B). The relatively mobility-restricted state (State C) could be due to a partial adsorption of the molten lipid on the test tube wall. State D is vanished due to the complete melting of the semisolid SNEDDS at 37 °C. As observed at 25 °C, the change in the formulation composition did not pronouncedly affect the  $T_2$ -relaxation time distribution (**Table 18**). However, the relatively mobility-restricted state (State B) area increased with the increase of the DPHS content in the formulation. Accordingly, the fitted  $T_2$ -relaxation time decreased with the increase of DPHS content. The 2 mobility states peaks (State A and B) could be fitted as a Gauss peaks after taking the logarithm of the X-axis. The fitted line width increased with the increase of the DPHS content (**Fig. 21**). This increase could be interpreted as a partial decrease in the formulations mobility. The reason could be the increase of the internal viscosity brought by the increase in the DPHS content. State B (the relatively mobility-restricted state) was more affected by the increase of DPHS content than State A (the relatively higher mobility one).

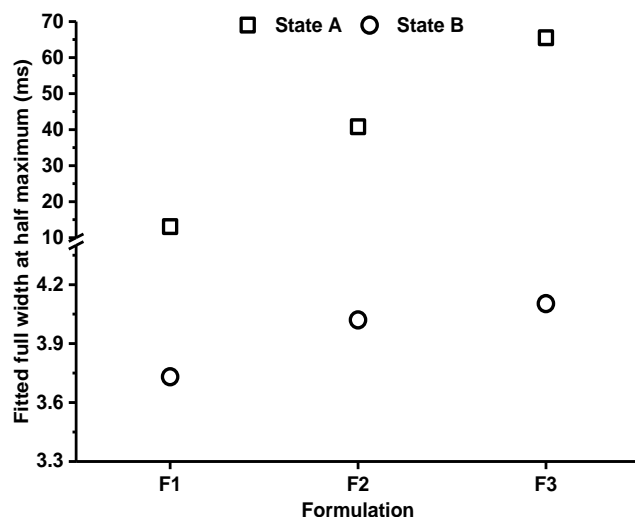


**Fig. 21** Fitted Gauss full line width at half maximum (FWHM) of the mobility states (State A and B) of the semisolid SNEDDS at 37 °C.

#### 4.2.5.5. Proton nuclear magnetic resonance ( $^1\text{H-NMR}$ )

$^1\text{H-NMR}$  spectroscopy measurements can provide good information about the structure and mobility of the lipid in the nanodispersed systems [116]. The mobility of nanodispersed systems is essential for its *in vivo* performance. After ingestion of lipids, different phases with different degrees of mobility are developed. The  $^1\text{H-NMR}$  signals of mobile lipids are characterized by narrow lines with high amplitudes. On the other hand, signals of less mobile lipids are characterized by broader lines and lower amplitudes. Immobile lipids cannot be detected by  $^1\text{H-NMR}$  spectroscopy because of their very short relaxation times [270, 323]. To facilitate the identification of the signals corresponding to each excipient in the nanoemulsions,  $^1\text{H-NMR}$  spectra of excipients were recorded at 37 °C in d-DMSO (**Fig. 22**).  $^1\text{H-NMR}$  spectra of 5 % (m/V) SNEDDS nanodispersions in  $\text{D}_2\text{O}$  at 37 °C as well as micellar dispersion of 3 % (m/V) HS15 at 37 °C in  $\text{D}_2\text{O}$  are shown in **Fig. 23**.

MCM is a medium chain complex lipid mixture of MG, DG and TG of caprylic acid ( $\text{C}_8$ ) and capric acid ( $\text{C}_{10}$ ) as well as free glycerol [324]. The assignment of the  $^1\text{H-NMR}$  signals to MCM was performed in agreement with the literature [325, 326]. The multiplet (e), with a shift between 4.0 and 4.2 ppm, corresponding to the esterified glycerol protons can be used to identify MCM in nanoemulsions. No interference of these signals with signals from the other excipients was observed. The MCM multiplet (e) was also detected in the three nanoemulsions (**Fig. 23** bottom center). The observed decrease in the signal (e) amplitudes from the self-nanoemulsifying formulations F1 to F3 is caused by the decrease of the MCM content in the formulations.

DPHS is an ABA block copolymer. The middle block (B) is a PEG chain while the two outer blocks (A) are poly(12-HSA) [309]. HS15 consists of a mixture of ~70 % PEG ME and DE of 12-HSA and ~30 % PEG [86, 320]. Due to the ownership of the same building blocks, DPHS and HS15 <sup>1</sup>H-NMR signals have nearly the same chemical shifts. However, the relative intensity of the signals and some line widths differ according to the different ratios of the building blocks and their different mobility.

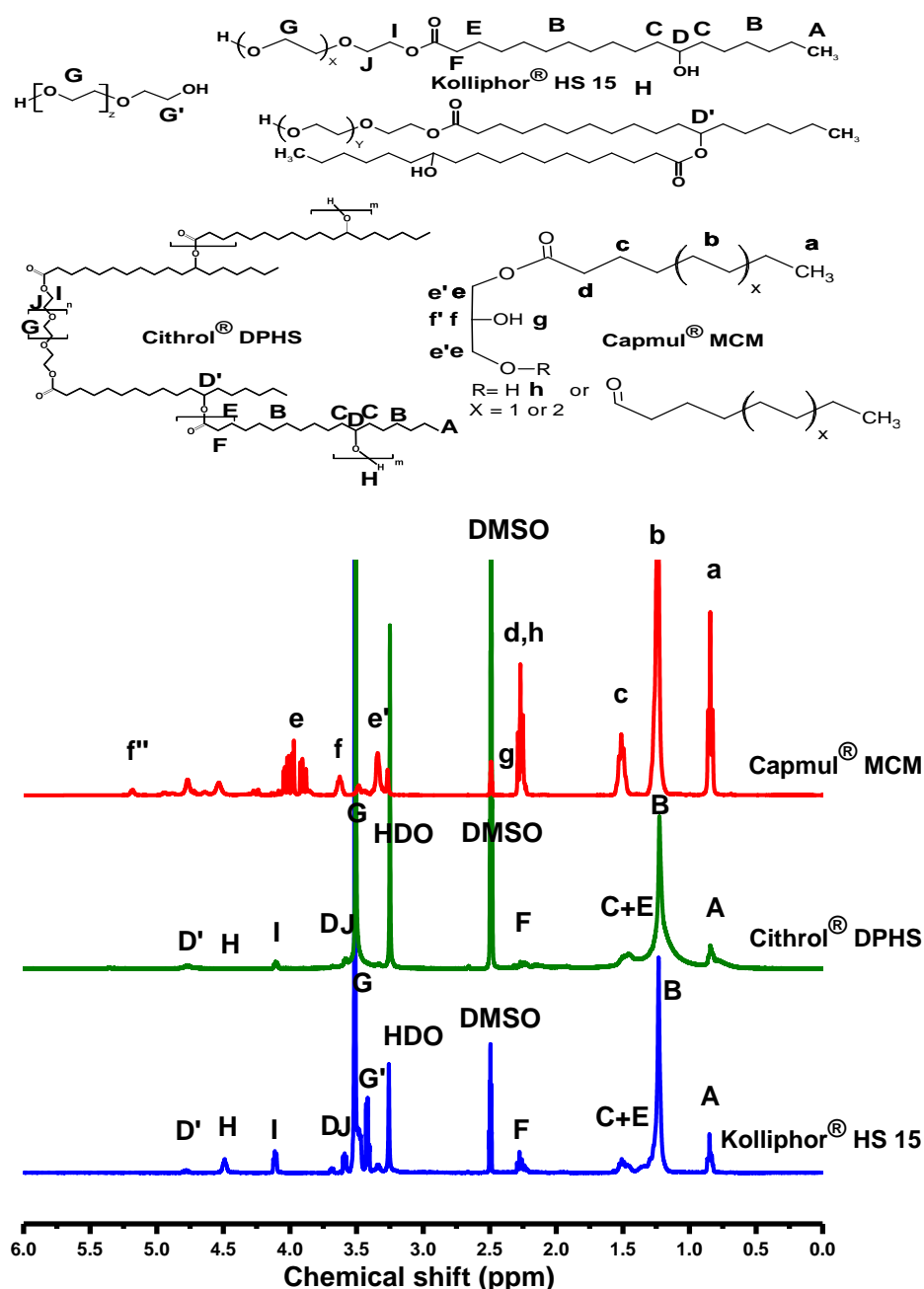


**Fig. 22** <sup>1</sup>H-NMR spectra of the excipients dissolved in d-DMSO at 37 °C. All signals are signed corresponding to the positions of the protons in the chemical formula above.

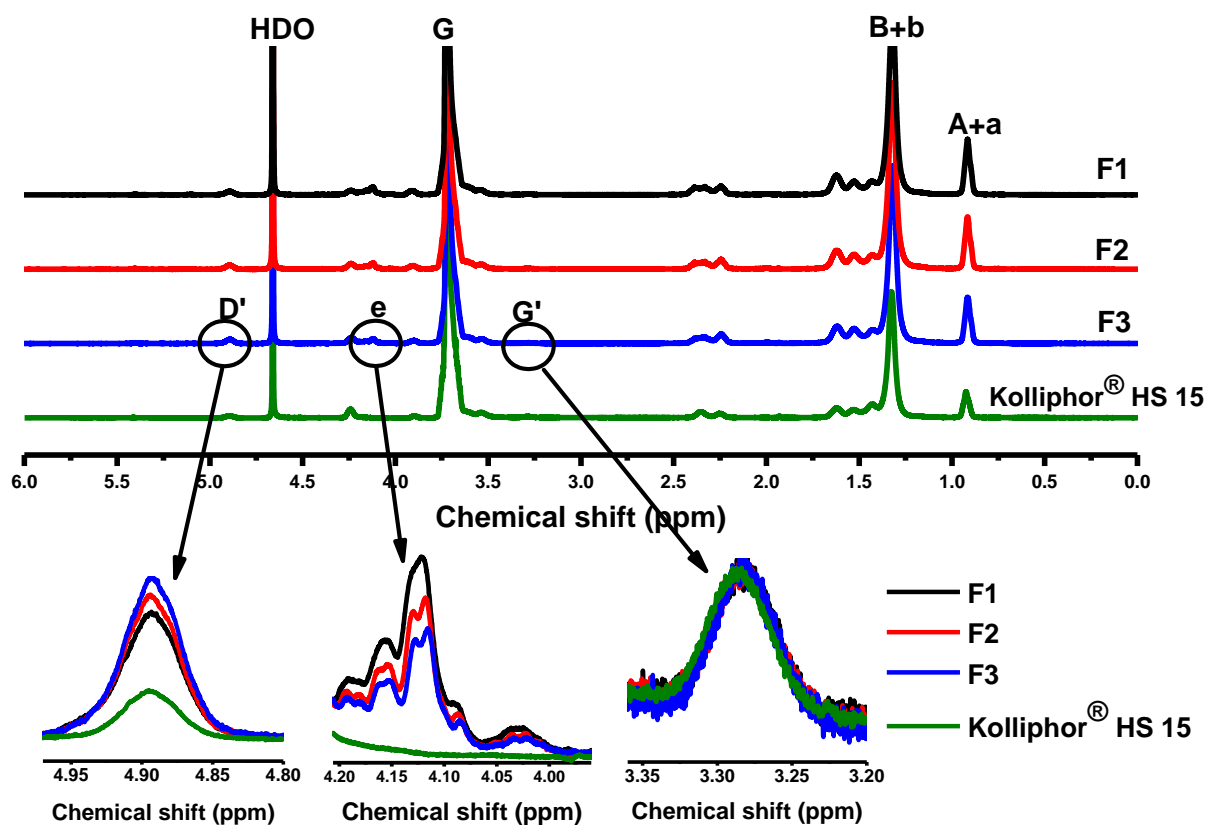


**Fig. 23**  $^1\text{H}$ -NMR spectra of 5 % (m/V) dispersions of the semisolid SNEDDS in  $\text{D}_2\text{O}$  at  $37\text{ }^\circ\text{C}$  compared to the micellar spectra of Kolliphor<sup>®</sup> HS 15 in  $\text{D}_2\text{O}$ .

In d-DMSO solution of DPHS, the PEG signal was broader due to the fact that PEG is localized in the central B block of the polymeric emulsifier (**Fig. 22**). Due to the covalent linkage at both sides, its flexibility is restricted compared to free PEG and PEG linked only at one end. Furthermore, all DPHS signals are very broad and - in contrast to HS15 - no real baseline could be observed in the region between 0.5 and 1.5 ppm. The PEG chains of HS15 are free either at one (the other linked to the 12-HSA) or even at both ends (free PEG content ~30 %). Therefore, compared to the DPHS, a higher mobility is expected. Indeed, the PEG specific proton NMR signals of HS15 solutions in d-DMSO have narrow line widths and high signal amplitudes with a good signal resolution (**Fig. 22**). The values of the chemical shifts of HS15 micelles (**Fig. 23**) are in a good agreement with literature data [327].

All signals of the micellar dispersion (**Fig. 23**) were shifted downfield compared to the HS15 signals in d-DMSO solutions (**Fig. 22**). The change of the solvent and the proximity of the amphiphilic chains to each other in the micellar structure may be responsible for such effect. Separated signals for the same protons, which could occur due to their localization in different environments (e.g. molecular dispersed in water and associated in micelles or SNEDDS

droplets), could not be observed in the aqueous dispersions (**Fig. 23**). One explanation for this observation would be the dominance of one species. Another reason could be a fast exchange between both species. Micelles are not static entities. They are constantly reorganizing themselves by rapid reversible exchange between the surfactant molecules localized in the micelles and molecularly dissolved surfactants. Under the used experimental setup, it could be assumed that this exchange is faster to the NMR-timescale. As a result, both signals are averaged and not recognizable as two different species.

The terminal methylene group of the free PEG (G') can serve as an identification of HS15 in the nanoemulsions (**Fig. 23** bottom right). Because of the constant free PEG fraction in the formulations, the signal area remained unchanged. However, it was more difficult to assign a signal for DPHS. Due to its higher molecular weight (~5000 D) compared to HS15 (~854 D) and its relatively lower content, DPHS mole fraction in the dispersions was too low to be compared to HS15. The (D') signal corresponding to C<sub>12</sub> in the DE is stronger in DPHS compared to HS15. An increase in the (D') signal area in the nanoemulsions was observed with the slight increase in DPHS mole fraction (**Fig. 23** bottom left).

<sup>1</sup>H-NMR spectra of the SNEDDS nanoemulsions showed four distinct signals: (a) the terminal methyl signal at 0.92 ppm, (b) the FA chain signal at 1.33 ppm, (c) the PEG signal at 3.70 ppm and (d) the HOD signal at 4.66 ppm. In order to assess the mobility of the hydrophilic and lipophilic part of the formulations, a comparison between expected and measured relative signal areas was constructed in **Table 19**. Furthermore, the spectra were assessed in terms of line width at half-amplitude of the respective signal (**Table 20**) [328, 329]. The line widths analysis indicates an overall high degree of mobility.

Due to its position, the terminal methyl signal is the most sensitive signal to the mobility of the hydrophobic part of the nanoemulsions. A small increase in line width was observed with the increase in DPHS content in the hydrophobic part of the formulations (**Table 20**). This reflects a slight decrease in mobility of the hydrophobic part with the increase of the local viscosity caused by an increased DPHS content. However, the restriction in the mobility was not pronounced compared to micellar HS15. The line width of the –CH<sub>2</sub>– groups of the FA chain signal did not considerably change between formulations (**Table 20**). Nevertheless, the signals were broader compared to micellar HS15 signals due to the incorporation of the hydrophobic part within the micelles. The measured  $\frac{-\text{CH}_3}{-\text{CH}_2-}$  ratios were nicely in agreement with the calculated ratios (**Table 19**), indicating that all excipients were in a mobile status.

**Table 19** Comparison between expected and measured relative signal areas of the SNEDDS nanodispersions.

	-CH <sub>2</sub> - / -CH <sub>3</sub>			PEG/fatty acids chain (-CH <sub>3</sub> + -CH <sub>2</sub> -)		
	Expected <sup>a</sup>	Measured	%	Expected <sup>b</sup>	Measured	%
<b>F1</b>	6.2:1	6.5:1	104.2	1.80:1	1.59:1	88.3
<b>F2</b>	6.8:1	7.0:1	103.4	1.77:1	1.44:1	81.1
<b>F3</b>	7.1:1	7.4:1	104.0	1.76:1	1.38:1	78.1

<sup>a</sup> Calculations based on the relative signal areas obtained from dissolved Cithrol<sup>®</sup> DPHS and Capmul<sup>®</sup> MCM in d-DMSO and micellar dispersion of Kolliphor<sup>®</sup> HS 15 in D<sub>2</sub>O.

<sup>b</sup> Calculations based on the relative signal areas obtained from dissolved Cithrol<sup>®</sup> DPHS in d-DMSO and micellar dispersion of Kolliphor<sup>®</sup> HS 15 in D<sub>2</sub>O.

**Table 20** Line width at half-amplitude of the main signals of the SNEDDS nanodispersions and micellar Kolliphor<sup>®</sup> HS 15.

	Line width at half-amplitude of the respective signal (Hz)		
	Terminal -CH <sub>3</sub> (0.92 ppm)	Chain -CH <sub>2</sub> - (1.33 ppm)	PEG (3.70 ppm)
<b>Kolliphor<sup>®</sup> HS 15</b>	13.6	16.0	4.4
<b>F1</b>	13.6	18.0	7.6
<b>F2</b>	14.0	17.6	6.8
<b>F3</b>	14.4	18.0	6.4

The PEG signal was used to evaluate the mobility of the hydrophilic part of the nanoemulsions (**Fig. 23**). The relative value of  $\frac{\text{PEG}}{-\text{CH}_2- + -\text{CH}_3}$  ratio of the <sup>1</sup>H-NMR signals of micellar HS15 was about 84 % of that of the dissolved HS15. This result can be attributed to the broadness of the micellar signals due to the decreased mobility of PEG at the interface. All nanoemulsions showed a broader PEG signal compared to the micellar HS15. Surprisingly, the observed PEG signal line width decreased with the increase of DPHS ratio. This could be attributed a partial replacement of HS15 by DPHS at the interface. The replaced HS15 would have a higher water affinity and show a narrow line width in the molecular dispersed state. The results indicate that only a part (78-88 %) of the PEG groups was detectable by NMR under the experimental conditions. The missing part is most likely localized at the lipid/water interface with a restricted mobility.

#### 4.2.5.6. Electron spin resonance (ESR)

ESR, also known as electron paramagnetic resonance (EPR), is a beneficial non-invasive tool to detect and characterize free radicals and other paramagnetic compounds. It is very useful to explore the microenvironment inside the drug delivery systems with the respect to micropolarity, mobility, microviscosity as well as pH. Most of the drug delivery systems are diamagnetic and EPR silent. Consequently, the incorporation of spin probes is essential. In

many cases, nitroxides are used, which show in solution three ESR lines due to the impact of the  $^{14}\text{N}$ -nuclear spin ( $I=1$ ). A wide range of spin probes with different physicochemical properties is commercially available [330]. Tempolbenzoate (TB) is a widely used poorly water-soluble spin probe with a submillimolar solubility in water,  $\log P$  of 2.46 [276] and HLB of 6.7 [331]. A typical spectrum of TB in the lipophilic environment and the important spectrum parameters are shown in **Fig. 24**. The hyperfine coupling constant ( $a_{\text{N}}$ ) can serve as an indication of the polarity of the microenvironment. The value of  $a_{\text{N}}$  increases with the increase of the polarity (**Fig. 25**).

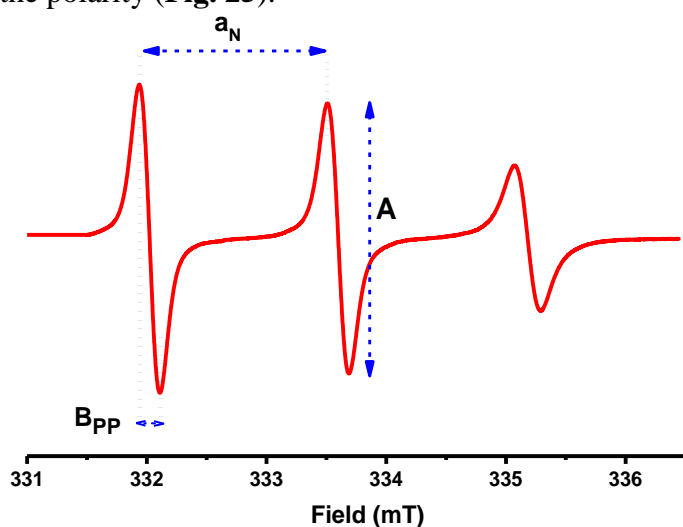


**Fig. 24** ESR spectrum of Tempolbenzoate in Capmul<sup>®</sup> MCM showing the important spectrum parameters: hyperfine constant ( $a_{\text{N}}$ ), peak-to-peak line width ( $B_{\text{pp}}$ ) and peak amplitude ( $A$ ).

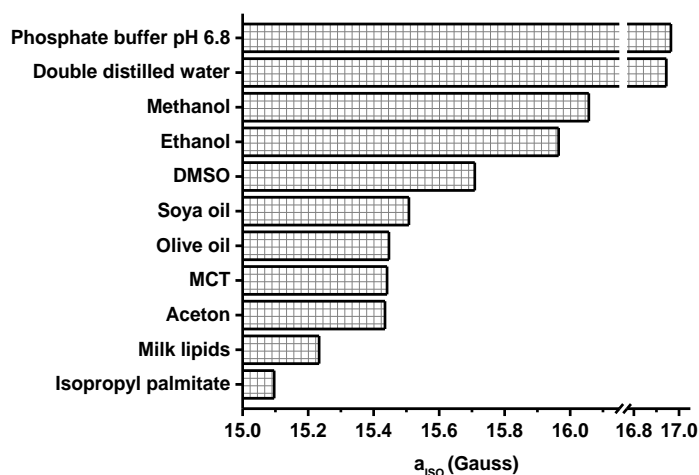


**Fig. 25** Fitted hyperfine coupling constant ( $a_{\text{iso}}$ ) of Tempolbenzoate in lipids and solvents that display different polarities.

The hyperfine coupling between the unpaired electron and the nuclear spin is anisotropic. Because of the non-spherical structure of the TB molecule, the spectrum can be described as a weighted average of two rotation states, a slower and a faster one. Microviscosity affects the tumbling speed expressed as the rotational correlation time ( $\tau_c$ ). In a low viscosity microenvironment, the anisotropy is nearly averaged due to the rapid movement of the spin probe and an isotropic hyperfine splitting is obtained. Under such conditions, the ESR spectra



of nitroxides show three similar lines with similar small line widths and signal amplitudes. An increase of the microviscosity results in an incomplete averaging of the anisotropy. Consequently, broader peaks are obtained. The broadening effect is different for each line and is most pronounced for the third peak [332]. ESR spectra of TB-loaded excipients at 37 °C and the results of their fitting are shown in **Fig. 26**.

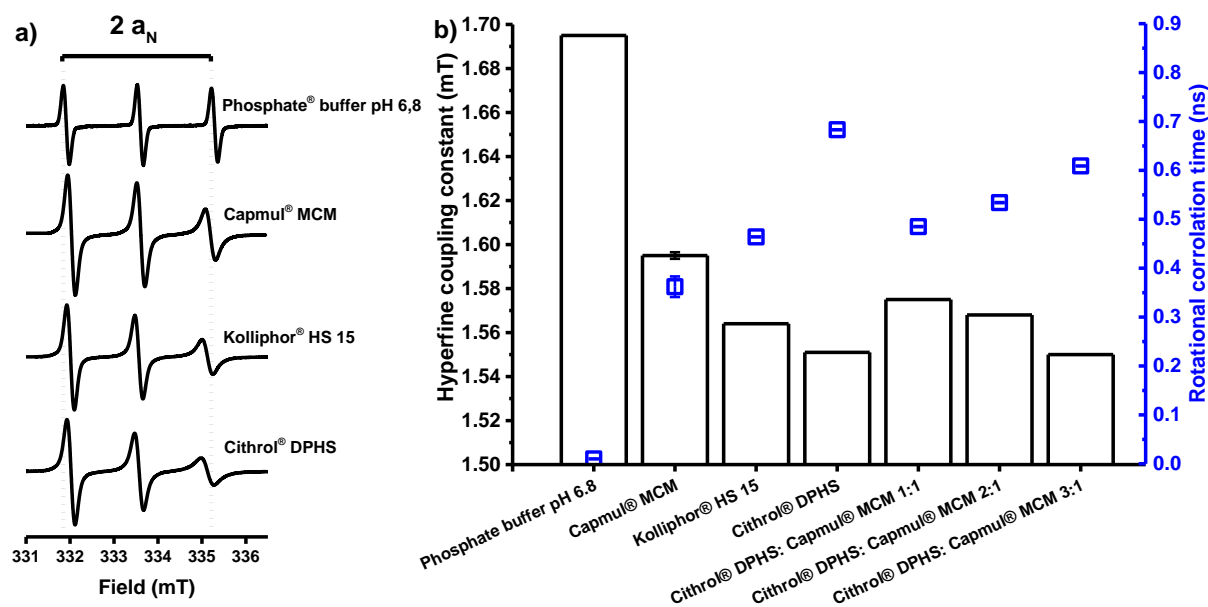


**Fig. 26** ESR spectra of different Tempolbenzoate-loaded excipients at 37 °C (a) and the values of the hyperfine coupling constant ( $a_N$ ) and rotational correlation time ( $\tau_c$ ) of Tempolbenzoate obtained after data fitting (b). Error bars are obtained from the fitting process and denote the accordance of the simulated states to the original data.

MCM showed the highest polarity and lowest viscosity. On the other hand, DPHS showed the lowest polarity and the highest viscosity. A decrease in polarity accompanied with an increase in viscosity was noticed with the increase of DPHS ratio in the lipophilic mixture. The ESR spectra of different MCM/DPHS combinations are shown in **Fig. 27**.

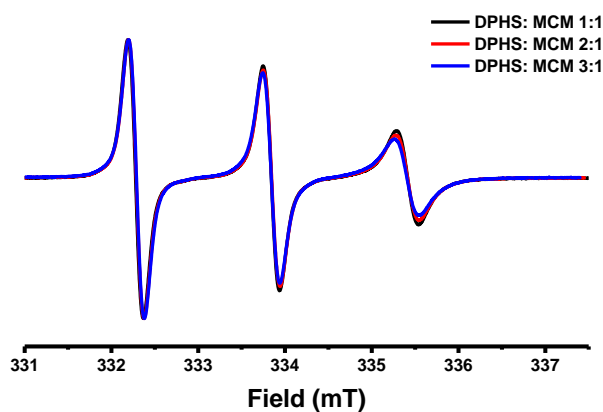


**Fig. 27** ESR spectra of different Tempolbenzoate-loaded combinations of Cithrol<sup>®</sup> DPHS and Capmul<sup>®</sup> MCM at 37 °C. The spectra are normalized to the same amplitude of the first peak.

The ESR spectra were normalized to the same first line amplitude. Accordingly, the effect of viscosity can be observed on the peak height of the third peak of the normalized spectra. The spectra indicate a slight increase of microviscosity with increasing DPHS content.

The results of the ESR fitting of the semisolid SNEDDS and their nanoemulsions are shown in **Fig. 28**. The data can be fitted into two rotation states: R1 and R2 (**Fig. 29**). The superposition of different rotation states is seen for both water-free SNEDDS as well as 5 % and 10 % SNEDDS nanodispersions. Compared to R2, R1 has a lower hyperfine coupling constant (indicating a lower polarity) and a higher rotational correlation time ( $\tau_c$ ) (indicating a higher viscosity). In water-free SNEDDS, increasing the temperature from 25 °C to 37 °C leads to a decrease of the R1/R2 differences in the hyperfine splittings (**Fig. 28a**) and to a decrease of the rotational correlation times (**Fig. 28c and d**). The data indicates that different nanocompartments exist at lower temperatures and that the temperature increase causes structural changes, which transform the SNEDDS towards a more isotropic, less-structured low viscous liquid. For SNEDDS dilutions, the hyperfine splittings are comparable to water-free SNEDDS despite a water content of 90 % or 95 % (**Fig. 28b vs. Fig. 28a**). The  $a_N$  value of R1 decreases with the increase of DPHS content (from F1 to F3), indicating the formation of a more lipophilic compartment. In contrast, the  $a_N$  value of the more polar rotation state R2 does not change from F1 to F3 (**Fig. 28b**). R2 accounts for ~70 % of the overall EPR signal intensity in the SNEDDS nanodispersions (**Fig. 28e and f**), but only to ~45 % (**Fig. 28c**) and ~30 % (**Fig. 28d**) for undiluted SNEDDS at 25 °C and 37 °C respectively. The SNEDDS composition (F1, F2 or F3) does not affect the rotational correlation time ( $\tau_c$ ) of the R2 rotation state (**Fig. 28d-f**), which was around 0.3 ns at 37 °C for both undiluted and diluted SNEDDS. In contrast, R1 changes from F1 over F2 to F3, especially in SNEDDS nanodispersions (from 0.7 to 1.1 ns). It also depends on the dilution degree, especially for the more hydrophilic SNEDDS nanodispersions of F1 and F2 (**Fig. 28e and f**).

An overlay of the normalized ESR spectra of the nanoemulsified formulation F2 spectra in phosphate buffer pH 6.8 is shown in **Fig. 30**. Samples were measured at high modulation and longer time to increase the signal-to-noise ratio. ESR spectra of the 1 % dispersions were difficult to be fitted because of the very low signal-to-noise ratio. However, the 1 % dispersion spectra clearly show a considerable localization of the spin probe in a polar environment, indicated by the line shape and shift of the third peak. It can be concluded that small molecules with a similar characteristics as TB (log P between 2 and 3; aqueous submillimolar solubility) will be mainly associated with the SNEDDS up to a dilution of 5 % and will translocate into

water with further dilution (or relocate *in vivo* into other sides such as proteins and lipid tissue). Furthermore, no evidence of TB precipitation was detected upon dilution.

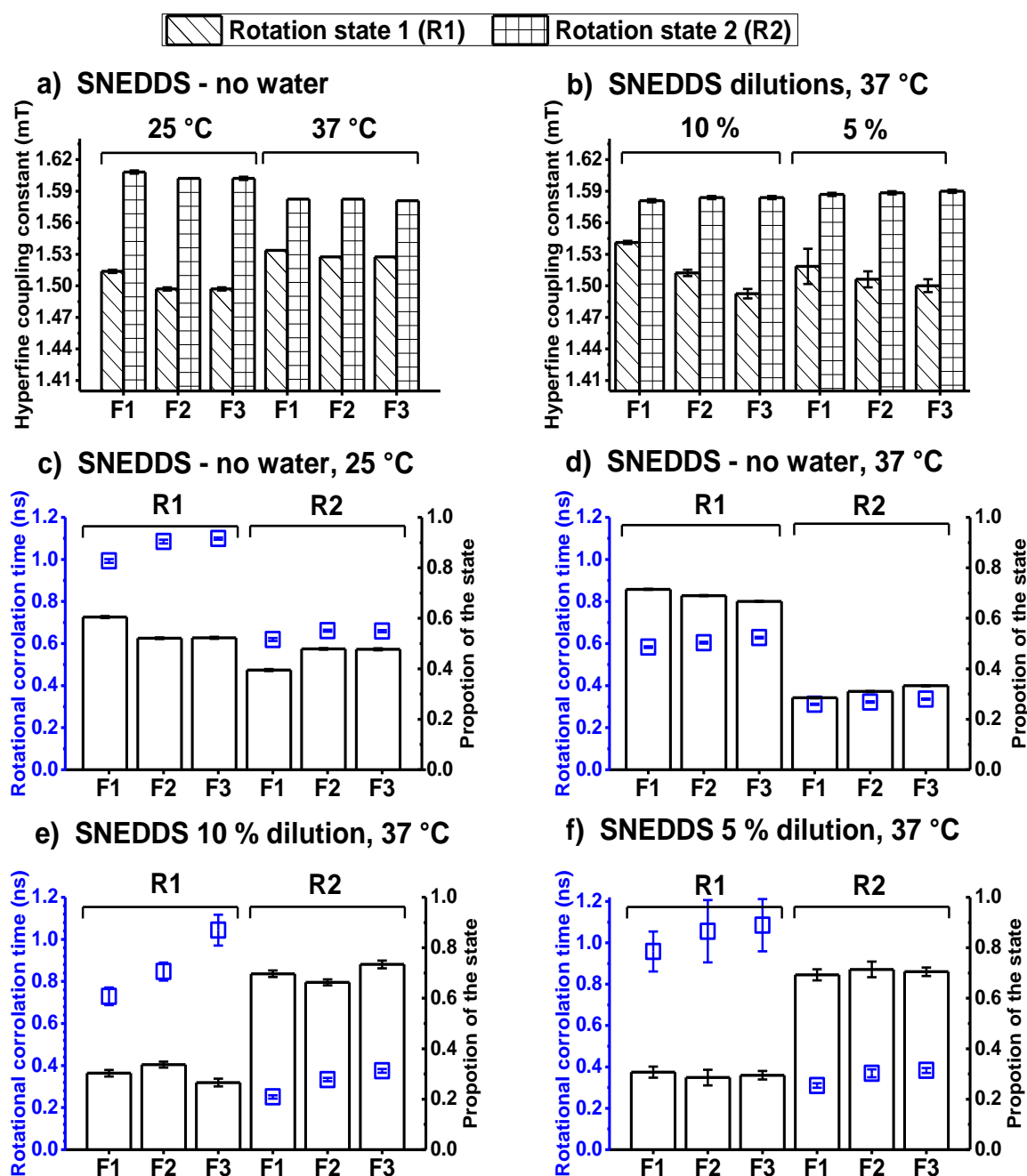


**Fig. 28** ESR fitting data of Tempolbenzoate-loaded semisolid SNEDDS and their nanoemulsions. (a) The hyperfine coupling constant ( $a_N$ ) in the anhydrous SNEDDS at 25 °C and 37 °C. (b) The  $a_N$  in 10 % and 5 % nanoemulsions. (c) The rotational correlation time ( $\tau_c$ ) and the proportion of each fitted states in the SNEDDS at 25 °C and (d) at 37 °C. (e) The  $\tau_c$  and the proportion of each fitted states in the 10 % and (f) 5 % nanoemulsions. Error bars are obtained from the fitting process and denote the accordance of the simulated states to the original data.

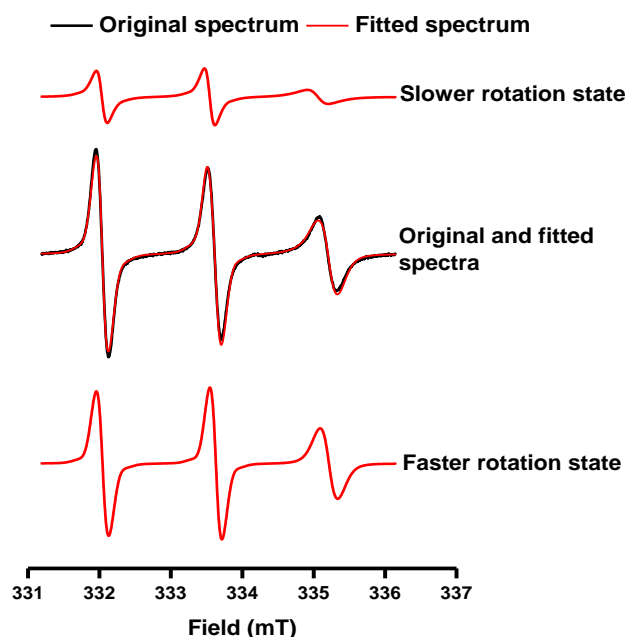


**Fig. 29** Original and fitted ESR spectra of the 10 % dispersion of Tempolbenzoate-loaded semisolid self-nanoemulsified formulation F2 in phosphate buffer pH 6.8 at 37 °C.

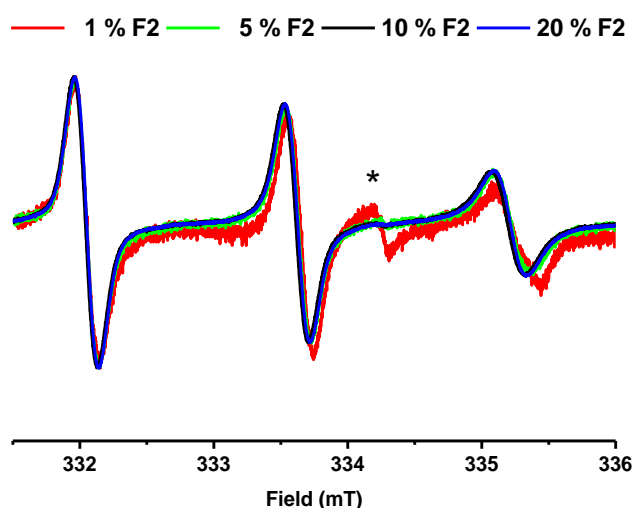


**Fig. 30** ESR spectra of different dispersions of Tempolbenzoate-loaded semisolid self-nanoemulsified formulation F2 in phosphate buffer pH 6.8. The spectra are normalized to the same amplitude of the first peak. The extra signal marked with (\*) is a background signal of the resonator.

#### 4.3. Preparation of the self-nanoemulsifying adsorbates

Based on the aforementioned data, the self-nanoemulsifying formulation F2 was selected as a promising formulation for further investigation and denoted as semisolid SNEDDS. F2 showed a rapid and pH-independent dispersibility in all media with a Z-average of less than 25 nm. Furthermore, F2 nanodispersions showed high mobility in physiological conditions. Although, semisolid SNEDDS are more advantageous than liquid ones, S-SNEDDS (especially tablets) have superior shelf-life stability, lower production cost and lower sensitivity to the storage conditions as well as higher patient compliance and palatability compared to both liquid and semisolid ones. Accordingly, it is more beneficial to transform the semisolid SNEDDS into a freely flowable powder to be compressed into tablets.

#### 4.3.1. Preliminary screening of the possible adsorbates

Selected common tableting excipients were screened for their ability to adsorb 30 % m/m of the semisolid SNEDDS. In the preformulation study, the adsorbates were tested only for the appearance and flowability (**Table S6**). Among tested tablets filler and binders, only Neusilin<sup>®</sup> US2 (N-US2) have shown superior adsorbing and flow properties. Among disintegrants, fine grades of cross-linked Povidones showed an acceptable adsorbing and flow properties. Therefore, they were used for the further formulations studies.

#### 4.3.2. Preparation of the Neusilin<sup>®</sup> US2/SNEDDS adsorbates

N-US2 is an amorphous, synthetic, neutral grade of Magnesium aluminometasilicate. It occurs in nanoporous, ultra-light granules prepared by spray drying. N-US2 is non-toxic and does not form gels upon contact with aqueous fluids. Furthermore, it has an excellent flowability, very high specific surface area and good compressibility [89, 238, 333]. N-US2 was recently used to solidify liquid self-emulsifying systems [127, 187, 230-232, 236, 237, 263, 334-342]. However, in some cases incomplete drug release was observed from N-US2 [263]. It was proposed that some SNEDDS form gels (as an intermediate phase during their dispersion) upon contact with the aqueous phase. Accordingly, N-US2 nanopores may be clogged and incomplete drug release may occur [237]. Therefore, it is very interesting to study how N-US2 interacts with semisolid SNEDDS that have higher viscosity and are more mobility-restricted compared to the liquid one.

The semisolid SNEDDS was loaded onto N-US2 at different concentration using a solvent-free method. The physical form of different adsorbates is shown in **Table 21**. The semisolid properties of the SNEDDS were not changed with the incorporation of 10 % N-US2 and the adsorbent seems to be dispersed within the semisolid SNEDDS matrix. Increasing the amount of N-US2 (20-30 %) resulted in an increase in the solid properties of the SNEDDS with the formation of plastic paste or rubbery solid that could be molded into tablet-like shapes. These type of adsorbates are favorable, when a high SNEDDS (or PWSD) load is essential in the final dosage form. They could be filled as minitables into hard gelatin capsules. Compared to soft gelatin capsules filled with liquid SNEDDS, these minitables might provide higher chemical and physical stability and less interaction with the capsule shell as well as higher resistance to temperature-induced PWSD precipitation.

A freely flowable powder was obtained at N-US2 concentration starting from 40 % m/m. This powder could also be filled into hard gelatin capsules or compressed into tablets. Due to the relatively low density of such adsorbates, tablets are more favorable than capsules as they

can hold 2-3 times more powder compared to capsules [237, 263]. However, the compression of SNEDDS-loaded adsorbates is not trivial. SNEDDS could be squeezed out during the compression. Furthermore, the hydrophobic environment inside the produced tablets hinders their disintegration and can lead to incomplete drug release, especially when gel-mediated SNEDDS dispersion takes place or irreversible interaction between the SNEDDS and adsorbent arises [237, 238]. Therefore, the SNEDDS/adsorbent interactions should be thoroughly evaluated.

**Table 21** The composition and the physical states of the Neusilin<sup>®</sup> US2/SNEDDS adsorbates.

Adsorbate	Neusilin <sup>®</sup> US2	SNEDDS	Physical form
N1	10	90	Semisolid
N2	20	80	Paste
N3	30	70	Rubbery
N4	40	60	Solid
N5	50	50	Solid
N6	60	40	Solid
N7	70	30	Solid
N8	80	20	Solid

### 4.3.3. Characterization of the Neusilin<sup>®</sup> US2/SNEDDS adsorbates

#### 4.3.3.1. Differential scanning calorimetry (DSC)

DSC was used in order to study the interaction between N-US2 and the SNEDDS and its effect on the melting behavior of the semisolid SNEDDS. DSC thermograms of different adsorbates are represented in **Fig. 31**.

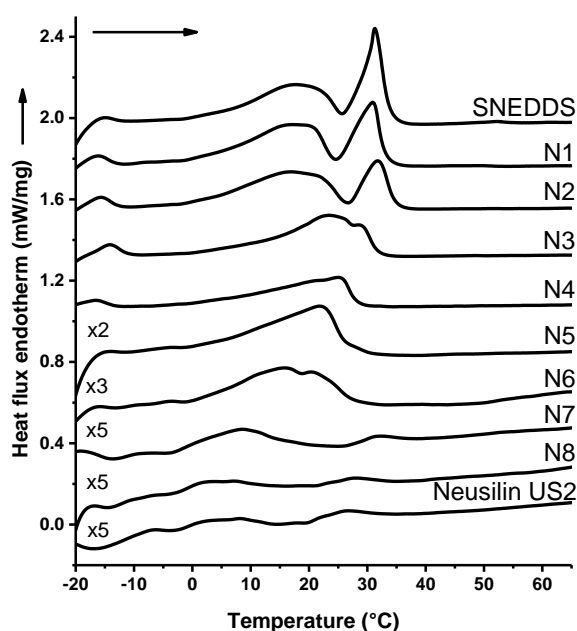


**Fig. 31** DSC thermograms of the semisolid SNEDDS, Neusilin<sup>®</sup> US2, and adsorbates.

The semisolid SNEDDS showed two melting isotherms at about 23.1 °C (very broad) and about 31.1 °C while N-US2 showed no characteristic peak in this temperature range. Incorporation of small amounts of N-US2 (10-20 %) resulted in a minor positive shift of the main melting peak. Further increase in the N-US2 amount led to a reduction of the melting point of the SNEDDS and broadening of the melting peak due to the incorporation of the semisolid SNEDDS in N-US2 nanopores with different pore sizes. The enthalpy decreased linearly ( $R^2 = 0.993$ ) with the decrease of the SNEDDS content in the adsorbates until a SNEDDS concentration of 30 % was achieved (**Fig. 32**). At lower SNEDDS concentrations, the influence of the adsorbed water on the DSC thermogram was more pronounced. The linear decrease in the enthalpy suggests that the interaction between the SNEDDS and N-US2 did not affect the SNEDDS crystallinity.

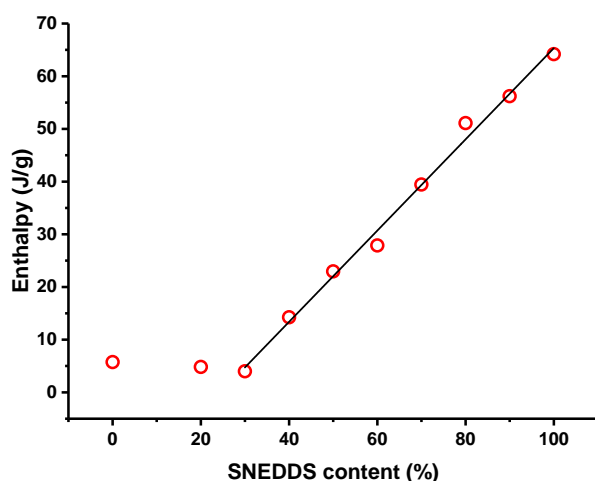


**Fig. 32** Effect of the semisolid SNEDDS content on the melting enthalpy.

#### 4.3.3.2. Benchtop nuclear magnetic resonance (BT-NMR)

BT-NMR was used to study the interaction between N-US2 and the semisolid SNEDDS. As the adsorption of the SNEDDS on N-US2 restricts their mobility, a negative shift in their  $T_2$ -relaxation time is expected. The strength of the  $T_2$ -relaxation time shift could reflect the degree of the SNEDDS adsorption [235, 322].  $T_2$ -relaxation time distribution curves of different adsorbates are shown in **Fig. 33**. Since the signal intensity is a function of the total number of nuclei [343], the area under the  $T_2$ -relaxation time distribution curves showed a linear correlation ( $R^2 = 0.996$ ) with the amount of adsorbed SNEDDS (**Fig. 34a**). The area of the zero lipid  $T_2$ -relaxation time distribution curve is corresponding to the adsorbed water. N-US2 have free silanol groups that form hydrogen bonds with water [235]. Therefore, a strongly adsorbed water state was detected at pure N-US2 (**Fig. 33**). N-US2 was subjected to the same adsorbates preparation conditions in order to determine the zero lipid area under the  $T_2$ -relaxation time distribution curve.

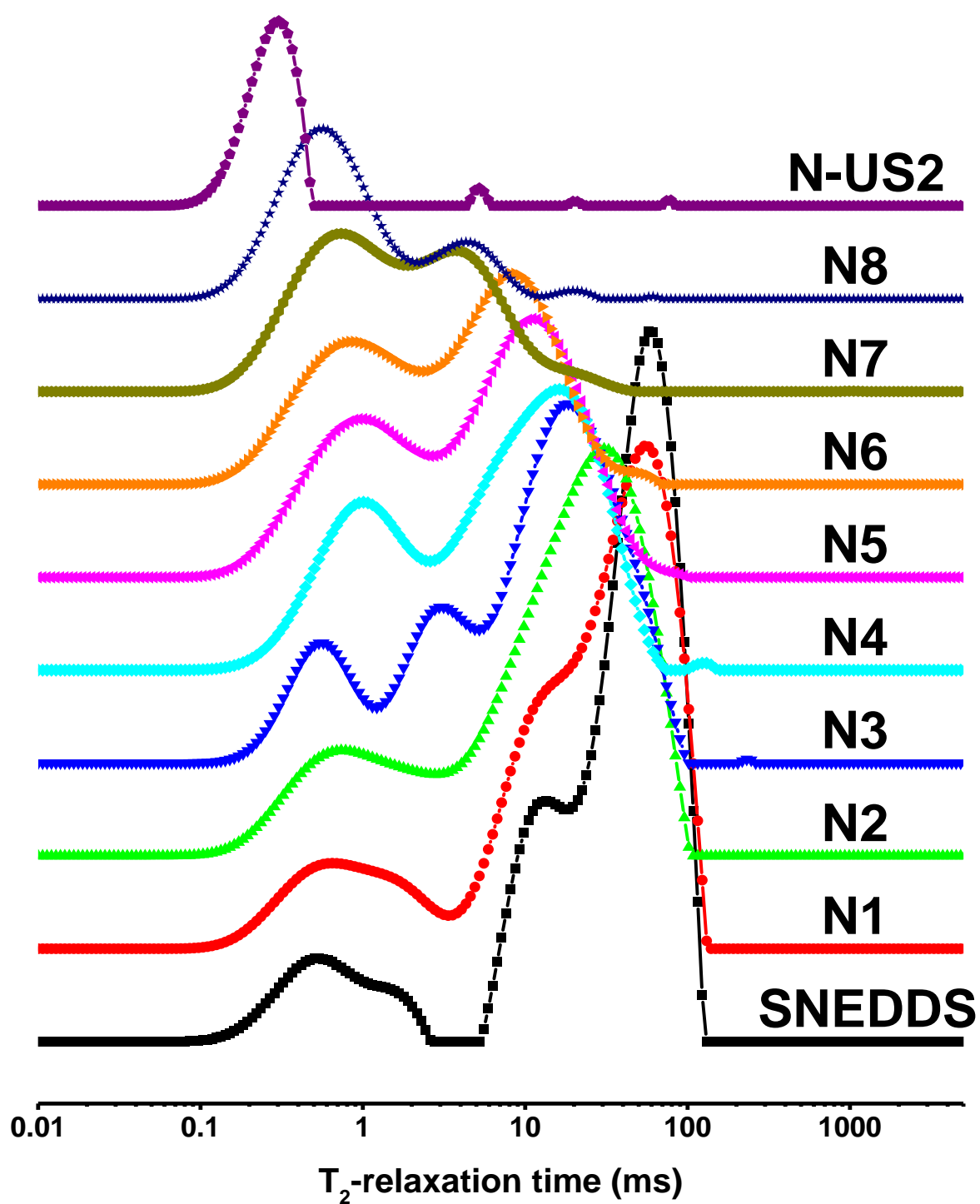


**Fig. 33** Influence of the semisolid SNEDDS content on the  $T_2$ -relaxation time distribution of the adsorbates.



Increasing the amount of N-US2 in the adsorbates resulted in a shift in the  $T_2$ -relaxation time to lower relaxation time due to the N-US2/SNEDDS physical interactions (**Table 22**). N-US2 forms hydrogen bonds with the adsorbed SNEDDS due to its free silanol groups. This type of interaction is much stronger than the hydrophobic interactions that take place with the other adsorbents lacking H-bond donors or acceptors [235]. However, the decrease in the fitted  $T_2$ -relaxation time was not linear (**Fig. 34b**). The semisolid SNEDDS showed a superposition of several mobility states with at least four visible  $T_2$ -relaxation states (**Fig. 33**). Incorporating 10 % of N-US2 (N1) had a minor effect on the  $T_2$ -relaxation time distribution.

**Table 22**  $T_2$ -relaxation time distribution of the semisolid SNEDDS, adsorbates and Neusilin<sup>®</sup> US2 at 25 °C.

	1 <sup>st</sup> peak (ms)	2 <sup>nd</sup> peak (ms)	3 <sup>rd</sup> peak (ms)	4 <sup>th</sup> peak (ms)	$T_2$ (ms) <sup>a</sup>
SNEDDS	57.7	13.5	1.4	0.54	47.1
N1	54.1	13.5	1.4	0.65	38.8
N2	30.6	0.74	--	--	27.6
N3	18.5	3.2	0.57	--	17.1
N4	16.3	1.0	--	--	16.2
N5	11.1	1.0	--	--	14.9
N6	8.7	0.89	--	--	6.7
N7	3.8	0.74	--	--	4.3
N8	4.3	0.75	--	--	2.3
N-US2	0.30	--	--	--	--

<sup>a</sup>  $T_2$ -relaxation time was calculated by fitting the exponential decay curves.

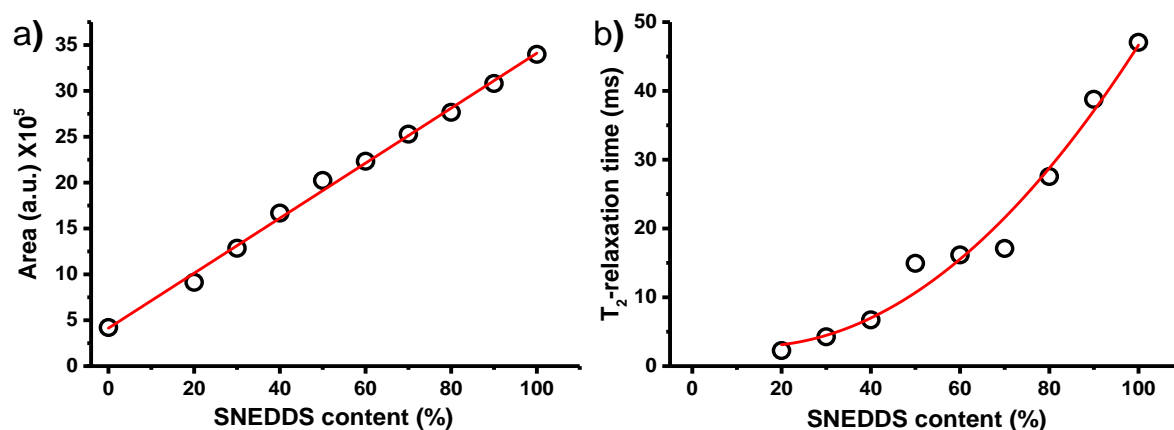


**Fig. 34** Effect of the semisolid SNEDDS content on the area under the  $T_2$ -relaxation time distribution curves (a) and the fitted  $T_2$ -relaxation time (b).  $T_2$ -relaxation time was calculated by fitting the exponential decay curves.

At 20 % N-US2 (N2), a shift in the  $T_2$ -relaxation time to a lower value was observed. Additionally, the main relaxation peak became broader and only two states could be observed. At 30 % N-US2 (N3), an intermediate mobility state could be observed. The three mobility states could be described as a slightly, moderately and strongly adsorbed SNEDDS depending on the strength of N-US2/SNEDDS physical interaction. Increasing the content of N-US2 (N4 – N8) resulted in the increase of the moderately to strongly adsorbed SNEDDS states area (**Fig. 35**).

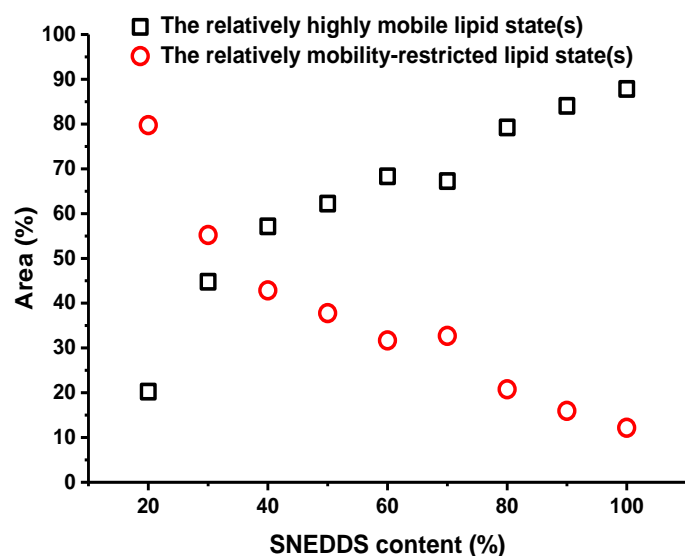


**Fig. 35** The relative areas of the relatively highly mobile and the relatively mobility-restricted stronger adsorbed lipid states.

This increase was almost linear ( $R^2 = 0.961$ ) until SNEDDS concentration of 30 % was achieved. At lower SNEDDS content (N8, 20 %), the influence of the adsorbed water on the distribution was more pronounced. High moisture content in the adsorbates could adversely affect the stability of the adsorbed SNEDDS and may precipitate the accompanied PWS. The influence of water could be reduced by heating N-US2 up to a constant weight prior to its utilization in the preparation of the S-SNEDDS. Above ~65 % of the N-US2, the strongly adsorbed state became the dominant one. In a previous study [235], the interaction between N-US2 and MCM was investigated in 3 different MCM concentrations. The  $T_2$ -relaxation time of MCM was shifted from ~200 ms to about (27, 7 and 2) ms, (26 and 7) ms and (32 and 10) ms upon MCM adsorption on N-US2 at a level of 30 %, 50 % and 70 % respectively. Compared to this study, it could be seen that the interaction between N-US2 and the liquid MCM was stronger than its interaction with the adsorbed semisolid SNEDDS. Due to its lower viscosity, MCM can deeply penetrates into the N-US2 nanopores with the subsequent increase in the strongly adsorbed state.

#### 4.3.4. Preparation of tablets for the preliminary studies

##### 4.3.4.1. Dispersibility

Semisolid and rubbery adsorbates (N1 – N3) were molded into tablet-like cylinders while freely flowable solid adsorbates (N4 – N8) were compressed into tablets. The produced tablets were dispersed into 0.1 N HCl and phosphate buffer pH 6.8 USP. Photos of selected dispersions are shown in **Fig. 36**. Molded tablets showed an acceptable dispersibility. Complete tablets dispersibility was accomplished within 2-3 h. On the other hand, compressed tablets were non-dispersible over 24 h (**Fig. 37**).

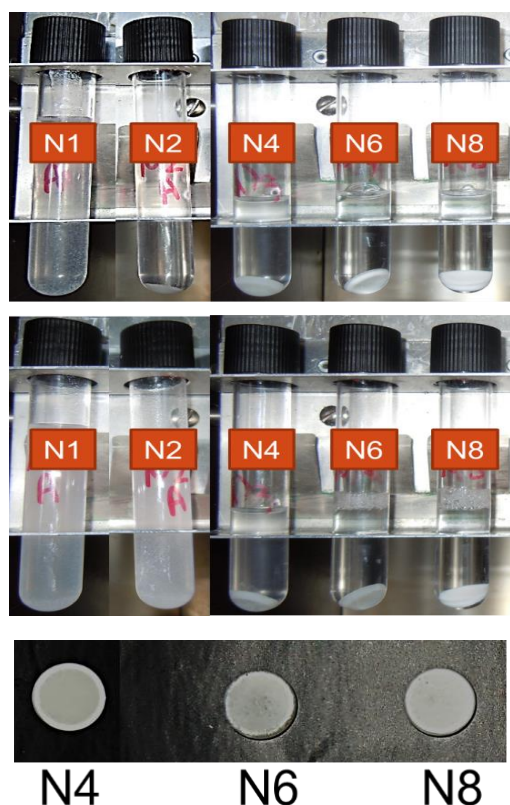


**Fig. 36** Photos of 1 % (m/V) dispersions of selected Neusilin® US2/SNEDDS tableted adsorbates in 0.1 N HCl after 15 min (above) and 180 min (below).

**Fig. 37** Photos of compressed N4, N6 and N8 adsorbates after 24 h incubation in 0.1 N HCl in an end over end mixer.

Desorption of the SNEDDS from the porous carrier is very critical for *in vivo* performance of the S-SNEDDS [263]. Ideal S-SNEDDS should be able to deliver the adsorbates in the form of fine dispersions so that rapid, complete exposure of SNEDDS to the aqueous media is ensured. SNEDDS-loaded tablets have a hydrophobic microenvironment because of the incorporated lipids [237]. Furthermore, moistened compressed silicates were reported to retard tablets disintegration by inhibiting moisture penetration into the tightly bonded silica particles [258]. In the case of molded tablets, the semisolid SNEDDS are typically outside the N-US2 nanopores. Therefore, they can readily disperse in the aqueous media. On the other hand, the SNEDDS are mostly inside the nanopores of the compressed N-US2 that displays retarded

water penetration. Therefore, the incorporation of a superdisintegrant is very essential to obtain an immediate SNEDDS dispersion.

#### 4.3.4.2. Effect of the disintegrant level on the fineness of the dispersion

Kollidon<sup>®</sup> CL-SF (CL-SF) was selected as a disintegrant. CL-SF is a water insoluble superdisintegrant that combines both swelling and wicking mechanisms. It occurs in porous granules with high specific surface area. CL-SF does not form gels upon water contact. Furthermore, it contributes to tablets hardness and reduces its friability due to its binding effect [344-346]. Three levels of CL-SF were mixed with N7 adsorbates and compressed into tablets: 5, 7.5 and 10 %. The appearance of the tablets dispersions after 10 and 60 min was microscopically evaluated (**Fig. 38**).

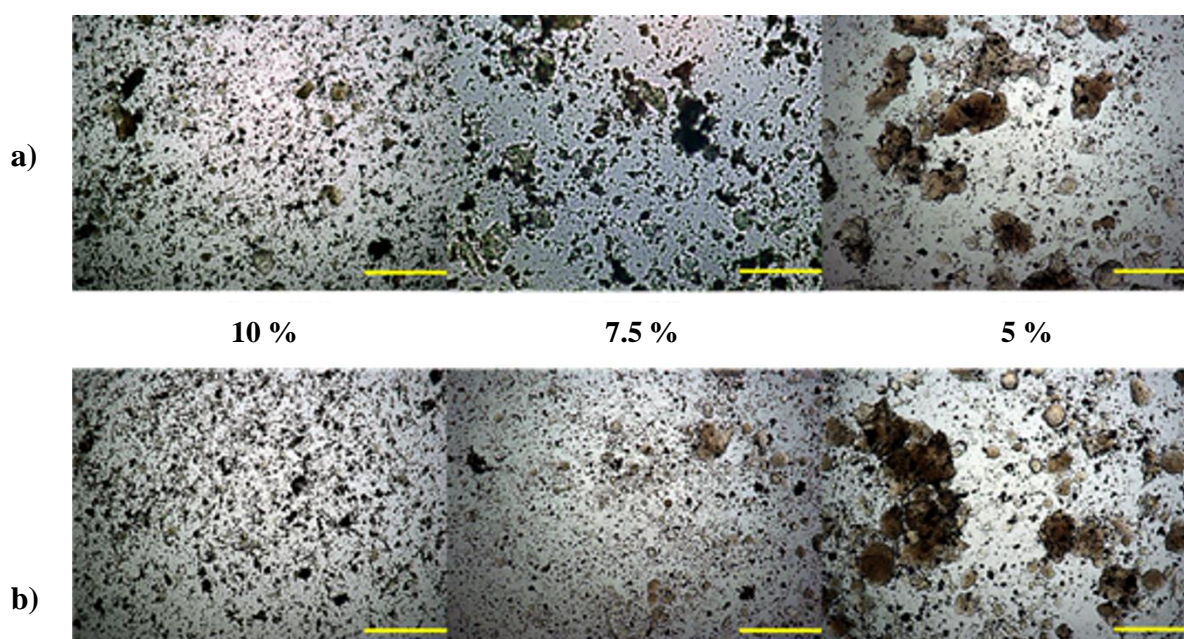


**Fig. 38** Effect of the disintegrant level on the fineness of the tablets dispersions after 10 min (a) and 60 min (b) in 0.1 N HCl. The yellow bar represents 500  $\mu$ m.

Tablets prepared with 10 % disintegrant were able to provide fine dispersions within 10 min. Longer time was required to obtain fine dispersions at a disintegrant level of 7.5 %. Tablets prepared with 5 % disintegrant did not provide fine dispersions for 2 hours. Accordingly, incomplete PWSD release is expected. Therefore, at least 7.5 % disintegrant is required to achieve high PWSD release rate. The pH of the media had no influence on the dispersion fineness.

#### 4.3.4.3. Effect of the compression force and tablets shape on the tablets properties

The compression force/pressure is a crucial parameter in preparing self-nanoemulsifying tablets. High compression forces always squeeze the lipids out of the adsorbates [238]. As a

result, tablets with oily surfaces are obtained. These tablets have lower patient palatability and are subjected to stability problems. On the other hand, insufficient compression forces yield tablets with unsatisfactory mechanical properties. Therefore, the selection of the optimum compression force is critical for the performance of the lipid-loaded tablets. T1 formulation (Table 14) was compressed into tablets at different compression forces (2-10 kN) corresponding to compression pressures (20-105 MPa). Two tablets shapes were also evaluated: the flat and the convex.

Optical microscopic images of the produced tablets are shown in Fig. 39. Increasing the compression force -more than 5 kN- resulted in tablets with excessive tablets chipping regardless to the tablets shape. The presence of the lipids on the tablets surface was non-avoidable and was dependent on the compression force. However, low surface lipids were observed below a compression force of 5 kN. Convex tablets were less prone to tablets chipping compared to the flat ones at 4 kN. However, their surface was rougher compared to the flat ones (Fig. 39b vs. a).

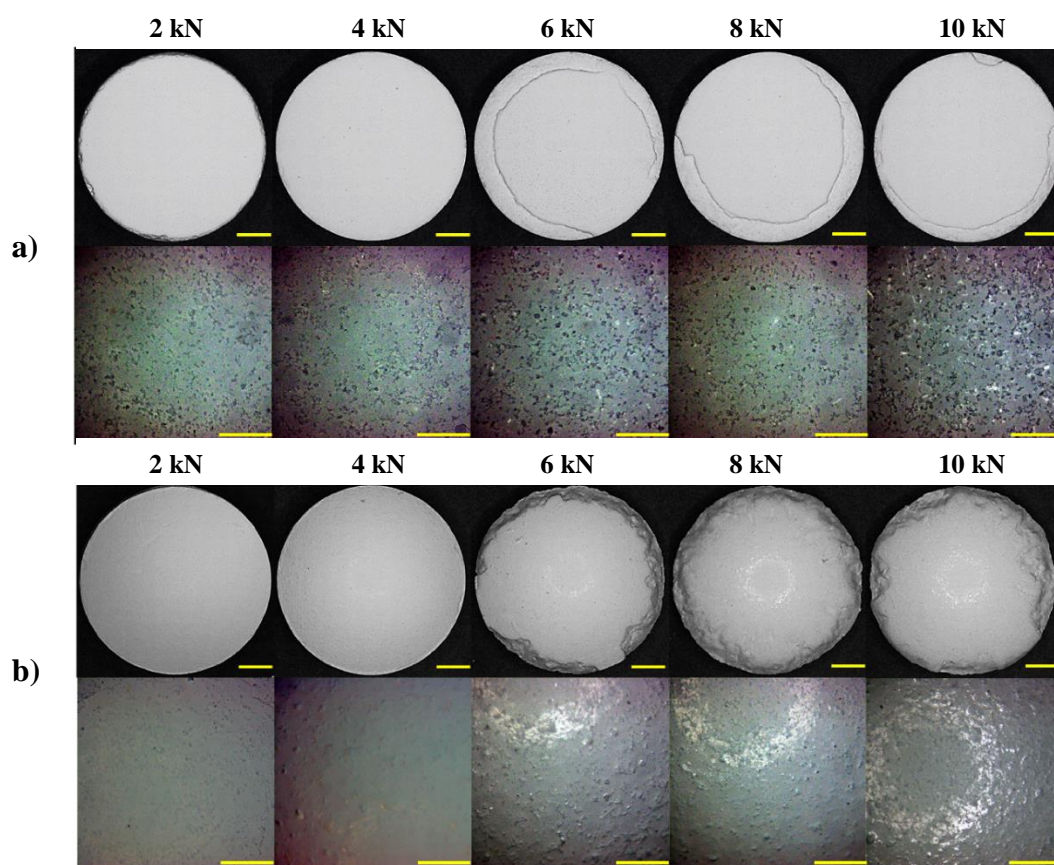


**Fig. 39** Optical microscopic images of flat (a) and convex (b) tablets prepared by compressing T1 formulation at different compression forces. The bar represents 2 mm (tablets, above) and 1 mm (surface, below).

The effect of the compression force on the physical properties of the produced SNEDDS tablets is illustrated in **Fig. 40**. Tableability is always assessed by the plot of the compression pressure against the tensile strength of the produced tablets [347]. Generally, tablets with tensile strength values of more than 1 MPa or hardness values of more than 50 N are considered to be adequate for handling and shelf-life. Low compression forces ( $\sim 2$  kN) yielded tablets with an unsatisfactory mechanical strength. Tablets with acceptable hardness and tensile strength were obtained at a compression force of 4-5 kN. Increasing the compression force resulted in an increase in tablets tensile strength (**Fig. 40** top right). However, massive tablets shipping was observed with a compression force above 5 kN.

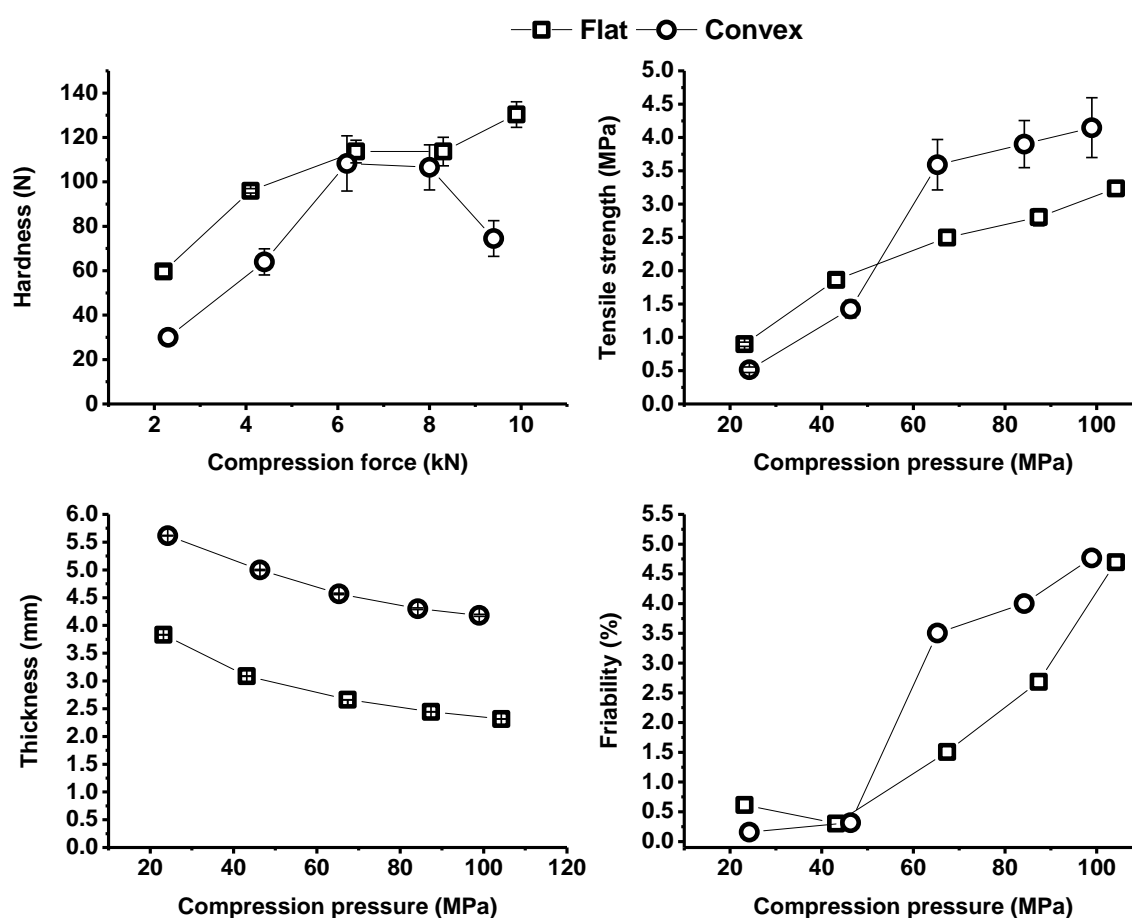


**Fig. 40** Effect of the compression force/pressure on the physical properties of the T1 tablets.

In one study, a compression pressure range of 45-135 MPa was considered to be adequate for the compression of SNEDDS-loaded N-US2 adsorbates in terms of tensile strength [237]. It is generally advisable that the compression pressure should be kept lower as possible. This could help reducing the lipid squeeze out, maintaining sufficient tablets porosity, minimizing the internal stress and elastic recovery and reducing the amount of the used disintegrant.

However, in contrary to this study, tablets with lower chipping were produced at higher compression pressure (up to 145 MPa) [237]. The difference between the 2 opposite behavior of the adsorbates upon increasing the compression pressure could be attributed to the difference in the nature (semisolid vs. liquid) and content (30 % vs. 50 %) of the incorporated SNEDDS that may lead to a difference in the N-US2/SNEDDS interaction strength (**Section 4.3.3.2**).

According to the USP, tablets with friability values of less than 1 % are considered to be acceptable. Only compression forces of less than 5 kN resulted in tablets with an acceptable friability. At lower compression forces (~2 kN), convex tablets showed a lower friability compared to the flat ones. The opposite behavior is observed at higher compression forces (**Fig. 40** bottom right). Increasing the compression force above 5 kN increases tablets chipping. Therefore, high weight loss percentage was calculated.

The effect of the compression force on the tablets thickness was 2 phasic. At lower compression forces (2-4 kN), the decrease in the tablets thickness was steeper than at higher compression forces. At a compression forces > 5 kN for flat tablets or 6 kN for convex ones, considerable lipid amount is probably squeezed out N-US2 granules to their surface. Therefore, the adsorbates compactability was partially hindered. Therefore, the slope of the curve is less steep than at lower compression forces (**Fig. 40** bottom left).

The disintegration of the tablets was not pronouncedly changed with the increase of the compression force and tablets shape (**Table 23**). Increasing the compression force retarded the disintegration time in terms of seconds and all tablets disintegrated within the first 2 min. Convex tablets disintegrated slower than flat ones at high compression force (~10 kN).

**Table 23** Effect of the compression force and pressure on the disintegration time of the T1 tablets.

Compression Force (kN)	Flat		Convex	
	0.1 N HCl	Phosphate Buffer pH 6.8	0.1 N HCl	Phosphate Buffer pH 6.8
2	< 30 s	< 30 s	< 30 s	< 30 s
4	< 30 s	< 30 s	< 30 s	< 30 s
6	< 45 s	< 45 s	< 45 s	< 45 s
8	< 60 s	< 75 s	< 60 s	< 60 s
10	< 60 s	< 90 s	< 120 s	< 120 s

#### 4.3.4.4. Lumogen® F305 release

In order to visualize the SNEDDS desorption process, Lumogen® F305 (F305) fluorescence dye was used as a PWSD model. F305 has a very high light and heat stability and a log P value of > 6.2 [348]. F305 was incorporated into T1 tablets (**Table 14**), which are composed of 10 %

CL-SF and N7 adsorbates (30 % SNEDDS). Tablets dispersibility was compared to the parent semisolid SNEDDS and N7 adsorbates (Fig. 41).

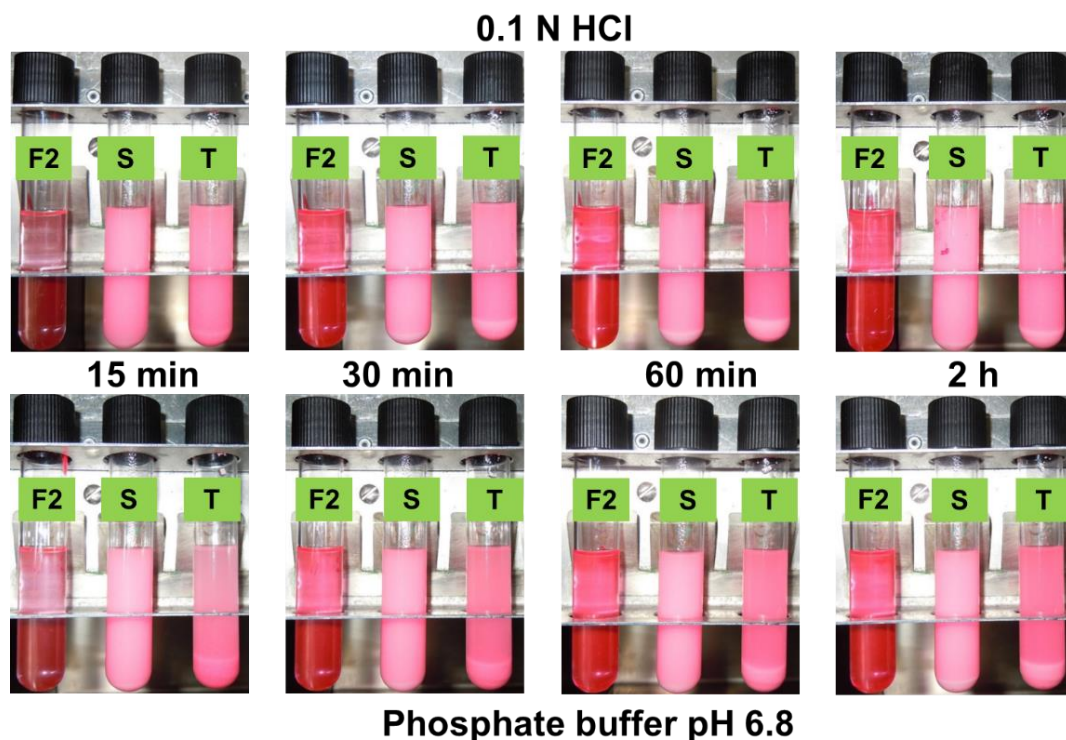


**Fig. 41** Photos of 1 % (m/V) dispersions of the semisolid SNEDDS (F2), the solid N7 adsorbates (S) and T1 tablets (T) in 0.1 N HCl (above) and phosphate buffer pH 6.8 USP (below). Lumogen<sup>®</sup> F305 was incorporated in the SNEDDS at a level of 0.2 % m/m.

F305-loaded SNEDDS were desorbed from the adsorbates and tablets. SNEDDS desorption rate was slower in the phosphate buffer pH 6.8 within the first 15 min compared to the 0.1 N HCl medium. After 2 h samples were centrifuged to separate N-US2 powder. Centrifuged samples did not show any color change between the parent SNEDDS, adsorbates and tablets. No pH-dependent dispersibility was observed.

#### 4.4. Incorporation of Progesterone

Progesterone was selected as a PWSD with a log P of 3.87 [349]. Progesterone is a steroid that is used in the treatment of many gynecological disorders [350]. It occurs in 2 polymorphic forms: form 1 ( $\alpha$ -form) and form 2 ( $\beta$ -form) [351]. Oral Progesterone administration is associated with poor bioavailability because of its very low water solubility as well as extensive hepatic first-pass metabolism [352]. Accordingly, Progesterone is a good candidate for SNEDDS-mediated bioavailability enhancement.



#### 4.4.1. Progesterone loading

The maximum solubility of a drug in its formulation limits the maximum drug load. **Table 24** shows the equilibrium solubility of Progesterone in excipients and the semisolid SNEDDS. DPHS is semisolid at room temperature and is not completely molten at 37 °C. Therefore, the measurements were performed at 50 °C. The Progesterone solubility in MCM was significantly higher than the other excipients. Progesterone solubility in DPHS was lower than HS15 despite its higher ester value. Surprisingly, increasing the ratio of DPHS in the formulations resulted in an increase in Progesterone solubility. The reason could be the enhanced mobility of DPHS in the formulation compared to its mobility alone observed in the ESR and <sup>1</sup>H-NMR study.

**Table 24** Equilibrium solubility of Progesterone in the excipients and the SNEDDS at 50 °C (mean ± SD, n=3).

Excipient/formulation	Progesterone solubility (µg/g)
Cithrol® DPHS	35.5 ± 2.3
Kolliphor® HS 15	55.7 ± 1.2
Capmul® MCM	104.7 ± 3.4
F1	49.0 ± 2.1
F2	54.8 ± 2.7
F3	64.6 ± 3.3

#### 4.4.2. Progesterone equilibrium solubility

Blank formulations were mixed with different dispersion media (1 % m/V) in order to assess the impact of their presence on Progesterone equilibrium solubility (**Fig. 42**). Furthermore, the solubility of Progesterone in bio-relevant dissolution media (FaSSIF and FeSSIF) was evaluated. Preliminary studies have shown that the solubility of Progesterone in the respective media did not change after 24 h of the incubation in the respective dissolution media. Therefore, the equilibrium solubility was conducted for 24 h. The solubility of Progesterone was pronouncedly enhanced when incorporated in FaSSIF and FeSSIF media compared to the bio-irrelevant ones. The presence of the SNEDDS, even at low concentration (1 % m/V), successfully enhanced the equilibrium solubility of Progesterone in all media. Despite the nearly same Progesterone solubility in both pH 1.2 and 6.8, a pronounced enhancement of the semisolid SNEDDS-mediated Progesterone equilibrium solubility was observed in 0.1 N HCl compared to phosphate buffer pH 6.8. The acid values of DPHS and MCM, which constitute the lipophilic core of the produced nanoemulsions, is ≤ 10 mg KOH/g and ≤ 4 mg KOH/g, respectively. Because the free carboxylic groups are protonated at the acidic pH, the polarity of the lipophilic core of the nanoemulsions is decreased with the subsequent increase of the

solubilization power to lipophilic drugs.

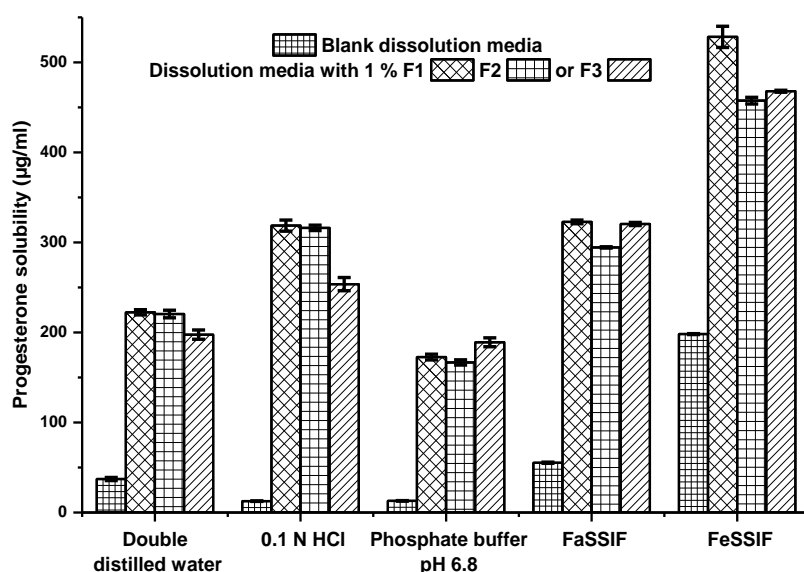


**Fig. 42** Equilibrium Progesterone solubility in different media in the presence of 1 % m/V dispersions of the different semisolid SNEDDS at 37 °C (mean  $\pm$  SD, n=3).

#### 4.4.3. Differential scanning calorimetry (DSC)

In order to assess the influence of Progesterone incorporation on the physical state and melting behavior of the semisolid SNEDDS (F2), DSC thermograms of Progesterone-loaded SNEDDS, Progesterone and the parent semisolid SNEDDS were evaluated (**Fig. 43**).

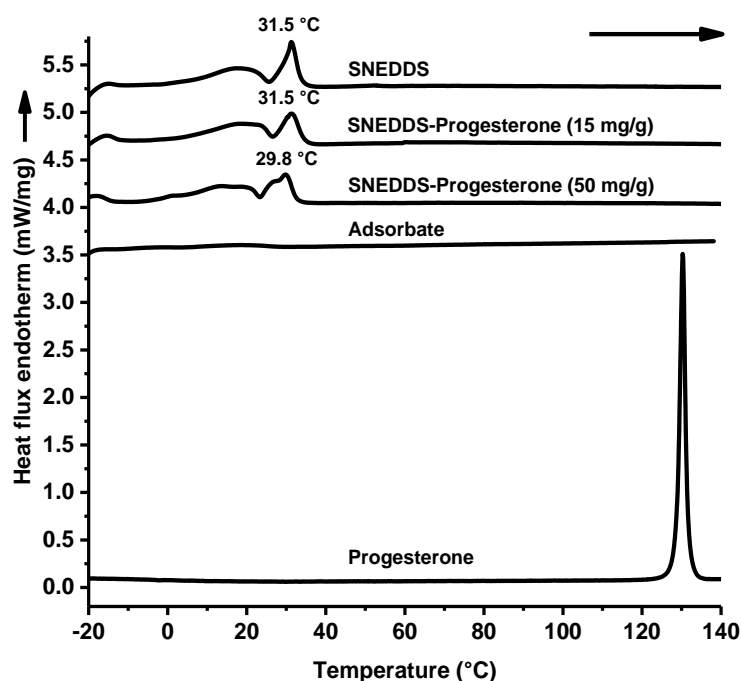


**Fig. 43** Heating DSC thermograms of the semisolid SNEDDS, Progesterone-loaded semisolid SNEDDS, its N7 adsorbates and Progesterone.

Two levels of Progesterone were tested: 15 mg/g and 50 mg/g. The physical state and the melting point were not affected by the incorporation of Progesterone at the level of 15 mg/g. However, a depression in the SNEDDS melting point was observed at the level of 50 mg/g. The

reduction of the melting point at the higher Progesterone content was expected as the molecularly dissolved Progesterone may act as a solute or impurity in the semisolid SNEDDS with the consequent depression of their melting point. Progesterone showed a melting endotherm at about 130 °C, which can be detected even in low sample weight (0.3 mg). Neither Progesterone-loaded semisolid SNEDDS nor N7 adsorbates showed the melting endotherm of the pure Progesterone. The absence of this characteristic melting endotherm is always interpreted in the direction of its molecular solubility. However, Progesterone could be also solubilized in the freshly molten SNEDDS during DSC measurement. Therefore, DSC cannot be used to confirm the solubility of Progesterone in the SNEDDS.

#### 4.4.4. Powder X-ray diffraction (PXRD)

PXRD was used to evaluate the solid state of the semisolid Progesterone-loaded SNEDDS (F2) and its adsorbates as well as Progesterone solubility in the SNEDDS (**Fig. 44**). The PXRD patterns of the excipients (DPHS and HS15) are shown in **Fig. S7** of the supplementary data. Based on the chemical composition, X-ray signals from lipid structures and from PEG-chains can be expected to occur. The diffraction pattern of the SNEDDS revealed the presence of broad signals between 15-30 °(2 $\theta$ ), which reflect the short spacings. The signals can be used to evaluate the cross-sectional packaging of the lipid hydrocarbon and PEG chains. Short spacing is independent on the chain length and can be used to characterize the polymorphism of lipids [353, 354]. Two stronger signals were observed at 4.6 Å and 3.8 Å. Overall, the signals indicate a partial amorphous/liquid and partial crystalline system with a superposition of different spacings. Due to the chemical composition of the excipients, the formation of crystals with very well-defined spacings and small line widths is not expected. The presence of an amorphous or a liquid part in the semisolid SNEDDS could be advantageous. It is generally well known that crystalline structures are not able to accommodate foreign molecules. Therefore, crystallization leads to drug expulsion [44, 355]. PXRD pattern of Progesterone conformed to the diffraction pattern of the orthorhombic Progesterone form 1 [351]. Progesterone-loaded SNEDDS retained the same diffraction pattern of the parent SNEDDS and did not show any diffraction pattern related to Progesterone. However, under this experimental setup, the solubility of Progesterone in the semisolid SNEDDS could not be confirmed because of its low concentration. A physical mixture between MCC and Progesterone at the same concentration (15 mg/g) did not also show the strong diffraction pattern of the Progesterone due to the low amount of the drug (insufficient sensitivity) (**Fig. S8** of the supplementary data). Being amorphous, N-US2 did not show any

diffraction pattern. PXRD pattern of Progesterone-loaded N7 adsorbates showed only the amorphous part. No evidence of lipid crystallinity was detected in the N7 adsorbates (**Fig. 31**).

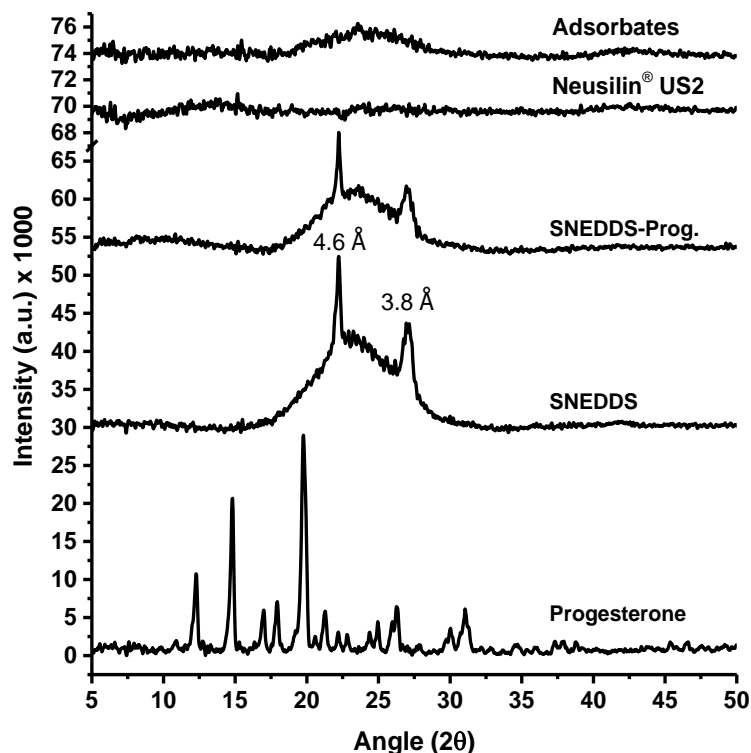


**Fig. 44** PXRD patterns of the semisolid SNEDDS, semisolid Progesterone-loaded SNEDDS, its N7 adsorbates, Neusilin® US2 and Progesterone.

#### 4.4.5. Fourier transform infrared spectroscopy (FTIR)

FTIR was used to study the interaction between the semisolid SNEDDS and Progesterone as well as between the adsorbed semisolid Progesterone-loaded SNEDDS and N-US2 (**Fig. 45**). FTIR spectra are typically composed of two regions: the fingerprint region (below  $1500\text{ cm}^{-1}$ ) and the function group region (above  $1500\text{ cm}^{-1}$ ). Progesterone fingerprint region conformed to the Progesterone polymorph 1 [351]. Furthermore, its FTIR spectrum showed 3 strong peaks at  $1615\text{ cm}^{-1}$  (C=C stretch),  $1661\text{ cm}^{-1}$  (conjugated cyclic C=O stretch) and  $1698\text{ cm}^{-1}$  (non-conjugated aliphatic methyl C=O stretch) as well as broad band at  $2975\text{--}2850\text{ cm}^{-1}$  corresponding to the skeleton C-H stretch [356]. The strong peaks in the semisolid SNEDDS were assigned according to the guidelines developed by Guillén and Cabo for the lipids FTIR [357]. Three strong peaks were observed at  $2922\text{ cm}^{-1}$  ( $\text{CH}_2$ , asymmetric stretch),  $2854\text{ cm}^{-1}$  ( $\text{CH}_2$ , symmetric stretch) and  $1733\text{ cm}^{-1}$  (C=O, ester stretch). Additionally, a broad peak at  $3474 \pm 5.4\text{ cm}^{-1}$  (OH) was observed. Progesterone-loaded semisolid SNEDDS showed a little deviation in the SNEDDS fingerprint region and a significant (t-Test,  $\alpha = 0.05$ ,  $n = 3$ ) shift in the OH region ( $3461 \pm 0.3\text{ cm}^{-1}$ ). This shift could be due to the intermolecular H-bonding between Progesterone and the SNEDDS and can prove Progesterone solubilization in the

SNEDDS. FTIR spectra of the N7 adsorbates demonstrated no chemical interactions between the SNEDDS and N-US2. The OH region of the adsorbates spectrum was shifted compared to both N-US2 and semisolid SNEDDS suggesting H-bond formation between the free silanol groups in N-US2 and the adsorbed SNEDDS. This physical interaction conformed to the effect observed by the BT-NMR study (**Fig. 33**).

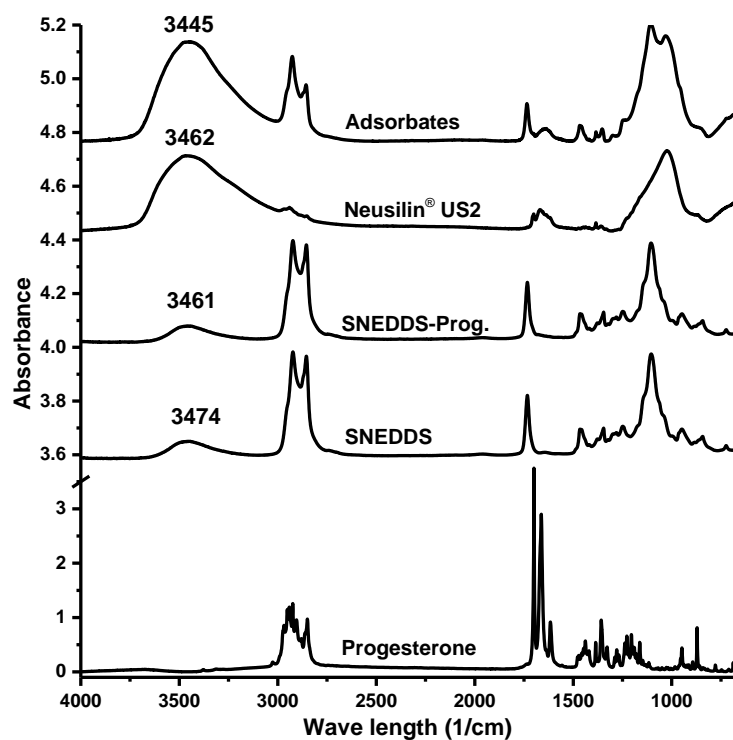


**Fig. 45** FTIR spectra of the semisolid SNEDDS, semisolid Progesterone-loaded SNEDDS, its N7 adsorbates, Neusilin® US2 and Progesterone.

#### 4.5. Powder properties

Lipid-loaded adsorbates showed in some cases poor flowability [347]. Modern tableting machines are operated at high speed. Therefore, excellent flowability is an essential property in order to ensure acceptable tablets weight uniformity [358]. The flowability of N-US2 as well as its Progesterone-loaded and progesterone-free adsorbates (30-50 % SNEDDS) was evaluated using angle of repose, compressibility index (CI) and Hausner ratio (HR). The flow properties as well as bulk and tapped densities of the SNEDDS adsorbates are summarized in **Table 25**.

Due to its spherical form and relatively large particle size (60-120  $\mu\text{m}$ ) [232], N-US2 showed an excellent angle of repose. At 30-50 % SNEDDS content, the SNEDDS are mainly located in the nanopores of N-US2 (**Fig. 33**). Consequently, the angle of repose was not pronouncedly affected by the incorporation of the semisolid SNEDDS and all adsorbates had a comparable, excellent flowability to N-US2. As expected, the bulk and tapped density increased with the increase of the SNEDDS content in the adsorbates. During the tableting process, a powder arch is always developed in the powder hopper. The breaking down of this arch is essential for the

effective tabletability and is dependent on the powder cohesiveness, moisture content, powder density as well as particle shape and size. Measuring CI and HR mirrors the straightforwardness of the arch breaking [359]. Lower CI and HR values reflect better flowability while higher values reflect lower flowability [280, 281]. N-US2 showed a good CI and HR. However, increasing the SNEDDS content within the adsorbates negatively affected the adsorbates CI and HR. Incorporation of Progesterone did not significantly influence the angle of repose. However, Progesterone incorporation seems to have an effect on the CI and HR. Progesterone-loaded adsorbates have a lower tapped density, compared to the Progesterone-free ones. Therefore, they have higher calculated CI and HR.

**Table 25** The flow properties, density and compressibility of Neusilin<sup>®</sup> US2 and the adsorbates.

Code	Angle of repose (degree)		Density (g/ml)		Compressibility index (%)		Hausner ratio	
	Value <sup>a</sup>	Classification <sup>b</sup>	Bulk	Tapped	Value	Classification <sup>b</sup>	Value	Classification <sup>b</sup>
N-US2	21.7	Excellent	0.17	0.20	14.66	Good	1.17	Good
30 %	22.0	Excellent	0.24	0.32	24.39	Passable	1.25	Fair
30 % – P	20.9	Excellent	0.24	0.27	13.10	Good	1.15	Good
40 %	23.4	Excellent	0.26	0.37	28.13	Poor	1.39	Poor
40 % – P	21.4	Excellent	0.27	0.32	16.25	Fair	1.19	Fair
50 %	23.5	Excellent	0.33	0.47	30.65	Poor	1.44	Poor
50 % – P	21.7	Excellent	0.31	0.37	15.38	Good	1.18	Good

<sup>a</sup> Mean, n = 5.

<sup>b</sup> The classification was made according to USP 32 and EP 8.0 [280, 281].

#### 4.6. Preparation and characterization of the self-nanoemulsifying tablets

Based on the aforementioned findings, compression pressures of 45-55 MPa were found to yield tablets with acceptable physical properties and low surface lipids. Furthermore, at this compression pressure range, tablets with convex shape showed a lower degree of tablets chipping than the flat ones. Therefore, convex tablets shape and ~50 MPa compression pressure were selected for further SNEDDS tablets preparation. The composition of the self-nanoemulsifying tablets is summarized in **Table 14**. Adsorbates containing 30-50 % of the semisolid SNEDDS were mixed with 10 % CL-SF (T1, T3 and T6). Kollidon<sup>®</sup> 90 F was also tested at a level of 2.5 % as a dry binder to reduce the tablets chipping and to increase the tablets tensile strength (T2, T4 and T6).

##### 4.6.1. Powder properties

The powder properties of the prepared formulations are summarized in **Table 26**. All formulations showed a passable CI (22-25 %) and HR (1.28-1.33). Incorporation of CL-SF into

the tablets formulations influenced the powder density and outweighed the negative effect on the CI and HR that was observed upon increasing the content of the semisolid SNEDDS in the adsorbates (**Table 25**). Progesterone and Kollidon® 90 F incorporation had only a very slight effect on the powder properties.

**Table 26** The density and compressibility of the self-nanoemulsifying tablets formulations.

Code	Density (g/ml)		Compressibility index (%)		Hausner ratio	
	Bulk	Tapped	Value	Classification <sup>a</sup>	Value	Classification <sup>a</sup>
T1	0.23	0.30	23.53	Passable	1.31	Passable
T1 – P	0.22	0.28	23.33	Passable	1.30	Passable
T2	0.24	0.31	24.39	Passable	1.32	Passable
T2 – P	0.22	0.29	22.09	Passable	1.28	Passable
T3	0.23	0.31	25.00	Passable	1.33	Passable
T3 – P	0.24	0.32	23.75	Passable	1.31	Passable
T4	0.24	0.32	24.39	Passable	1.32	Passable
T4 – P	0.25	0.32	22.50	Passable	1.29	Passable
T5	0.28	0.37	22.81	Passable	1.30	Passable
T5 – P	0.27	0.36	24.66	Passable	1.33	Passable
T6	0.30	0.38	22.58	Passable	1.29	Passable
T6 – P	0.28	0.36	23.61	Passable	1.31	Passable

<sup>a</sup>The classification was made according to USP 32 and EP 8.0 [280, 281].

#### 4.6.2. Physical properties and optical microscopy

The physical properties of the Progesterone-loaded and Progesterone-free tablets are summarized in **Table 27**. Formulation containing 30-40 % of the SNEDDS-loaded adsorbates (T1 – T4) were successfully compressed into tablets with acceptable physical properties (**Fig. 46**). All tablets had adequate hardness and tensile strength. Incorporation of Kollidon® 90 F did not show pronounced tensile strength enhancement at the tested compression pressure. Progesterone containing tablets were less friable than Progesterone-free ones despite the lower tensile strength (**Table 27**).

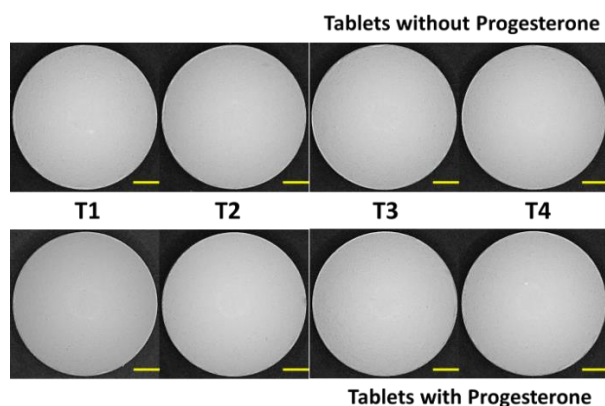


**Fig. 46** Optical microscopic images of the convex tablets prepared by compressing T1 – T4 formulations containing either 27 % or 36 % of the semisolid SNEDDS. The bar represents 2 mm.

**Table 27** Hardness, thickness, tensile strength and friability of the self-nanoemulsifying tablets.

Code	Hardness (N)	Thickness (mm)	Tensile Strength (MPa)	Friability (%)
T1	66.3 ± 5.3	4.96 ± 0.02	1.59 ± 0.13	0.16
T1 – P	61.5 ± 3.4	5.09 ± 0.01	1.40 ± 0.08	0.08
T2	67.3 ± 6.5	4.93 ± 0.02	1.61 ± 0.15	0.47
T2 – P	58.3 ± 4.4	5.08 ± 0.01	1.24 ± 0.09	0.16
T3	53.8 ± 3.4	4.82 ± 0.00	1.49 ± 0.08	0.24
T3 – P	50.3 ± 3.4	4.83 ± 0.01	1.28 ± 0.09	0.08
T4	46.5 ± 2.4	4.76 ± 0.02	1.37 ± 0.07	0.24
T4 – P	50.0 ± 3.0	4.80 ± 0.01	1.43 ± 0.09	0.08

On the other hand, the compression of formulations containing 50 % of the SNEDDS-loaded adsorbates (T5 and T6) resulted in tablets with massive chipping (**Fig. 47**). The tablets chipping could be probably avoided by using tablets shape without any sharp edges.

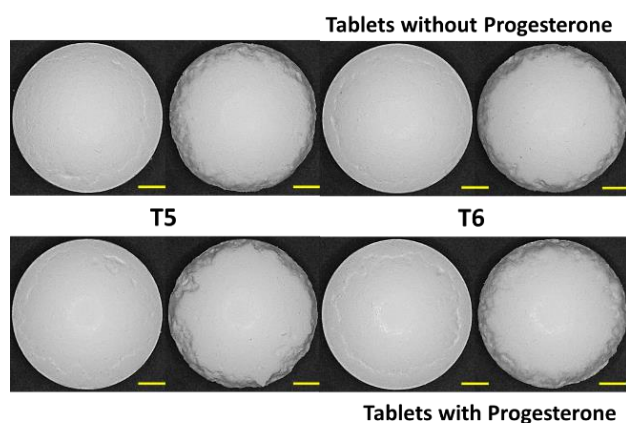


**Fig. 47** Optical microscopic images of the convex tablets prepared by compressing T5 and T6 formulations containing 45 % of the semisolid SNEDDS. All tablets showed massive tablets chipping that could be easily removed by the hand (right images). The bar represents 2 mm.

#### 4.6.3. Droplet size distribution

Progesterone was incorporated in the SNEDDS at a level of 15-27 mg/g. Furthermore, Progesterone loaded N7 adsorbates (15 mg/g) were prepared and compressed into T1 tablets. The selection of these Progesterone levels was based on its equilibrium solubility assessed in **Section 4.4.2**. At this level, no Progesterone precipitation is expected upon dilution in the three test media (double distilled water, 0.1 N HCl and phosphate buffer pH 6.8). Progesterone remained in the solubilized state in the semisolid SNEDDS and no phase separation or crystallization was observed upon storage of the Progesterone-loaded semisolid SNEDDS at 23°C for few months. The droplet size distribution of 1 % m/V dispersions of the semisolid SNEDDS, N7 adsorbates and T1 tablets in different media at 37 °C is summarized in **Table 28**. 1 % m/V dispersions of the semisolid SNEDDS (F2 formulation) showed monomodal volume distributions in all media with an average hydrodynamic diameter of less than 25 nm. The effect of the ionic strength, pH and filtration on the droplet size distribution of the SNEDDS



nanodispersions was minimal (**Section 4.2.5.1**). Centrifugation of the samples (12045 g / 5 min) resulted in the reduction of the PDI with a minor change in the Z-average. The lipid recovery after centrifugation ranged from 94 % to 99 % depending on the dispersion media. Higher lipid recovery was observed in double distilled water and phosphate buffer pH 6.8 media compared to 0.1 N HCl medium. Incorporation of Progesterone did not cause a pronounced change in the average hydrodynamic diameter. Furthermore, centrifuged dispersions of adsorbates and tablets did not show a pronounced change in the droplet size compared to the centrifuged SNEDDS nanodispersions in the three tested media.

**Table 28** Average droplet size diameter of the nanoemulsions produced by dispersing 1 % (m/V) of the semisolid SNEDDS, N7 adsorbates and T1 tablets in different media measured by dynamic light scattering at 37 °C (mean, n=3).

Formulation	Double distilled water		0.1 N HCl		Phosphate buffer pH 6.8	
	Z-average (nm)	PDI	Z-average (nm)	PDI	Z-average (nm)	PDI
SNEDDS	18.2	0.245	21.5	0.299	21.7	0.272
SNEDDS – Cent. <sup>a</sup>	17.8	0.150	19.1	0.090	21.2	0.114
SNEDDS – P	20.1	0.214	23.5	0.287	23.2	0.262
SNEDDS – P – Cent. <sup>a</sup>	19.3	0.167	20.1	0.122	21.2	0.117
Adsorbates <sup>a</sup>	16.6	0.178	18.9	0.107	16.7	0.185
Adsorbates – P <sup>a</sup>	18.3	0.259	20.8	0.205	19.4	0.145
Tablets <sup>a</sup>	18.9	0.233	20.2	0.213	17.3	0.200
Tablets – P <sup>a</sup>	20.3	0.124	21.4	0.235	18.6	0.178

<sup>a</sup>The samples were centrifuged at 12045 g for 5 min.

#### 4.6.4. Benchtop nuclear magnetic resonance (BT-NMR)

BT-NMR was used to study the desorption process of the semisolid SNEDDS from both Progesterone-loaded N7 adsorbates and T2 tablets. The dispersion media were composed of 0.1 N deuterated HCl in D<sub>2</sub>O and phosphate buffer pH 6.8 prepared in D<sub>2</sub>O. T<sub>2</sub>-relaxation time distributions of different 5 % m/V dispersions are shown in **Fig. 48**. Deuterated dispersion media were chosen to avoid the contribution of the water protons to the BT-NMR signals. The contribution of the buffer salts to the signal was very low (**Fig. 48a**). Compared to the semisolid SNEDDS, the T<sub>2</sub>-relaxation time distributions of both adsorbates and tablets were shifted to lower mobility because of the strong physical interaction with the nanoporous carrier (N-US2). Compression of the N7 adsorbates even increased the strength of the interaction (**Fig. 48a**). Indeed, the T<sub>2</sub>-relaxation time distributions of the T2 tablets were slightly shifted to lower mobility. Upon the dispersion of the semisolid SNEDDS in D<sub>2</sub>O, the main T<sub>2</sub>-relaxation time distribution peak was shifted to lower mobility. The dispersion of the SNEDDS into the aqueous

phase is associated with the formation of various lipids states that have different degrees of mobility. At high dilution level such as 95 %, lipids could be localized in the nanodroplets core, lipid/water interface and/or in the bulk aqueous phase as free amphiphiles monomers. Therefore, a superposition of various mobility states was observed in the SNEDDS nanodispersions with the subsequent broadening of the main lipid  $T_2$ -relaxation time peak (**Fig. 48a**). Due to the large interfacial area of the nanodroplets, it is believed that the interfacial lipids have the highest contribution to the  $T_2$ -relaxation time distribution. Compared to the melted SNEDDS, interfacial lipids have lower mobility (**Fig. 19 vs. Fig. 48a**).

The  $T_2$ -relaxation time distributions of the SNEDDS nanodispersions in deuterated 0.1 N HCl and deuterated phosphate buffer have also shown a superposition of several mobility states. A physical mixture between Progesterone and N-US2 showed a small contribution of Progesterone to the  $T_2$ -relaxation time distributions that was masked by SNEDDS superposition (**Fig. 48c and d**). Two main  $T_2$ -relaxation time peaks could be observed in the distribution curves: State A and State B. State A represents the relatively higher mobility lipid species while State B represents the relatively mobility-restricted ones. In addition, due to the exchange between the deuterated protons and some lipids protons, a small water peak could be observed at ~1000 ms (denoted as (W) in **Fig. 48b**). Increasing the dispersion time of the semisolid SNEDDS from 60 min to 120 min allowed better dispersibility with the consequent shift of the distribution peaks to higher mobility states (**Fig. 48b**). Furthermore, the ratio of the State A: State B areas increased with the increase of the dispersion time (**Table 29**). In addition, the distribution peaks were broader in the case of the phosphate buffer dispersions at 60 min compared to the 0.1 N HCl ones. The  $T_2$ -relaxation time distributions of both adsorbates and tablets were more or less comparable to the SNEDDS nanodispersions (**Fig. 48c and d**). However, both State A and B were shifted towards lower mobility.

After 120 min of the dispersion, the ratios between the 2 mobility states areas did not pronouncedly change between adsorbates and tablets and was comparable to those of SNEDDS nanodispersions at 60 min (**Table 29**). However, a slight increase in the State A areas was observed in adsorbates compared to tablets. Based on the relative area calculations, it could be assumed that the release of the SNEDDS after 2 h from both adsorbates and tablets was about 89-93 %. As observed in the SNEDDS nanodispersions, broader State A distributions were observed in phosphate buffer compared to 0.1 N HCl.

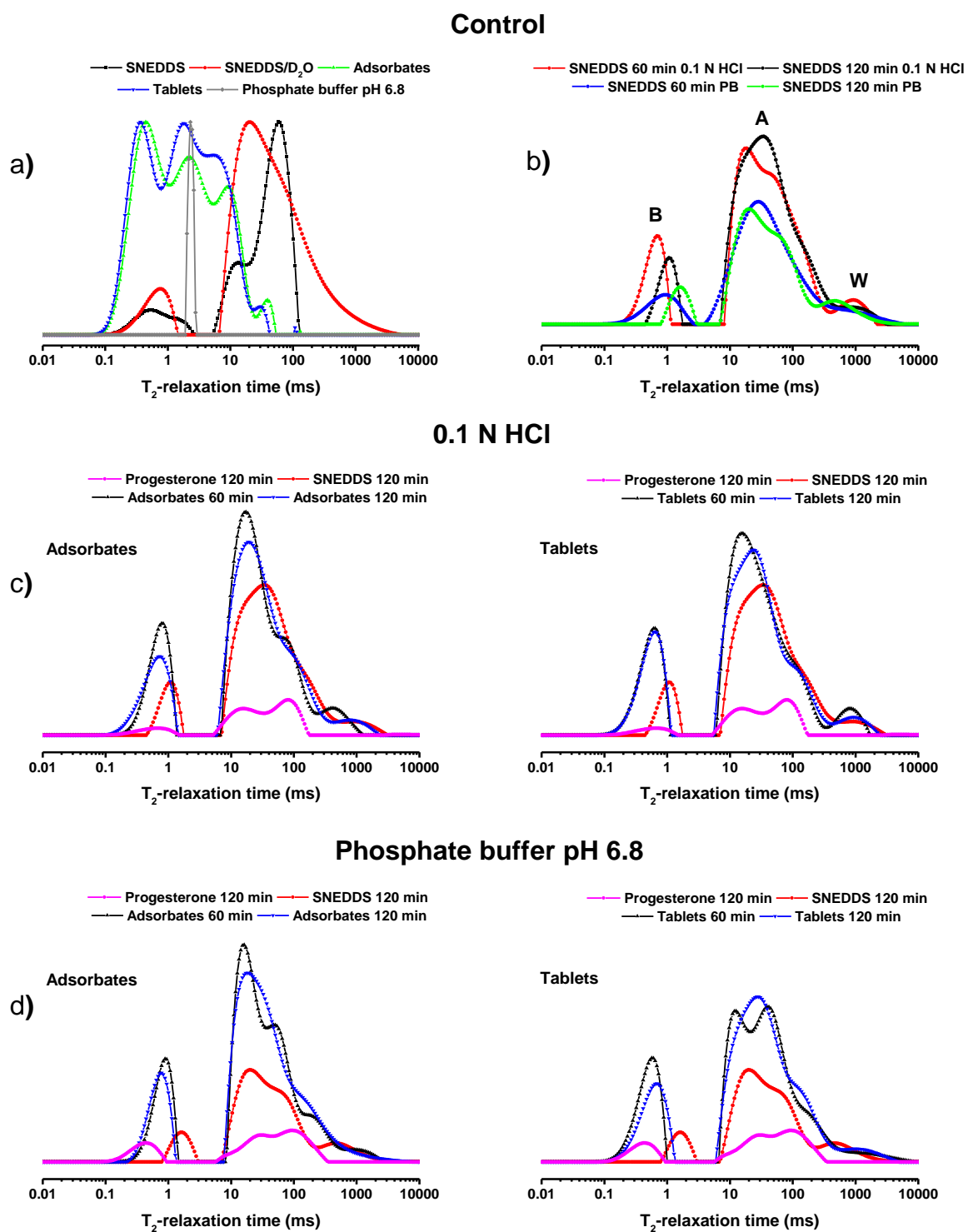


**Fig. 48**  $T_2$ -relaxation time distributions of the Progesterone-loaded semisolid SNEDDS (b), N7 adsorbates and T2 tablets after the dispersion for 60 min and 120 min in deuterated 0.1 N HCl (c) and deuterated phosphate buffer pH 6.8 (d) at 37 °C. The first figure (a) represents the  $T_2$ -relaxation time distributions of the anhydrous semisolid SNEDDS, N7 adsorbates and T2 tablets as well as the deuterated buffer and the SNEDDS nanodispersions in deuterated water. The distributions curves (a) were normalized to the same amplitude of the highest peak.

**Table 29** Percentage of State A and B in the T<sub>2</sub>-relaxation time distributions of the Progesterone-loaded semisolid SNEDDS, N7 adsorbates and T2 tablets after dispersion in deuterated 0.1 N HCl and deuterated phosphate buffer pH 6.8 at 37 °C.

Time (min)	SNEDDS		Adsorbates		Tablets	
	State A	State B	State A	State B	State A	State B
<b>Deuterated 0.1 N HCl</b>						
60	84.7	15.3	80.4	19.6	80.2	19.8
120	90.4	9.6	81.9	18.1	80.0	20.0
<b>Deuterated phosphate buffer pH 6.8</b>						
60	84.0	16.0	82.9	17.1	79.7	20.3
120	90.7	9.3	84.2	15.8	82.2	17.8

#### 4.6.5. *In vitro* drug release

Progesterone-loaded T2 tablets (15 mg/g) were selected for the release study. The release profile of Progesterone was evaluated in different media (0.1 N HCl, phosphate buffer pH 6.8 USP, FaSSIF and FeSSIF) in an end over end mixer (**Fig. 49**). The dashed lines represent the equilibrium solubility of Progesterone in the corresponding media. The semisolid SNEDDS, N7 adsorbates and T2 tablets were able to enhance the Progesterone solubility in all media. As expected, Progesterone release rate was in the order of SNEDDS > adsorbates > tablets.

In 0.1 N HCL, Progesterone-loaded SNEDDS were completely released from tablets and adsorbates within 2 h. In phosphate buffer pH 6.8, precipitation of Progesterone was observed from the semisolid SNEDDS. The maximum amount of Progesterone that remained dissolved was about 85 % of the loaded dose. Compared to the semisolid SNEDDS, the release of Progesterone from the adsorbates was completed within 1 h whereas incomplete Progesterone release was observed from the tablets. The Progesterone release from the tablets was much slower in phosphate buffer than in 0.1 N HCl. The reason could be the relatively slower SNEDDS dispersibility in buffer compared to acid media and the formation of gel-like intermediates during the SNEDDS dispersibility in the buffer media that may clog N-US2 nanopores with subsequent reduction of the release rate and extent [237]. This dispersion pattern was only observed in the phosphate buffer media. The release rate of Progesterone-loaded SNEDDS from tablets and adsorbates in the bio-relevant media was faster compared to the bio-irrelevant media. Bio-relevant media contain PL and BS mixed micelles that interact with the released SNEDDS and Progesterone. This interaction hinders the release of the Progesterone-loaded SNEDDS. Complete Progesterone release from tablets and adsorbates was observed in both FaSSIF and FeSSIF media. The release rate was higher in the fed state

(FeSSIF) medium compared to the fasted state (FaSSIF) medium due to the higher proportion of both PL and BS.

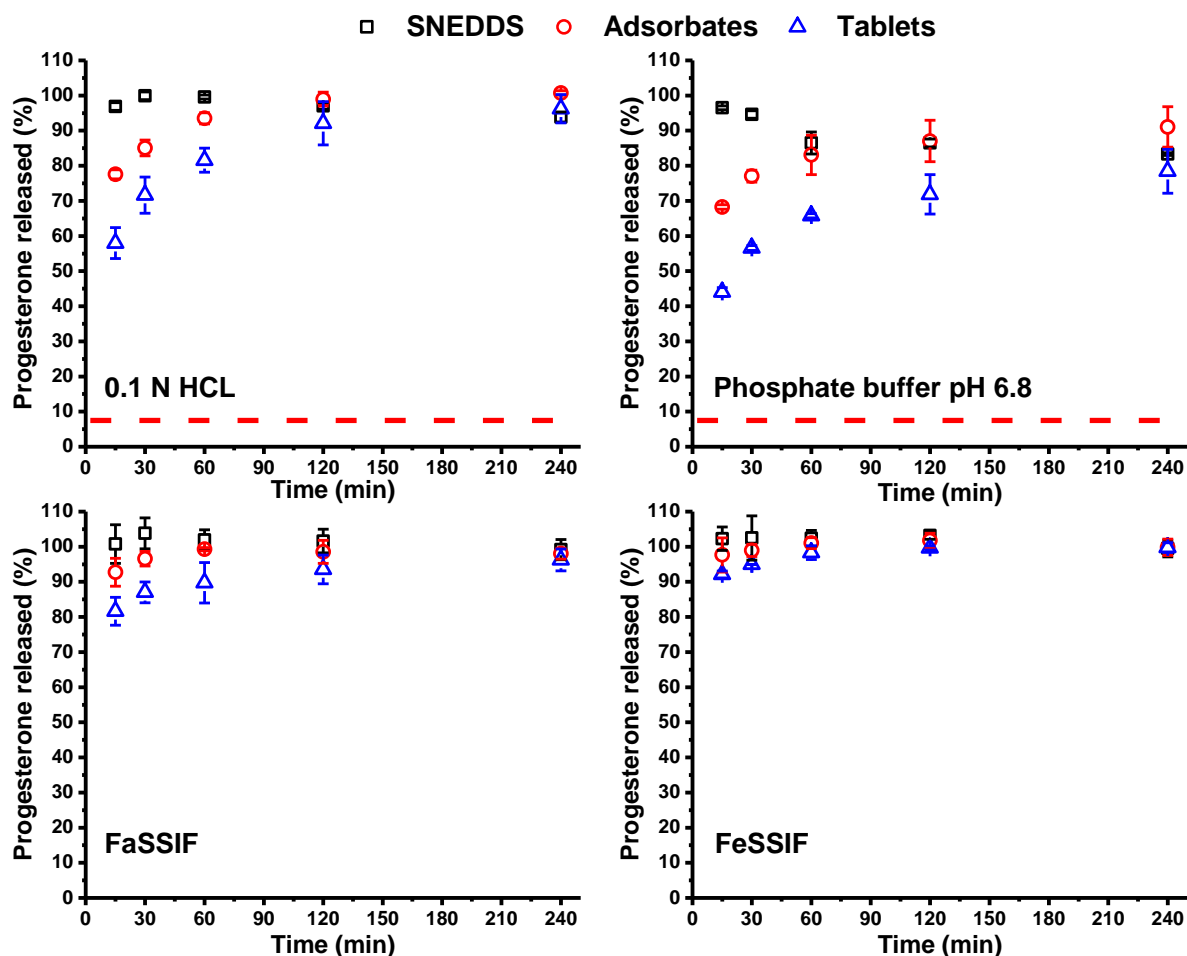


**Fig. 49** Percentage of Progesterone released (or remained dissolved) after the 1 % (m/V) dispersion of the Progesterone-loaded semisolid SNEDDS, N7 adsorbates and T2 tablets in 0.1 N HCl, phosphate buffer pH 6.8 USP, FaSSIF and FeSSIF media (mean  $\pm$  SD, n=3). The dashed line represents the equilibrium solubility of Progesterone in the SNEDDS-free medium.

#### 4.7. *In vitro* lipid digestion

Oral administration of lipids stimulates the secretion of several lipolytic enzymes. Examples are HGL, HPL, PLA2, CEH and PLRP2. Lipolytic enzymes hydrolyze the lipids ester bonds. For example, TG are hydrolyzed into two free FA and 2-MAG [52]. The breakdown products are then incorporated in the bile mixed micelles with the subsequent increase of its PWSDs solubilization capacity. However, lipid digestion might also decrease the PWSDs solubilization capacity of the carrier and - as a consequence - PWSD precipitation might occur. Therefore, *in vitro* lipid digestion studies, using bio-relevant dissolution media, are recommended to evaluate the performance of SNEDDS [265, 271-273].

#### 4.7.1. Digestibility of the excipients

##### 4.7.1.1. Preparation and particle size of the excipient dispersions

Lipases work on the oil/water interface [360], which is highly affected by the droplet size. Therefore, the droplet size distributions of the excipient dispersions (1 % m/V) were evaluated by either static or dynamic laser diffraction (**Table 30**). MCM formed unstable dispersions in Sorensen's phosphate buffer pH 6.8, which have a very broad droplet size distribution and is dependent on the agitation speed. Furthermore, droplets coalescence occurred after stopping the agitation. Therefore, it was difficult to evaluate its particle size distribution. HS15 formed a stable micellar dispersion with an average micellar size of ~11 nm.

**Table 30** Droplet size distribution data of Cithrol® DPHS and Kolliphor® HS 15 dispersions.

Preparation method	d (0.1)	d (0.5)	d (0.9)	D [4,3]	Z-average	PDI
Cithrol® DPHS – UTM <sup>a</sup>	23.4 μm	208.2 μm	470.8 μm	232.4 μm		
Cithrol® DPHS – SEM <sup>a</sup>	5.2 μm	13.6 μm	35.5 μm	18.3 μm		
Kolliphor® HS 15 <sup>b</sup>				10.1 nm	11.1	0.014

<sup>a</sup> Determined by static laser diffraction at ambient temperature.

<sup>b</sup> Determined by dynamic laser diffraction at 37 °C.

Compared to MCM and HS15, DPHS was difficult to be dispersed in the buffer by simple agitation. DPHS is semisolid at room temperature and does not completely melt at 37 °C. Therefore, high shear stress was applied using Ultra-Turrax® (Ultra-Turrax® method, UTM). The produced dispersion had a wide droplet size distribution with an average size of ~232 μm. In order to reduce the droplet size and the polydispersity of the dispersion, another preparation method was developed (solvent displacement method, SDM). The SDM resulted in ~13 times reduction of DPHS average droplet size and a decrease in the polydispersity of the dispersion (**Fig. 50**). DPHS dispersions prepared by both methods were evaluated for their digestibility.

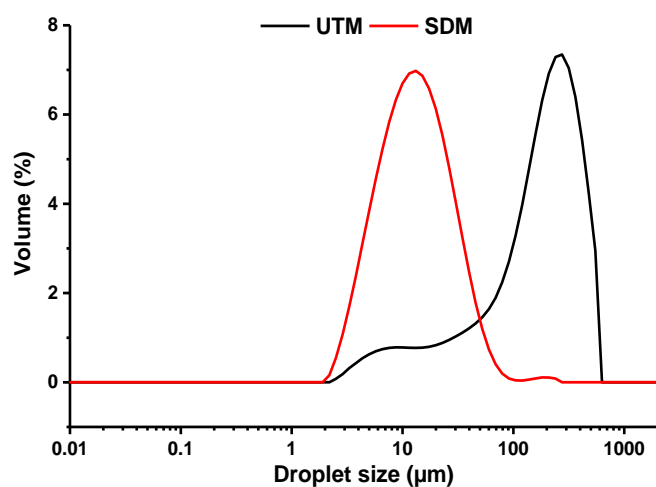


**Fig. 50** Droplet size volume distribution of Cithrol® DPHS dispersions, prepared either by the Ultra-Turrax® method (UTM) or solvent displacement method (SDM), measured by static laser diffraction.

#### 4.7.1.2. pH-stat method

pH-stat method was used in order to investigate the susceptibility of lipid excipients and the semisolid SNEDDS to pancreatin-mediated digestion. Fat digestion was initiated by addition of pancreatin powder (450 U/ml). The digestion products are mostly FA, partial glycerides, PEG and PEG esters. The free FA can be titrated with a standard sodium hydroxide solution (0.1 N) until a constant pH is achieved. The titration rate and the extent of the titration volume, needed to keep the pH constant, reflect the degree of lipid digestibility.

**Fig. 51** shows the cumulative consumption of sodium hydroxide during the *in vitro* digestion of the excipients in both FaSSIF and FeSSIF media. The titration curve has normally 2 phases. The first phase (5-15 min) shows a high initial consumption of sodium hydroxide, corresponding to a high output of free FA. The second phase shows a slow, constant increase in the free FA output.

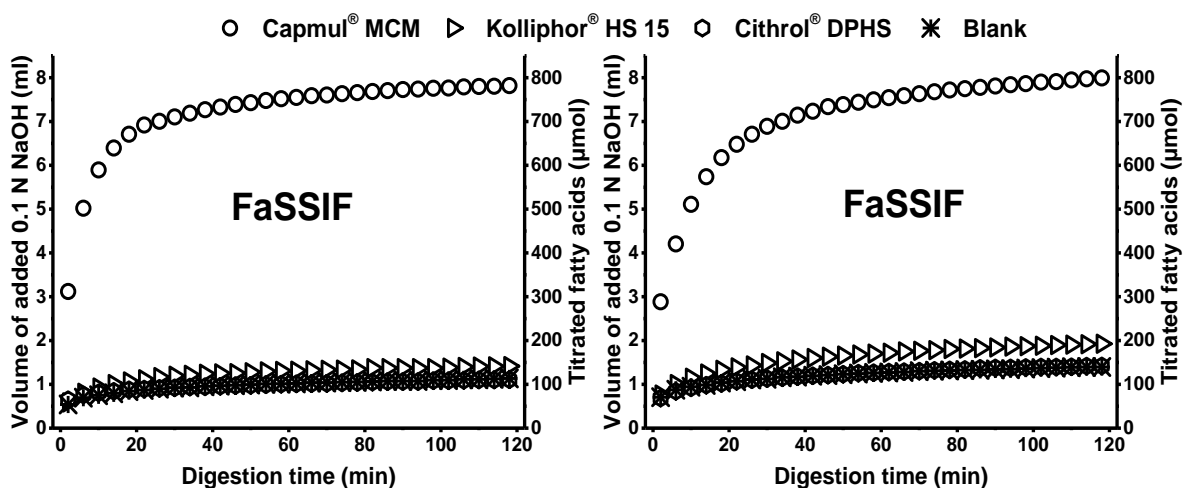


**Fig. 51** Fatty acids concentrations determined by pH-stat titration during the *in vitro* digestion of the excipients in both FaSSIF (left) and FeSSIF (right) media (mean, n=3).

For blank digestion media, the digestion speed was approximately the same in both fasted and fed state conditions. However, the total consumption of sodium hydroxide was higher for the blank FeSSIF compared to the blank FaSSIF. This effect can be attributed to the higher content of both PL and BS in FeSSIF compared to FaSSIF. PL are substrates to PLA2, PLRP2 and CEH. In addition, BS clean the lipid/water interface by the incorporation of the digestion products, especially long chain MG and FA, into mixed micelles. Otherwise, accumulation of the digestion products at the interface would inhibit the action of HPL. Furthermore, PL digestion is enhanced when incorporated in BS mixed micelles [52, 69].

HS15, being a PEG ester of 12-HSA, is susceptible to digestion. It is reported that HPL has no significant activity on PEG esters digestion compared to PLRP2 and CEH [65]. Furthermore,

incomplete digestion of HS15 was reported due to its inhibitory effect on the lipolytic enzymes [283, 361]. The digestion of HS15 was significantly higher in FeSSIF medium compared to FaSSIF due to the higher content of PL and BS.

MCM dispersions showed the highest rate and extent of digestion in both FaSSIF and FeSSIF media. In contrast, the sodium hydroxide consumptions of the DPHS dispersions prepared by UTM were comparable to those of the blank media (control) (Fig. 51). The titration curves of DPHS dispersions prepared by SDM did also match with the control (blank) in the FaSSIF medium. However, a small degree of digestibility was observed under FeSSIF conditions (Fig. 52).

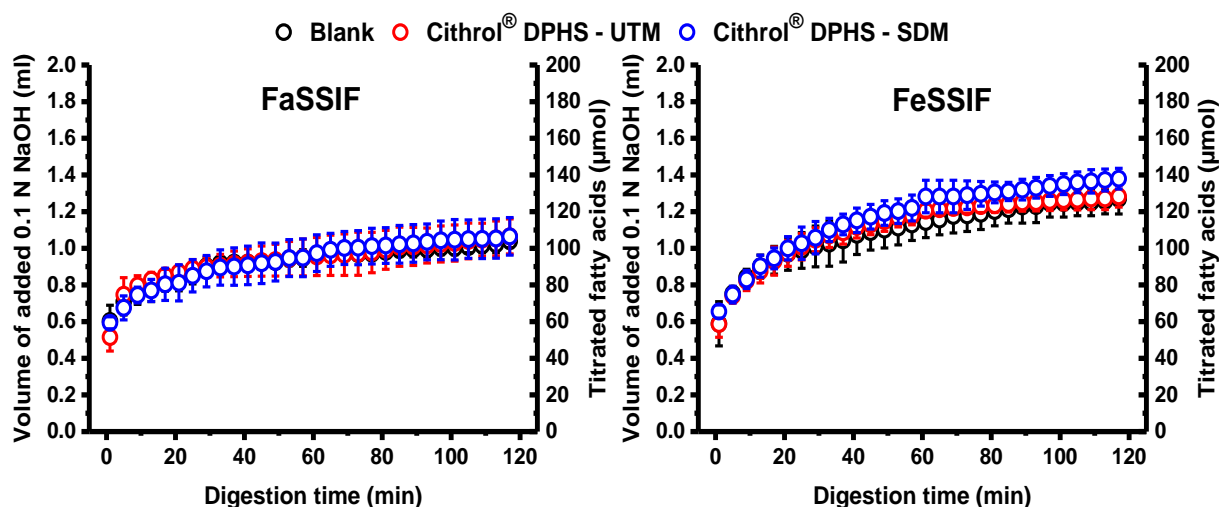


**Fig. 52** Fatty acids concentrations determined by pH-stat titration during the *in vitro* digestion of Cithrol® DPHS in both FaSSIF (left) and FeSSIF (right) media (mean  $\pm$  SD,  $n=3$ ).

The pH-stat titration method is strongly sensitive to the degree of FA ionization, which is governed by their pKa, pH and the ionic strength of the media. The apparent pKa of FA is dependent on their phase behavior, chain length as well as the BS concentration [69, 283, 362]. Medium chain FA have lower pKa than long chain ones. This leads to a higher degree of ionization at pH 6.8. In addition, they are more water-soluble compared to the long chains FA. Consequently, medium chain FA are easily detected by the pH-stat method while long chain FA are often underestimated. Hence, other methods should be used to re-evaluate the digestibility of long chain lipid excipients (DPHS and HS15).

#### 4.7.1.3. Back titration method

Back titration is a potential option to re-evaluate the digestibility of long chain lipids [65]. Due to their higher apparent pKa values, long chain FA are not completely ionized at pH 6.8 [363, 364]. Therefore, the pH of the digestion medium was raised from 6.8 to 9 at the end of



the pH-stat titration. The required volume of sodium hydroxide was recorded (**Table 31**). The difference in sodium hydroxide consumption between excipients and blank medium reflects the degree of underestimation by the pH-stat method. In both FaSSIF and FeSSIF media, the required sodium hydroxide volume for all excipients was significantly higher compared to the blank media (t-Test,  $\alpha = 0.05$ ). Furthermore, the consumption of sodium hydroxide was significantly lower in FeSSIF compared to FaSSIF. DPHS dispersions prepared by SDM showed higher sodium hydroxide consumption compared to those prepared by UTM. The difference in the droplet size contributes to this result. Furthermore, the results also proved the underestimation of MCM digestibility by pH-stat method at pH 6.8.

**Table 31** Volume of sodium hydroxide (ml) required to raise the pH from 6.8 to 9 at the end of pH-stat titration (mean  $\pm$  SD, n = 3).

	FaSSIF	FeSSIF
<b>Blank media</b>	6.04 $\pm$ 0.27	5.15 $\pm$ 0.17
<b>Cithrol® DPHS – UTM</b>	6.49 $\pm$ 0.09	5.40 $\pm$ 0.06
<b>Cithrol® DPHS – SEM</b>	6.67 $\pm$ 0.09	5.82 $\pm$ 0.06
<b>Kolliphor® HS 15</b>	6.36 $\pm$ 0.10	5.48 $\pm$ 0.04
<b>Capmul® MCM</b>	6.55 $\pm$ 0.04	5.77 $\pm$ 0.03

#### 4.7.1.4. Lipid analysis by high-performance thin layer chromatography (HPTLC) combined with spectrodensitometry

In order to precisely determine the extent of excipients digestion, HPTLC combined with spectrodensitometry was used [275]. This technique provides a better overview of all digestion products such as FA, MG, DG, TG as well as other digestion products (e.g. PEG esters). On the other side, pH-stat combined with the back titration method provides only the total released FA concentration [69]. Under these experimental conditions, the recovery rate of MCM digestion products (with chain lengths of C<sub>8</sub> and C<sub>10</sub>) was low and highly variable due to their evaporation during the processing of the plate at 150 °C. These problems do not occur with long chain lipids (C<sub>16</sub>, C<sub>18</sub> and higher). 12-HSA is the main digestion product of HS15 and DPHS. Therefore, calibration curves of standard 12-HSA solutions were prepared and used to quantify the FA released during their digestion process. The relation between the mass of 12-HSA and the area under the peak was linear until saturation was achieved. Then a change in the slope was observed. Therefore, the calibration curves were fitted as Hill slope (**Fig. 53**). The results of HPTLC/spectrodensitometry analysis are presented in **Fig. 54**. The release rate of 12-HSA was faster in the first 30 min. Afterward slower 12-HSA release was observed. The digestibility of both DPHS and HS15 was underestimated by pH-stat combined with back titration method in both media (**Table 32**).

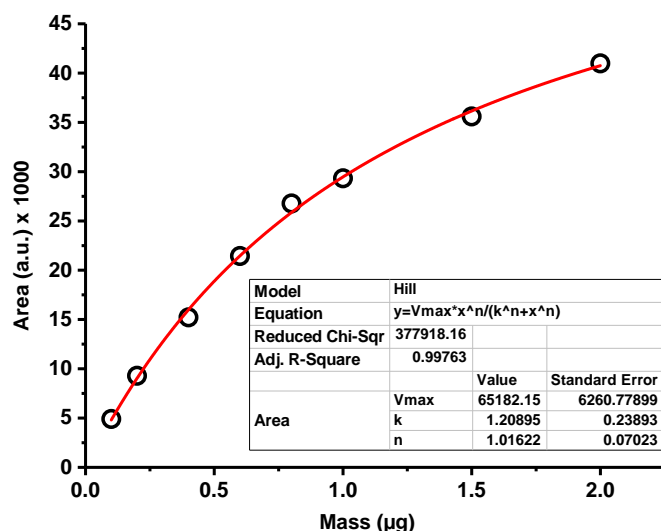


**Fig. 53** Calibration curve for HPTLC/spectrodensitometry of 12-hydroxystearic acid. The curve was fitted as a Hill slope.

In addition, the digestibility of HS15 was higher than DPHS despite its lower ester value (~125 mg KOH/g for DPHS compared to ~60 mg KOH/g for HS15). The difference in droplet size and molecular weight could attribute to this finding. Furthermore, DPHS is an ABA block copolymer. The middle block (B) is the hydrophilic poly(ethylene oxide) while the two outer blocks (A) are poly(12-HSA). Most lipolytic enzymes act on the lipid/water interface. Due to the DPHS interfacial packing, the lipophilic part (poly(12-HSA)) is mainly shielded in the oil core from the action of the lipolytic enzymes while few ester bonds are available at the interface. In addition, after cleavage at the interface, the produced poly(12-HSA) is expected to be slowly digested due to its relatively low polarity.

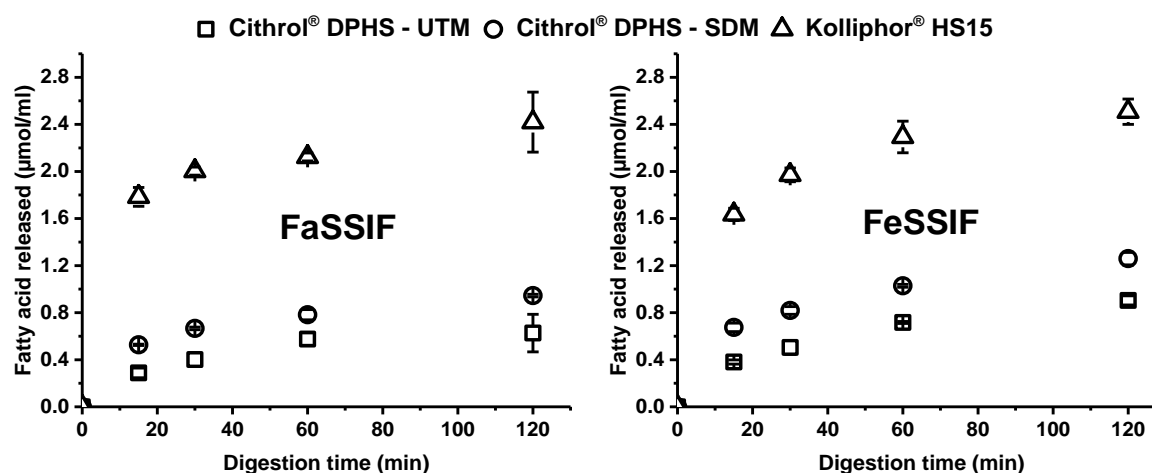


**Fig. 54** Digestion-induced formation of 12-hydroxystearic acid from Cithrol® DPHS and Kolliphor® HS 15 in both FaSSIF and FeSSIF media analyzed by HPTLC/spectrodensitometry (mean  $\pm$  SD,  $n=3$ ).

As expected, DPHS dispersions prepared by SDM showed higher 12-HSA release compared to dispersions prepared by UTM. However, both dispersions showed less than 6 % of the

expected FA release (**Table 32**). The incomplete digestion of long chain lipids was reported [52, 274, 365]. Furthermore, the digestion rate was higher in FeSSIF medium compared to the FaSSIF one. Because of their low polarity, long chain FA are accumulated at the interface with consequent deactivation of lipolytic enzymes. Therefore, the incorporation of long chain FA into the BS mixed micelles is essential for long chain lipids digestion [52]. Consequently, the digestibility of long chain lipids is more sensitive to BS concentration than medium chain ones [69].

**Table 32** Comparison between the fatty acids concentration determined by both pH-stat method and HPTLC/spectrodensitometry after 120 min of digestion (mean, n = 3) of 1 % (m/V) Kolliphor<sup>®</sup> HS15 and Cithrol<sup>®</sup> DPDS dispersions in FaSSIF and FeSSIF.

Excipient	Fatty acids available for digestion (mM) <sup>a</sup>	Fatty acids determined by HPTLC method (mM)	Fatty acids determined by pH-stat method (mM) <sup>b</sup>	Percentage of fatty acids detected by pH-stat method (%)	Digestion (%)
<b>FaSSIF</b>					
Kolliphor <sup>®</sup> HS15	10.69	2.42	0.80	33.1	22.6
Cithrol <sup>®</sup> DPDS – UTM	22.28	0.63	0.45	71.4	2.8
Cithrol <sup>®</sup> DPDS – SDM	22.28	0.95	0.63	66.3	4.3
<b>FeSSIF</b>					
Kolliphor <sup>®</sup> HS15	10.69	2.51	0.87	34.7	23.5
Cithrol <sup>®</sup> DPDS – UTM	22.28	0.90	0.25	27.8	4.0
Cithrol <sup>®</sup> DPDS – SDM	22.28	1.26	0.70	55.6	5.7

<sup>a</sup> Fatty acids estimation is based on the ester values of both Cithrol<sup>®</sup> DPDS (125 mg KOH/g) and Kolliphor<sup>®</sup> HS 15 (60 mg KOH/g).

<sup>b</sup> Calculations are based on the titrated fatty acids obtained during the pH-stat method and the back titration method. The fatty acids titrated during blank media digestion were subtracted from the results.

#### 4.7.2. Digestibility of the semisolid SNEDDS

The semisolid DPDS-SNEDDS showed a significant increase in the sodium hydroxide consumption compared to blank media (**Fig. 55**). Both DPDS and HS15 are slowly and incompletely digested (**Table 32**). On the other hand, based on its ester values (~270 mg KOH/g) and pH-stat combined with back titration digestibility data, MCM showed complete digestibility in FaSSIF (99.7 %) and FeSSIF (100.1 %). Accordingly, the source of FA, available for pH-stat titration, is mainly MCM. Therefore, a decreasing tendency of the overall titrated FA was observed with decreasing the MCM contents in the semisolid SNEDDS. In addition, the digestibility of the SNEDDS did not significantly changed in either FaSSIF or FeSSIF media.

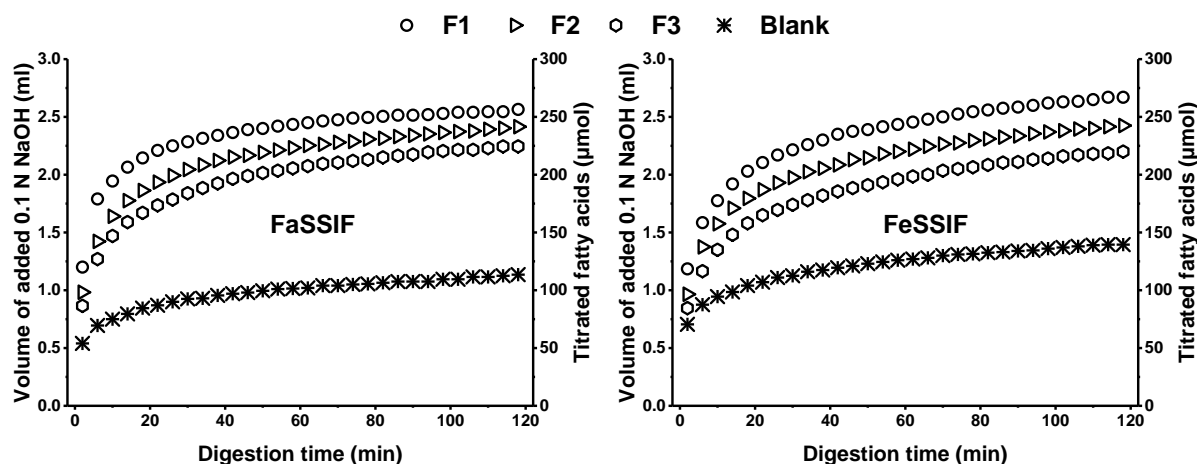


**Fig. 55** Fatty acids concentrations determined by pH-stat titration during the *in vitro* digestion of the semisolid SNEDDS in both FaSSIF and FeSSIF media (mean, n=3).

Based on the ester values of the excipients, an estimation of expected FA release during the SNEDDS nanodispersions digestion was calculated (**Table 33**).

**Table 33** Comparison between the estimated and measured fatty acids concentration determined by pH-stat method after 120 min of digestion (mean, n = 3) of the 1 % (m/V) SNEDDS nanodispersions in FaSSIF and FeSSIF.

Formulation	Predicted amount of fatty acids available for titration based on the ester values of the excipients (µmol)				Fatty acids determined by pH-stat method (µmol) <sup>a</sup>	Percentage formulations digestibility based on ester values (%)
	MCM	DPHS	HS15	Total		
<b>FaSSIF</b>						
<b>F1</b>	144	32	206	382	143	37.4
<b>F2</b>	96	43	206	345	129	37.4
<b>F3</b>	72	48	206	326	112	34.4
<b>FeSSIF</b>						
<b>F1</b>	144	32	206	382	128	33.5
<b>F2</b>	96	43	206	345	104	30.1
<b>F3</b>	72	48	206	326	88	27.1

<sup>a</sup> Calculations are based on the titrated fatty acids obtained during the pH-stat method. The fatty acids titrated during blank media digestion were subtracted from the results.

According to the calculations, incomplete digestion of DPHS formulations was observed and only 27-38 % of the possible ester groups were cleaved under the experimental conditions. This result was surprising because lipases work on the oil/water interface, which is strongly dependent on the droplet size. Due to the tiny size (< 25 nm) of the SNEDDS nanodispersions, a higher degree of the nanodispersions digestibility was expected owing to their larger

interfacial surface area. An explanation for this result could depend on the difference in the interfacial packing between the single excipient and SNEDDS nanodispersions. In the case of the SNEDDS nanodispersions, PEG loops are projecting on the interface. Therefore, a steric hindrance could be developed on the interface that may hinder the HPL/co-lipase interfacial anchoring and prevent the HPL activation. Feeney et al. [366] have reported the resistance of stealth (PEGylated) nanoparticles to the pancreatin-mediated digestion due to the formation of a steric barrier on the nanoparticles surface. The inhibitory effect was found to be dependent on the molecular weight and the packing density of the surface PEG.

#### 4.7.3. Possible drug precipitation during digestion

Orally administered SNEDDS should be able to keep the incorporated PWSD in the solubilized form throughout the GI tract in different LC as well as colloidal structures. However, lipid digestion usually changes the solubilization capacity and PWSD precipitation sometimes occurs [10]. Therefore, the influence of the digestion on the PWSD solubilization and the possible precipitation should be studied in both fasted and fed state. **Fig. 56** demonstrates that Progesterone remained almost completely dissolved after the digestion of 1 % m/V of the formulations in both FaSSIF and FeSSIF.

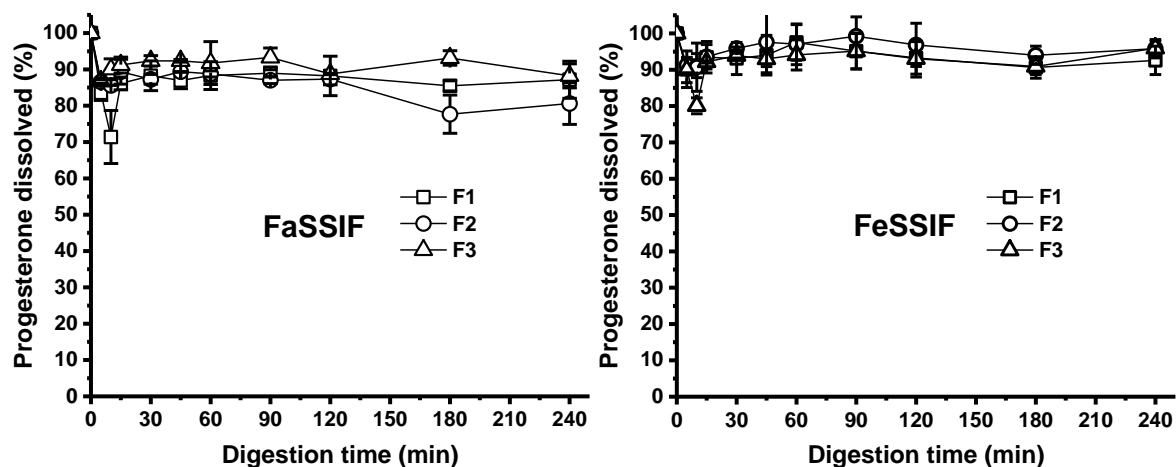


**Fig. 56** Percentage of Progesterone that remained dissolved after the digestion of 1 % (m/V) of the self-nanoemulsifying formulations in both FaSSIF (left) and FeSSIF (right) media (mean  $\pm$  SD, n=3).

A small amount of Progesterone starts to precipitate at the beginning of the digestion process. The maximum precipitation has been seen after 15 min of digestion in both media. The reason could be the higher digestibility of the formulation (mainly the MCM part) that is usually observed at this period (the first phase of the pH-stat titration diagrams, **Fig. 55**). The

precipitation rate was lower in FeSSIF compared to FaSSIF. Subsequently, an increase of the solubilization capacity of the formulations was observed. DPHS-SNEDDS are composed mainly of long chain lipids (DPHS and HS15). Long chain lipids have lower polarity and show slower, incomplete digestibility (**Table 32**) compared to medium chain lipids [69]. Consequently, they have higher capability to maintain the solubilization capacity of the accompanied PWSDs when incorporated into the bile mixed micelles, even in lower concentrations [47]. More than 80 % (FaSSIF) and 90 % (FeSSIF) of Progesterone remained in the solubilized form after 4 h of digestion. The difference between DPHS formulations was not pronounced.

#### 4.7.4. Effect of digestion on the drug release from adsorbates and tablets

The effect of digestion on the release profile of the self-nanoemulsifying T2 tablets in both FaSSIF and FeSSIF is shown in **Fig. 57**.

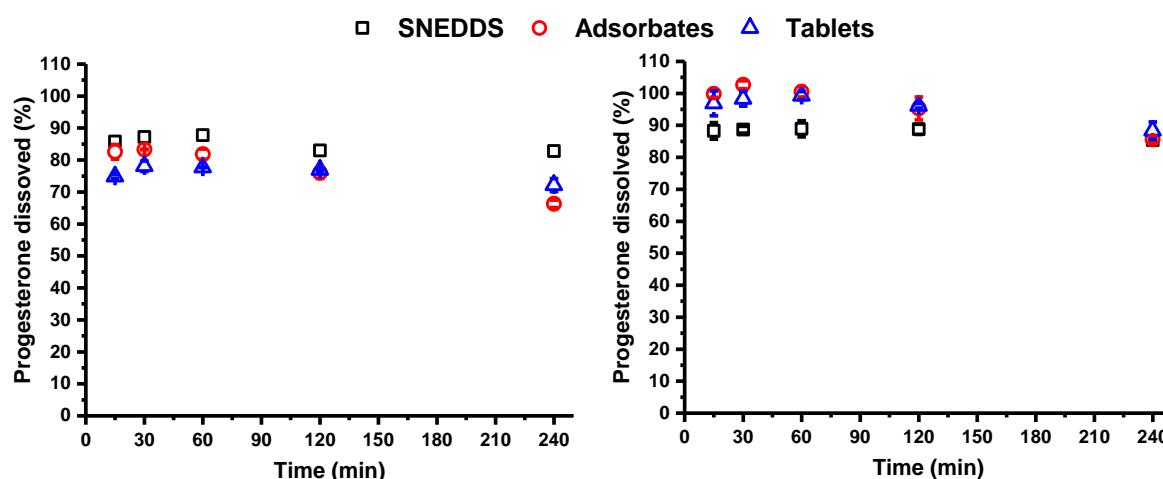


**Fig. 57** Percentage of Progesterone that remained dissolved after the digestion of 1 % (m/V) of the Progesterone-loaded semisolid SNEDDS, N7 adsorbates and T2 tablets in both FaSSIF (left) and FeSSIF (right) media (mean  $\pm$  SD, n=3).

DPHS-based semisolid SNEDDS were able to protect Progesterone against digestion-induced precipitation. Only 10-15 % of Progesterone was precipitated upon SNEDDS digestion in FaSSIF and FeSSIF media. Adsorbates and tablets showed lower Progesterone level than the semisolid SNEDDS upon digestion in FaSSIF medium. The opposite behavior was observed upon digestion in FeSSIF medium. The protection of Progesterone against precipitation upon tablets and adsorbates digestion in FeSSIF medium is not fully understood.

## 5. Conclusion

The feasibility of using the polymeric emulsifier PEG-30-dipolyhydroxystearate (DPHS) as a lipophilic excipient for the production of SNEDDS as well as its *in vitro* digestibility are for the first time explored. The optimized SNEDDS have semisolid consistency at room temperature and are able to provide very fine dispersions (less than 25 nm) in various media regardless to the pH and the ionic strength. Furthermore, SNEDDS nanodispersions have shown a high degree of molecular mobility, which is essential for their *in vivo* performance. In addition, the optimized SNEDDS are able to enhance the equilibrium solubility of the accompanied PWSD (Progesterone) in various media. The digestibility of DPHS and its semisolid SNEDDS are incomplete in both FaSSIF and FeSSIF media. Protection of Progesterone against digestion-induced precipitation is the main advantage obtained from the developed semisolid SNEDDS. Further advantages could be the avoidance of co-solvents and the higher shelf-life stability due to the lack of unsaturation.

Freely flowable powders can be prepared by the incorporation of the optimized semisolid SNEDDS into Neusilin<sup>®</sup> US2 at up to 60 % m/m. The formed adsorbates can be compressed into tablets with acceptable mechanical properties. The upper limit of the SNEDDS content in the adsorbates intended for tablets preparation is ~45 % m/m. The optimum compression pressure of the tablets compression is 45-55 MPa. At higher SNEDDS content or higher compression pressure, extensive tablets chipping occurs. Minitablets prepared with higher SNEDDS load (70-90 %) should be also considered as a potential solution when higher drug load is essential. The produced tablets are able to completely release the accompanied PWSD in the bio-relevant media.

## 6. Summary and outlook

### 6.1. English version

Poorly water-soluble drugs (PWSDs) are associated with some limitations such as inter- and intra-patient variability as well as poor bioavailability. Furthermore, their dose is always augmented to reach the therapeutic blood level. This leads to local GI tract irritation, toxicity, patient incompliance, higher costs as well as inefficient treatment. Unfortunately, the number of potential drug candidates that have poor aqueous solubility is progressively increasing. Accordingly, the problem has become dominant in the pharmaceutical industry. Among different approaches that have developed to enhance the aqueous solubility, the use of the self-nanoemulsifying drug delivery systems (SNEDDS) has drawn considerable attention and ultimately therapeutical and commercial success in the oral delivery of PWSDs. They provide the PWSDs in the form of solubilized nanodispersions. Consequently, the rate-limiting step of the PWSDs dissolution is bypassed. Nonetheless, SNEDDS are typically filled in soft gelatin capsules, which might cause the following problems: interaction with the capsule shell, instability, higher production cost and possible drug precipitation. Therefore, alternative formulation strategies, e.g. the inclusion of SNEDDS into a solid or semisolid dosage form, are desirable; nevertheless, very challenging.

Therefore, it was the aim of this work to develop and optimize novel semisolid/solid SNEDDS for the oral delivery of PWSDs. Tablets were selected as a final dosage form. The prepared SNEDDS should conform to the following criteria: (a) Semisolid or solid consistency at room temperature. (b) pH-independent self-nanoemulsification upon mild agitation at 37 °C. (c) High lipid mobility after dilution at physiological conditions. (d) High shelf-life stability due to the avoidance of unsaturated lipid excipients. (e) Less PWSDs precipitation due to the avoidance of co-solvents as well as high content of long chain lipids.

Among the screened semisolid and solid excipients, Cithrol<sup>®</sup> DPHS (PEG-30-dipolyhydroxystearate, DPHS) formulations have shown potential advantages that enable DPHS to be a good candidate for SNEDDS development. However, its potential use as a lipophilic excipient in SNEDDS was not yet explored. Based on phase diagrams and dilution assay, semisolid SNEDDS with good self-nanoemulsifying properties were successfully prepared. The SNEDDS were composed of DPHS along with Capmul<sup>®</sup> MCM (MCM) and Kolliphor<sup>®</sup> HS 15 (HS15). The semisolid SNEDDS showed a partial crystalline and partial amorphous systems at room temperature. The formulations and the produced nanodispersions were comprehensively characterized for droplet size distributions, dispersion clarity, excipients



interactions, physical form as well as for the molecular mobility of the dispersed SNEDDS components at body temperature. The characterizations were performed by photon correlation spectroscopy (PCS), UV-visible spectrophotometry, differential scanning calorimetry (DSC), powder X-ray diffraction (PXRD), benchtop nuclear magnetic resonance (BT-NMR), proton nuclear magnetic resonance ( $^1\text{H-NMR}$ ) and electron spin resonance (ESR). The presence of MCM was found to be essential for the self-nanoemulsifying process. Higher MCM contents resulted in a pH and ionic strength dependent dispersibility while lower MCM contents led to a slower dispersibility. The ratio DPHS: MCM 2:1 was found to be ideal in terms of the droplets size, dispersibility and stability of the formed nanoemulsions. F2 and F3 formulations showed monomodal volume distributions in all tested media with an average hydrodynamic diameter of less than 25 nm. DSC study exposed the capability of MCM to dissolve both DPHS and HS15, which could point to its importance in the self-nanoemulsification process. All excipients can be detected by standard  $^1\text{H-NMR}$  in their dispersions, reflecting a high molecular mobility, which is essential for the *in vivo* performance of the SNEDDS. The measured fatty acids chain signal areas conformed to the predicted ratios. However, the PEG signal areas were less than expected due to a partial replacement of HS15 by DPHS at the interface. An increase in the microviscosity within the SNEDDS was observed with the increase of DPHS content in the formulations. ESR study showed that the PWSD model Tempolbenzoate was mainly associated with the SNEDDS up to a dilution of 5 % and then translocated into water with further dilution.

The semisolid SNEDDS was incorporated (20-90 %) in Neusilin<sup>®</sup> US2 (N-US2) using solvent-free method. Freely flowable powders were obtained at SNEDDS content of up to 60 % m/m. BT-NMR and DSC were used to study the interaction between the semisolid SNEDDS and the nanoporous carrier. The strength of the N-US2/SNEDDS interaction depended on their relative content. The increase in the N-US2 content led to a reduction of the melting point, broadening of the melting peak and reduction of the fitted  $T_2$ -relaxation time of the SNEDDS. The effect of the disintegrant level, compression pressure and tablets shape were evaluated. At least 7.5 % disintegrant was required to obtain fine tablets dispersions. The compression pressure of 45-55 MPa was found to be optimal for the production of tablets with acceptable mechanical properties. At this compression pressure range, convex tablets were superior to flat ones. The self-nanoemulsifying tablets were able to release the incorporated Lumogen<sup>®</sup> F305 fluorescence dye in a comparable rate to both the adsorbates and the semisolid SNEDDS.

Progesterone was selected as a PWSD model. Progesterone loading was studied in the single excipients (DPHS, MCM and HS15) as well as in their semisolid SNEDDS formulations. Progesterone-loaded SNEDDS retained the physical form of the parent semisolid SNEDDS.

Increasing the DPHS content in the formulations resulted in a higher Progesterone load. Moreover, the SNEDDS were able to enhance the equilibrium solubility of Progesterone at different media. Progesterone remained in the solubilized state in the semisolid SNEDDS and no phase separation or crystallization was observed. Progesterone loaded adsorbates and semisolid SNEDDS were comprehensively characterized by DSC, PCS, PXRD and Fourier transform infrared spectroscopy (FTIR).

Increasing the SNEDDS content in the adsorbates adversely affected their compressibility index (CI). However, incorporation of Progesterone was found to enhance the CI of the SNEDDS-loaded adsorbates without affecting their angle of repose. The upper limit of the SNEDDS content in the adsorbates intended for tablets preparation was found to be ~45 % m/m. At higher SNEDDS content, extensive tablets chipping occurs. Tablets chipping could be probably reduced by the avoidance of the tablets sharp edges. The release of Progesterone from tablets and adsorbates was found to be medium-dependent. Complete Progesterone release was observed in bio-relevant media.

The digestibility of DPHS along with MCM and HS15 as well as the semisolid SNEDDS was evaluated by means of an *in vitro* pancreatin digestion assay under both fasted (FaSSIF) and fed (FeSSIF) states. The pH-stat method was not sensitive to detect DPHS long chain digestion products. Therefore, two other methods were used to study the digestibility of DPHS: the back titration method and the HPTLC combined with spectrodensitometry. An incomplete (< 6 %), size dependent digestibility was observed in both FaSSIF and FeSSIF media. DPHS showed a lower digestibility than HS15 despite its higher ester value. The reason could be its higher molecular weight, larger droplet size and its interfacial packing. Incomplete digestion of the semisolid SNEDDS was observed and only 27-38 % of the possible ester groups were cleaved under the experimental conditions. Depending on the digestion media, more than 80-90 % of Progesterone remained in the solubilized form after 4 h of digestion. Protection of Progesterone against digestion-induced precipitation is the main advantage obtained from the developed semisolid SNEDDS.

Further studies should be focused on the evaluation of the shelf-life stability of the optimized semisolid SNEDDS, SNEDDS adsorbates and the self-nanoemulsifying tablets. Minitablets prepared with higher SNEDDS load (70-90 %) should be also considered as a potential solution when higher drug load is essential. However, the SNEDDS/capsule shell interaction should be thoroughly studied. Furthermore, the SNEDDS-mediated bioavailability enhancement of different PWSDs with various lipophilicity and physicochemical properties should be assessed. In addition, the lymphatic uptake of such systems should be evaluated.

## 6.2. German version

Schwer wasserlösliche Wirkstoffe sind mit therapeutischen Herausforderungen wie beispielsweise patienteninter- und -intraindividuelle Variabilität sowie geringer Bioverfügbarkeit verbunden. Weiterhin müssen sie oft in hoher Dosis verabreicht werden, um einen therapeutischen Blutspiegel zu erreichen. Dies kann zu lokalen Magen-Darm-Reizungen und verminderter Therapietreue des Patienten, toxischen Effekten, höheren Kosten und ineffizienter Behandlung führen. Dennoch steigt die Anzahl der schwerlöslichen Substanzen unter potentiellen Wirkstoffen stark an und aus diesem Grund wird dieses Thema für die pharmazeutische Industrie immer wichtiger. Unter den verschiedenen Ansätzen, die entwickelt wurden, um die Wasserlöslichkeit der Wirkstoffe zu erhöhen, erscheint der Einsatz von selbstnanoemulgierenden Systemen (SNEDDS) besonders interessant und könnte schlussendlich zum therapeutischen und kommerziellen Erfolg der Wirkstoffe als Formulierung zur oralen Anwendung führen. SNEDDS enthalten den schwer wasserlöslichen Wirkstoff in Form von solubilisierten Nanodispersionen. Aus diesem Grund wird der geschwindigkeitsbestimmende Schritt der Auflösung des Wirkstoffs umgangen. SNEDDS werden typischerweise in Weichgelatine kapseln gefüllt, aber damit sind typische Probleme wie die Interaktion mit der Kapselhülle, Instabilität, hohe Produktionskosten und mögliche Wirkstoffpräzipitation verbunden. Daher sind alternative Formulierungsstrategien wie zum Beispiel die Einbindung von SNEDDS in eine feste oder halbfeste Arzneiform erwünscht, wenn auch sehr anspruchsvoll.

Zielsetzung der vorliegenden Arbeit war daher die Entwicklung und Optimierung von neuartigen halbfesten oder festen SNEDDS für die orale Administration von schwer wasserlöslichen Wirkstoffen. Schlussendlich wurden Tabletten als passende Arzneiform ausgewählt. Die hergestellten SNEDDS sollten die folgenden Eigenschaften besitzen: (a) Halbfester oder fester Zustand bei Raumtemperatur. (b) pH-unabhängige Selbstnanoemulgierung durch schwaches Schütteln bei 37°C. (c) Hohe Mobilität der Lipide nach Verdünnung unter physiologischen Bedingungen. (d) Hohe Lagerstabilität durch Vermeidung von ungesättigten Lipidhilfsstoffen. (e) Geringe Wirkstoffpräzipitation durch Vermeidung von Cosolventien sowie eines hohen Anteils an langkettigen Lipiden.

Unter den untersuchten halbfesten und festen Hilfsstoffen haben Formulierungen mit Cithrol® DPHS (PEG-30-Dipolyhydroxystearat, DPHS) vorteilhafte Eigenschaften gezeigt, die DPHS als einen vielversprechenden Hilfsstoff zur Entwicklung von SNEDDS erscheinen lassen. Jedoch wurde DPHS als lipophiler Hilfsstoff in der Entwicklung von SNEDDS bisher

noch nicht untersucht. Auf der Basis von Phasendiagrammen und Verdünnungsanalysen wurden halbfeste SNEDDS mit guten selbstnanoemulgierenden Eigenschaften erfolgreich hergestellt. Die SNEDDS bestanden aus DPHS zusammen mit Capmul® MCM (MCM) und Kolliphor® HS 15 (HS15). Die halbfesten SNEDDS zeigten eine teils kristalline und teils amorphe Struktur bei Raumtemperatur. Die Formulierungen sowie die Nanodispersionen wurden umfassend auf Tröpfchengrößenverteilung, Klarheit der Dispersion, Interaktionen der Hilfsstoffe, physikalische Form sowie auf die molekulare Mobilität der dispergierten Hilfsstoffe der SNEDDS bei Körpertemperatur untersucht. Die Charakterisierung erfolgte mittels Photonenkorrelationsspektroskopie (PCS), UV-Vis-Spektrophotometrie, dynamischer Differenzkalorimetrie (DSC), Pulver-Röntgenbeugung (PXRD), Benchtop Kernspinresonanzspektroskopie (BT-NMR), Standard Protonen-Kernspinresonanzspektroskopie ( $^1\text{H-NMR}$ ) und Elektronenspinresonanzspektroskopie (EPR). Der Einsatz von MCM stellte sich als unerlässlich für den Selbstnanoemulsionsprozess heraus. Ein hoher Anteil an MCM hatte eine pH-Wert- und Ionenstärken-abhängige Dispergierbarkeit zur Folge, während geringere MCM Anteile zu einer langsameren Dispersion führten. Das Verhältnis DPHS zu MCM 2:1 erwies sich als ideal in Bezug auf Tröpfchengröße, Dispergierbarkeit und Stabilität der entstandenen Nanoemulsionen. Die Formulierungen F2 und F3 zeigten monomodale Volumenverteilungen in allen untersuchten Dispersionmedien mit einem durchschnittlichen hydrodynamischen Durchmesser von weniger als 25 nm. DSC-Untersuchten zeigten die Löslichkeit sowohl von DPHS als auch HS15 in MCM, was eine Ursache für die Unabdingbarkeit von MCM für den Emulsionsprozessein könnte. Alle Hilfsstoffe konnten mittels Standard  $^1\text{H-NMR}$  in ihren Dispersionen nachgewiesen werden, was auf eine hohe molekulare Mobilität hinweist, die für die *in-vivo* Wirksamkeit der SNEDDS sehr wichtig ist. Die gemessenen Flächenintegrale der Signale der Fettsäuren entsprachen den vorhergesagten berechneten Verhältnissen. Allerdings waren die gemessenen Signalflächen des PEG aufgrund eines anteiligen Austausches von HS15 durch DPHS an der Grenzfläche geringer als erwartet. Ein steigender Anteil an DPHS führte zu einer Erhöhung der Mikroviskosität in den SNEDDS. EPR-Untersuchungen zeigten, dass der Modellstoff Tempolbenzoat mit den SNEDDS bis zu einer Verdünnung von 5 % vorwiegend verbunden war und sich erst bei weiterer Verdünnung in das wässrige Medium verteilte.

Die halbfesten SNEDDS wurden mit einem lösungsmittelfreien Verfahren zu 20-90 % in Neusilin® US2 (N-US2) eingearbeitet. Frei fließfähige Pulver wurden bei einem SNEDDS-Anteil von bis zu 60 % m/m erhalten. BT-NMR und DSC wurden verwendet, um die

Interaktionen zwischen den halbfesten SNEDDS und den nanoporösen Träger zu untersuchen. Das Ausmaß der N-US2/SNEDDS Interaktion war abhängig von deren relativen Anteilen. Ein steigender Anteil an N-US2 führte zu einer Verringerung des Schmelzpunktes, Verbreiterung des Schmelzpeaks und Verminderung der T<sub>2</sub>-Relaxationszeit der SNEDDS.

Bei der Herstellung von Tabletten wurde der Einfluss des Sprengmittelanteils, des Pressdrucks und der Tablettenform ausgewertet. Mindestens 7,5 % Sprengmittel waren erforderlich, um eine feine Dispersion der Tabletten zu erhalten. Der Kompressionsdruck von 45-55 MPa wurde als optimal für die Herstellung von selbstnanoemulgierenden Tabletten mit akzeptablen mechanischen Eigenschaften festgestellt. In diesem Bereich des Kompressionsdruck waren bikonvexe Tabletten biplanen Tabletten überlegen. Die selbstnanoemulgierenden Tabletten konnten den Fluoreszenzfarbstoff Lumogen<sup>®</sup> F305 in einer vergleichbaren Geschwindigkeit zu den Adsorbaten und den halbfesten SNEDDS freisetzen.

Progesteron wurde als lipophile Modellschubstanz ausgewählt. Die Wirkstoffbeladung der einzelnen Hilfsstoffe (DPHS, MCM und HS15) sowie deren halbfesten SNEDDS-Formulierungen wurde untersucht. Mit Progesteron beladene SNEDDS behielten die physikalische Form der ursprünglichen SNEDDS. Ein steigender Anteil an DPHS in den SNEDDS führte zu einer höheren Progesteronbeladung. Außerdem waren die SNEDDS in der Lage, die Sättigungslöslichkeit von Progesteron in verschiedenen Medien zu erhöhen. Progesteron blieb in den halbfesten SNEDDS gelöst, weder Phasentrennung noch Kristallisation wurde beobachtet. Die mit Progesteron beladenen Adsorbate und die halbfesten SNEDDS wurden umfassend mit Hilfe von DSC, PCS, PXRD und Fourier-Transformation-Infrarot-Spektroskopie (FTIR) charakterisiert.

Ein steigender Anteil an SNEDDS in den Adsorbaten beeinflusste ihren Kompressibilitätsindex (KI) nachteilig. Jedoch verbesserte der Zusatz des Progesterons den KI der SNEDDS-Adsorbate, aber ohne deren Böschungswinkel zu beeinflussen. Die obere Grenze des SNEDDS-Anteils der Adsorbate zur Herstellung von Tabletten wurde mit ~45 % m/m festgestellt. Bei höheren SNEDDS-Anteilen trat ein starkes Deckeln der Tabletten auf. Dies könnte wahrscheinlich durch die Vermeidung von scharfen Kanten der Tabletten vermeiden werden. Die Freisetzung des Progesterons aus Tabletten und Adsorbaten zeigte sich stark vom Freisetzungsmedium abhängig. In biorelevanten Medien wurde allerdings die vollständige Freisetzung von Progesteron beobachtet.

Die Verdaubarkeit von DPHS zusammen mit MCM und HS15 sowie den halbfesten SNEDDS wurde mittels eines *in-vitro* Pankreatin Verdauungstestes in künstlichen intestinalen

Flüssigkeiten für den nüchternen (FaSSIF) und postprandialen (FeSSIF) Zustand untersucht. Das pH-Stat-Verfahren eignete sich nicht dazu, die langkettigen Verdauungsprodukte von DPHS vollständig zu detektieren. Daher wurden zwei andere Methoden verwendet, um die Verdauung von DPHS zu untersuchen: die Rücktitration und die HPTLC/Densitometrie. Eine unvollständige (< 6 %), von der Tröpfchengröße abhängige Verdaubarkeit wurde in FaSSIF und FeSSIF Medien festgestellt. DPHS zeigte eine geringere Verdauung als HS15 trotz höherer Esterzahl. Der Grund dafür könnte dessen höheres Molekulargewicht, größere Tröpfchengröße und Grenzflächenanordnung sein. Da nur 27-38 % der möglichen Estergruppen unter den experimentellen Bedingungen gespalten wurden, muss von einer unvollständigen Verdauung der halbfesten SNEDDS ausgegangen werden. Abhängig vom Verdaumedium verblieben mehr als 80-90 % des Progesterons auch nach 4 h Verdauung in ihrer solubilisierten Form. Der Schutz des Progesterons gegen die verdauungsinduzierte Präzipitation ist der Hauptvorteil der entwickelten halbfesten SNEDDS.

Weitere Studien sollten sich auf die Bewertung der Lagerstabilität der optimierten halbfesten SNEDDS, der Adsorbaten und der selbstnanoemulgierenden Tabletten fokussieren. Sofern eine höhere Wirkstoffbeladung wichtig ist, könnten Minitabletten mit höherer SNEDDS Beladung (70-90%) als eine mögliche Lösung in Betracht gezogen werden. In Bezug auf die halbfesten SNEDDS sollten die Wechselwirkungen zwischen SNEDDS und Kapselhülle eingehend untersucht werden. Darüber hinaus sollte die durch die SNEDDS verbesserte Bioverfügbarkeit verschiedener schwer wasserlöslicher Wirkstoffe mit unterschiedlicher Lipophilie und physikochemischen Eigenschaften bewertet werden. Ebenfalls sollte man die lymphatische Aufnahme solcher Systeme evaluieren.

---

## 7. References

1. Lipinski, CA, et al., *Experimental and computational approaches to estimate solubility and permeability in drug discovery and development settings*. *Advanced Drug Delivery Reviews*, 1997. **23**(1-3): p. 3-25.
2. Lipinski, CA, et al., *Experimental and computational approaches to estimate solubility and permeability in drug discovery and development settings*. *Advanced Drug Delivery Reviews*, 2001. **46**(1-3): p. 3-26.
3. Kim, C-K, and Park, J-S, *Solubility enhancers for oral drug delivery*. *American Journal of Drug Delivery*, 2004. **2**(2): p. 113-130.
4. Singh, A, et al., *Oral formulation strategies to improve solubility of poorly water-soluble drugs*. *Expert Opinion on Drug Delivery*, 2011. **8**(10): p. 1361-1378.
5. Moriguchi, I, et al., *Simple method of calculating octanol/water partition coefficient*. *Chemical and Pharmaceutical Bulletin*, 1992. **40**(1): p. 127-130.
6. Lipinski, CA, *Drug-like properties and the causes of poor solubility and poor permeability*. *Journal of Pharmacological and Toxicological Methods*, 2000. **44**(1): p. 235-249.
7. Amidon, G, et al., *A theoretical basis for a biopharmaceutic drug classification: the correlation of in vitro drug product dissolution and in vivo bioavailability*. *Pharmaceutical Research*, 1995. **12**(3): p. 413-420.
8. Lennernäs, H, and Abrahamsson, B, *The biopharmaceutics classification system*, in John, BT, et al., Editors, *Comprehensive medicinal chemistry II*. 2007, Elsevier: Oxford. p. 971-988.
9. Yu, L, et al., *Biopharmaceutics classification system: the scientific basis for biowaiver Extensions*. *Pharmaceutical Research*, 2002. **19**(7): p. 921-925.
10. Pouton, CW, *Formulation of poorly water-soluble drugs for oral administration: Physicochemical and physiological issues and the lipid formulation classification system*. *European Journal of Pharmaceutical Sciences*, 2006. **29**(3-4): p. 278-287.
11. Di, L, et al., *Bridging solubility between drug discovery and development*. *Drug Discovery Today*, 2012. **17**(9-10): p. 486-495.
12. Di, L, et al., *Drug-like property concepts in pharmaceutical design*. *Current Pharmaceutical Design*, 2009. **15**(19): p. 2184-2194.
13. Bergström, CA, et al., *Poorly soluble marketed drugs display solvation limited solubility*. *Journal of Medicinal Chemistry*, 2007. **50**(23): p. 5858-5862.
14. Anuta, V, et al., *Biopharmaceutical profiling of new antitumor pyrazole derivatives*. *Molecules*, 2014. **19**(10): p. 16381-16401.

## References

---

15. Kakran, M, et al., *Overcoming the challenge of poor drug solubility*. Pharmaceutical Engineering, 2012. **32**(4): p. 1-7.
16. Williams, HD, et al., *Strategies to address low drug solubility in discovery and development*. Pharmacological Reviews, 2013. **65**(1): p. 315-499.
17. Savjani, KT, et al., *Drug solubility: Importance and enhancement techniques*. ISRN Pharmaceutics, 2012. **2012**: p. 1-10.
18. Timpe, C, *Drug solubilization strategies: Applying nanoparticulate formulation and solid dispersion approaches in drug development*. American Pharmaceutical Review, 2010. **13**(1): p. 12-21.
19. Singh, B, et al., *Self-emulsifying drug delivery systems (SEDDS): Formulation development, characterization, and applications*. Critical Reviews™ in Therapeutic Drug Carrier Systems, 2009. **26**(5): p. 427-521.
20. Rahman, MA, et al., *Oral lipid based drug delivery system (LBDDS): Formulation, characterization and application: A review*. Current Drug Delivery, 2011. **8**(4): p. 330-345.
21. Alam, MA, et al., *Solid dispersions: A strategy for poorly aqueous soluble drugs and technology updates*. Expert Opinion on Drug Delivery, 2012. **9**(11): p. 1419-1440.
22. Tiwari, R, et al., *Solid dispersions: An overview to modify bioavailability of poorly water soluble drugs*. International Journal of PharmTech Research, 2009. **1**(4): p. 1338-1349.
23. Fahy, E, et al., *A comprehensive classification system for lipids*. Journal of Lipid Research, 2005. **46**(5): p. 839-861.
24. Fahy, E, et al., *Update of the LIPID MAPS comprehensive classification system for lipids*. Journal of Lipid Research, 2009. **50 Suppl**: p. S9-14.
25. Fahy, E, et al., *Lipid classification, structures and tools*. Biochimica et Biophysica Acta (BBA) - Molecular and Cell Biology of Lipids, 2011. **1811**(11): p. 637-647.
26. Hauss, DJ, *Oral lipid-based formulations*. Advanced Drug Delivery Reviews, 2007. **59**(7): p. 667-676.
27. Akoh, CC, and Min, DB, *Food lipids chemistry, nutrition, and biotechnology*. 3<sup>rd</sup> ed. 2008, CRC Press: Boca Raton.
28. Small, D, *A classification of biologic lipids based upon their interaction in aqueous systems*. Journal of the American Oil Chemists Society, 1968. **45**(3): p. 108-119.
29. Hauss, DJ, et al., *Lipid-based delivery systems for improving the bioavailability and lymphatic transport of a poorly water-soluble LTB4 inhibitor*. Journal of Pharmaceutical Sciences, 1998. **87**(2): p. 164-169.
30. O'Driscoll, CM, *Lipid-based formulations for intestinal lymphatic delivery*. European Journal of Pharmaceutical Sciences, 2002. **15**(5): p. 405-415.



31. Pouton, CW, *Lipid formulations for oral administration of drugs: Non-emulsifying, self-emulsifying and 'self-microemulsifying' drug delivery systems*. European Journal of Pharmaceutical Sciences, 2000. **11**: p. S93-S98.
32. Pouton, CW, and Porter, CJ, *Formulation of lipid-based delivery systems for oral administration: materials, methods and strategies*. Advanced Drug Delivery Reviews, 2008. **60**(6): p. 625-637.
33. Gupta, S, et al., *Formulation strategies to improve the bioavailability of poorly absorbed drugs with special emphasis on self-emulsifying systems*. ISRN Pharmaceutics 2013. **2013**: p. 848043.
34. Mu, H, et al., *Lipid-based formulations for oral administration of poorly water-soluble drugs*. International Journal of Pharmaceutics, 2013. **453**(1): p. 215-224.
35. Chakraborty, S, et al., *Lipid – An emerging platform for oral delivery of drugs with poor bioavailability*. European Journal of Pharmaceutics and Biopharmaceutics, 2009. **73**(1): p. 1-15.
36. Balaji, A, et al., *Liquisolid technology- A latest review*. International Journal of Applied Pharmaceutics, 2014. **6**(1): p. 11-19.
37. Spicer, P, *Cubosome processing: Industrial nanoparticle technology development*. Chemical Engineering Research and Design, 2005. **83**(11): p. 1283-1286.
38. Anton, N, and Vandamme, TF, *Nano-emulsions and micro-emulsions: Clarifications of the critical differences*. Pharmaceutical Research, 2011. **28**(5): p. 978-985.
39. Narang, AS, et al., *Stable drug encapsulation in micelles and microemulsions*. International Journal of Pharmaceutics, 2007. **345**(1-2): p. 9-25.
40. Nanjwade, BK, et al., *Functions of lipids for enhancement of oral bioavailability of poorly water-soluble drugs*. Scientia Pharmaceutica, 2011. **79**(4): p. 705-727.
41. Park, MJ, et al., *Polymeric nanocapsules with SEDDS oil-core for the controlled and enhanced oral absorption of cyclosporine*. International Journal of Pharmaceutics, 2013. **441**(1-2): p. 757-764.
42. Surabhi, K, et al., *Microemulsions: Developmental aspects*. Research Journal of Pharmaceutical, Biological and Chemical Sciences, 2010. **1**(4): p. 683-706.
43. Porter, CJ, et al., *Enhancing intestinal drug solubilisation using lipid-based delivery systems*. Advanced Drug Delivery Reviews, 2008. **60**(6): p. 673-691.
44. Mehnert, W, and Mäder, K, *Solid lipid nanoparticles: Production, characterization and applications*. Advanced Drug Delivery Reviews, 2001. **47**(2-3): p. 165-196.
45. Singhal, GB, et al., *Solid lipid nanoparticles and nano lipid carriers: As novel solid lipid based drug carrier*. International Research Journal of Pharmacy, 2011. **2**(2): p. 20-52.

46. Humberstone, AJ, and Charman, WN, *Lipid-based vehicles for the oral delivery of poorly water soluble drugs*. *Advanced Drug Delivery Reviews*, 1997. **25**(1): p. 103-128.
47. Porter, CJH, et al., *Lipids and lipid-based formulations: Optimizing the oral delivery of lipophilic drugs*. *Nature Reviews Drug Discovery*, 2007. **6**(3): p. 231-248.
48. Rahman, MA, et al., *Role of excipients in successful development of self-emulsifying/microemulsifying drug delivery system (SEDDS/SMEDDS)*. *Drug Development and Industrial Pharmacy*, 2013. **39**(1): p. 1-19.
49. Song, WH, et al., *Enhanced dissolution of celecoxib by supersaturating self-emulsifying drug delivery system (S-SEDDS) formulation*. *Archives of Pharmacal Research*, 2013. **36**(1): p. 69-78.
50. Borovicka, J, et al., *Regulation of gastric and pancreatic lipase secretion by CCK and cholinergic mechanisms in humans*. *American Journal of Physiology-Gastrointestinal and Liver Physiology*, 1997. **36**(2): p. G374-G380.
51. Thomson, ABR, et al., *Intestinal aspects of lipid absorption: In review*. *Canadian Journal of Physiology and Pharmacology*, 1989. **67**(3): p. 179-191.
52. N'Goma, JCB, et al., *Understanding the lipid-digestion processes in the GI tract before designing lipid-based drug-delivery systems*. *Therapeutic Delivery*, 2012. **3**(1): p. 105-124.
53. Sternby, B, et al., *Pancreatic lipolytic enzymes in human duodenal contents radioimmunoassay compared with enzyme activity*. *Scandinavian Journal of Gastroenterology*, 1991. **26**(8): p. 859-866.
54. Abrams, CK, et al., *Gastric lipase: Localization in the human stomach*. *Gastroenterology*, 1988. **95**(6): p. 1460-1464.
55. Lengsfeld, H, et al., *Physiology of gastrointestinal lipolysis and therapeutical use of lipases and digestive lipase inhibitors*, in, *Lipases and phospholipases in drug development*. 2005, Wiley-VCH Verlag GmbH & Co. KGaA: Weinheim. p. 195-229.
56. Carrière, F, et al., *Quantitative study of digestive enzyme secretion and gastrointestinal lipolysis in chronic pancreatitis*. *Clinical Gastroenterology and Hepatology*, 2005. **3**(1): p. 28-38.
57. Carriere, F, et al., *Secretion and contribution to lipolysis of gastric and pancreatic lipases during a test meal in humans*. *Gastroenterology*, 1993. **105**(3): p. 876-888.
58. Renou, C, et al., *Effects of lansoprazole on human gastric lipase secretion and intragastric lipolysis in healthy human volunteers*. *Digestion*, 2001. **63**(4): p. 207-213.
59. Hamosh, M, et al., *Fat digestion in the newborn: characterization of lipase in gastric aspirates of premature and term infants*. *Journal of Clinical Investigation*, 1981. **67**(3): p. 838-846.

## References

---

60. Bezzine, S, et al., *Human pancreatic lipase: Colipase dependence and interfacial binding of lid domain mutants*. *Biochemistry*, 1999. **38**(17): p. 5499-5510.
61. Dahim, M, and Brockman, H, *How colipase–fatty acid interactions mediate adsorption of pancreatic lipase to interfaces*. *Biochemistry*, 1998. **37**(23): p. 8369-8377.
62. Hildebrand, P, et al., *Hydrolysis of dietary fat by pancreatic lipase stimulates cholecystokinin release*. *Gastroenterology*, 1998. **114**(1): p. 123-129.
63. McLaughlin, J, et al., *Fatty acid chain length determines cholecystokinin secretion and effect on human gastric motility*. *Gastroenterology*, 1999. **116**(1): p. 46-53.
64. Hunt, J, and Knox, M, *A relation between the chain length of fatty acids and the slowing of gastric emptying*. *The Journal of Physiology*, 1968. **194**(2): p. 327-336.
65. Fernandez, S, et al., *Lipolysis of the semi-solid self-emulsifying excipient gelucire® 44/14 by digestive lipases*. *Biochimica et Biophysica Acta (BBA) - Molecular and Cell Biology of Lipids*, 2008. **1781**(8): p. 367-375.
66. Duane, WC, et al., *Effects of fasting on bile acid metabolism and biliary lipid composition in man*. *Journal of Lipid Research*, 1976. **17**(3): p. 211-219.
67. Erlinger, S, *Bile secretion*. *British Medical Bulletin*, 1992. **48**(4): p. 860-876.
68. Hernell, O, et al., *Physical-chemical behavior of dietary and biliary lipids during intestinal digestion and absorption. 2. Phase analysis and aggregation states of luminal lipids during duodenal fat digestion in healthy adult human beings*. *Biochemistry*, 1990. **29**(8): p. 2041-2056.
69. Sek, L, et al., *Evaluation of the in-vitro digestion profiles of long and medium chain glycerides and the phase behaviour of their lipolytic products*. *Journal of Pharmacy and Pharmacology*, 2002. **54**(1): p. 29-41.
70. Kossena, GA, et al., *Probing drug solubilization patterns in the gastrointestinal tract after administration of lipid-based delivery systems: A phase diagram approach*. *Journal of Pharmaceutical Sciences*, 2004. **93**(2): p. 332-348.
71. Kossena, GA, et al., *Influence of the intermediate digestion phases of common formulation lipids on the absorption of a poorly water-soluble drug*. *Journal of Pharmaceutical Sciences*, 2005. **94**(3): p. 481-492.
72. Westergaard, H, and Dietschy, JM, *The mechanism whereby bile acid micelles increase the rate of fatty acid and cholesterol uptake into the intestinal mucosal cell*. *Journal of Clinical Investigation*, 1976. **58**(1): p. 97-108.
73. Dulfer, WJ, et al., *Effect of fatty acids and the aqueous diffusion barrier on the uptake and transport of polychlorinated biphenyls in Caco-2 cells*. *Journal of lipid research*, 1996. **37**(5): p. 950-961.
74. Thomson, ABR, et al., *Lipid absorptions passing through the unstirred layers, brush-border membrane, and beyond*. *Canadian Journal of Physiology and Pharmacology*, 1993. **71**(8): p. 531-555.

## References

---

75. Simmonds, WJ, *The role of micellar solubilization in lipid absorption*. Immunology and Cell Biology, 1972. **50**(4): p. 403-421.
76. Shiau, Y, et al., *Acidic mucin layer facilitates micelle dissociation and fatty acid diffusion*. American Journal of Physiology - Gastrointestinal and Liver Physiology, 1990. **259**(4 Part 1): p. G671-G675.
77. Nordskog, BK, et al., *An examination of the factors affecting intestinal lymphatic transport of dietary lipids*. Advanced Drug Delivery Reviews, 2001. **50**(1-2): p. 21-44.
78. Porter, CJH, and Charman, WN, *Intestinal lymphatic drug transport: An update*. Advanced Drug Delivery Reviews, 2001. **50**(1-2): p. 61-80.
79. Cater, NB, et al., *Comparison of the effects of medium-chain triacylglycerols, palm oil, and high oleic acid sunflower oil on plasma triacylglycerol fatty acids and lipid and lipoprotein concentrations in humans*. The American Journal of Clinical Nutrition, 1997. **65**(1): p. 41-45.
80. Bergstedt, SE, et al., *A comparison of absorption of glycerol tristearate and glycerol trioleate by rat small intestine*. American Journal of Physiology - Gastrointestinal and Liver Physiology, 1990. **259**(3): p. G386-G393.
81. Ockner, RK, et al., *Differences in the intestinal absorption of saturated and unsaturated long chain fatty acids*. Gastroenterology. **62**(5): p. 981-992.
82. van Greevenbroek, MMJ, et al., *Effects of saturated, mono-, and polyunsaturated fatty acids on the secretion of apo B containing lipoproteins by Caco-2 cells*. Atherosclerosis, 1996. **121**(1): p. 139-150.
83. Charman, WNA, and Stella, VJ, *Estimating the maximal potential for intestinal lymphatic transport of lipophilic drug molecules*. International Journal of Pharmaceutics, 1986. **34**(1-2): p. 175-178.
84. Trevaskis, NL, et al., *An examination of the interplay between enterocyte-based metabolism and lymphatic drug transport in the rat*. Drug Metabolism and Disposition, 2006. **34**(5): p. 729-733.
85. Pantaleo, G, et al., *Role of lymphoid organs in the pathogenesis of human immunodeficiency virus (HIV) infection*. Immunological Reviews, 1994. **140**(1): p. 105-130.
86. Strickley, RG, *Solubilizing excipients in oral and injectable formulations*. Pharmaceutical Research, 2004. **21**(2): p. 201-230.
87. Qi, XL, et al., *Self-double-emulsifying drug delivery system (SDEDDS): A new way for oral delivery of drugs with high solubility and low permeability*. International Journal of Pharmaceutics, 2011. **409**(1-2): p. 245-251.
88. Date, AA, et al., *Self-nanoemulsifying drug delivery systems: Formulation insights, applications and advances*. Nanomedicine, 2010. **5**(10): p. 1595-1616.

- 
89. Dokania, S, and Joshi, AK, *Self-microemulsifying drug delivery system (SMEDDS) – Challenges and road ahead*. Drug Delivery, 2014. DOI:10.3109/10717544.2014.896058: p. .
  90. Niederquell, A, and Kuentz, M, *Proposal of stability categories for nano-dispersions obtained from pharmaceutical self-emulsifying formulations*. International Journal of Pharmaceutics, 2013. **446**(1-2): p. 70-80.
  91. Khan, AW, et al., *Potentials and challenges in self-nanoemulsifying drug delivery systems*. Expert Opinion on Drug Delivery, 2012. **9**(10): p. 1305-1317.
  92. Vonderscher, J, and Meinzer, A. *Rationale for the development of sandimmune neoral*. in *Transplantation proceedings*. 1994. Elsevier.
  93. Singh, B, et al., *Recent advances in self-emulsifying drug delivery systems (SEDDS)*. Critical Reviews™ in Therapeutic Drug Carrier Systems, 2014. **31**(2): p. 121-185.
  94. Ravichandiran, V, et al., *Bioavailability enhancement of poorly soluble drugs: Self emulsifying drug delivery system - A novel approach*. International Journal of Pharmaceutical Sciences Review and Research, 2011. **10**(2): p. 72-77.
  95. Kumar, A, et al., *Self emulsifying drug delivery system (SEDDS): Future aspects*. International Journal of Pharmacy and Pharmaceutical Sciences, 2010. **2**(SUPPL. 4): p. 7-13.
  96. Mallikarjun, V, and Rajesh Babu, V, *Recent trends in development of solid-self emulsifying drug Delivery (S-SEDDS) systems: An overview*. International Research Journal of Pharmacy, 2011. **2**(6): p. 18-22.
  97. Tang, B, et al., *Development of solid self-emulsifying drug delivery systems: Preparation techniques and dosage forms*. Drug Discovery Today, 2008. **13**(13-14): p. 606-612.
  98. Gugulothu, D, et al., *Self-microemulsifying suppository formulation of beta-artemether*. AAPS PharmSciTech, 2010. **11**(3): p. 1179-1184.
  99. Kim, JY, and Ku, YS, *Enhanced absorption of indomethacin after oral or rectal administration of a self-emulsifying system containing indomethacin to rats*. International Journal of Pharmaceutics, 2000. **194**(1): p. 81-89.
  100. Lee, S, et al., *Design and evaluation of prostaglandin E1 (PGE1) intraurethral liquid formulation employing self-microemulsifying drug delivery system (SMEDDS) for erectile dysfunction treatment*. Biological and Pharmaceutical Bulletin, 2008. **31**(4): p. 668-672.
  101. Yao, J, et al., *Development of docetaxel self-microemulsifying drug delivery system (SMEDDS) for parenteral delivery: Preparation, characterization and in vivo evaluation*. Asian Journal of Pharmaceutical Sciences, 2012. **7**(4): p. 18-27.
  102. He, S, et al., *A cremophor-free self-microemulsified delivery system for intravenous injection of teniposide: Evaluation in vitro and in vivo*. AAPS PharmSciTech, 2012. **13**(3): p. 846-852.

## References

---

103. Borhade, VB, et al., *Development and characterization of self-microemulsifying drug delivery system of tacrolimus for intravenous administration*. Drug Development and Industrial Pharmacy, 2009. **35**(5): p. 619-630.
104. Lo, J-T, et al., *Self-emulsifying O/W formulations of paclitaxel prepared from mixed nonionic surfactants*. Journal of Pharmaceutical Sciences, 2010. **99**(5): p. 2320-2332.
105. Chae, GS, et al., *Enhancement of the stability of BCNU using self-emulsifying drug deliver systems (SEDDS) and in vitro antitumor activity of self-emulsified BCNU-loaded PLGA water*. International Journal of Pharmaceutics, 2005. **301**(1-2): p. 6-14.
106. El Maghraby, GM, *Self-microemulsifying and microemulsion systems for transdermal delivery of indomethacin: Effect of phase transition*. Colloids and Surfaces B-Biointerfaces, 2010. **75**(2): p. 595-600.
107. Zargar-Shoshtari, S, et al., *Formulation and physicochemical characterization of imwitor 308 based self microemulsifying drug delivery systems*. Chemical and Pharmaceutical Bulletin, 2010. **58**(10): p. 1332-1338.
108. Ahmed, OAA, et al., *Optimization of self-nanoemulsifying systems for the enhancement of in vivo hypoglycemic efficacy of glimepiride transdermal patches*. Expert Opinion on Drug Delivery, 2014. **11**(7): p. 1005-1013.
109. Elnaggar, YSR, et al., *Sildenafil citrate nanoemulsion vs. self-nanoemulsifying delivery systems: Rational development and transdermal permeation*. International Journal of Nanotechnology, 2011. **8**(8-9): p. 749-763.
110. El-Say, KM, et al., *Enhanced permeation parameters of optimized nanostructured simvastatin transdermal films: Ex vivo and in vivo evaluation*. Pharmaceutical Development and Technology, 2014. DOI:10.3109/10837450.2014.938859.
111. Li, SH, and Quan, DQ, *Preparation and in vitro evaluation of an ilomastat microemulsion gel by a self-microemulsifying system*. Pharmazie, 2012. **67**(2): p. 156-160.
112. Czajkowska-Kosnik, A, and Sznitowska, M, *Solubility of ocular therapeutic agents in self-emulsifying oils I. Self-emulsifying oils for ocular drug delivery: Solubility of indomethacin, aciclovir and hydrocortisone*. Acta Poloniae Pharmaceutica, 2009. **66**(6): p. 709-713.
113. Czajkowska-Kosnik, A, et al., *Self-emulsifying oils for ocular drug delivery. II. In vitro release of indomethacin and hydrocortisone*. Acta Poloniae Pharmaceutica, 2012. **69**(2): p. 309-317.
114. Sigward, E, et al., *Formulation and cytotoxicity evaluation of new self-emulsifying multiple W/O/W nanoemulsions*. International Journal of Nanomedicine, 2013. **8**: p. 611.
115. ElKasabgy, NA, *Ocular supersaturated self-nanoemulsifying drug delivery systems (S-SNEDDS) to enhance econazole nitrate bioavailability*. International Journal of Pharmaceutics, 2014. **460**(1-2): p. 33-44.

116. El Maghraby, GM, and Bosela, AA, *Investigation of self-microemulsifying and microemulsion systems for protection of prednisolone from gamma radiation*. Pharmaceutical Development and Technology, 2011. **16**(3): p. 237-242.
117. Reiss, H, *Entropy-induced dispersion of bulk liquids*. Journal of Colloid and Interface Science, 1975. **53**(1): p. 61-70.
118. Wakerly, MG, et al., *Self-emulsification of vegetable oil-nonionic surfactant mixtures*, in Scamehorn, JF, Editor, *Phenomena in mixed surfactant systems*. 1986, American Chemical Society: Washington. p. 242-255.
119. Pouton, CW, *Self-emulsifying drug delivery systems: Assessment of the efficiency of emulsification*. International Journal of Pharmaceutics, 1985. **27**(2-3): p. 335-348.
120. Pouton, CW, *Formulation of self-emulsifying drug delivery systems*. Advanced Drug Delivery Reviews, 1997. **25**(1): p. 47-58.
121. Chen, XQ, et al., *Application of lipid-based formulations in drug discovery*. Journal of Medicinal Chemistry, 2012. **55**(18): p. 7945-7956.
122. Jannin, V, et al., *Approaches for the development of solid and semi-solid lipid-based formulations*. Advanced Drug Delivery Reviews, 2008. **60**(6): p. 734-746.
123. Cao, Y, et al., *Predictive relationships for the effects of triglyceride ester concentration and water uptake on solubility and partitioning of small molecules into lipid vehicles*. Journal of Pharmaceutical Sciences, 2004. **93**(11): p. 2768-2779.
124. Charman, WN, and Stella, VJ, *Transport of lipophilic molecules by the intestinal lymphatic system*. Advanced Drug Delivery Reviews, 1991. **7**(1): p. 1-14.
125. Bandyopadhyay, S, et al., *Optimized self nano-emulsifying systems of ezetimibe with enhanced bioavailability potential using long chain and medium chain triglycerides*. Colloids and Surfaces B-Biointerfaces, 2012. **100**: p. 50-61.
126. Caliph, SM, et al., *Effect of short-, medium-, and long-chain fatty acid-based vehicles on the absolute oral bioavailability and intestinal lymphatic transport of halofantrine and assessment of mass balance in lymph-cannulated and non-cannulated rats*. Journal of Pharmaceutical Sciences, 2000. **89**(8): p. 1073-1084.
127. Beg, S, et al., *Development of solid self-nanoemulsifying granules (SSNEGs) of ondansetron hydrochloride with enhanced bioavailability potential*. Colloids and Surfaces B-Biointerfaces, 2013. **101**: p. 414-423.
128. Thomas, N, et al., *Influence of lipid composition and drug load on the in vitro performance of self-nanoemulsifying drug delivery systems*. Journal of Pharmaceutical Sciences, 2012. **101**(5): p. 1721-1731.
129. Patel, V, et al., *Self emulsifying drug delivery system: A conventional and alternative approach to improve oral bioavailability of lipophilic drugs*. International Journal of Drug Development and Research, 2010. **2**(4): p. 859-870.

## References

---

130. Kohli, K, et al., *Self-emulsifying drug delivery systems: an approach to enhance oral bioavailability*. Drug Discovery Today, 2010. **15**(21-22): p. 958-965.
131. Wei, LL, et al., *Investigations of a novel self-emulsifying osmotic pump tablet containing carvedilol*. Drug Development and Industrial Pharmacy, 2007. **33**(9): p. 990-998.
132. Zhang, X, et al., *Controlled release of cyclosporine A self-nanoemulsifying systems from osmotic pump tablets: Near zero-order release and pharmacokinetics in dogs*. International Journal of Pharmaceutics, 2013. **452**(1-2): p. 233-240.
133. Bagul, N, et al., *Design and development of solid self emulsifying osmotic delivery system of nifedipine*. Archives of Pharmacy Practice, 2012. **3**(2): p. 128-135.
134. Setthacheewakul, S, et al., *Controlled release of oral tetrahydrocurcumin from a novel self-emulsifying floating drug delivery system (SEFDDS)*. AAPS PharmSciTech, 2011. **12**(1): p. 152-164.
135. Wang, YP, et al., *Novel gastroretentive sustained-release tablet of tacrolimus based on self-microemulsifying mixture: In vitro evaluation and in vivo bioavailability test*. Acta Pharmacologica Sinica, 2011. **32**(10): p. 1294-1302.
136. Whittle, B, and Guy, G, *Mucoadhesive pharmaceutical formulations*. 2002. World Patent **WO02/064109A2**.
137. Trickler, WJ, et al., *A novel nanoparticle formulation for sustained paclitaxel delivery*. AAPS PharmSciTech, 2008. **9**(2): p. 486-493.
138. Khan, MA, and Nazzal, S, *Eutectic-based self-nanoemulsified drug delivery system*. 2003. United States Patent **US2003/0147927A1**.
139. Nazzal, S, et al., *Preparation and in vitro characterization of a eutectic based semisolid self-nanoemulsified drug delivery system (SNEDDS) of ubiquinone: Mechanism and progress of emulsion formation*. International Journal of Pharmaceutics, 2002. **235**(1-2): p. 247-265.
140. Ruan, JH, et al., *Preparation and evaluation of self-nanoemulsified drug delivery systems (SNEDDSs) of matrine based on drug-phospholipid complex technique*. International Journal of Pharmaceutics, 2010. **386**(1-2): p. 282-290.
141. Shanmugam, S, et al., *Solid self-nanoemulsifying drug delivery system (S-SNEDDS) containing phosphatidylcholine for enhanced bioavailability of highly lipophilic bioactive carotenoid lutein*. European Journal of Pharmaceutics and Biopharmaceutics, 2011. **79**(2): p. 250-257.
142. Milovic, M, et al., *Solid self-emulsifying phospholipid suspension (SSEPS) with diatom as a drug carrier*. European Journal of Pharmaceutical Sciences, 2014. **63**: p. 226-232.
143. Zhou, H, et al., *A new strategy for enhancing the oral bioavailability of drugs with poor water-solubility and low liposolubility based on phospholipid complex and supersaturated SEDDS*. Plos One, 2014. **9**(2): p. e91605.



144. Zhou, H, et al., *A new strategy for enhancing the oral bioavailability of drugs with poor water-solubility and low liposolubility based on phospholipid complex and supersaturated SEDDS*. Plos One, 2013. **8**(12).
145. Gao, P, et al., *Enhanced oral bioavailability of a poorly water soluble drug PNU-91325 by supersaturatable formulations*. Drug Development and Industrial Pharmacy, 2004. **30**(2): p. 221-229.
146. Bandyopadhyay, S, et al., *Development of optimized supersaturable self-nanoemulsifying systems of ezetimibe: Effect of polymers and efflux transporters*. Expert Opinion on Drug Delivery, 2014. **11**(4): p. 479-492.
147. Nan, Z, et al., *Evaluation of carbamazepine (CBZ) supersaturatable self-microemulsifying (S-SMEDDS) formulation in-vitro and in-vivo*. Iranian Journal of Pharmaceutical Research, 2012. **11**(1): p. 257-264.
148. Thomas, N, et al., *Supersaturated self-nanoemulsifying drug delivery systems (super-SNEDDS) enhance the bioavailability of the poorly water-soluble drug simvastatin in dogs*. AAPS Journal, 2013. **15**(1): p. 219-227.
149. Wei, Y, et al., *Enhanced oral bioavailability of silybin by a supersaturatable self-emulsifying drug delivery system (S-SEDDS)*. Colloids and Surfaces A: Physicochemical and Engineering Aspects, 2012. **396**: p. 22-28.
150. Chen, Y, et al., *Development of a solid supersaturatable self-emulsifying drug delivery system of docetaxel with improved dissolution and bioavailability*. Biological and Pharmaceutical Bulletin, 2011. **34**(2): p. 278-286.
151. Gao, P, et al., *Characterization and optimization of AMG 517 supersaturatable self-emulsifying drug delivery system (S-SEDDS) for improved oral absorption*. Journal of Pharmaceutical Sciences, 2009. **98**(2): p. 516-528.
152. Gao, P, and Morozowich, W, *Development of supersaturatable self-emulsifying drug delivery system formulations for improving the oral absorption of poorly soluble drugs*. Expert Opinion on Drug Delivery, 2006. **3**(1): p. 97-110.
153. Gao, P, et al., *Development of a supersaturable SEDDS (S-SEDDS) formulation of paclitaxel with improved oral bioavailability*. Journal of Pharmaceutical Sciences, 2003. **92**(12): p. 2386-2398.
154. Gosangari, S, and Dyakonov, T, *Enhanced dissolution performance of curcumin with the use of supersaturatable formulations*. Pharmaceutical Development and Technology, 2013. **18**(2): p. 475-480.
155. Mukherjee, T, and Plakogiannis, FM, *Development and oral bioavailability assessment of a supersaturated self-microemulsifying drug delivery system (SMEDDS) of albendazole*. The Journal of Pharmacy and Pharmacology, 2010. **62**(9): p. 1112-1120.
156. Peng, X, et al., *Preparation and evaluation of silymarin supersaturation self-emulsifying drug delivery system*. Chinese Traditional and Herbal Drugs, 2010. **41**(1): p. 40-44.

## References

---

157. Thomas, N, et al., *In vitro and in vivo performance of novel supersaturated self-nanoemulsifying drug delivery systems (super-SNEDDS)*. Journal of Controlled Release, 2012. **160**(1): p. 25-32.
158. Zhang, N, et al., *Studies on preparation of carbamazepine (CBZ) supersaturatable self-microemulsifying (S-SMEDDS) formulation and relative bioavailability in beagle dogs*. Pharmaceutical Development and Technology, 2011. **16**(4): p. 415-421.
159. Venkatesan, N, et al., *Liquid filled nanoparticles as a drug delivery tool for protein therapeutics*. Biomaterials, 2005. **26**(34): p. 7154-7163.
160. Gershanik, T, et al., *Interaction of a self-emulsifying lipid drug delivery system with the everted rat intestinal mucosa as a function of droplet size and surface charge*. Pharmaceutical Research, 1998. **15**(6): p. 863-869.
161. Parthasarathi, KP, et al., *Formulation and evaluation of positively charged self-emulsifying drug delivery system containing ibuprofen*. International Research Journal of Pharmacy, 2011. **2**(8): p. 82-91.
162. Mudit, D, et al., *Formulation and evaluation of positively charged self-emulsifying drug delivery system containing a NSAID*. International Journal of Pharmaceutical Sciences, 2010. **2**(3): p. 792-803.
163. Chen, Y, et al., *Self-microemulsifying drug delivery system (SMEDDS) of vincopetine: Formulation development and in vivo assessment*. Biological and Pharmaceutical Bulletin, 2008. **31**(1): p. 118-125.
164. Holmberg, C, and Siekmann, B, *Self emulsifying drug delivery system*. 2010. United States Patent **US7736666B2**.
165. Arien, AME, et al., *Polymeric micromulsions*. 2006. United States Patent **US2006/0034797**.
166. Fernandez-Tarrio, M, et al., *Pluronic and tetronic copolymers with polyglycolized oils as self-emulsifying drug delivery systems*. AAPS PharmSciTech, 2008. **9**(2): p. 471-479.
167. Shively, M, *Self-emulsifying glasses*. 1991. World Patent **WO1991/018613**.
168. Myers, SL, and Shively, ML, *Preparation and characterization of emulsifiable glasses: Oil-in-water and water-in-oil-in-water emulsions*. Journal of Colloid and Interface Science, 1992. **149**(1): p. 271-278.
169. Lv, L-Z, et al., *Enhanced absorption of hydroxysafflor yellow A using a self-double-emulsifying drug delivery system: In vitro and in vivo studies*. International Journal of Nanomedicine, 2012. **7**: p. 4099.
170. Zhang, L, et al., *Enhanced absorption of Stachydrine using a self-double-emulsifying drug delivery systems (SDEDDS): In vitro and in vivo studies*. Life Science Journal, 2013. **10**(4).
171. Padole, A, and Bodhankar, M, *Self double emulsifying drug delivery system (SDEDDS): A review*. Journal of Drug Delivery and Therapeutics, 2012. **2**(6).

172. Singh, G, and Pai, RS, *Enhanced oral bioavailability of (+)-catechin by a self double-emulsifying drug delivery system (SDEDDS): A new platform for oral delivery of biopharmaceutics classification system Class III drugs*. *Nanomedicine and Nanobiology*, 2014. **1**(1): p. 51-56.
173. Atef, E, and Belmonte, AA, *Formulation and in vitro and in vivo characterization of a phenytoin self-emulsifying drug delivery system (SEDDS)*. *European Journal of Pharmaceutical Sciences*, 2008. **35**(4): p. 257-263.
174. Gunstone, FD, et al., *The Lipid Handbook*. 3<sup>rd</sup> ed. 2007, CRC Press: Boca Raton.
175. Zhu, X, et al., *Target release rate of antioxidants to extend induction period of lipid oxidation*. *Food Research International*, 2012. **47**(1): p. 1-5.
176. Bowtle, WJ, *Materials, process, and manufacturing considerations for lipid-based hard-capsule formats*, in Hauss, DJ, Editor, *Oral lipid-based formulations: Enhancing the bioavailability of poorly water-soluble drugs*. 2007, Informa Healthcare: New York. p. 97-106.
177. Serajuddin, ATM, et al., *Water migration from soft gelatin capsule shell to fill material and its effect on drug solubility*. *Journal of Pharmaceutical Sciences*, 1986. **75**(1): p. 62-64.
178. Gullapalli, RP, *Soft gelatin capsules (softgels)*. *Journal of Pharmaceutical Sciences*, 2010. **99**(10): p. 4107-4148.
179. Chen, F-J, et al., *Effects of lipophilic components on the compatibility of lipid-based formulations with hard gelatin capsules*. *Journal of Pharmaceutical Sciences*, 2010. **99**(1): p. 128-141.
180. Zhang, F, and DiNunzio, J, *Solubilized formulations*, in Williams III, RO, et al., Editors, *Formulating poorly water soluble drugs*. 2012, Springer: New York. p. 171-208.
181. Abdalla, A, and Mäder, K, *Preparation and characterization of a self-emulsifying pellet formulation*. *European Journal of Pharmaceutics and Biopharmaceutics*, 2007. **66**(2): p. 220-226.
182. Lei, Y, et al., *Solid self-nanoemulsifying cyclosporin A pellets prepared by fluid-bed coating: Preparation, characterization and in vitro redispersibility*. *International Journal of Nanomedicine*, 2011. **6**: p. 795-805.
183. Swamy, NGN, and Shiny, EK, *Formulation and evaluation of telmisartan liquisolid tablets*. *Rajiv Gandhi University of Health Sciences Journal of Pharmaceutical Sciences*, 2013. **3**(3): p. 49-57.
184. Sohn, Y, et al., *Development of self-microemulsifying bilayer tablets for pH-independent fast release of candesartan cilexetil*. *Pharmazie*, 2012. **67**(11): p. 917-924.
185. Soliman, KA, et al., *Formulation of risperidone as self-nanoemulsifying drug delivery system in form of effervescent tablets*. *Journal of Dispersion Science and Technology*, 2012. **33**(8): p. 1127-1133.

186. Zidan, AS, et al., *Taste-masked orodispersible tablets of cyclosporine self-nanoemulsion lyophilized with dry silica*. *Pharmaceutical Development and Technology*, 2014. DOI:10.3109/10837450.2014.908307: p. .
187. Agarwal, V, et al., *Powdered self-emulsified lipid formulations of meloxicam as solid dosage forms for oral administration*. *Drug Development and Industrial Pharmacy*, 2013. **39**(11): p. 1681-1689.
188. Huang, Y, et al., *A novel plug-controlled colon-specific pulsatile capsule with tablet of curcumin-loaded SMEDDS*. *Carbohydrate Polymers*, 2013. **92**(2): p. 2218-2223.
189. Bremmell, KE, et al., *Tableting lipid-based formulations for oral drug delivery: A case study with silica nanoparticle–lipid–mannitol hybrid microparticles*. *Journal of Pharmaceutical Sciences*, 2013. **102**(2): p. 684-693.
190. Nguyen, T-H, et al., *Silica–lipid hybrid (SLH) formulations enhance the oral bioavailability and efficacy of celecoxib: An in vivo evaluation*. *Journal of Controlled Release*, 2013. **167**(1): p. 85-91.
191. Zhang, Y, et al., *Mesoporous silica nanoparticles for increasing the oral bioavailability and permeation of poorly water soluble drugs*. *Molecular Pharmaceutics*, 2012. **9**(3): p. 505-513.
192. Tan, A, et al., *Silica-lipid hybrid (SLH) microcapsules: A novel oral delivery system for poorly soluble drugs*. *Journal of Controlled Release*, 2009. **134**(1): p. 62-70.
193. Attama, AA, and Nkemnele, MO, *In vitro evaluation of drug release from self micro-emulsifying drug delivery systems using a biodegradable homolipid from Capra hircus*. *International Journal of Pharmaceutics*, 2005. **304**(1-2): p. 4-10.
194. Hu, YX, et al., *Preparation and evaluation of 5-FU/PLGA/gene nanoparticles*. *Key Engineering Materials*, 2005. **288**: p. 147-150.
195. Xiao, L, et al., *A new self-microemulsifying mouth dissolving film to improve the oral bioavailability of poorly water soluble drugs*. *Drug Development and Industrial Pharmacy*, 2013. **39**(9): p. 1284-1290.
196. Patil, P, and Paradkar, A, *Porous polystyrene beads as carriers for self-emulsifying system containing loratadine*. *AAPS PharmSciTech*, 2006. **7**(1): p. E1-E7.
197. Sriraksa, S, et al., *Floating alginate beads as carriers for self-emulsifying system containing tetrahydrocurcumin*. *Advanced Materials Research*, 2012. **506**: p. 517-520.
198. Kuentz, M, and Roethlisberger, D, *Self emulsifying lipid matrix (SELM)*. 2006. European Patent **EP1349541B1**.
199. Kattaboina, S, et al., *Approaches for the development of solid self-emulsifying drug delivery systems and dosage forms*. *Asian Journal of Pharmaceutical Sciences*, 2009. **4**(4): p. 240-253.
200. Tan, A, et al., *Transforming lipid-based oral drug delivery systems into solid dosage forms: An overview of solid carriers, physicochemical properties, and*

- biopharmaceutical performance*. *Pharmaceutical Research*, 2013. **30**(12): p. 2993-3017.
201. Patel, N, et al., *Development of solid SEDDS: II. Application of acconon C-44 and gelucire 44/14 as solidifying agents for self-emulsifying drug delivery systems of medium chain triglyceride*. *Journal of Excipients and Food Chemicals*, 2012. **3**(2): p. 54-66.
202. Patel, N, et al., *Development of solid SEDDS: III. Application of acconon C-50® and gelucire 50/13® as both solidifying and emulsifying agents for medium chain triglycerides*. *Journal of Excipients and Food Chemicals*, 2012. **3**(2): p. 83-92.
203. Albertini, B, et al., *Formulation of spray congealed microparticles with self-emulsifying ability for enhanced glibenclamide dissolution performance*. *Journal of Microencapsulation*, 2014. DOI:10.3109/02652048.2014.985341.
204. Breitzkreitz, MC, et al., *Characterization of semi-solid self-emulsifying drug delivery systems (SEDDS) of atorvastatin calcium by raman image spectroscopy and chemometrics*. *Journal of Pharmaceutical and Biomedical Analysis*, 2013. **73**: p. 3-12.
205. Chambin, O, et al., *Influence of drug polarity upon the solid-state structure and release properties of self-emulsifying drug delivery systems in relation with water affinity*. *Colloids and Surfaces B-Biointerfaces*, 2009. **71**(1): p. 73-78.
206. Shah, AV, and Serajuddin, AT, *Development of solid self-emulsifying drug delivery system (SEDDS) I: Use of poloxamer 188 as both solidifying and emulsifying agent for lipids*. *Pharmaceutical Research*, 2012. **29**(10): p. 2817-2832.
207. Li, P, et al., *Development of clinical dosage forms for a poorly water-soluble drug II: Formulation and characterization of a novel solid microemulsion concentrate system for oral delivery of a poorly water-soluble drug*. *Journal of Pharmaceutical Sciences*, 2009. **98**(5): p. 1750-1764.
208. Kanaujia, P, et al., *Solid self-emulsifying drug delivery system (S-SEDDS) for improved dissolution rate of fenofibrate*. *Journal of Microencapsulation*, 2014. **31**(3): p. 293-298.
209. Chambin, O, et al., *Influence of cryogenic grinding on properties of a self-emulsifying formulation*. *International Journal of Pharmaceutics*, 2004. **278**(1): p. 79-89.
210. Nanda Kishore, R, et al., *Solid self microemulsification of Atorvastatin using hydrophilic carriers: A design*. *Drug Development and Industrial Pharmacy*, 2014. DOI:10.3109/03639045.2014.938655.
211. Cavallari, C, et al., *Thermal and fractal analysis of diclofenac/gelucire 50/13 microparticles obtained by ultrasound-assisted atomization*. *Journal of Pharmaceutical Sciences*, 2005. **94**(5): p. 1124-1134.
212. Li, F, et al., *Preparation and pharmacokinetics evaluation of oral self-emulsifying system for poorly water-soluble drug Lornoxicam*. *Drug Delivery*, 2014. DOI:10.3109/10717544.2014.885615.

213. Ahmed, IS, and Aboul-Einien, MH, *In vitro and in vivo evaluation of a fast-disintegrating lyophilized dry emulsion tablet containing griseofulvin*. European Journal of Pharmaceutical Sciences, 2007. **32**(1): p. 58-68.
214. Corveleyn, S, and Remon, JP, *Formulation of a lyophilized dry emulsion tablet for the delivery of poorly soluble drugs*. International Journal of Pharmaceutics, 1998. **166**(1): p. 65-74.
215. Abdalla, A, et al., *A new self-emulsifying drug delivery system (SEDDS) for poorly soluble drugs: Characterization, dissolution, in vitro digestion and incorporation into solid pellets*. European Journal of Pharmaceutical Sciences, 2008. **35**(5): p. 457-464.
216. Abbaspour, M, et al., *Development and evaluation of a solid self-nanoemulsifying drug delivery system for loratadin by extrusion-spheronization*. Advanced Pharmaceutical Bulletin, 2014. **4**(2): p. 113-119.
217. Desai, NS, and Nagarsenker, MS, *Design and evaluation of self-nanoemulsifying pellets of repaglinide*. AAPS PharmSciTech, 2013. **14**(3): p. 994-1003.
218. Hu, X, et al., *Sirolimus solid self-microemulsifying pellets: Formulation development, characterization and bioavailability evaluation*. International Journal of Pharmaceutics, 2012. **438**(1-2): p. 123-133.
219. Iosio, T, et al., *Bi-layered self-emulsifying pellets prepared by co-extrusion and spheronization: Influence of formulation variables and preliminary study on the in vivo absorption*. European Journal of Pharmaceutics and Biopharmaceutics, 2008. **69**(2): p. 686-697.
220. Iosio, T, et al., *Oral bioavailability of silymarin phytocomplex formulated as self-emulsifying pellets*. Phytomedicine, 2011. **18**(6): p. 505-512.
221. Miao, Y, et al., *Characterization and evaluation of self-nanoemulsifying sustained-release pellet formulation of ziprasidone with enhanced bioavailability and no food effect*. Drug Delivery, 2014. DOI:10.3109/10717544.2014.950768.
222. Nikolakakis, I, and Malamataris, S, *Self-emulsifying pellets: Relations between kinetic parameters of drug release and emulsion reconstitution-influence of formulation variables*. Journal of Pharmaceutical Sciences, 2014. **103**(5): p. 1453-1465.
223. Sermkaew, N, et al., *Liquid and solid self-microemulsifying drug delivery systems for improving the oral bioavailability of andrographolide from a crude extract of *Andrographis paniculata**. European Journal of Pharmaceutical Sciences, 2013. **50**(3-4): p. 459-466.
224. Tuleu, C, et al., *Comparative bioavailability study in dogs of a self-emulsifying formulation of progesterone presented in a pellet and liquid form compared with an aqueous suspension of progesterone*. Journal of Pharmaceutical Sciences, 2004. **93**(6): p. 1495-1502.

## References

---

225. Uppugalla, S, et al., *Self-emulsifying systems of aceclofenac by extrusion/spheronization: Formulation and evaluation*. Journal of Chemical and Pharmaceutical Research, 2011. **3**(2): p. 280-289.
226. Wang, ZY, et al., *Solid self-emulsifying nitrendipine pellets: Preparation and in vitro/in vivo evaluation*. International Journal of Pharmaceutics, 2010. **383**(1-2): p. 1-6.
227. Yanyu, X, et al., *Self-emulsifying bifendate pellets: Preparation, characterization and oral bioavailability in rats*. Drug Development and Industrial Pharmacy, 2012. **39**(5): p. 724-732.
228. Zhang, Y, et al., *Characterization and evaluation of self-microemulsifying sustained-release pellet formulation of puerarin for oral delivery*. International Journal of Pharmaceutics, 2012. **427**(2): p. 337-344.
229. Mahmoud, EA, et al., *Preparation and evaluation of self-nanoemulsifying tablets of carvedilol*. AAPS PharmSciTech, 2009. **10**(1): p. 183-192.
230. Mura, P, et al., *New solid self-microemulsifying systems to enhance dissolution rate of poorly water soluble drugs*. Pharmaceutical Development and Technology, 2012. **17**(3): p. 277-284.
231. Beg, S, et al., *Development, optimization, and characterization of solid self-nanoemulsifying drug delivery systems of valsartan using porous carriers*. AAPS PharmSciTech, 2012. **13**(4): p. 1416-1427.
232. Gumaste, SG, et al., *Development of solid SEDDS, IV: Effect of adsorbed lipid and surfactant on tableting properties and surface structures of different silicates*. Pharmaceutical Research, 2013. **30**(12): p. 3170-3185.
233. Kang, JH, et al., *Effects of solid carriers on the crystalline properties, dissolution and bioavailability of flurbiprofen in solid self-nanoemulsifying drug delivery system (solid SNEDDS)*. European Journal of Pharmaceutics and Biopharmaceutics, 2012. **80**(2): p. 289-297.
234. Kang, MJ, et al., *Immediate release of ibuprofen from fujicalin(R)-based fast-dissolving self-emulsifying tablets*. Drug Development and Industrial Pharmacy, 2011. **37**(11): p. 1298-1305.
235. Kutza, C, et al., *Toward a detailed characterization of oil adsorbates as "solid liquids"*. European Journal of Pharmaceutics and Biopharmaceutics, 2013. **84**(1): p. 172-182.
236. Deshmukh, A, and Kulkarni, S, *Solid self-microemulsifying drug delivery system of ritonavir*. Drug Development and Industrial Pharmacy, 2014. **40**(4): p. 477-487.
237. Gumaste, SG, et al., *Development of solid SEDDS, V: Compaction and drug release properties of tablets prepared by adsorbing lipid-based formulations onto neusilin (r) US2*. Pharmaceutical Research, 2013. **30**(12): p. 3186-3199.
238. Sander, C, and Holm, P, *Porous magnesium aluminometasilicate tablets as carrier of a cyclosporine self-emulsifying formulation*. AAPS PharmSciTech, 2009. **10**(4): p. 1388-1395.

## References

---

239. Kamel, AO, and Mahmoud, AA, *Enhancement of human oral bioavailability and in vitro antitumor activity of rosuvastatin via spray dried self-nanoemulsifying drug delivery system*. Journal of Biomedical Nanotechnology, 2013. **9**(1): p. 26-39.
240. Nekkanti, V, et al., *Solid self-microemulsifying formulation for candesartan cilexetil*. AAPS PharmSciTech, 2010. **11**(1): p. 9-17.
241. Qi, X, et al., *Solid self-microemulsifying dispersible tablets of celastrol: Formulation development, characterization and bioavailability evaluation*. International Journal of Pharmaceutics, 2014. **472**(1-2): p. 40-47.
242. Taha, EI, et al., *Preparation, in vitro and in vivo evaluation of solid-state self-nanoemulsifying drug delivery system (SNEDDS) of vitamin A acetate*. Journal of Drug Targeting, 2009. **17**(6): p. 468-473.
243. Akhter, MH, et al., *Formulation and development of CoQ10-loaded s-SNEDDS for enhancement of oral bioavailability*. Journal of Pharmaceutical Innovation, 2014. **9**(2): p. 121-131.
244. Alinaghi, A, et al., *Impact of solidification on the performance of lipid-based colloidal carriers: Oil-based versus self-emulsifying systems*. Current Drug Delivery, 2014. DOI:10.2174/1567201811666140716122644
245. Balakrishnan, P, et al., *Enhanced oral bioavailability of dexibuprofen by a novel solid self-emulsifying drug delivery system (SEDDS)*. European Journal of Pharmaceutics and Biopharmaceutics, 2009. **72**(3): p. 539-545.
246. Kim, DW, et al., *Development of novel flurbiprofen-loaded solid self-microemulsifying drug delivery system using gelatin as solid carrier*. Journal of Microencapsulation, 2012. **29**(4): p. 323-330.
247. Kim, GG, et al., *Enhancement of oral bioavailability of fenofibrate by solid self-microemulsifying drug delivery systems*. Drug Development and Industrial Pharmacy, 2013. **39**(9): p. 1431-1438.
248. Singh, SK, et al., *A comparison between use of spray and freeze drying techniques for preparation of solid self-microemulsifying formulation of valsartan and in vitro and in vivo evaluation*. Biomed Research International, 2013. **2013**: p. 1-13.
249. Li, L, et al., *Effects of spray-drying and choice of solid carriers on concentrations of labrasol (r) and transcutool (r) in solid self-microemulsifying drug delivery systems (SMEDDS)*. Molecules, 2013. **18**(1): p. 545-560.
250. Marasini, N, et al., *Statistical modeling, optimization and characterization of spray-dried solid self-microemulsifying drug delivery system using design of experiments*. Chemical and Pharmaceutical Bulletin, 2013. **61**(2): p. 184-193.
251. Oh, DH, et al., *Comparison of solid self-microemulsifying drug delivery system (solid SMEDDS) prepared with hydrophilic and hydrophobic solid carrier*. International Journal of Pharmaceutics, 2011. **420**(2): p. 412-418.



252. Onoue, S, et al., *Novel solid self-emulsifying drug delivery system of coenzyme Q<sub>10</sub> with improved photochemical and pharmacokinetic behaviors*. European Journal of Pharmaceutical Sciences, 2012. **46**(5): p. 492-499.
253. Quan, Q, et al., *Physicochemical characterization and in vivo evaluation of solid self-nanoemulsifying drug delivery system for oral administration of docetaxel*. Journal of Microencapsulation, 2013. **30**(4): p. 307-314.
254. Seo, YG, et al., *Preparation and pharmaceutical evaluation of new tacrolimus-loaded solid self-emulsifying drug delivery system*. Archives of Pharmacal Research, 2014. DOI:10.1007/s12272-014-0459-5.
255. Yan, YD, et al., *Enhanced oral bioavailability of curcumin via a solid lipid-based self-emulsifying drug delivery system using a spray-drying technique*. Biological and Pharmaceutical Bulletin, 2011. **34**(8): p. 1179-1186.
256. Yi, T, et al., *A new solid self-microemulsifying formulation prepared by spray-drying to improve the oral bioavailability of poorly water soluble drugs*. European Journal of Pharmaceutics and Biopharmaceutics, 2008. **70**(2): p. 439-444.
257. Yin, YM, et al., *Preparation, characterization and in vitro intestinal absorption of a dry emulsion formulation containing atorvastatin calcium*. Drug Delivery, 2009. **16**(1): p. 30-36.
258. Nazzal, S, and Khan, MA, *Controlled release of a self-emulsifying formulation from a tablet dosage form: Stability assessment and optimization of some processing parameters*. International Journal of Pharmaceutics, 2006. **315**(1-2): p. 110-121.
259. Nazzal, S, et al., *Optimization of a self-nanoemulsified tablet dosage form of ubiquinone using response surface methodology: Effect of formulation ingredients*. International Journal of Pharmaceutics, 2002. **240**(1): p. 103-114.
260. Patel, J, et al., *Quality by design approach for oral bioavailability enhancement of irbesartan by self-nanoemulsifying tablets*. Drug Delivery, 2014. **21**(6): p. 412-435.
261. Krupa, A, et al., *Preparation of solid self-emulsifying drug delivery systems using magnesium aluminometasilicates and fluid-bed coating process*. Powder Technology, 2014. **266**: p. 329-339.
262. Lei, Y, et al., *Solid self-nanoemulsifying cyclosporine A pellets prepared by fluid-bed coating: Stability and bioavailability study*. Journal of Biomedical Nanotechnology, 2012. **8**(3): p. 515-521.
263. Williams, HD, et al., *Lipid-based formulations solidified via adsorption onto the mesoporous carrier neusilin® US2: Effect of drug type and formulation composition on in vitro pharmaceutical performance*. Journal of Pharmaceutical Sciences, 2014. **103**(6): p. 1734-1746.
264. Christiansen, ML, et al., *Cinnarizine food-effects in beagle dogs can be avoided by administration in a self nano emulsifying drug delivery system (SNEDDS)*. European Journal of Pharmaceutical Sciences, 2014. **57**: p. 164-172.

## References

---

265. Christophersen, PC, et al., *Fed and fasted state gastro-intestinal in vitro lipolysis: In vitro in vivo relations of a conventional tablet, a SNEDDS and a solidified SNEDDS*. European Journal of Pharmaceutical Sciences, 2014. **57**: p. 232-239.
266. Garti, N, et al., *A DSC study of water behavior in water-in-oil microemulsions stabilized by sucrose esters and butanol*. Colloids and Surfaces A: Physicochemical and Engineering Aspects, 2000. **170**(1): p. 1-18.
267. Clause, D, *Thermal behaviour of emulsions studied by differential scanning calorimetry*. Journal of Thermal Analysis and Calorimetry, 1998. **51**(1): p. 191-201.
268. Dalmazone, C, et al., *Application of DSC for emulsified system characterization*. Oil and Gas Science and Technology - Revue de l'IFP, 2008. **64**(5): p. 543-555.
269. Ullrich, S, *Amphiphilic sucrose esters as new ingredients for lipid based drug delivery systems*. PhD Thesis, Martin-Luther-Universität Halle-Wittenberg, 2013.
270. Jores, K, et al., *Physicochemical investigations on solid lipid nanoparticles and on oil-loaded solid lipid nanoparticles: A nuclear magnetic resonance and electron spin resonance study*. Pharmaceutical Research, 2003. **20**(8): p. 1274-1283.
271. Fatouros, DG, and Mullertz, A, *In vitro lipid digestion models in design of drug delivery systems for enhancing oral bioavailability*. Expert Opinion on Drug Metabolism and Toxicology, 2008. **4**(1): p. 65-76.
272. Phan, S, et al., *Self-assembled structures formed during lipid digestion: Characterization and implications for oral lipid-based drug delivery systems*. Drug Delivery and Translational Research, 2014. **4**(3): p. 275-294.
273. Thomas, N, et al., *Characterising lipid lipolysis and its implication in lipid-based formulation development*. AAPS Journal, 2012. **14**(4): p. 860-871.
274. Williams, HD, et al., *Toward the establishment of standardized in vitro tests for lipid-based formulations, part 1: Method parameterization and comparison of in vitro digestion profiles across a range of representative formulations*. Journal of Pharmaceutical Sciences, 2012. **101**(9): p. 3360-3380.
275. Sek, L, et al., *Characterisation and quantification of medium chain and long chain triglycerides and their in vitro digestion products, by HPTLC coupled with in situ densitometric analysis*. Journal of Pharmaceutical and Biomedical Analysis, 2001. **25**(3-4): p. 651-661.
276. Abdalla, A, and Mäder, K, *ESR studies on the influence of physiological dissolution and digestion media on the lipid phase characteristics of SEDDS and SEDDS pellets*. International Journal of Pharmaceutics, 2009. **367**(1-2): p. 29-36.
277. Noack, A, et al., *In vitro digestion of curcuminoid-loaded lipid nanoparticles*. Journal of Nanoparticle Research, 2012. **14**(9): p. 1-19.
278. Carr, RL, *Evaluating flow properties of solids*. Chemical Engineering, 1965. **18**: p. 163-168.

## References

---

279. Bulk density and tapped density of powders, in, *European Pharmacopeia 8.0*. 2013, Council of Europe: Strasbourg, France. p. 343-346.
280. Powder flow <1174>, in, *The United States Pharmacopeia 32 - National Formulary 27 (USP/NF)*. 2009, United States Pharmacopeial Convention: Rockville, USA. p. 688.
281. Powder flow, in, *European Pharmacopeia 8.0*. 2013, Council of Europe: Strasbourg, France. p. 346-349.
282. Tablet breaking force <1217>, in, *The United States Pharmacopeia 32 - National Formulary 27 (USP/NF)*. 2009, United States Pharmacopeial Convention: Rockville, USA. p. 726.
283. Klein, S, *In vitro lipolysis assay as a prognostic tool for the development of lipid based drug delivery systems*. PhD Thesis, Martin-Luther-Universität Halle-Wittenberg, 2013.
284. Rube, A, et al., *Monitoring of in vitro fat digestion by electron paramagnetic resonance spectroscopy*. *Pharmaceutical Research*, 2006. **23**(9): p. 2024-2029.
285. Oidtmann, JM, *Mikroverkapselung von bioaktiven Inhaltsstoffen aus der Heidelbeere (Vaccinium myrtillusL.)*. PhD Thesis, Martin-Luther-Universität Halle-Wittenberg, 2013.
286. Tho, I, et al., *Disintegrating pellets from a water-insoluble pectin derivative produced by extrusion/spheronisation*. *European Journal of Pharmaceutics and Biopharmaceutics*, 2003. **56**(3): p. 371-380.
287. Kranz, H, et al., *Drug release from MCC- and carrageenan-based pellets: Experiment and theory*. *European Journal of Pharmaceutics and Biopharmaceutics*, 2009. **73**(2): p. 302-309.
288. Al-Nimry, SS, et al., *Adsorption of ketotifen onto some pharmaceutical excipients*. *International Journal of Pharmaceutics*, 1997. **149**(1): p. 115-121.
289. Basit, AW, et al., *Formulation of ranitidine pellets by extrusion-spheronization with little or no microcrystalline cellulose*. *Pharmaceutical Development and Technology*, 1999. **4**(4): p. 499-505.
290. Lee, ES, et al., *Binary mixing of micelles using pluronics for a nano-sized drug delivery system*. *Colloids and Surfaces B-Biointerfaces*, 2011. **82**(1): p. 190-195.
291. Lerk, CF, et al., *Effect of hydrophilization of hydrophobic drugs on release rate from capsules*. *Journal of Pharmaceutical Sciences*, 1978. **67**(7): p. 935-939.
292. Rasenack, N, et al., *Micronization of anti-inflammatory drugs for pulmonary delivery by a controlled crystallization process*. *Journal of Pharmaceutical Sciences*, 2003. **92**(1): p. 35-44.
293. Warren, DB, et al., *Using polymeric precipitation inhibitors to improve the absorption of poorly water-soluble drugs: A mechanistic basis for utility*. *Journal of Drug Targeting*, 2010. **18**(10): p. 704-731.

## References

---

294. Guo, ZF, et al., *The utilization of drug-polymer interactions for improving the chemical stability of hot-melt extruded solid dispersions*. Journal of Pharmacy and Pharmacology, 2014. **66**(2): p. 285-296.
295. Djuris, J, et al., *Effect of composition in the development of carbamazepine hot-melt extruded solid dispersions by application of mixture experimental design*. Journal of Pharmacy and Pharmacology, 2014. **66**(2): p. 232-243.
296. Lim, H, and Hoag, SW, *Plasticizer effects on physical-mechanical properties of solvent cast soluplus(r) films*. AAPS PharmSciTech, 2013. **14**(3): p. 903-910.
297. Djuris, J, et al., *Preparation of carbamazepine-soluplus (r) solid dispersions by hot-melt extrusion, and prediction of drug-polymer miscibility by thermodynamic model fitting*. European Journal of Pharmaceutics and Biopharmaceutics, 2013. **84**(1): p. 228-237.
298. Terife, G, et al., *Hot melt mixing and foaming of soluplus (r) and indomethacin*. Polymer Engineering and Science, 2012. **52**(8): p. 1629-1639.
299. Maniruzzaman, M, et al., *Dissolution enhancement of poorly water-soluble APIs processed by hot-melt extrusion using hydrophilic polymers*. Drug Development and Industrial Pharmacy, 2013. **39**(2): p. 218-227.
300. Cespi, M, et al., *Rheological characterization of polyvinyl caprolactam-polyvinyl acetate-polyethylene glycol graft copolymer (soluplus (r)) water dispersions*. Colloid and Polymer Science, 2014. **292**(1): p. 235-241.
301. Zhang, K, et al., *Increased dissolution and oral absorption of itraconazole/soluplus extrudate compared with itraconazole nanosuspension*. European Journal of Pharmaceutics and Biopharmaceutics, 2013. **85**(3 Part B): p. 1285-1292.
302. Yu, H, et al., *Supersaturated polymeric micelles for oral cyclosporine A delivery*. European Journal of Pharmaceutics and Biopharmaceutics, 2013. **85**(3 Part B): p. 1325-1336.
303. Shamma, RN, and Basha, M, *Soluplus (r): A novel polymeric solubilizer for optimization of carvedilol solid dispersions: Formulation design and effect of method of preparation*. Powder Technology, 2013. **237**: p. 406-414.
304. Pokharkar, VB, et al., *Bicalutamide nanocrystals with improved oral bioavailability: In vitro and in vivo evaluation*. Pharmaceutical Development and Technology, 2013. **18**(3): p. 660-666.
305. Hughey, JR, et al., *The use of inorganic salts to improve the dissolution characteristics of tablets containing soluplus (r)-based solid dispersions*. European Journal of Pharmaceutical Sciences, 2013. **48**(4-5): p. 758-766.
306. Linn, M, et al., *Soluplus (r) as an effective absorption enhancer of poorly soluble drugs in vitro and in vivo*. European Journal of Pharmaceutical Sciences, 2012. **45**(3): p. 336-343.

307. Song, WH, et al., *In situ intestinal permeability and in vivo oral bioavailability of celecoxib in supersaturating self-emulsifying drug delivery system*. Archives of Pharmacal Research, 2014. **37**(5): p. 626-635.
308. Croda GmbH, *Arlacel<sup>TM</sup> LC information sheet*. 2013.
309. Croda GmbH, *Cithrol<sup>TM</sup> DPHS information sheet*. 2009.
310. Ferrari, M, and da Rocha, PA, *Multiple emulsions containing amazon oil: acai oil (Euterpe oleracea)*. Revista Brasileira De Farmacognosia-Brazilian Journal of Pharmacognosy, 2011. **21**(4): p. 737-743.
311. Vasiljevic, DD, et al., *Rheological and droplet size analysis of W/O/W multiple emulsions containing low concentrations of polymeric emulsifiers*. Journal of the Serbian Chemical Society, 2009. **74**(7): p. 801-816.
312. Vasiljevic, D, et al., *An investigation into the characteristics and drug release properties of multiple W/O/W emulsion systems containing low concentration of lipophilic polymeric emulsifier*. International Journal of Pharmaceutics, 2006. **309**(1-2): p. 171-177.
313. Dai, YJ, et al., *In vitro studies on the application of colloidal emulsion aphrons to drug overdose treatment*. International Journal of Pharmaceutics, 2006. **311**(1-2): p. 165-171.
314. Vasiljevic, D, et al., *The characterization of the semi-solid W/O/W emulsions with low concentrations of the primary polymeric emulsifier*. International Journal of Cosmetic Science, 2005. **27**(2): p. 81-87.
315. Kanouni, M, et al., *Preparation of a stable double emulsion (W<sub>1</sub>/O/W<sub>2</sub>): Role of the interfacial films on the stability of the system*. Advances in Colloid and Interface Science, 2002. **99**: p. 229-254.
316. Committee for veterinary medicinal products, *Polyethylene glycol stearates and polyethylene glycol 15 hydroxystearate*, 2003. Available from: [http://www.ema.europa.eu/docs/en\\_GB/document\\_library/Maximum\\_Residue\\_Limits\\_-\\_Report/2009/11/WC500015762.pdf](http://www.ema.europa.eu/docs/en_GB/document_library/Maximum_Residue_Limits_-_Report/2009/11/WC500015762.pdf) Last accessed on: 22.08.2014.
317. Croda GmbH, *Cithrol<sup>TM</sup> DPHS-SO-(MV) safety data sheet*. 2010.
318. Coon, JS, et al., *Solutol HS 15, nontoxic polyoxyethylene esters of 12-hydroxystearic acid, reverses multidrug resistance*. Cancer Research, 1991. **51**(3): p. 897-902.
319. Kraus, C, et al., *Hemolytic activity of mixed micellar solutions of solutol® HS 15 and sodium deoxycholate*. Acta Pharmaceutica Technologica, 1990. **36**(4): p. 221-225.
320. BASF AG, *Kolliphor<sup>TM</sup> HS 15 information sheet*. 2012.
321. Koynova, R, and Tenchov, B, *Lipids: Phase Transitions*, in Begley, TP, Editor, *Wiley encyclopedia of chemical biology*. 2007, John Wiley & Sons, Inc.: Hoboken. p. 1-15.
322. Metz, H, and Mäder, K, *Benchtop-NMR and MRI-A new analytical tool in drug delivery research*. International Journal of Pharmaceutics, 2008. **364**(2): p. 170-175.

323. Schubert, MA, et al., *Structural investigations on lipid nanoparticles containing high amounts of lecithin*. European Journal of Pharmaceutical Sciences, 2006. **27**(2-3): p. 226-236.
324. Chen, S, et al., *Drug–excipient complexation in lipid based delivery systems: An investigation of the Tipranavir-1,3-dioctanolyglycerol complex*. Journal of Pharmaceutical Sciences, 2009. **98**(5): p. 1732-1743.
325. Lie Ken Jie, MSF, and Lam, CC, *<sup>1</sup>H-Nuclear magnetic resonance spectroscopic studies of saturated, acetylenic and ethylenic triacylglycerols*. Chemistry and Physics of Lipids, 1995. **77**(2): p. 155-171.
326. Knothe, GH, *<sup>1</sup>H-NMR spectroscopy of fatty acids and their derivatives: glycerol esters*, 2006. Available from: <http://lipidlibrary.aocs.org/nmr/1NMRglyc/index.htm> Last accessed on: 02.07.2013.
327. Momot, KI, and Kuchel, PW, *Pulsed field gradient nuclear magnetic resonance as a tool for studying drug delivery systems*. Concepts in Magnetic Resonance Part A, 2003. **19A**(2): p. 51-64.
328. Noack, A, *Development and characterization of curcuminoid-loaded lipid nanoparticles*. PhD Thesis, Martin-Luther-Universität Halle-Wittenberg, 2012.
329. Jores, K, *Lipid nanodispersions as drug carrier systems - A physicochemical characterization*. PhD Thesis, Martin-Luther-Universität Halle-Wittenberg, 2004.
330. Kempe, S, et al., *Application of electron paramagnetic resonance (EPR) spectroscopy and imaging in drug delivery research – Chances and challenges*. European Journal of Pharmaceutics and Biopharmaceutics, 2010. **74**(1): p. 55-66.
331. Kuentz, M, and Cavegn, M, *Critical concentrations in the dilution of oral self-microemulsifying drug delivery systems*. Drug Development and Industrial Pharmacy, 2010. **36**(5): p. 531-538.
332. Mäder, K, *Characterization of nanoscaled drug delivery systems by electron spin resonance (ESR)*, in Kumar, CSSR, Editor, *Nanosystem characterization tools in the life sciences*. 2006, Wiley-VCH: Weinheim. p. 241-258.
333. Ruhland, T, et al., *Nanoporous magnesium aluminometasilicate tablets for precise, controlled, and continuous dosing of chemical reagents and catalysts: Applications in parallel solution-phase synthesis*. Journal of combinatorial chemistry, 2007. **9**(2): p. 301-305.
334. Pund, S, et al., *Improvement of anti-inflammatory and anti-angiogenic activity of berberine by novel rapid dissolving nanoemulsifying technique*. Phytomedicine, 2014. **21**(3): p. 307-314.
335. Patel, A, et al., *Development and optimization of solid self-nanoemulsifying drug delivery system (S-SNEDDS) using Scheffe's design for improvement of oral bioavailability of nelfinavir mesylate*. Drug Delivery and Translational Research, 2014. **4**(2): p. 171-186.

## References

---

336. Kallakunta, V, et al., *A gelucire 44/14 and labrasol based solid self emulsifying drug delivery system: Formulation and evaluation*. Journal of Pharmaceutical Investigation, 2013. **43**(3): p. 185-196.
337. Janga, KY, et al., *In situ absorption and relative bioavailability studies of zaleplon loaded self-nanoemulsifying powders*. Journal of Microencapsulation, 2013. **30**(2): p. 161-172.
338. Kanuganti, S, et al., *Paliperidone-loaded self-emulsifying drug delivery systems (SEDDS) for improved oral delivery*. Journal of Dispersion Science and Technology, 2012. **33**(4): p. 506-515.
339. Kallakunta, V, et al., *Oral self emulsifying powder of lercanidipine hydrochloride: Formulation and evaluation*. Powder Technology, 2012. **221**: p. 375-382.
340. Agrawal, AG, et al., *Formulation of solid self-nanoemulsifying drug delivery systems using N-methyl pyrrolidone as cosolvent*. Drug Development and Industrial Pharmacy, 2014. DOI:10.3109/03639045.2014.886695.
341. Durgacharan, B, and John I, DS, *Development of solid self micro emulsifying drug delivery system with neusilin US2 for enhanced dissolution rate of telmisartan*. International Journal of Drug Development and Research, 2012. **4**(4): p. 398-407.
342. Ramasahayam, B, et al., *Development of isradipine loaded self-nano emulsifying powders for improved oral delivery: In vitro and in vivo evaluation*. Drug Development and Industrial Pharmacy, 2014. DOI:10.3109/03639045.2014.900081.
343. Li, R, et al., *<sup>1</sup>H NMR studies of water in chicken breast marinated with different phosphates*. Journal of Food Science, 2000. **65**(4): p. 575-580.
344. Mohanachandran, P, et al., *Superdisintegrants: An overview*. International Journal of Pharmaceutical Sciences Review and Research, 2011. **6**(1): p. 105-109.
345. Pahwa, R, and Gupta, N, *Superdisintegrants in the development of orally disintegrating tablets: A review*. International Journal of Pharma Sciences and Research, 2011. **2**: p. 2767-2780.
346. Rahman, M, et al., *Effect of mode of addition of disintegrants on dissolution of model drug from wet granulation tablets*. International Journal of Pharma Sciences and Research, 2011. **2**(2): p. 84-92.
347. Nazzal, S, et al., *Effect of extragranular microcrystalline cellulose on compaction, surface roughness, and in vitro dissolution of a self-nanoemulsified solid dosage form of ubiquinone*. Pharmaceutical Technology, 2002. **26**(4): p. 86-98.
348. BASF AG, *Lumogen® F Red 305: Safety data sheet 2013*.
349. Bard, B, et al., *High throughput UV method for the estimation of thermodynamic solubility and the determination of the solubility in biorelevant media*. European Journal of Pharmaceutical Sciences, 2008. **33**(3): p. 230-240.

## References

---

350. McAuley, JW, et al., *Oral administration of micronized progesterone: A review and more experience*. *Pharmacotherapy: The Journal of Human Pharmacology and Drug Therapy*, 1996. **16**(3): p. 453-457.
351. Araya-Sibaja, AM, et al., *Dissolution properties, solid-state transformation and polymorphic crystallization: Progesterone case study*. *Pharmaceutical Development and Technology*, 2014. **19**(7): p. 779-788.
352. Sitruk-Ware, R, et al., *Oral micronized progesterone: Bioavailability pharmacokinetics, pharmacological and therapeutic implications — A review*. *Contraception*, 1987. **36**(4): p. 373-402.
353. D'Souza, V, et al., *Short spacings and polymorphic forms of natural and commercial solid fats: A review*. *Journal of the American Oil Chemists Society*, 1990. **67**(11): p. 835-843.
354. deMan, JM, *X-ray diffraction spectroscopy in the study of fat polymorphism*. *Food Research International*, 1992. **25**(6): p. 471-476.
355. Müller, RH, et al., *Solid lipid nanoparticles (SLN) for controlled drug delivery – A review of the state of the art*. *European Journal of Pharmaceutics and Biopharmaceutics*, 2000. **50**(1): p. 161-177.
356. Zoppetti, G, et al., *Solid state characterization of progesterone in a freeze dried 1:2 progesterone/HPBCD mixture*. *Journal of Pharmaceutical Sciences*, 2007. **96**(7): p. 1729-1736.
357. Guillén, MD, and Cabo, N, *Infrared spectroscopy in the study of edible oils and fats*. *Journal of the Science of Food and Agriculture*, 1997. **75**(1): p. 1-11.
358. Gohel, M, and Jogani, PD, *A review of co-processed directly compressible excipients*. *Journal of Pharmacy and Pharmaceutical Sciences*, 2005. **8**(1): p. 76-93.
359. Puttewar, TY, et al., *Formulation and evaluation of orodispersible tablet of taste masked doxylamine succinate using ion exchange resin*. *Journal of King Saud University (Science)*, 2010. **22**(4): p. 229-240.
360. Chapus, C, et al., *Mechanism of pancreatic lipase action. 1. Interfacial activation of pancreatic lipase*. *Biochemistry*, 1976. **15**(23): p. 4980-4987.
361. Christiansen, A, et al., *Effects of non-ionic surfactants on in vitro triglyceride digestion and their susceptibility to digestion by pancreatic enzymes*. *European Journal of Pharmaceutical Sciences*, 2010. **41**(2): p. 376-382.
362. Small, DM, et al., *The ionization behavior of fatty acids and bile acids in micelles and membranes*. *Hepatology*, 1984. **4**(5 Suppl): p. 77s-79s.
363. Maeda, H, et al., *Hydrogen ion titration of oleic acid in aqueous media*. *The Journal of Physical Chemistry*, 1992. **96**(25): p. 10487-10491.



364. Fukuda, H, et al., *Electron spin resonance study of the pH-induced transformation of micelles to vesicles in an aqueous oleic acid/oleate system*. *Langmuir*, 2001. **17**(14): p. 4223-4231.
365. Williams, HD, et al., *Toward the establishment of etandardized in vitro tests for lipid-based formulations. 2. The effect of bile salt concentration and drug loading on the performance of type I, II, IIIA, IIIB, and IV formulations during in vitro digestion*. *Molecular Pharmaceutics*, 2012. **9**(11): p. 3286-3300.
366. Feeney, OM, et al., *'Stealth' lipid-based formulations: Poly(ethylene glycol)-mediated digestion inhibition improves oral bioavailability of a model poorly water soluble drug*. *Journal of Controlled Release*, 2014. **192**: p. 219-227.
367. Seyfoddin, A, and Al-Kassas, R, *Development of solid lipid nanoparticles and nanostructured lipid carriers for improving ocular delivery of acyclovir*. *Drug Development and Industrial Pharmacy*, 2013. **39**(4): p. 508-519.
368. Prajapati, H, et al., *A comparative evaluation of mono-, di- and triglyceride of medium chain fatty acids by lipid/surfactant/water phase diagram, solubility determination and dispersion testing for application in pharmaceutical dosage form development*. *Pharmaceutical Research*, 2012. **29**(1): p. 285-305.
369. Dixit, RP, and Nagarsenker, MS, *Optimized microemulsions and solid microemulsion systems of simvastatin: Characterization and in vivo evaluation*. *Journal of Pharmaceutical Sciences*, 2010. **99**(12): p. 4892-4902.
370. Núñez, FAA, and Yalkowsky, SH, *Correlation between log P and ClogP for some steroids*. *Journal of Pharmaceutical Sciences*, 1997. **86**(10): p. 1187-1189.

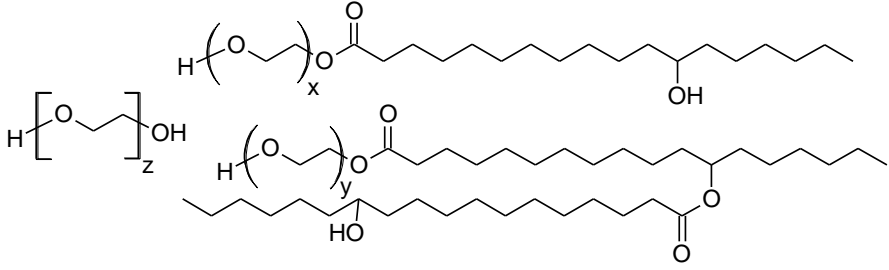
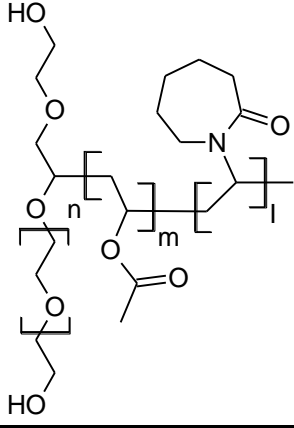


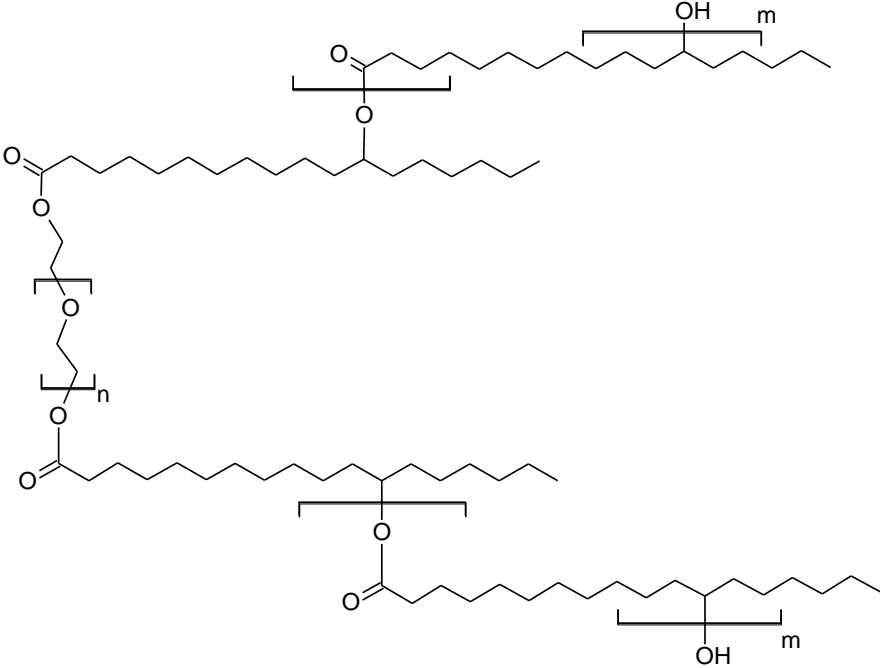
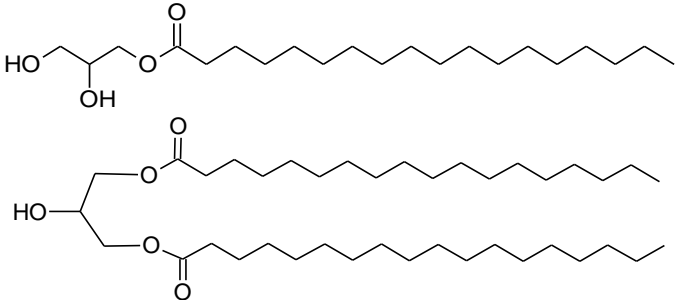
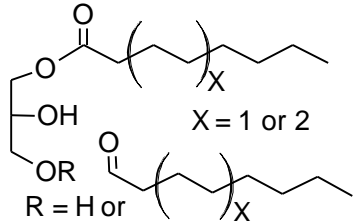
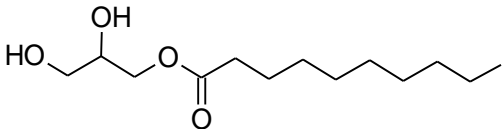
## 8. Appendices

### 8.1. Supplementary data

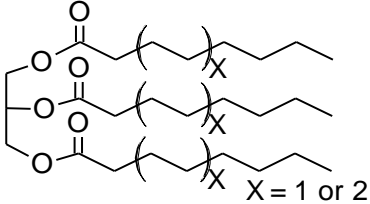
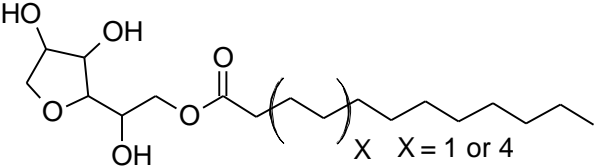
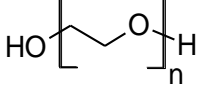
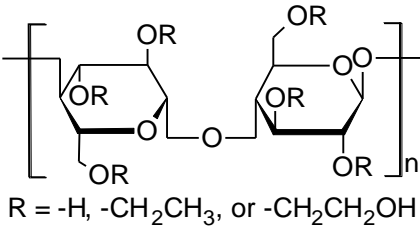
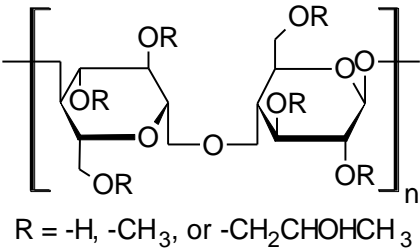
#### 8.1.1. Supplementary tables

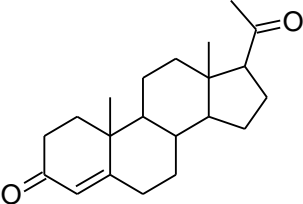
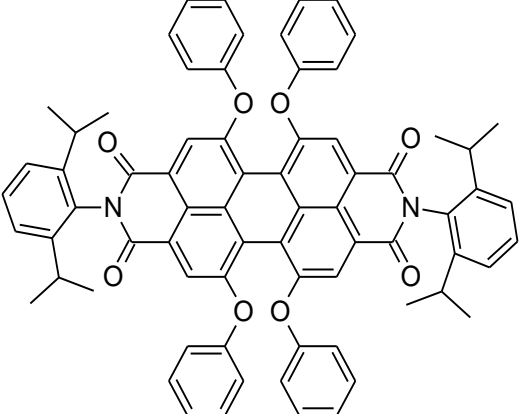
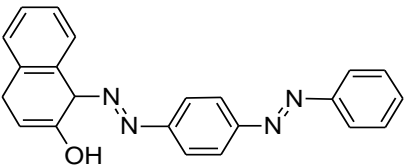
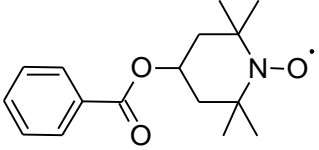
**Table S1** Chemical structures, properties and batch numbers of the used excipients, chemicals and reagents.

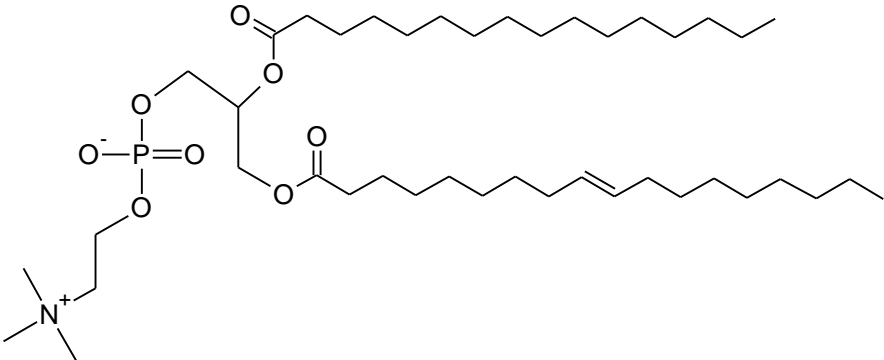
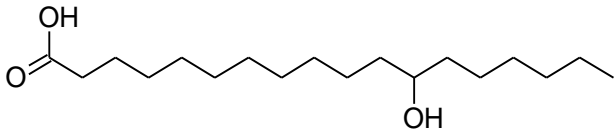
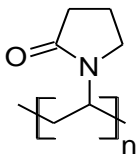
Material (Old name)	Physicochemical properties	Batch number	Supplier
<b>More hydrophilic amphiphiles</b>			
<b>Kolliphor® HS 15</b> (Solutol® HS 15)	Polyoxyethylene-660-12-hydroxystearate, ~70 % (PEG mono- and di-esters of 12-HAS) and ~30 % PEG HLB: 14-16 CMC: 0.005-0.02 % [320] Semisolid	<b>16087036W0</b> <b>97922356P0</b>	BASF AG, Germany
			
<b>Soluplus®</b>	Polyvinyl caprolactam-polyvinyl acetate-polyethylene glycol graft copolymer HLB: 14 CMC: 7.6-46.3 mg/L [49] Solid	<b>39844268E0</b>	BASF AG, Germany
			
<b>More hydrophobic amphiphiles</b>			
<b>Cithrol® DPHS</b> (Arlacel® P130)	PEG-30-dipolyhydroxystearate, polyester-polyether-polyester ABA block copolymer, the middle chain B is a PEG chain while the two tails A are poly(12-HSA) HLB: 5.5 [309] Semisolid	<b>0000725643</b>	Croda GmbH, Germany

			
<p><b>Cithrol® GMS 40</b></p>	<p>Mono- and di-glycerides of stearic acid HLB: 3-5 [367] Solid</p> 	<p><b>21727</b></p>	<p>Croda GmbH, Germany</p>
<p><b>Capmul® MCM EP</b></p>	<p>Medium chain mono (60 %) and diglyceride (35 %) of 83 % m/m caprylic acid (C<sub>8</sub>) and 17 % m/m capric acid (C<sub>10</sub>) HLB: 4.7 [368] Liquid</p>  <p>X = 1 or 2 R = H or</p>	<p><b>110301-6</b></p>	<p>Abitec Corporation, USA</p>
<p><b>Capmul® MCM C10</b></p>	<p>Glyceryl monocaprate HLB: 5-6 [369] Solid</p> 	<p><b>121005-8</b></p>	<p>Abitec Corporation, USA</p>

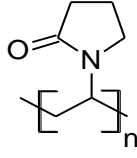
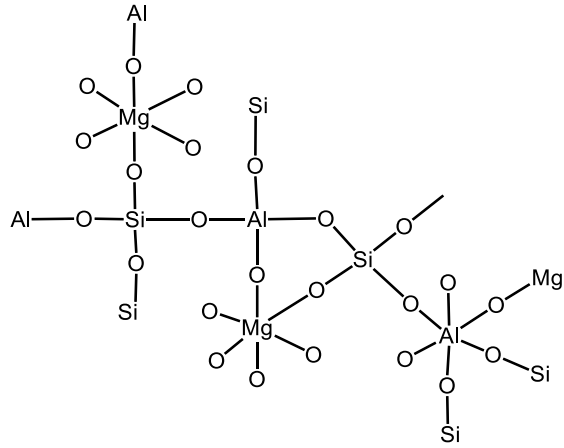
Appendices

<p><b>Captex® 355 EP/NF</b></p>	<p>Medium chain triglyceride of caprylic acid (C<sub>8</sub>) and capric acid (C<sub>10</sub>) at 55:45 ratio HLB: 0 [368] Liquid</p>	<p><b>090915UT14</b></p>	<p>Abitec Corporation, USA</p>
			
<p><b>Arlacel® LC</b></p>	<p>1:1 mixture of sorbitan stearate (HLB 4.7) and sorbityl laurate (HLB 8.6) [308] Solid</p>	<p><b>0000472666</b></p>	<p>Croda GmbH, Germany</p>
			
<p><b>Polymers</b></p>			
<p><b>PEG</b></p>	<p>Polyethylene oxide, different molecular weights</p>	<p>-</p>	<p>Clariant GmbH, Germany</p>
			
<p><b>Tylose® H 20 P2</b> <b>Tylose® H 30000 P2</b></p>	<p>Hydroxyethyl Cellulose Viscosity of 2 % solution: 20 mPa.s (20 P2) and 30000 mPa.s (30000 P2)</p>	<p><b>DEAC 086562</b> <b>DEAC 058993</b></p>	<p>Clariant GmbH, Germany</p>
			
<p><b>Metolose® 60SH-50</b> <b>Metolose® 60SH-10000</b></p>	<p>Hydroxypropyl Methylcellulose Viscosity of 2 % solution: 50 mPa.s (60SH-50) and 10000 mPa.s (60SH-10000)</p>	<p><b>912638</b> <b>001523</b></p>	<p>Shin-Etsu Chemical Co., Ltd, Japan</p>
			

Poorly water-soluble drug models			
Progesterone	Pregn-4-ene-3,20-dione Log P: 3.87 [370]	SLBC0269V	Sigma-Aldrich, Germany
			
Lumogen® F305	2,9-bis(2,6-diisopropylphenyl)-5,6,12,13-tetraphenoxyanthra[2,1,9-def:6,5,10-d'e'f]diisoquinoline-1,3,8,10(2H,9H)-tetraone Log P: > 6.2 [348]	00050007376	BASF AG, Germany
			
Sudan III	1-((4-(phenyldiazenyl)phenyl)azonaphthalen-2-ol Log P: 5.737 [290]	BCBB0830	Sigma-Aldrich, Germany
			
Proton nuclear magnetic resonance ( <sup>1</sup> H-NMR)			
Deuterium oxide	D <sub>2</sub> O	MKBB2073	Sigma-Aldrich, Germany
Deuterated DMSO	CD <sub>3</sub> -SO-CD <sub>3</sub>	03728HD	
Electron spin resonance (ESR)			
Tempolbenzoate	4-Hydroxy-2,2,6,6-tetramethylpiperidine 1-oxyl benzoate, 4-Hydroxy-TEMPO benzoate Log P: 2.46 [276]	13112PU	Sigma-Aldrich, Germany
			

<b>Equilibrium solubility and digestion</b>			
<b>Bile extract porcine</b>	Mixture of glycine and taurine conjugates of hyodeoxycholic acid and other BS BS concentration as determined by Ecoline S+: 0.986 µmol/mg	<b>013K0129</b>	Sigma-Aldrich, Germany
<b>Porcine pancreatin powder</b>	Mixture of several digestive enzymes 4 × USP specifications Lipase activity: 13.5 USP units/mg (110M1429V) and 15.5 USP units/mg (081M1275V)	<b>110M1429V</b> <b>081M1275V</b>	
<b>Phospholipon® 90G</b>	92-98 % purified phosphatidyl choline from soybean lecithin	<b>50680</b>	Lipoid, Germany
			
<b>Titrisol®</b>	Standard sodium hydroxide solution, 1 M	<b>50035846</b>	Merck, Germany
<b>HPTLC</b>			
<b>12-Hydroxystearic acid</b>	12-Hydroxyoctadecanoic acid	<b>19519JOV</b>	Sigma-Aldrich, Germany
			
<b>HPLC</b>			
<b>Acetonitrile HPLC</b>	CH <sub>3</sub> CN	-	VWR, Germany
<b>Double distilled water</b>	Double distilled water was prepared using a GFL bidistillator 2108 (GFL, Burgwedel, Germany)		
<b>Tablets</b>			
<b>Kollidon® 90 F</b>	Polyvinylpyrrolidone	<b>57535716K0</b>	BASF AG, Germany
			

Appendices

	Polyvinylpyrrolidone, cross-linked	<b>98242316K0</b>	BASF AG, Germany
<b>Kollidon® CL-SF</b>			
	Synthetic, amorphous Magnesium aluminometasilicate, $\text{Al}_2\text{O}_3 \cdot \text{MgO} \cdot 1.7\text{SiO}_2 \cdot x\text{H}_2\text{O}$ Granules Specific surface area: 300 m <sup>2</sup> /g Particle size distribution: 44-177 μm. Average pore size: 50-60 Angstrom.	<b>510013</b> <b>909015</b>	Fuji Chemical Industry Co., Ltd, Japan
<b>Neusilin® US2</b>			



**Table S2** Preliminary studied formulations composed of 90 % self-emulsifying formulation with 10 % of the selected polymeric excipient (m %). The self-emulsifying formulation is composed of 50 % m/m Kolliphor® HS 15 as a more hydrophilic amphiphile and 50 % m/m Cithrol® GMS 40 as a more lipophilic amphiphile [181].

Code	SEDDS	PEG (molecular weight)	Tylose® H 20P2	Tylose® H 30000P2	Metolose® 60SH-50	Metolose® 60SH-10000
P1	90	10 (4000)				
P3	90	10 (8000)				
P3	90	10 (20000)				
P4	90	10 (35000)				
P5	90		10			
P3	90			10		
P7	90				10	
P8	90					10

**Table S3** Preliminary studied Soluplus® formulations (m %).

Code	Cithrol® GMS 40	Captex® 355 EP/NF	Capmul® MCM	Soluplus®	Kolliphor® HS 15	PEG (molecular weight)	Physical state
P9	50			50			Solid
P10	33			67			Solid
P11	45			45		10 (4000)	Solid
P12	45			45		10 (8000)	Solid
P13	45			45		10 (20000)	Solid
P14	45			45		10 (35000)	Solid
P15		25	25	50			Semisolid
P16		16.5	16.5	67			Solid
P17		15	15	70			Solid
P18	50			25	25		Solid
P19	25			50	25		Rubbery
P20	16.5			67	16.5		Sticky mass with oily surface
P21		25	25	25	25		Gel-like
P22		15	15	45	25		Rubbery
P23		15	15	55	15		Rubbery
P24		10	10	55	25		Sticky mass with oily surface
P25		10	10	70	10		Solid

**Table S4** Preliminary studied Arlachel<sup>®</sup> LC formulations (m %).

Code	Cithrol <sup>®</sup> GMS 40	Captex <sup>®</sup> 355 EP/NF	Capmul <sup>®</sup> MCM	Kolliphor <sup>®</sup> HS 15	Soluplus <sup>®</sup>	Arlachel <sup>®</sup> LC	Physical state
P26						100	Solid
P27	50					50	Solid
P28		25	25			50	Semisolid
P29				50		50	Semisolid
P30					50	50	Solid
P31				33.33	33.33	33.34	Sticky mass with oily surface
P32	20			40		40	Semisolid
P33	30			35		35	Solid
P34	50			25		25	Solid
P35	70			15		15	Solid
P36	80			10		10	Solid

**Table S5** Preliminary studied Cithrol<sup>®</sup> DPMS formulations (m %).

Code	Cithrol <sup>®</sup> DPMS	Cithrol <sup>®</sup> GMS 40	Capmul <sup>®</sup> MCM	Kolliphor <sup>®</sup> HS 15	Soluplus <sup>®</sup>	Physical state
P37	50				50	Rubbery
P38	50			50		Semisolid
P39	25	25		25	25	Rubbery
P40	12	48		40		Semisolid
P41	30	30		40		Semisolid
P42	48	12		40		Semisolid
P43	33.33	16.67		50		Semisolid
P44	25	25		50		Semisolid
P45	16.67	33.33		50		Semisolid
P46	8	32		60		Semisolid
P47	20	20		60		Semisolid
P48	32	8		60		Semisolid
P49	15	15		70		Semisolid
P50	10	10		80		Semisolid
P51	25		25	50		Semisolid
P52	20		20	60		Semisolid
P53	26.67		13.33	60		Semisolid
P54	26.67		13.33		60	Rubbery
P55	26.67		13.33	30	30	Semisolid

**Table S6** Screened possible adsorbates containing 30 % of the semisolid SNEDDS. Grade A is powder with an excellent flowability, grade B is powder with a reasonable flowability, grade C is wet powder with a reasonable flowability, D is wet powder with a bad flowability, and E is a wet sticky mass.

<b>Excipient</b>	<b>Description</b>	<b>Flow grade</b>
<b>Filler</b>		
<b>Avicel® PH101</b>	Microcrystalline Cellulose (MCC)	C
<b>Emcocel® HD90</b>	Spray-dried medium size standard MCC grade	B
<b>Emcompress®</b>	Dibasic calcium phosphate	E
<b>Flowlac® 100</b>	Spray-dried $\alpha$ -lactose monohydrate	E
<b>Fujicalin®</b>	Porous spheres dibasic calcium phosphate anhydrous	B
<b>Galen® IQ 721</b>	Agglomerated spherical Isomalt	C
<b>Granulac® 200</b>	Fine Lactose particles	E
<b>Hylon® VII</b>	Unmodified high amylose corn starch	E
<b>Neosorp® P100T</b>	Sorbitol Powder	C
<b>Neusilin® UFL2</b>	Magnesium aluminometasilicate	B
<b>Neusilin® US2</b>	Magnesium aluminometasilicate	A
<b>Pullulan®</b>	Polysaccharide	B
<b>Vivapur® 302</b>	Medium size standard MCC grade	B
<b>Co-processed diluent</b>		
<b>Cellactose® 80</b>	75 % $\alpha$ -Lactose monohydrate + 25 % Cellulose powder	C
<b>F-Melt® type C</b>	Directly compressible and co-spray dried powder, containing 5 pharmaceutical excipients designed for orally disintegrating tablets	D
<b>Ludiflash®</b>	90 % Mannitol + 5 % Kollidon® CL-SF + 5 % Kollicoat® SR 30 D	C
<b>Ludipress®</b>	93 % Lactose + 3.5 % Kollidon® 30 + Kollidon® CL	C
<b>Ludipress® LCE</b>	96.5 % Lactose + 3.5 % Kollidon® 30	D
<b>Prosolv® 50</b>	98 % MCC and 2 % Colloidal silicon dioxide	B
<b>Prosolv® 90</b>	98 % MCC and 2 % Colloidal silicon dioxide	B
<b>Vivapur® MCG 591 P</b>	MCC and Carboxymethyl cellulose sodium	D
<b>Disintegrant</b>		
<b>Explotab®</b>	Sodium Starch Glycolate	E
<b>Kollidon® CL-F</b>	Cross-linked Polyvinylpyrrolidone, fine grade	B
<b>Kollidon® CL-M</b>	Cross-linked Polyvinylpyrrolidone, micronized	B
<b>Kollidon® CL-SF</b>	Cross-linked Polyvinylpyrrolidone, super fine grade	B
<b>Protacid® F120 NM</b>	Algenic acid	D
<b>Vivasol®</b>	Croscarmellose sodium	E

### 8.1.2. Supplementary figures

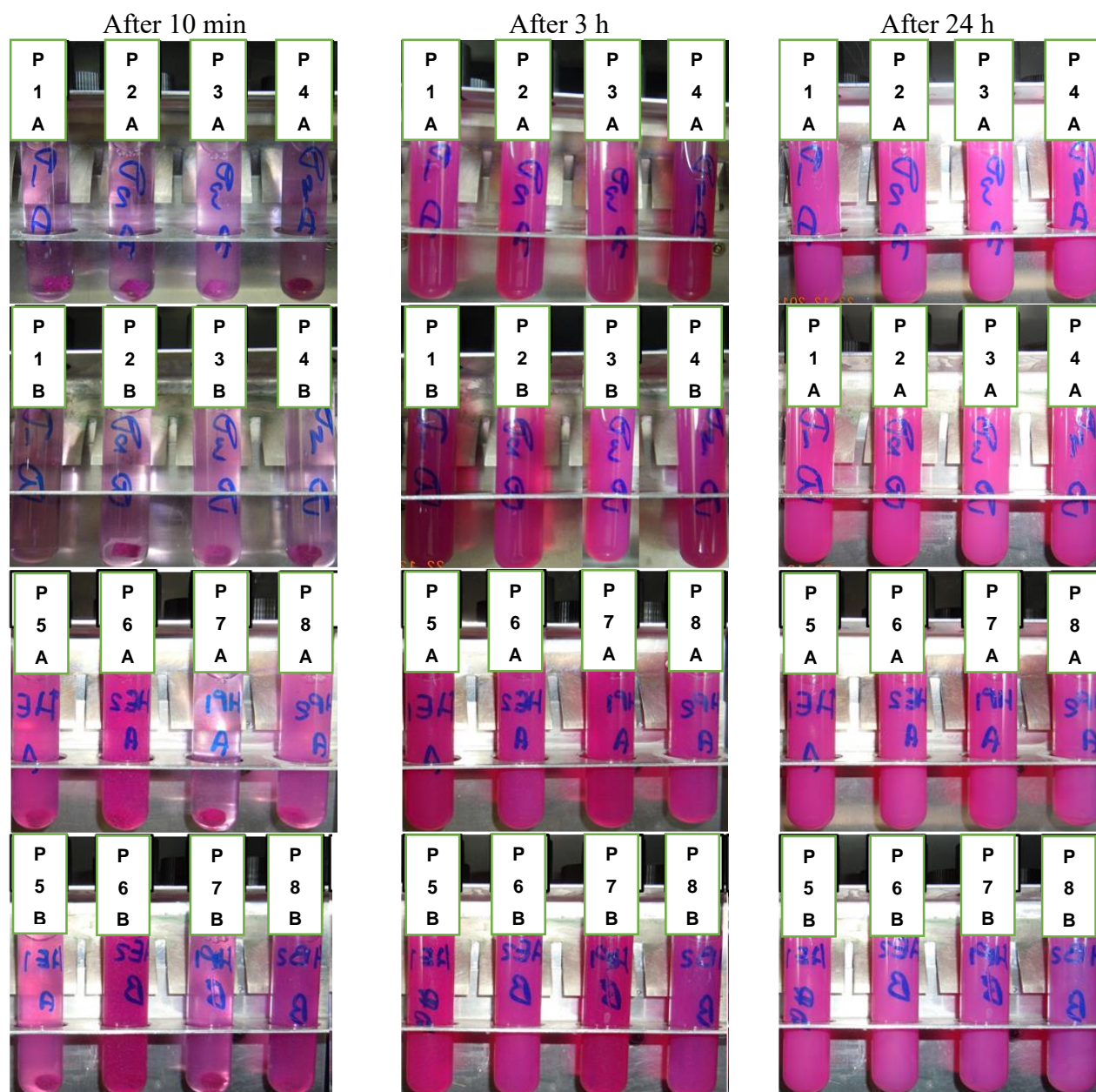


**Fig. S1** Photos of 1 % (m/V) dispersions of P1 – P8 in 0.1 N HCl (A) and phosphate buffer pH 6.8 (B) after incubation in an end over end mixer at 37 °C.

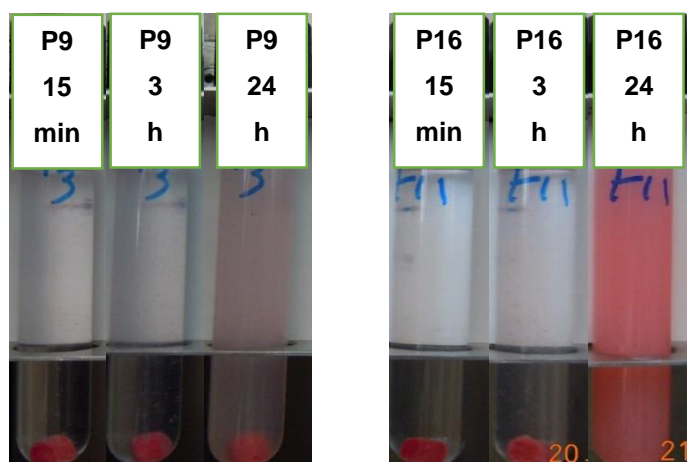


**Fig. S2** Photos of 1 % (m/V) dispersions of P9 and P16 in phosphate buffer pH 6.8 after incubation in an end over end mixer at 37 °C.

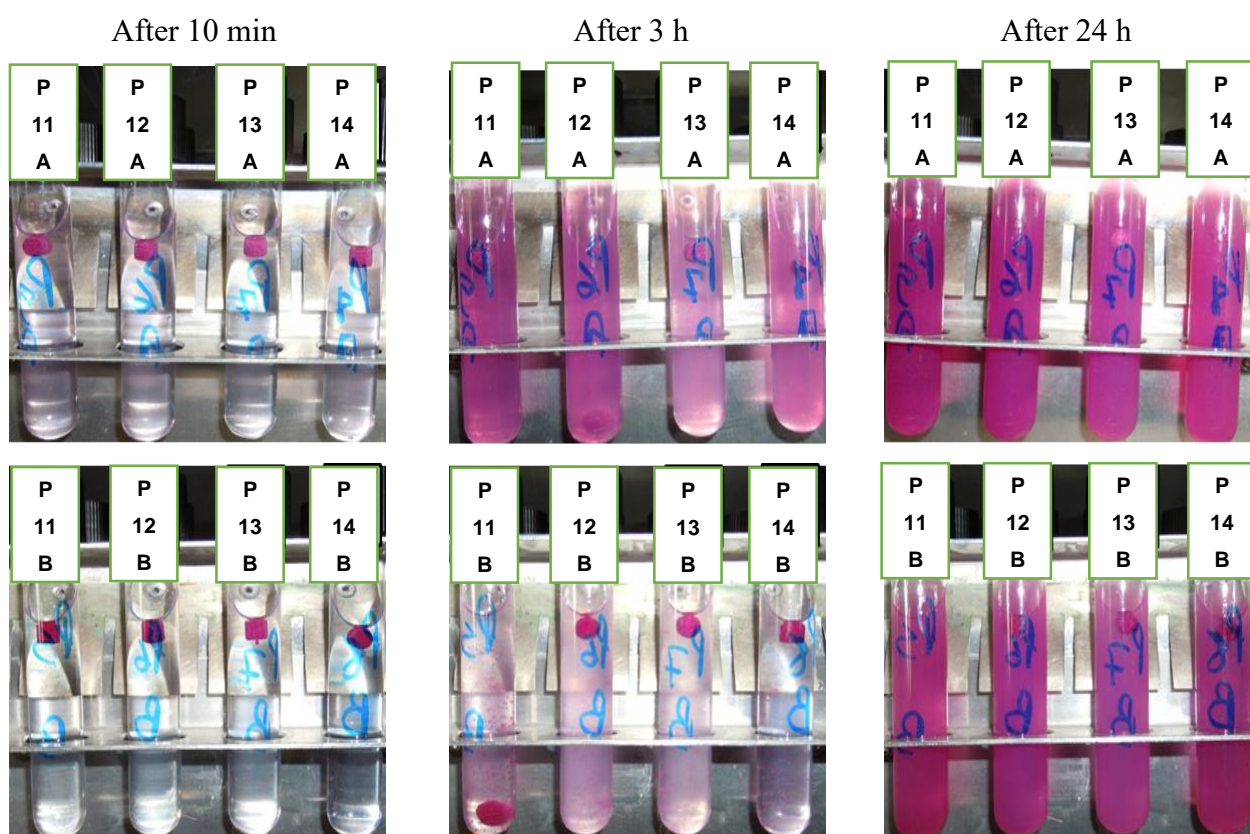


**Fig. S3** Photos of 1 % (m/V) dispersions of P11 – P14 in 0.1 N HCl (A) and phosphate buffer pH 6.8 (B) after incubation in an end over end mixer at 37 °C.

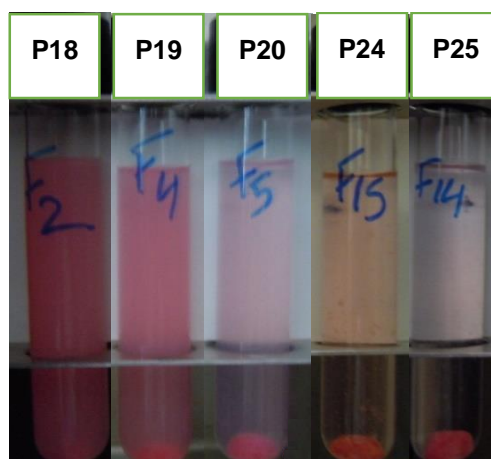


**Fig. S4** Photos of 1 % (m/V) dispersions of P18 – P20, P24 and P25 in phosphate buffer pH 6.8 after 3 h incubation in an end over end mixer at 37 °C.

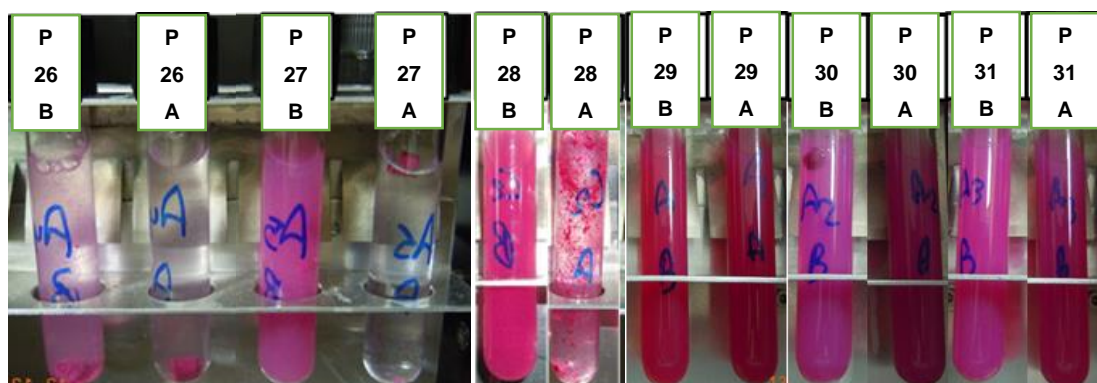


**Fig. S5** Photos of 1 % (m/V) dispersions of P26 – P31 in 0.1 N HCl (A) and phosphate buffer pH 6.8 (B) after 3 h incubation in an end over end mixer at 37 °C.

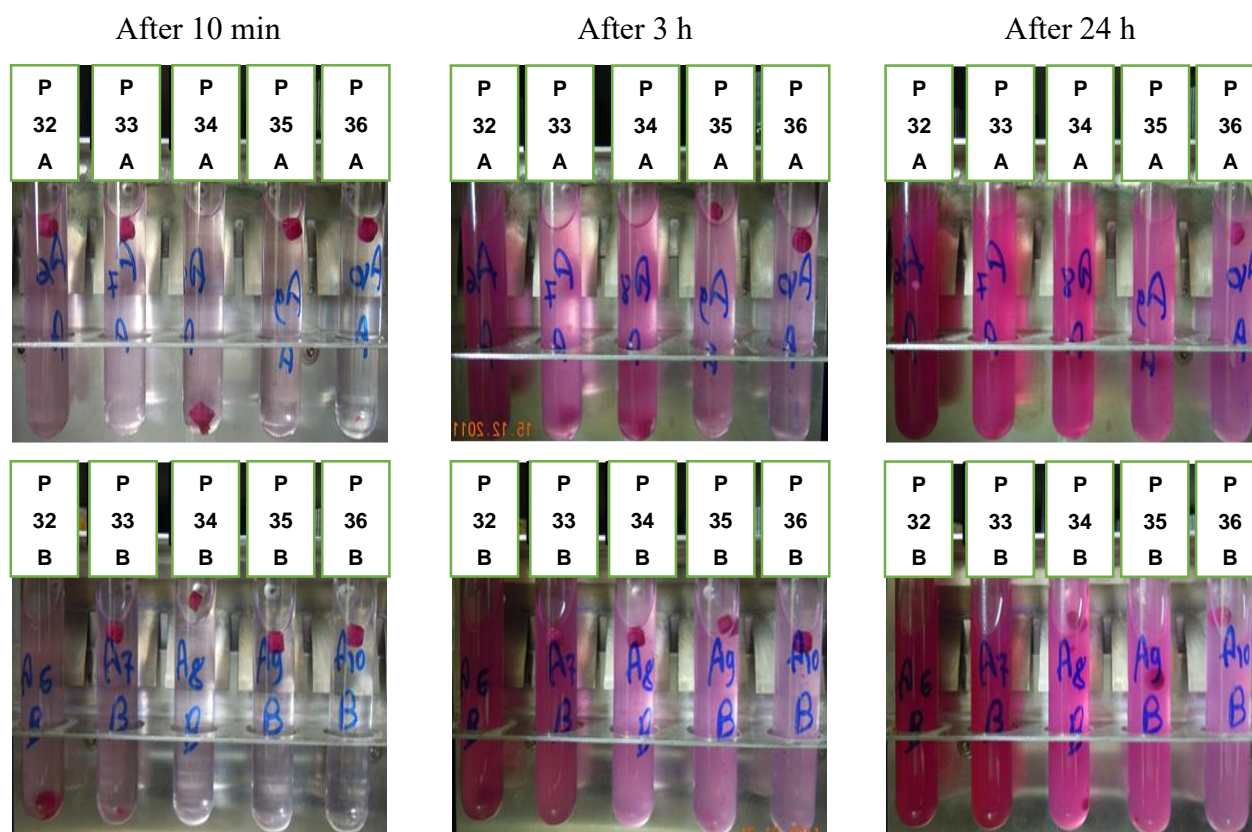


**Fig. S6** Photos of 1 % (m/V) dispersions of P32 – P36 in 0.1 N HCl (A) and phosphate buffer pH 6.8 (B) after incubation in an end over end mixer at 37 °C.

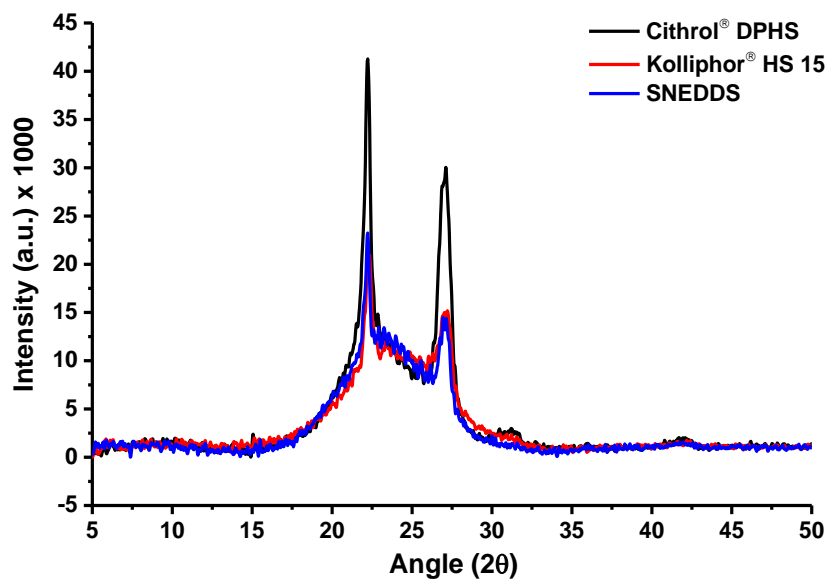


**Fig. S7** PXRD patterns of Cithrol® DPHS and Kolliphor® HS 15 and the semisolid SNEEDDS.

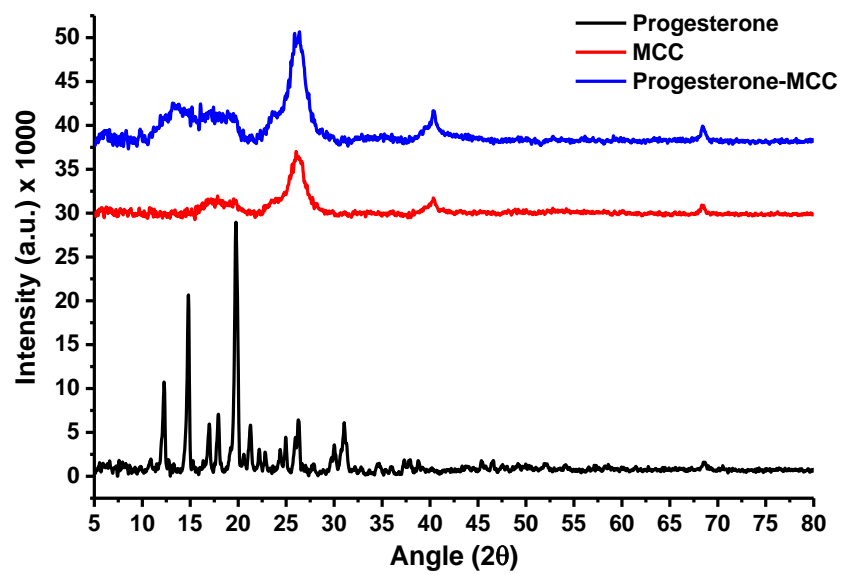


**Fig. S8** PXRD patterns of Progesterone-loaded MCC (15 mg/g), pure MCC and Progesterone.



## 8.2. Acknowledgement

I would like to express my sincere gratitude to my supervisor, Prof. Karsten Mäder, for accepting me as a PhD student in this challenging multi aspects research topic as well as the flexibility and freedom in the research he offered me during my PhD study. Prof. Mäder has provided a continuous support not only for me but also for my wife during our stay in Germany.

Prof. Peter Imming is highly acknowledged for his support in the  $^1\text{H-NMR}$  data analysis and for the continuous reinforcement and encouragement to my wife and myself.

Dr. Hendrik Metz is gratefully acknowledged for his guidance in the ESR and BT-NMR experiments, fitting of the ESR data as well as his fruitful discussions and suggestions in various physicochemical aspects.

I am grateful to the whole workgroup of Prof. Mäder for their help and nice working environment. Special thanks to Frederike Tenambergen, Dr. Martin Gernot Hahn, Claudia Kutza (geb. Kegel), Dr. Johannes Oidtman, Dr. Andreas Noack, Abdul-Karim Barakat and Rashad Al-Mwalad for their kind help during my start in the group and the introduction to various lab facilities. Furthermore, I would like to thank my former and current officemates Dr. Jun Li and Alexandre Rodrigues for their friendship and the nice everyday life discussions. Martha Heider is acknowledge for the HPTLC/spectrodensitometry measurements, Christin Zlomke (geb. Nitzschke) for proofreading of the German summary, Mrs. Heike Rudolf for the FTIR measurements Dr. Dieter Ströhl for the  $^1\text{H-NMR}$  measurements and Dr. Christoph Wagner for the introduction to PXRD.

Additionally, my thanks go to the lab technicians: Mrs. Kerstin Schwarz and Mrs. Ute Mentzel for their kindness, helpfulness and lab assistance. Mrs. Schwarz is further acknowledged for the DSC measurements and Mrs. Mentzel for the help in the HPLC analysis. I would like to express my appreciation to Mrs. Claudia Bertram for her continuous help in the daily paperwork during my stay in Germany and her always optimistic encouragement. Moreover, I would like to thank my students: Stefanie Voigt, Sophia Gebhardt, Margarita Aksenov, Irmak Kaya and Felicia Meyer for their contribution to my preliminary experiments during their mandatory elective subject.

I thank the Egyptian Ministry of Higher Education and Scientific Research and the Deutscher Akademischer Austauschdienst (DAAD) for the financial support in the frame of the German Egyptian Research Long-Term Scholarship (GERLS) program. Abitec Corporation, BASF AG, Croda GmbH and Fuji Chemical Industry Co., Ltd are gratefully acknowledged for the excipients donation.

My special gratitude is due to my wife (Marwa) and to my family for their continuous encouragement, love and invaluable support.

All praise be to Allah, for granting his bounties on me in my whole life and for giving me the strength to finish this work.



### 8.3. Curriculum vitae

#### PERSONAL INFORMATION

Name	Tamer Hassanen Hamed Ahmed Hassan
Birth date	02.09.1982 in Port Said, Egypt
Nationality	Egyptian
Marital status	Married

#### WORK HISTORY

04. 2011 – 03. 2015	Research and teaching assistant in the workgroup of Prof. Dr. Karsten Mäder, Institute of Pharmacy, Martin-Luther-University Halle-Wittenberg, Halle (Saale), Germany.
Since 05. 2009	Assistant lecturer, Pharmaceutics and Industrial Pharmacy Department, Faculty of Pharmacy, Suez Canal University, Ismailia, Egypt.
09. 2004 – 05. 2009	Demonstrator, Pharmaceutics and Industrial Pharmacy Department, Faculty of Pharmacy, Suez Canal University, Ismailia, Egypt.
Since 07. 2004	Part-time pharmacist in private and hospital pharmacies.

#### EDUCATION AND TRAINING

04. 2011 – 01. 2015	PhD student in the workgroup of Prof. Dr. Karsten Mäder, Institute of Pharmacy, Martin-Luther-University Halle-Wittenberg, Halle (Saale), Germany.
10. 2010 – 03. 2011	German language course at Herder Institute, Leipzig University, Leipzig, Germany. Graduation Grade: DSH Stufe 3.
05. 2010 – 08. 2010	Preparation Course for GERLS Scholarship Holders including 2 months German language course at Goethe Institute, Cairo, Egypt (Graduation Grade: Start 2: 88 %) and soft skills workshops.
04. 2009	MSc. Pharmaceutical Science (Pharmaceutics), Faculty of Pharmacy, Suez Canal University, Ismailia, Egypt. Title of Master thesis: “Preparation and Evaluation of Sustained Release Diclofenac Sodium Tablets”.
07. 2004	BSc. Pharmaceutical Science, Faculty of Pharmacy, Suez Canal University, Ismailia, Egypt. Graduation Grade: Excellent with Honors. (Ranked 1 <sup>st</sup> out of 246 students).

#### GRANTS/AWARDS

10. 2010 – 03. 2015	German Egyptian Long-Term Scholarship (GERLS).
---------------------	------------------------------------------------

## 8.4. List of publications

### 8.4.1. Research articles

- Hassan, T. H. and Mäder, K., **2015**. *Novel semisolid SNEDDS based on PEG-30-di-(polyhydroxystearate): Progesterone incorporation and in vitro digestion*. Int. J. Pharm., 486(1-2), 77-87.
- Hassan, T. H., Metz, H. and Mäder, K., **2014**. *Novel semisolid SNEDDS based on PEG-30-dipolyhydroxystearate: Development and characterization*. Int. J. Pharm., 477(1-2), 506-518.
- Sayed, H. A., Ghorab, M. M. and Hamed, T. H., **2008**. *Preparation and evaluation of sustained-release diclofenac sodium tablets*. Zag. J. Pharm. Sci., 17(2), 1-5.

### 8.4.2. Conferences contributions

- Hassan, T. H., Metz, H. and Mäder, K., **2014**. *Preparation and characterization of self-nanoemulsifying adsorbates based on semisolid SNEDDS*. DPhG Annual Meeting – Trends and perspectives in pharmaceutical sciences, Frankfurt, Germany, 199-200 (Poster and abstract).
- Hassan, T. H. and Mäder, K., **2013**. *Screening of Soluplus<sup>®</sup> as an ingredient in solid self-emulsifying formulations*. DPhG Annual Meeting – Drug discovery inspired by nature, Freiburg, Germany, 250-251 (Poster and abstract).

## 8.5. Declaration of the original authorship

### Selbständigkeitserklärung

Hiermit erkläre ich gemäß § 5 der Promotionsordnung der Naturwissenschaftlichen Fakultät I der Martin-Luther-Universität Halle-Wittenberg, dass ich die Ergebnisse der vorliegenden Dissertationsarbeit

**„Formulation and evaluation of self-nanoemulsifying tablets for the delivery of poorly water-soluble drugs“**

am Institut für Pharmazie der Martin-Luther-Universität Halle-Wittenberg unter Anleitung von Herrn Professor Dr. rer. nat. habil. Karsten Mäder selbständig erarbeitet und die Dissertation ohne fremde Hilfe verfasst habe. Ich habe keine anderen als die von mir angegebenen Quellen und Hilfsmittel benutzt und die den verwendeten Werken wörtlich oder inhaltlich entnommenen Stellen als solche kenntlich gemacht. Weiterhin habe ich diese Arbeit bisher an keiner in- oder ausländischen Fakultät als Dissertationsschrift vorgelegt.

*Halle (Saale), den 20.01.2015*

---

Ort, Datum

*sgd. Tamer H. Hassan*

---

Tamer Hassanen Hamed Ahmed Hassan, MSc.